# Sensory Mapping in Zebrin-positive Modules in the Cerebellum

# Representatie van sensorische input in zebrin-positieve modules in het cerebellum

Proefschrift

ter verkrijging van de graad van doctor aan de
Erasmus Universiteit Rotterdam
op gezag van de
rector magnificus

prof.dr. H.A.P. Pols

en volgens besluit van het College voor Promoties.
De openbare verdediging zal plaatsvinden op

woensdag 27 januari 2016 om 9.30 uur

**Chiheng Ju**
geboren te Dalian
(China)

Erasmus University Rotterdam

**Promotiecommissie:**

**Promotor:** **Prof.dr. C.I. de Zeeuw**

**Overige leden:** **Prof.dr. J. van der Steen**
**Prof.dr. M.A. Frens**
**Prof.dr. H.J. Groenewegen**

**Copromotor:** **Dr. L.W.J. Bosman**

# TABLE OF CONTENTS

**Chapter 1** General introduction ........ 5

**Chapter 2** Cerebellar modules operate at different frequencies ........ 69

**Chapter 3** Differential Purkinje cell simple spike activity and pausing behavior related to cerebellar modules ........ 97

**Chapter 4** Climbing fiber responses of individual Purkinje cells in crus 1 of the cerebellar cortex to tactile, auditory and visual inputs in awake mice ........ 121

**Chapter 5** Cellular resolution imaging of climbing fibers responding to single whisker stimulation ........ 135

**Chapter 6** General discussion ........ 153

**Summary** ........ 161

**Samenvatting** ........ 163

**Curriculum vitae** ........ 165

**PhD Portfolio** ........ 166

**Acknowledgments** ........ 167

# Chapter 1

# General introduction

The cerebellum is one of the most structurally conserved parts of the vertebrate nervous system with a striking homogeneity in its micro-circuitry. The cerebellum contains a limited number of well-defined classes of neurons of which the Purkinje cells in the cerebellar cortex play a key role. The structural similarity across different species allows the use of mice as a model organism for investigating the cerebellar functions also in other species, including humans.

The homogeneous cyto-architecture of the cerebellar cortex does, however, not mean that Purkinje cells function the same throughout the whole cerebellar cortex. In fact, subgroups of Purkinje cells can be distinguished by the expression pattern of various molecular markers. Of these markers, zebrin II has been particularly well studied. We found a significant difference in the intrinsic activity of Purkinje cells expressing or not expressing zebrin II. But even within regions with the same zebrin II-expression pattern, functional heterogeneity in Purkinje cell function can be found. We exploited somatosensory input from the face to study functional heterogeneity in cerebellar lobule crus 1, a zebrin II-positive area.

In the following I will introduce the basic structure of cerebellum with a focus on the cerebellar cortex, the Purkinje cells and the sensory input pathways to the Purkinje cells. I will relate this to sensory maps and to the whisker system as a model system for our sensory mapping studies.

### *1.1 Cerebellum*

The cerebellum is an area of the hindbrain which is present in all true vertebrates. This is especially striking in birds and mammals (Sultan and Glickstein 2007). The cerebellum consists of two parts: the cerebellar cortex and the cerebellar nuclei. Both parts receive input from two main excitatory pathways: the mossy fibers and the climbing fibers. The climbing fibers originate exclusively from the inferior olive while the mossy fibers have diverse origins. The cerebellar cortex projects exclusively to the cerebellar and – to a lesser degree - the vestibular nuclei. For this reason, the cerebellar cortex is generally perceived as the output structure of cerebellum. In this thesis, I focus on the cerebellar cortex.

The cerebellar cortex consist of a worm-like middle part called “vermis” that is bordered on both sides by the cerebellar hemispheres. The cerebellar cortex is transversely divided into three lobes, which are the anterior, the posterior and the flocculo-nodular lobes. These lobes can be further subdivided into lobules(Figure 1).

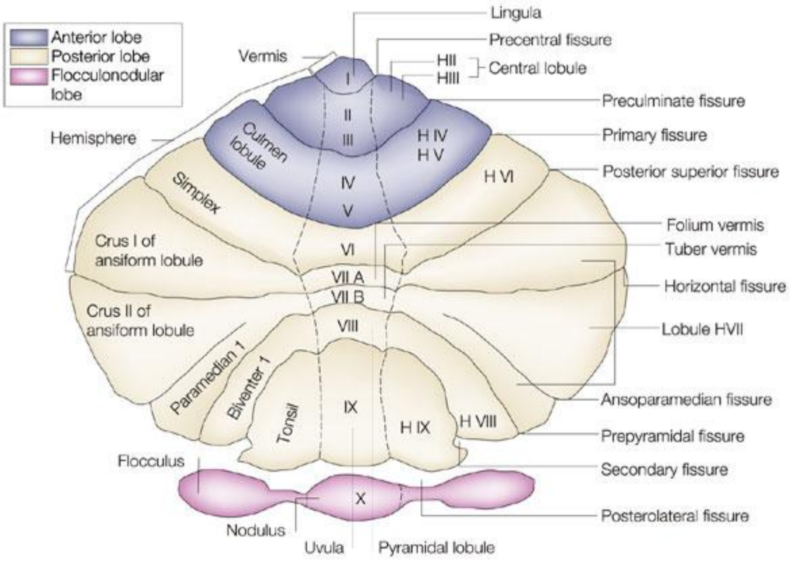
Anterior lobe
Posterior lobe
Flocculonodular lobe
Vermis
Hemisphere
Lingula
Precentral fissure
HII
HIII
Central lobule
Preculminate fissure
Primary fissure
Posterior superior fissure
Folium vermis
Tuber vermis
Horizontal fissure
Lobule HVII
Ansoparamedian fissure
Prepyramidal fissure
Secondary fissure
Posterolateral fissure
Culmen lobule
Simplex
Crus I of ansiform lobule
Crus II of ansiform lobule
Paramedian 1
Biventer 1
Tonsil
Flocculus
Nodulus
Uvula
Pyramidal lobule
I
II
III
IV
V
VI
VII A
VII B
VIII
IX
X
H IV
H V
H VI
H VIII
H IX

***Figure 1 – Unfolded view of the cerebellar cortex showing lobes, lobules (by name and number) and main fissures.*** *Adapted from (Manni & Petrosini 2004).*

In addition to the transversal lobular structure, the cerebellar cortex is also divided into a number of longitudinal zones. The longitudinal zones are characterized by the area of the inferior olive from which they receive climbing fiber input and the specific cerebellar (sub)nucleus to which they project. Initially, seven of these longitudinal zones (termed A, B, C1, C2, C3, D1 and D2) were distinguished (Voogd, 1964; Groenewegen and Voogd 1977; Groenewegen, Voogd, and Freedman 1979)(Figure 2).

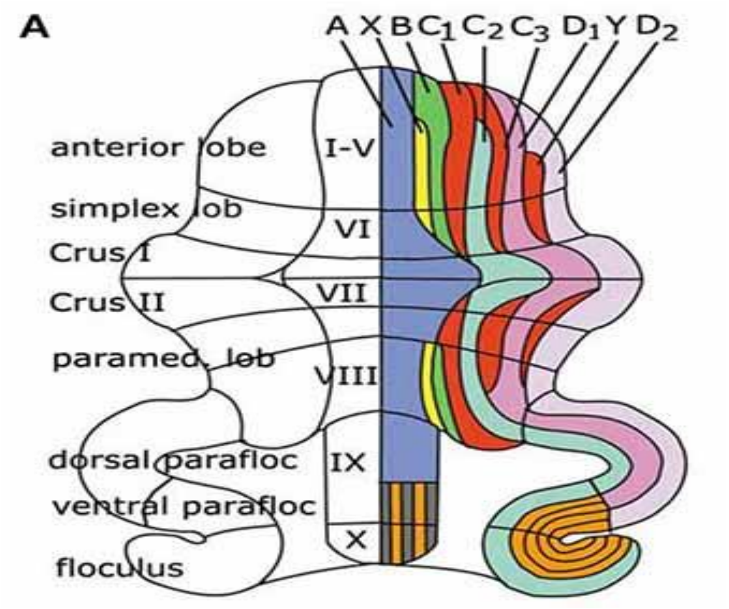
A
A X B C1 C2 C3 D1 Y D2
anterior lobe
I-V
simplex lob
VI
Crus I
VII
Crus II
paramed. lob
VIII
dorsal parafloc
IX
ventral parafloc
X
floculus

***Figure 2 –Seven longitutional zones in unfolded cerebellar cortex. Adapted from (Voogd 2014).***

Based on the expression pattern of zebrin II, these longitudinal zones were further subdivided into smaller parasagittal stripes. The zebrin II-stripes are symmetrically distributed across the midline and are highly reproducible between individuals (Brochu, Maler, and Hawkes 1990),(Richard Hawkes, Colonnier, and Leclerc 1985),(R. Hawkes and Leclerc 1987)(Figure 3).

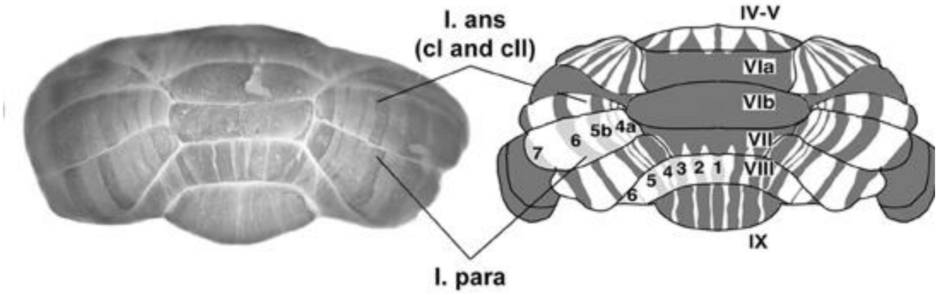
l. ans
(cl and cll)
IV-V
VIa
VIb
VII
VIII
IX
7
6
5b
4a
5
4
3
2
1
6
l. para

***Figure 3 – A dorsal overview of the complementary stripe arrays revealed by immunoperoxidase-staining for zebrin II/aldolase C in the adult mouse.*** *Adapted from (Consalez and Hawkes 2013).*

## *1.2 Purkinje cells*

*The cerebellar Purkinje cell is one of the largest and most complex neurons in the mammalian nervous system. Each adult Purkinje cells is innervated by a single climbing fiber that forms an extraordinary strong synaptic connection. In addition, Purkinje cells receive indirect mossy fiber input via the cerebellar granule cells that give rise to the numerous parallel fibers. Granule cells are the smallest and the most abundant type of neurons in the brain*

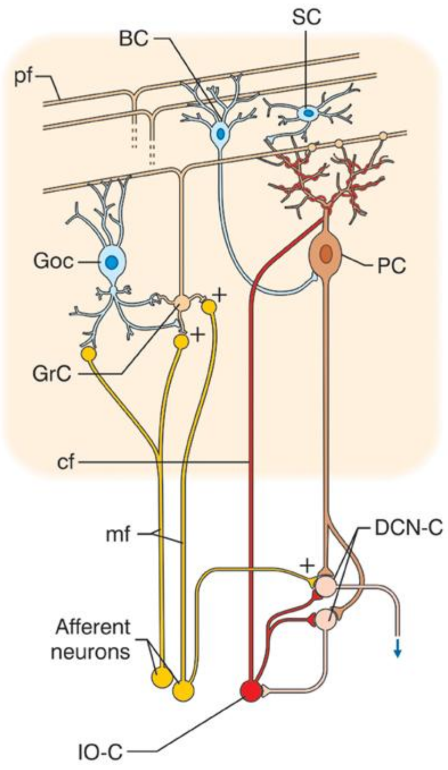

*(Braitenberg and Atwood 1958; Zagon, McLaughlin, and Smith 1977). The parallel fiber-to-Purkinje cell synapses are weak, but up to more than 100,000 parallel fiber can converge on a single Purkinje cell. Purkinje cells also receive inhibitory input from the molecular layer interneurons: the basket and stellate cells. These interneurons receive excitatory inputs from both parallel and climbing fibers (Jörntell and Ekerot 2002)(Figure 4). Purkinje cells produce two kinds of spikes: simple spikes at rates of 50-125 Hz and complex spikes at rates around 1 Hz* in vivo *(Latham 1971). Purkinje commonly operate in the upstate and have a high firing rate, even at rest, but can also produce pauses of several seconds (Loewenstein et al. 2005).*

***Figure 4 – Schematic representation of the cerebellar circuit.*** *DCN cells (DCN -C) IO cells (IO-C). granule cells (GrC), Golgi cells (GoC), Purkinje cells (PC), stellate and basket cells (SC, BC), mossy fibers (mf) climbing fibers (cf) parallel fibers (pf). Adapted from (D'Angelo and Casali, 2013).*

Purkinje cells are the sole output neurons of the cerebellar cortex to the cerebellar nuclei. They provide inhibitory input to the neurons of the cerebellar and vestibular nuclei (Palkovits et al. 1977; De Zeeuw and Berrebi 1995, Gauck and Jaeger 2000). This implies that the pauses in Purkinje cell simple spike activity are potentially functionally relevant in cerebellar information processing.

### *1.3 Inferior Olive*

Climbing fibers originate solely from the contralateral inferior olive. In rodents, the inferior olive consists of three primary subdivisions: the principal olive (PO), the medial accessory olive (MAO), and the dorsal accessory olive (DAO). The inferior olive contains predominantly excitatory projection neurons. These are either curly cells, having a relatively small cell somata and curly dendrites, or straight cells that have large cell somata and long, relatively straight dendrites (Scheibel and Scheibel 1975; Devor and Yarom 2002). Another interesting fact is that there are very few (<0.1% of all neurons) GABAergic interneurons in the inferior olive (Nelson and Mugnaini 1988; Walberg and Ottersen 1989). There are several characteristic features of inferior olivary neurons. First, they have gap junction-mediated electrical synapses which are composed of the protein connexin36 (Llinas, Baker, and Sotelo 1974). Another feature is that inferior olivary neurons exhibit spontaneous subthreshold oscillations of their membrane potential in slice experiments. The oscillation frequency is about 4–6 Hz with amplitude of 5–10 mV.

The sources of afferent fibers to the inferior olive are spinal cord segments (Matsushita, Yaginuma, and Tanami 1992) and midbrain nuclei such as the parvocellular red nucleus, the interstitial nucleus of Cajal, the nucleus of Darkschewitsch, and the caudomedial extremity of the subparafascicular nucleus (Saint-Cyr and Courville 1981). In addition the sensory trigeminal nuclei were also found to project to inferior olive (Van Ham and Yeo 1992).

## *1.4 sensory maps*

The most famous example of a sensory map is the sensory homunculus in the somatosensory cortex. The homunculus in the somatosensory cortex has the same shape as the skin, although some areas have a larger representation than others. Such a homunculus, or ordered somatotopy, is absent in the cerebellar cortex. The sensory maps of the cerebellar cortex looks as if an orderly somatotopic map has been fractured into many pieces and was then reassembled in a new arrangement. Hence, it has "fractured somatotopy" (Figure 5). Such an organization is true for both the mossy fibers (Shambes, Gibson, and Welker 1978) and the climbing fibers (Robertson 1984). But we are still lacking a high-resolution sensory map in the cerebellar cortex. Knowing whether there is a detailed map of sensory input could help us understand how sensory information is processed in cerebellum.

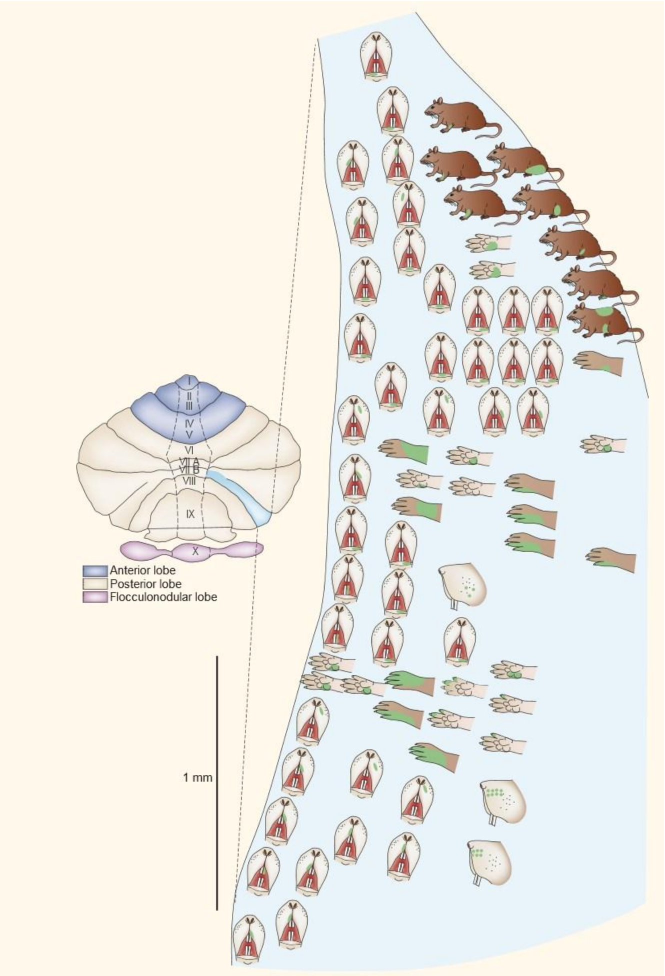

***Figure 5 – The fractured somatotopy of the paramedian lobule.*** *The receptive fields of granule cells in the rat cerebellar cortex reveal multiple representations of the same body parts in different locations. Adapted from (Manni and Petrosini, 2004)*

## *1.5 The mouse whisker system*

### 1.5.1 *A model system to study somatosensory input to Purkinje cells.*

Beginning with the 1970s discovery of "barrels" in the rat and mouse brain, the rodent whisker system has become a fruitful system to investigate tactile sensory inputs to the central nervous system. There is evidence that both the mossy fiber–parallel fiber and the climbing fiber pathways convey sensory information from the whiskers to the cerebellar cortex (Kleinfeld, Berg, and O'Connor 1999). The spatial arrangement of whiskers in mice is highly conserved across individuals in very precise rows and arcs on both sides of the animal's head. This makes it relatively easy to access and stimulate whiskers and the simulation could be accurately repeated across individual animals. All these points make mouse whisker system an ideal model to investigate tactile sensory input to cerebellar cortex.

# 1.5.2

# Anatomical pathways involved in generating and sensing rhythmic whisker movements

Laurens W.J. Bosman[1,2], Arthur R. Houweling[1], Cullen B. Owens[1], Nouk Tanke[1], Olesya T. Shevchouk[1], Negah Rahmati[1], Wouter H.T. Teunissen[1], Chiheng Ju[1], Wei Gong[1], Sebastiaan K.E. Koekkoek[1] & Chris I. De Zeeuw[1,2*]

**Front Integr Neurosci. 2011**

## Abstract

The rodent whisker system is widely used as a model system for investigating sensorimotor integration, neural mechanisms of complex cognitive tasks, neural development, and robotics. The whisker pathways to the barrel cortex have received considerable attention. However, many subcortical structures are paramount to the whisker system. They contribute to important processes, like filtering out salient features, integration with other senses and adaptation of the whisker system to the general behavioral state of the animal. We present here an overview of the brain regions and their connections involved in the whisker system. We do not only describe the anatomy and functional roles of the cerebral cortex, but also those of subcortical structures like the striatum, superior colliculus, cerebellum, pontomedullary reticular formation, zona incerta and anterior pretectal nucleus as well as those of level setting systems like the cholinergic, histaminergic, serotonergic and noradrenergic pathways. We conclude by discussing how these brain regions may affect each other and how they together may control the precise timing of whisker movements and coordinate whisker perception.

## Keywords

1. Vibrissa
2. Follicle-sinus complex
3. Barrel cortex
4. Basal ganglia
5. Cerebellum
6. Sensorimotor integration
7. Rhythmic movements
8. Anatomy

## 1. Introduction

Rodents have highly mobile whiskers, with which they can rapidly locate and discriminate objects in their environment. The rodent whisker system has become a popular model system for brain development, experience-dependent plasticity, perceptual learning, repetitive, timed motor responses, sensorimotor integration and robotics. Of the many brain regions involved in the whisker system, the trigeminal brainstem, thalamus and primary somatosensory cortex (S1), and to a lesser extent the whisker motor cortex (wM1), have attracted most attention (for reviews see Kleinfeld et al., 1999;Deschênes et al., 2005;Brecht, 2007;Petersen, 2007;Alloway, 2008;Diamond et al., 2008). Other brain regions and the structures of the whisker pad itself have received less attention. Here we aim to integrate the current knowledge on sub-cortical structures into the well-known whisker pathways, thus presenting an overview of the most important structures of the whisker system and their interconnections as a whole. In addition, we discuss how these structures may cooperate to generate and sense whisker movements.

Tactile hairs are specialized hairs that, due to the presence of sensitive mechanoreceptors at their follicles, provide accurate somatosensory input. Tactile hairs which grow from a follicle-sinus complex are called “vibrissae” or “whiskers”. Almost all mammals, except humans and egg-laying mammals (monotremes), have vibrissae (Chernova, 2006;Muchlinski, 2010). Vibrissae can grow from all body parts, but are mainly located on the face (Sarko et al., 2011). Most likely, all vibrissae can be moved, but there is a large variability in movement mechanics. Some vibrissae, like the genal vibrissae in the hamster, lack musculature and are moved solely by vascular and connective tissue dynamics (Wineski, 1985). Other vibrissae can be moved by muscles involved in the erection of hairs (m. arrector pili) (Hyvärinen et al., 2009), while mystacial vibrissae can be moved by a group of specialized muscles (Brecht et al., 1997;Haidarliu et al., 2010;Sarko et al., 2011). In some species, including shrews (Munz et al., 2010) and rodents such as rats, mice, gerbils, hamsters, chinchillas and porcupines (Woolsey et al., 1975), the mystacial vibrissae can move fast and rhythmically. This behavior is called “whisking”, and in accordance we reserve the term “whiskers” here for those vibrissae that can be whisked. Whisking behavior is absent in most species, including well-studied species like rabbits, cats and seals (Woolsey et al., 1975;Dehnhardt and Kaminski, 1995). The main function of vibrissae is to complement or replace near-vision (Welker, 1964;Gogan et al., 1981;Ahl, 1986). In addition, marine mammals use their vibrissae for long-distance sensing. For instance, a seal may “feel” prey fish at more than 180 m distance (Dehnhardt et al., 2001). Vibrissae also help to locate, identify and capture prey (Anjum et al., 2006;Munz et al., 2010;Favaro et al., 2011). In addition, vibrissae inform about body posture, especially in water (Ahl, 1982), and play a central role in social behavior (Miller, 1975;Blanchard et al., 1977).

Well-timed, rhythmic whisker movements are instrumental in exploring the environment (Carvell and Simons, 1990;Grant et al., 2009;Hartmann, 2011). When doing so, rats make large whisker movements at a relatively low frequency (5-15 Hz). Once their interest has been caught, they can thrust their whiskers forward and make smaller movements at higher frequencies (15-25 Hz) to identify objects and textures (Carvell and Simons, 1995;Harvey et al., 2001;Berg and Kleinfeld, 2003a). Small variations in surface texture may halt the whisker tip for a short while, after which it slips past the fine obstruction (Fig. 1B) (Neimark et al., 2003;Ritt et al., 2008;Wolfe et al., 2008). Such “slip-stick” movements can trigger stereotypical neuronal responses allowing the animal to sense subtle features of surfaces (Fig. 1C) (Jadhav et al., 2009). The combination of rhythmic movements and precisely timed sensory input thus greatly increases the acuity of whisker input.

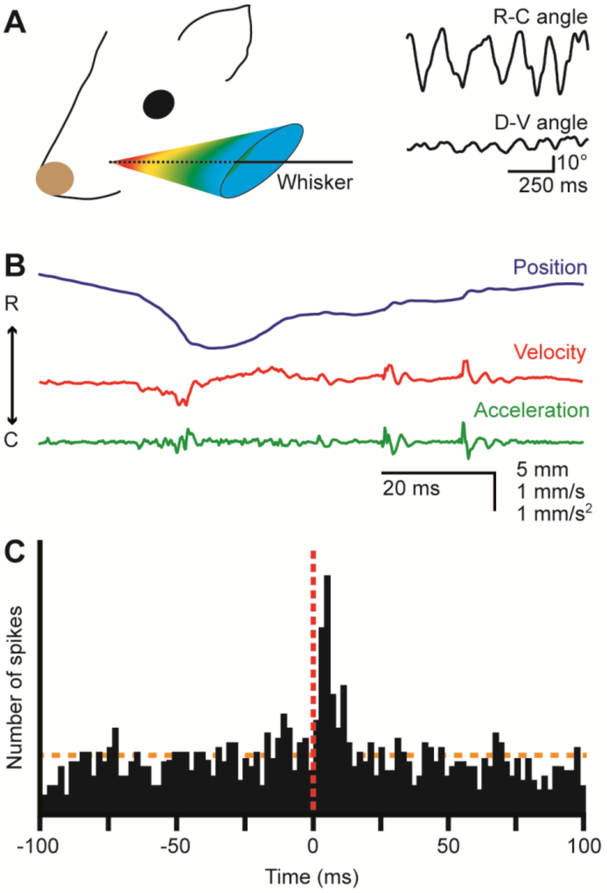

***Figure 1 – Whisker movements***
***A** | Whiskers move rhythmically back-and-forth during exploratory whisking in the rat. The deflection along the rostro-caudal axis is much larger than that on the dorso-ventral axis. The left panel is a schematic drawing of the space in which a whisker can be moved, based on Bermejo et al. (2002). The right panels are reproduced with permission from Hill et al. (2008). **B** | Position, velocity and acceleration of a rat D3 whisker during one whisking cycle on P150 sandpaper. Irregularities in the sandpaper surface cause “slip-stick” movements. Reproduced with permission from Wolfe et al. (2008). **C** | Slips can trigger neuronal responses in rat wS1, as shown by a peri-stimulus time histogram of the spike times of a single neuron aligned on the first slips of whisker movements. Reproduced with permission from Jadhav et al. (2009).*

## 2. Whiskers

### 2.1. The whisker pad

The organization of the whiskers on the mystacial pad varies greatly between different species, but is relatively similar between rats and mice (Woolsey et al., 1975;Brecht et al., 1997). Rats and mice have five rows of whiskers. The upper two rows (A-B) have four whiskers each, while the lower three rows (C-E) each contain about seven whiskers. In addition, there are four particularly large whiskers (“straddlers”), labeled - , at the caudal edge of the mystacial pad (Fig. 2A). The muscles of the mystacial pad are divided into extrinsic and intrinsic muscles, all of which are innervated by specific branches of the facial nerve (Fig. 2A) (Dörfl, 1985). The intrinsic muscles are completely situated within the mystacial pad, while the extrinsic muscles have their origins outside the mystacial region (Dörfl, 1982;Jin et al., 2004;Haidarliu et al., 2010). During a normal, exploratory whisking cycle, the whiskers first protract and then retract. Whisker protraction is initiated by contraction of the medial inferior and medial superior parts of the extrinsic muscle m. nasolabialis profundus and completed by contraction of the intrinsic capsular muscles. Subsequent whisker retraction is under control of two extrinsic muscles, the m. nasolabialis and the m. maxillolabialis (Fig. 2A-B) (Berg and Kleinfeld, 2003a;Hill et al., 2008;Simony et al., 2010). Whisker retraction during foveal whisking is a relatively passive process, involving virtually no muscle activity; during foveal whisking the vibrissae are thrust forward and palpate objects with low-amplitude movements at high frequency (Berg and Kleinfeld, 2003a). Rodents can also move the whole mystacial pad. Pad movements may contribute to the normal whisking cycle (Bermejo et al., 2005), but can also involve rotation or resizing of the whisker pad to optimize object contact (Haidarliu et al., 2010;Towal et al., 2011). For instance, contraction of m. nasolabialis superficialis moves the A and B rows dorsally, and contraction of m. buccinatorius pars orbicularis oris moves the C-E rows ventrally, thereby adjusting the mystacial field size (Haidarliu et al., 2010). Although the general structure of the mystacial pad is similar in mice (Dörfl, 1982), hamsters (Wineski, 1985) and rats (Haidarliu et al., 2010), minor differences between species do occur, mainly in the organization of the m. nasolabialis profundus (cf. Haidarliu et al. (2010)).

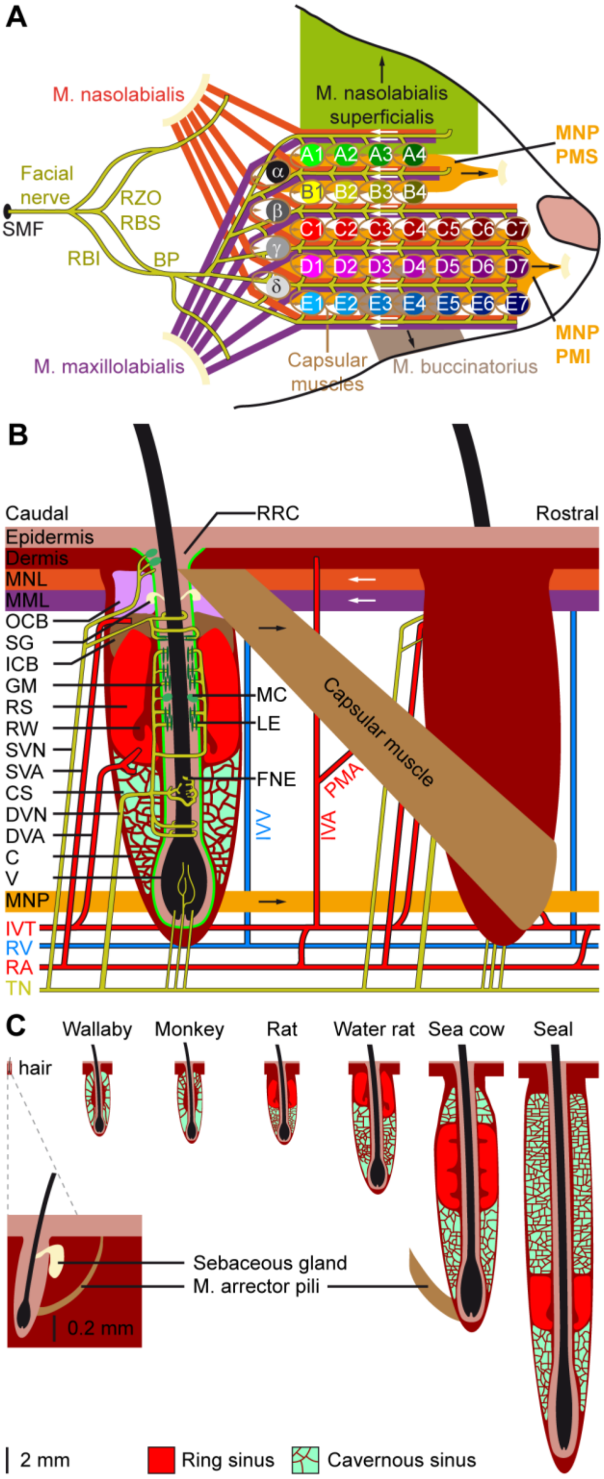
A
M. nasolabialis
M. nasolabialis superficialis
MNP
PMS
Facial nerve
SMF
RZO
RBS
RBI
BP
α
β
γ
δ
A1 A2 A3 A4
B1 B2 B3 B4
C1 C2 C3 C4 C5 C6 C7
D1 D2 D3 D4 D5 D6 D7
E1 E2 E3 E4 E5 E6 E7
MNP
PMI
M. maxillolabialis
Capsular muscles
M. buccinatorius
B
Caudal
RRC
Rostral
Epidermis
Dermis
MNL
MML
OCB
SG
ICB
GM
RS
RW
SVN
SVA
CS
DVN
DVA
C
V
MNP
IVT
RV
RA
TN
MC
LE
FNE
Capsular muscle
PMA
IVV
IVA
C
Wallaby
Monkey
Rat
Water rat
Sea cow
Seal
hair
Sebaceous gland
M. arrector pili
0.2 mm
2 mm
🟥 Ring sinus
▨ Cavernous sinus

***Figure 2 – Location and structure of the whiskers***

***A*** *| The whiskers are organized in rows on the mystacial pad. Mice and rats have five rows of whiskers, as well as four "straddlers" caudal to these rows. Each whisker is associated with an intrinsic capsular muscle (see also B). Extrinsic muscles connect to multiple whiskers. The m. nasolabialis profundis (MNP) consists of two parts, the mediosuperior (PMS) and the medioinferior (PMI) parts, both of which are involved in whisker protraction. The m. nasolabialis and m. maxillolabialis are involved in whisker retraction. The other extrinsic whiskers, including the m. nasolabialis superficialis and the m. buccinatorius, are involved in resizing the entire mystacial pad. The mystacial muscles are almost exclusively innervated by the facial nerve, which leaves the skull via the stylomastoid foramen (SMF). After leaving the SMF, the facial nerve splits up in two streams. The lower stream consists of the rami buccolabialis superior (RBS) and inferior (RBI), which anastomose in the buccal plexus (BP). From the BP all extrinsic and intrinsic whisker muscles are innervated, with the exception of m. nasolabialis, which is innervated by the upper stream, which includes the ramus zygomatico-orbitalis (RZO).* ***B*** *| Schematic drawing of the follicle-sinus complex (FSC) of the rat. The vibrissa (V) lies within a follicle that is derived from the epidermis and that is surrounded by the glassy membrane (GM). Around the follicle is a blood sinus derived from the dermis, and which is composed of two sinuses: the cavernous sinus (CS), which has numerous collagenous trabeculae, and the ring sinus (RS), which is an open structure. At the bottom of the ring sinus, there is an asymmetric structure of connective tissue: the ringwulst (RW). At the distal end of the ring sinus, the inner conical body (ICB) links the follicle strongly to the capsule (C). Distal to the ICB is the outer conical body (OCB) that contains the sebaceous gland (SG). Intrinsic capsular muscles connect pairs of FSCs. Extrinsic muscles are located just below the skin (m. nasolabialis (MNL) and m. maxillolabialis (MML)), or at the lower end of the FSC (m. nasolabialis profundus (MNP)). The arrows indicate whether contraction of the muscle causes pro- or retraction of the vibrissae. The vibrissae are surrounded by three different types of mechanoreceptors: Merkel cells (MC), lanceolate endings (LE) and free nerve endings (FNE). Mechanoreceptors in the upper part of the FSC are innervated by superficial vibrissal nerves (SVN) and those in the lower part by the deep vibrissal nerve (DVN). In addition, there are some small-caliber fibers at the bottom. The sensory fibers come together with fibers from other parts of the face to form the infra-orbital branch of the trigeminal nerve (TN). Blood supply to the FSCs is organized via row arteries (RA) located between the whisker rows, with superficial vibrissal arteries (SVA) supplying the upper parts and deep vibrissal arteries (DVA) the lower parts of the FSCs. The DVA does not directly branch from a RA, but from the anastomozing intervibrissal trunks (IVT).*

*In between the FSCs are intervibrissal arteries (IVA) that supply the skin and hair follicles. The capsular muscles receive their blood from arterioles (PMA) branching from the IVA and directly from the IVT. Venal drainage is organized by intervibrissal veins (IVV) that empty in row veins (RV).* ***C*** *| Schematic drawings of the follicle of a typical, mammalian body hair (left) and of the structure of the blood sinuses of FSCs in different species. A hair follicle lacks a blood sinus and can be moved by contraction of the m. arrector pili. In marsupials and primates, the blood sinus is composed of a single compartment (the cavernous sinus), as illustrated for the tammar wallaby (Macropus eugenii) (Marotte et al., 1992) and the rhesus monkey (Van Horn, 1970). Most species, however, have two sinuses: the ring sinus and the cavernous sinus, as illustrated for the rat (Rattus sp.) (Ebara et al., 2002) and the Australian water rat (Hydromys chrysogaster) (Dehnhardt et al., 1999). Pinnipeds have tricompartite blood sinuses, including an outer cavernous sinus, as illustrated for a sea cow, the Florida manatee (Trichechus manatus latirostris) (Reep et al., 2001), and the ringed seal (Phoca hispida) (Hyvärinen et al., 2009). Non-whisking species can generally move their vibrissae using m. arrector pili muscles, as indicated for the FSC of the sea cow.*

### 2.2. Follicle-sinus complexes

Vibrissae differ from other (pelagic) hairs in that each of their (epidermal) follicles is surrounded by a (dermal) blood sinus, which in most species is composed of a distal ring sinus and a proximal cavernous sinus (Fig. 2B-C) (Szymonowicz, 1895;Ebara et al., 2002;Kim et al., 2011). It has been suggested that animals can modulate the dynamic range of the vibrissal mechanoreceptors by changing the blood pressure in the blood sinus (Vincent, 1913;Nilsson, 1969;Gottschaldt et al., 1973). In addition, the size of the follicle-sinus complex (FSC) seems to be adapted for the behavior and environment of the animals. In general, the largest FSCs are found in marine mammals, intermediate FSCs in semi-aquatic species, like otters and water rats, and the smallest FSCs in purely terrestrial mammals (Dehnhardt et al., 1999;Hyvärinen et al., 2009). Larger FSCs make the vibrissal movements more resistant to water, which has a much higher density than air, and allows better thermal insulation of mechanoreceptors to cold or warm water (Dehnhardt et al., 1998;Dehnhardt et al., 1999). The larger size of the FSCs of marine mammals is due to the presence of a second, external cavernous sinus (Fig. 2C) (Sarko et al., 2007;Hyvärinen et al., 2009). In species where the vibrissal system is relatively unimportant, such as marsupials and primates, the FSCs lack a ring sinus (Van Horn, 1970;Hollis and Lyne, 1974;Marotte et al., 1992). Thus, the adaptations in the FSC-anatomy are in line with specific behavioral requirements.

Cavernous sinuses contain trabeculae of connective tissue, with the spaces in between filled with blood and nerve fibers (Rice, 1993;Hyvärinen et al., 2009;Kim et al., 2011). The ring sinus is an open structure, lacking trabeculae. At the bottom of the ring sinus, most species have an asymmetric, collagenous appendix: the ringwulst. Most likely, the rigid ringwulst transmits vibrations to the soft ring sinus with which it is associated (Stephens et al., 1973), while the ring sinus probably acts to dampen these vibrations (Yohro, 1977). This would imply that the anatomy of the blood sinus, including that of the ringwulst, determines the sensitivity range, which can be fine-tuned by modulating the pressure of the blood sinus. In conclusion, specific adaptations to environmental conditions and behavioral requirements, may have led to variations in the anatomy of the FSC. Such diversity can also be observed between FSCs at various body regions of a single animal. In the Florida manatee, for instance, the facial FSCs are substantially larger and more complex than those at other body regions (Sarko et al., 2007), consistent with the prominent role of facial vibrissae during feeding (Reep et al., 2001).

## 3. Transduction of sensory input

### 3.1. Trigeminal nerve

### 3.1.1 Mechanoreceptors

Vibrissal vibrations are detected by several types of mechanoreceptors with different functional properties. Each FSC is innervated by several small superficial vibrissal nerves

(SVN), a single, large deep vibrissal nerve (DVN) containing 100-200 fibers (Rice et al., 1986), as well as a number of unmyelinated fibers at the base of the FSC (Fig. 2B). The SVN and the DVN contain mainly Aß and Aδ fibers. Thickly myelinated Aß fibers have Merkel cell endings, which are slowly adapting mechanoreceptors, or lanceolate endings, which are rapidly adapting. Hence, Merkel cell endings will primarily signal ongoing movements, while lanceolate endings will predominantly detect unexpected movements (Gottschaldt et al., 1973;Halata et al., 2010;Lumpkin et al., 2010). Merkel cells are located within the epidermis at two regions: at the rete ridge collar and at the level of the ring sinus (Ebara et al., 2002). Remarkably, in the mystacial FSCs of rats, the Merkel cells at the rete ridge collar are almost exclusively found at the caudal site of the FSC, implying that they predominantly transmit backward deflections (Fundin et al., 1994;Ebara et al., 2002). Circumferentially oriented lanceolate endings are mainly located at the level of the inner conical body, while longitudinally oriented lanceolate endings are mostly restricted to the level of the ring sinus (Ebara et al., 2002). The thinly myelinated Aδ fibers supply a highly heterogeneous group of other endings, including spindle-like, club-like, reticular, spiny and encapsulated endings. These endings are dispersed through the epidermal sheet of the FSC, but enriched at the level of the cavernous sinus (Ebara et al., 2002;Sarko et al., 2007). The specific functions of these mechanoreceptors are presently unclear. At the base of the FSC are unmyelinated C fibers (Ebara et al., 2002). Since C fibers predominantly conduct nociceptive stimuli, they could signal pulling of the vibrissae.

### 3.1.2. Trigeminal ganglion

The cell bodies of the trigeminal nerve fibers are located either in the trigeminal ganglion or in the mesencephalic nucleus (see 3.1.3). As a rule, each neuron in the trigeminal ganglion receives input only from a single vibrissa (Kerr and Lysak, 1964;Zucker and Welker, 1969;Lichtenstein et al., 1990). However, neurons receiving input from very small vibrissae may be connected to two or three individual vibrissae (Kerr and Lysak, 1964). In addition, very large deflections of a single vibrissa can cause deformation of the skin, and in that way also activate mechanoreceptors of adjacent FSCs (Simons, 1985). The receptive fields of the trigeminal ganglion are loosely arranged in a somatotopic fashion, with the caudal part of the face projecting to the dorsal part of the ganglion, and the rostral part of the face to the ventral part of the ganglion. The whisker projections follow this general pattern (Erzurumlu and Killackey, 1983;Leiser and Moxon, 2006). Originally, it was reported that dorsal vibrissae are represented medially and ventral vibrissae laterally within the trigeminal ganglion (Zucker and Welker, 1969), but Leiser and Moxon (2006) could not reproduce this medio-lateral patterning.

During rest, when the vibrissae are neither moving nor being touched, the neurons of the trigeminal ganglion are silent (Gibson and Welker, 1983;Lichtenstein et al., 1990;Leiser and Moxon, 2007). Based on their response pattern to vibrissal movement, the majority of trigeminal ganglion neurons are classified as slowly adapting (SA), while the others are rapidly adapting (RA) (Fitzgerald, 1940;Kerr and Lysak, 1964;Lichtenstein et al., 1990;Leiser and Moxon, 2007). During whisking in air, SA neurons fire about three times as often as RA neurons (Leiser and Moxon, 2007). Upon touching an object, both SA and RA neurons increase their firing rate. Both types of neurons reach similar firing rates upon whisker touching (Jones et al., 2004;Leiser and Moxon, 2007). Overall, trigeminal ganglion neurons have a broad range of activation thresholds that vary mainly in amplitude and speed, but also in direction of whisker movement (Arabzadeh et al., 2005;Leiser and Moxon, 2007;Khatri et al., 2009;Gerdjikov et al., 2010). Most trigeminal ganglion neurons receive whisker sensory input via the DVN rather than the SVN, but the information content of both types of fibers seems to be very similar (Waite and Jacquin, 1992).

### 3.1.3. Trigeminal mesencephalic nucleus

A subset of trigeminal nerve fibers does not have their somata in the trigeminal ganglion, but in the trigeminal mesencephalic nucleus (MeV). Thus, MeV houses primary sensory neurons within the CNS, which makes it a unique structure. MeV neurons mainly innervate muscle spindles in the masticatory and extraocular muscles and are thus involved in proprioception. In addition, several other types of receptors in the dental, oral and peri-oral domain are innervated by MeV neurons (Lazarov, 2002). Although whisker muscles lack spindles, MeV contains neurons that innervate the mystacial pad and that respond to spontaneous whisker movements (Mameli et al., 2010). MeV projects to, among others, the dorsomedial part of the principal trigeminal nucleus, the pontomedullary reticular formation and the superior colliculus (Matesz, 1981;Ndiaye et al., 2000).

## 3.2. Sensory trigeminal nuclei

The sensory trigeminal nuclei form the main entrance to the brain for whisker input. The principal trigeminal nucleus (PrV) lies anterior to the spinal trigeminal nucleus (SpV), which consists of an oral (SpVo), an interpolar (SpVi) and a caudal part (SpVc) (Fig. 3A). Afferent fibers of the trigeminal root bifurcate to form a rostral branch ascending to PrV and a caudal branch descending to SpV (Hayashi, 1980). Of the individual fibers, some target only PrV or SpV, while others bifurcate and innervate both. Afferents to SpV can terminate in all three subregions (Hayashi, 1980). All compartments, except SpVo and the rostral part of SpVi, have barrelettes, discrete groups of neurons that receive input from the same vibrissa and that can be visualized by cytochrome oxidase staining (Fig. 3B) (Belford and Killackey, 1979;Ma, 1991;Li et al., 1994;Erzurumlu et al., 2010). Neurons in the barrelettes are relatively small and their dendritic trees are confined within the borders of the barrelette (Veinante and Deschênes, 1999). Roughly one-third of the neurons dedicated to whisker input are located between the barrelettes. These interbarrelette cells have widespread dendritic trees and receive input from multiple vibrissae, mainly located within a single row on the mystacial pad (Veinante and Deschênes, 1999). The barrelettes are organized according to an inverted somatotopy, with dorsal whiskers having a ventral representation and rostral whiskers a medial one (Ma, 1991;Erzurumlu et al., 2010). In addition to the large barrelettes representing the whiskers, smaller barrelettes can be seen that mainly represent the facial micro-vibrissae (Fig. 3B). We will restrict ourselves to the description of the neuronal circuitry of the whiskers, rather than that of the other vibrissae.

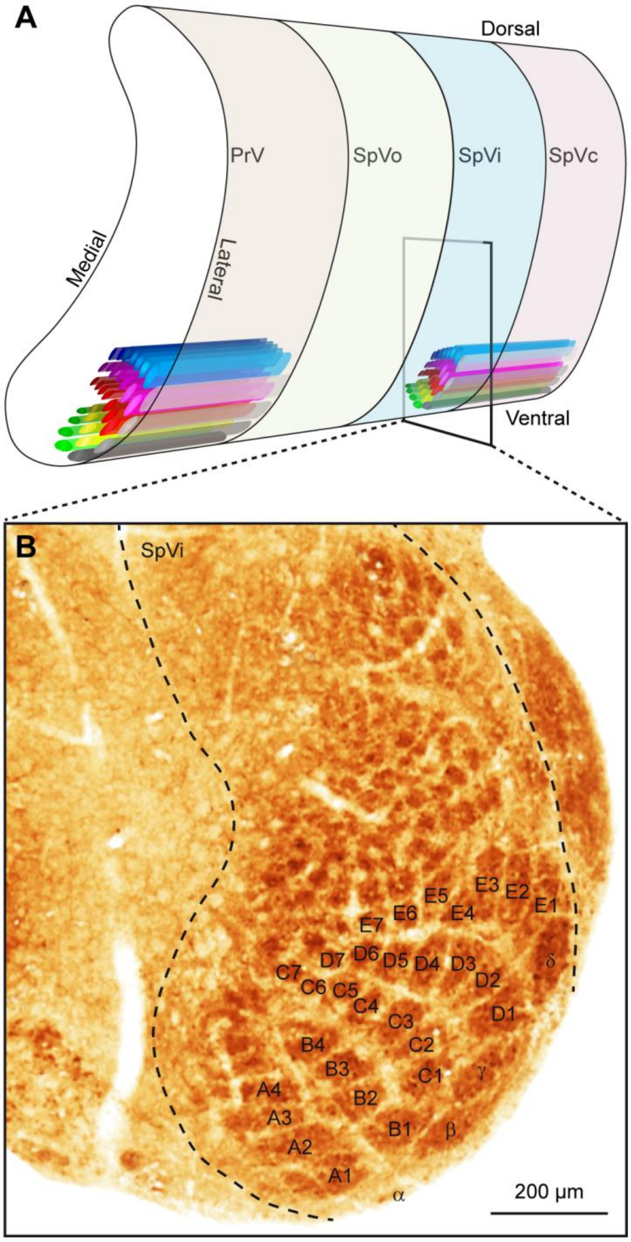

***Figure 3 – The trigeminal nuclei***
***A** | The sensory trigeminal nuclei consist of two nuclei, oriented along the antero-posterior axis. The principal nucleus (PrV) is located at the anterior end and the spinal nucleus (SpV) at the posterior site. The SpV can be subdivided into an oral (SpVo), interpolar (SpVi) and caudal part (SpVc). The facial vibrissae project to the ventral part of the trigeminal nuclei. In PrV, SpVc and the caudal part of SpVi, each vibrissa has its own projection field: a barrelette. The orientation of the barrelettes of the facial macro-vibrissae is indicated schematically. **B** | Coronal section of a neonatal mouse brain, showing the location of the barrelettes of the facial macro-vibrissae in the ventral part of SpVi. Following cytochrome oxidase staining, barrelettes appear as dark patches. Note the inverted somatotopy: dorsal vibrissae project to ventral barrelettes. The smaller patches dorsal to the barrelettes of the E-row are the receptive fields of the facial micro-vibrissae. The photomicrograph was kindly provided by Dr. R.S. Erzurumlu.*

In PrV, output neurons can be found both within and between barrelettes (Veinante and Deschênes, 1999). In SpVi, however, single-whisker neurons project mainly within the trigeminal nuclei, while multi-whisker neurons project to other brain regions (Woolston et al., 1983;Jacquin et al., 1989a;Jacquin et al., 1989b). The small single-whisker neurons of SpVi are part of an extensive, inter-trigeminal network. GABAergic and glycinergic neurons of SpVc project to SpVi, and GABAergic and glycinergic neurons of SpVi project to PrV (Furuta et al., 2008). In addition, glutamatergic interneurons of SpVc project to both SpVi and PrV (Furuta et al., 2008). In this way, SpV can modulate the sensitivity of PrV to whisker inputs (Timofeeva et al., 2005;Furuta et al., 2008;Lee et al., 2008a). This SpV-mediated modulation of PrV in turn is subject to modulation by the somatosensory cortex (Furuta et al., 2010). This allows for central control of the whisker sensitivity. Most likely, this pathway is being used during active whisking, when the whisker-induced output of PrV is suppressed (Lee et al., 2008a). Since there is no strong, direct pathway from wM1 to SpV, this effect is most likely mediated by the whisker area of S1 (wS1). Thus, activity in wM1 activates wS1, which in turn activates the inhibitory projection from SpVi to PrV, reducing the output of PrV (Lee et al., 2008a). This could help the trigeminal nuclei to filter out irrelevant inputs, which may be particularly prominent during movement. Another way to reduce irrelevant input is selective adaptation. PrV responses triggered by weak sensory inputs rapidly desensitize, but are relatively unaffected by repeated strong inputs (Ganmor et al., 2010). Finally, the activity of the sensory trigeminal nuclei can be modulated by several inputs that mainly reflect the general state of alertness, including a cholinergic projection from the pedunculopontine tegmental nuclei (Timofeeva et al., 2005;Beak et al., 2010), a serotonergic projection from the raphe nuclei (Lee et al., 2008c) and a noradrenergic projection from the locus coeruleus (Moore and Bloom, 1979). Taken together, the level of detail of the sensory information forwarded to the rest of the brain by the trigeminal nuclei depends on the behavioral state of the animal.

Apart from the contralateral projections to the thalamus described in detail below, there are also contralateral projections from the trigeminal nuclei to the pontine nuclei (see 4.5.1), the inferior olive (see 4.5.2), the superior colliculus (see 4.4) and the zona incerta (see 4.7.2). In addition, there are predominantly ipsilateral connections to the cerebellum (see 4.5.2), the pontomedullary reticular formation (see 4.7.1) and the lateral facial nucleus. The trigemino-facial connections originate from all four subnuclei, but mainly from SpVc (Erzurumlu and Killackey, 1979;Pinganaud et al., 1999;Hattox et al., 2002). Since the lateral facial nucleus houses whisker motor neurons (Klein and Rhoades, 1985;Herfst and Brecht, 2008), this connection forms a direct feedback loop (Nguyen and Kleinfeld, 2005). It has been suggested that SpV also receives motor input from wS1, the information of which might be forwarded to the lateral facial nucleus via the direct connection (Matyas et al., 2010).

### 3.3. Thalamus and trigemino-thalamo-cortical pathways

The thalamus is the main gateway to the cerebral cortex. It is composed of several nuclei, two of which are critically involved in the transmission of whisker stimuli to wS1: the ventral posterior medial nucleus (VPM) and the medial posterior nucleus (Pom). There are at least six pathways conveying whisker input from the trigeminal nuclei to the cerebral cortex (Fig. 4E). To some extent, these pathways convey different aspects of whisker sensation (Yu et al., 2006). The pathways that make synapses in VPM convey whisker input with short-latencies, while those via Pom have considerably longer latencies. VPM receives both single- and multiple-whisker input, Pom only multi-whisker input. An anatomical difference between VPM and Pom is that VPM, in contrast to Pom, contains barreloids, analogous to the barrelettes in the trigeminal nuclei and the barrels in wS1. The barreloids are prominent in the dorsomedial part of VPM (VPMdm), but fade away towards the ventrolateral part (VPMvl) (Van der Loos, 1976;Land et al., 1995;Haidarliu and Ahissar, 2001). As a consequence, VPMdm processes mainly single-whisker input and VPMvl multi-whisker input. Within a barreloid, the neurons are ordered according to their angular preference (Timofeeva et al., 2003).

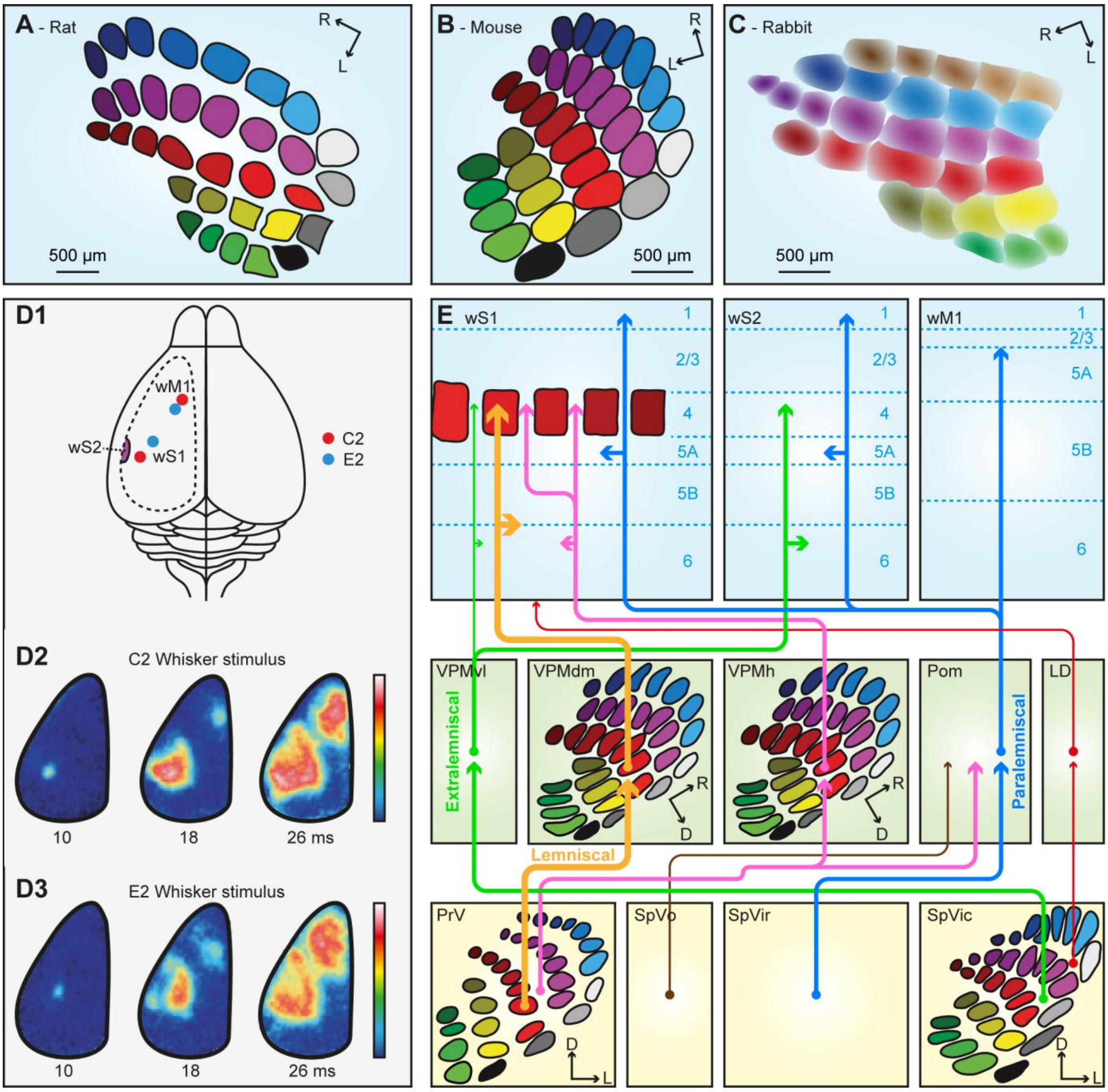
A - Rat
R
L
500 µm
B - Mouse
R
L
500 µm
C - Rabbit
R
L
500 µm
D1
wM1
wS2
wS1
C2
E2
D2
C2 Whisker stimulus
10
18
26 ms
D3
E2 Whisker stimulus
10
18
26 ms
E
wS1
1
2/3
4
5A
5B
6
wS2
1
2/3
4
5A
5B
6
wM1
1
2/3
5A
5B
6
VPMvl
VPMdm
VPMh
Pom
LD
Extralemniscal
Lemniscal
Paralemniscal
R
D
R
D
PrV
SpVo
SpVir
SpVic
D
L
D
L

***Figure 4 – The trigemino-thalamo-cortical pathways***
*Schematic drawingw of the organization of the barrels in layer 4 of a tangential slice of an adult rat (**A**), mouse (**B**) and rabbit (**C**). Note that the septa are prominent in rats but very small in mice. In adult rabbits, barrels are absent. Instead, the somatotopic representation of the vibrissae is more gradual. **D1** | Schematic drawing of a rat brain. The dotted line indicates the recording area for the panels D2 and D3. The red dots indicate the representations of the C2 whisker, and the blue dots those of the E2 whisker in wS1 and wM1. wS2 is partially visible on the extreme left of the recording area. **D2** | Voltage-sensitive dye images in urethane-anesthetized mice showing that stimulation of the contralateral C2 whisker initially evokes a very local signal in the C2 barrel of wS1. Consecutively, the signal spreads over the rest of wS1, and also to wM1, and to a lesser extent also to wS2. The time points indicate the time since the onset of whisker deflection, the scale bar the fluorescent signal (blue = weak, white = high). **D3** | Idem, but for the E2 whisker. Note that the early responses to the C2 and E2 whiskers are at different locations, but this difference is less obvious during later phases of the response. Panel D is reproduced with permission from Aronoff et al. (2010). **E** | Schematic representation of the trigemino-thalamo-cortical pathways discussed in the main text. The arrowheads indicate the termination areas of the axons. Note that (in the cerebral cortex) the postsynaptic cells may have their somata in other layers. The line thickness indicates the relative importance of the pathways. The barreloids in VPM are indicated in an oblique coronal slice, the barrelettes of the trigeminal nuclei in coronal slices. D = dorsal, L = lateral, LD = laterodorsal nucleus of the thalamus, Pom = medial posterior nucleus of the thalamus, PrV = primary trigeminal nucleus, R =*

*rostral, SpVic = caudal part of spinal trigeminal nucleus pars interpolaris, SpVio = oral part of SpVi, SpVo = spinal trigeminal nucleus pars oralis, VPMdm = dorsomedial part of the ventroposterior medial nucleus of the thalamus, VPMh = "head" area of VPM, VPMvl = ventrolateral part of VPM, wM1 = whisker motor cortex, wS1 = whisker part of primary sensorimotor cortex, wS2 = whisker part of secondary sensorimotor cortex.*

Of all trigemino-thalamo-cortical pathways, the lemniscal pathway is the only one that predominantly conveys single-whisker input. This disynaptic pathway links the barrelettes of PrV to the barrels of wS1 via the barreloids of VPMdm (Erzurumlu et al., 1980;Williams et al., 1994;Veinante and Deschênes, 1999). The main targets are the barrels of layer 4 in wS1, but there are also terminals in layers 5/6 of wS1 (Killackey, 1973;Koralek et al., 1988;Chmielowska et al., 1989;Lu and Lin, 1993;Bureau et al., 2006;Petreanu et al., 2009;Meyer et al., 2010a). The thalamic relay cells in the barreloids of VPMdm respond with precisely timed single action potentials to deflections of a single principle whisker at short latencies (4-8 ms) (Ito, 1988;Simons and Carvell, 1989;Armstrong-James and Callahan, 1991;Diamond et al., 1992b;Brecht and Sakmann, 2002b).

A second pathway synapsing in VPM is the extralemniscal pathway. In contrast to the lemniscal pathway, the extralemniscal pathway passes through VPMvl, where the barreloids are not as distinct as in VPMdm. The input of the extralemniscal pathway originates from the multi-whisker, interbarrelette cells of the caudal part of SpVi, and the output is targeted to layers 4 and 6 of wS2, as well as the septal columns of wS1 (Pierret et al., 2000).

The third pathway, the paralemniscal pathway, arises from the multi-whisker cells in the rostral part of SpVi (Erzurumlu and Killackey, 1980;Peschanski, 1984;Williams et al., 1994;Veinante et al., 2000a), contacts relay cells in Pom and targets wS1, wS2 and wM1. Pom axons terminate mainly throughout layers 5a and 1 of wS1 as well as in layer 4 of the septa (Koralek et al., 1988;Chmielowska et al., 1989;Lu and Lin, 1993;Bureau et al., 2006;Petreanu et al., 2009;Wimmer et al., 2010), where they also provide synaptic input to pyramidal neurons in layers 3 and 5a (Bureau et al., 2006;Petreanu et al., 2009;Meyer et al., 2010a). In addition, Pom terminals are found in wS2 and wM1(Carvell and Simons, 1987). From Pom, there are also projections to the striatum (Alloway et al., 2006), the perirhinal cortex and the insular cortex (Deschênes et al., 1998). Responses of relay cells in Pom to single-whisker deflections differ from those in VPM: in Pom, the receptive fields are larger, the latencies longer and more variable and the activity is under control of a strong cortical feedback (Diamond et al., 1992b;Ahissar et al., 2000). The variable and relatively long response latencies (19-27 ms) of Pom cells are likely caused by inhibitory inputs from the zona incerta gating peripheral inputs to Pom (Trageser and Keller, 2004).

In addition, there are at least three other trigemino-thalamo-cortical pathways. All of these convey multi-whisker information. The first arises from the interbarrelette cells of PrV, projects to Pom and to multi-whisker relay cells in the "heads" of the barreloids at the dorsomedial margin of VPM (VPMh) (Veinante and Deschênes, 1999;Urbain and Deschênes, 2007b). The head barreloid cells send axons to the septal columns of wS1 (Furuta et al., 2009). A second multi-whisker pathway involves projections from SpVi to the thalamic laterodorsal nucleus (LD), which projects mainly to the cingulate and retrosplenial cortex, and only sparsely to wS1 (Bezdudnaya and Keller, 2008). And finally, there is a relatively sparse and poorly characterized pathway originating from multi-whisker neurons in SpVo and projecting to caudal thalamic regions including the most posterior parts of VPM and Pom (Jacquin and Rhoades, 1990;Veinante et al., 2000a). These thalamic regions receive inputs from different sensory modalities and project to the perirhinal cortex, striatum and amygdala (Groenewegen and Witter, 2004).

Apart from being the relay station between the trigeminal nuclei and the cerebral cortex, the thalamus also contains intra-thalamic projections. As such the reticular nucleus

(RT) is involved in several negative feedback loops that modulate the flow of information through trigemino-thalamo-cortical pathways discussed above. RT forms a sheet of GABAergic neurons surrounding the thalamus and it contains a somatotopic body map with a large representation of the whiskers (Shosaku et al., 1984;Guillery and Harting, 2003;Pinault, 2004). Axons of VPM and Pom cells give off collaterals in RT (Crabtree et al., 1998;Lam and Sherman, 2011), while RT in turn provides strong inhibitory input to VPM and Pom (Pinault et al., 1995;Cox et al., 1997;Brecht and Sakmann, 2002b). The VPM-projections from RT cells are whisker-specific: they target the barreloid of their own principle whisker (Desilets-Roy et al., 2002). Since RT neurons adapt stronger to repeated, high-frequency stimulation than VPM neurons, strong whisker stimulation can lead to disinhibition of VPM neurons (Hartings et al., 2003;Ganmor et al., 2010). Furthermore, VPM cells can influence activity in Pom through intra-thalamic pathways involving RT (Crabtree et al., 1998). Additional indirect inhibitory feedback loops to Pom involve the zona incerta (see 4.7), which receives both peripheral and cortico-thalamic input and provides a significant portion of GABAergic synaptic terminals in Pom (Barthó et al., 2002;Bokor et al., 2005).

### 3.4 Primary somatosensory cortex (S1)

The whisker part of S1 (wS1) is of crucial importance for perception and processing of whisker input. For instance, wS1 is required for whisker-based object localization (O'Connor et al., 2010a), gap-crossing (Hutson and Masterton, 1986) and aperture width discrimination (Krupa et al., 2001). Direct stimulation of wS1 in rabbits can substitute for peripheral vibrissa stimulation (Leal-Campanario et al., 2006). This suggests that wS1 can form sensory percepts, but does not differentiate between peripheral and central stimulation (see also Huber et al. (2008)). Recent evidence indicates that wS1 also has a previously unanticipated role in motor control of whisker retraction (Matyas et al., 2010).

As all cortical areas, wS1 is composed of layers. Layer 4 is the main input layer, and in mice it is organized in patches (“barrels”) of neurons primarily receiving input from a single whisker (Fig. 4B) (Woolsey and Van der Loos, 1970). Within a mouse barrel, most neurons are found at the borders, leaving the barrel center relatively empty. In rats, a similar organization is found (Fig. 4A), but the barrel diameters are larger (~400 µm) than in mice (~280 µm), and the cells are equally distributed within the barrels (Welker and Woolsey, 1974). In mice, a single barrel column contains, distributed over all layers, ~6,500 neurons (C2 barrel; Lefort et al. (2009)), while the rat C2 barrel contains ~19,000 neurons (Meyer et al., 2010b). The barrels are strictly organized in a somatotopic pattern (Welker, 1971). In between the barrels are the septa, which mainly receive multi-whisker input (Brumberg et al., 1999;Furuta et al., 2009). The septa are larger in rats than in mice (Welker, 1971;Woolsey et al., 1975). Within the class of mammals, rats and mice are quite exceptional in having barrels in wS1. Barrels are only present in some rodents, as well as a few other species (Woolsey et al., 1975;Rice, 1985). In adult rabbits, for instance, barrels cannot be identified. Yet, also rabbits probably have a somatotopic representation of their vibrissae in S1, but the borders between the whisker receptive fields are fuzzier than in animals with barrels (Fig. 4C) (Woolsey et al., 1975;McMullen et al., 1994).

Throughout wS1, sensory-evoked responses are sparse and near-simultaneous, but the response probabilities are layer- and cell type-specific (Brecht and Sakmann, 2002a;Brecht et al., 2003;Manns et al., 2004;De Kock et al., 2007). In the barrel columns, spiking responses in excitatory neurons across all layers are largely restricted to deflections of the principle whisker, except for thick-tufted layer 5 pyramidal neurons (Welker, 1971;Simons, 1978;Manns et al., 2004;De Kock et al., 2007). Subthreshold synaptic responses, however, can also be triggered by the movement of several whiskers surrounding the principle whisker (Brecht and Sakmann, 2002a). Sensory evoked responses in layer 4 cells are brief due to the recruitment of powerful thalamocortical feedforward inhibition (Swadlow, 2002;Gabernet et al., 2005;Sun et al., 2006;Cruikshank et al., 2007). Angular tuning domains have been observed within individual barrels (Bruno et al., 2003), although their existence in layer 2/3 is debated (Andermann and Moore, 2006;Kerr et al., 2007). During free whisking, neurons across all layers respond to active touch (Curtis and Kleinfeld, 2009;O'Connor et al., 2010b;Crochet et al., 2011) and to slip-stick motion events (Fig. 1C) (Jadhav et al., 2009). Sensory evoked activity patterns in wS1 correlate well with psychophysical performance in whisker-dependent tactile discrimination tasks (Krupa et al., 2004;von Heimendahl et al., 2007;Stüttgen and Schwarz, 2008;O'Connor et al., 2010b). The activity of wS1 neurons encodes the spatial location of the whiskers over time (Fee et al., 1997;Crochet and Petersen, 2006;De Kock and Sakmann, 2009). This is also true for GABAergic interneurons (Gentet et al., 2010). Such a reference signal is required for decoding horizontal object position (Diamond et al., 2008), for example by neurons in wS1 for which phase in the whisk cycle gates the response to touch (Curtis and Kleinfeld, 2009).

In comparison to responses in the barrel columns, those in the septal columns are less whisker-specific. The barrel and septal columns have been proposed to represent two partially segregated circuits that process different aspects of whisker movements (Kim and Ebner, 1999;Shepherd and Svoboda, 2005;Alloway, 2008). However, the segregation between barrels and septa, while prominent in rats, is not so clear in other species, like mice which have only very thin septa (cf. Bureau et al. (2006)).

The microcircuit of wS1 has been extensively characterized, yielding increasingly detailed connectivity schemes (Lübke and Feldmeyer, 2007;Schubert et al., 2007;Lefort et al., 2009;Petreanu et al., 2009). Layer 4 barrel neurons, which are the main recipients of the lemniscal pathway, project to all layers within their own barrel column, but most prominently to other layer 4 cells as well as layer 2/3 pyramidal cells (Kim and Ebner, 1999;Lübke et al., 2000;Petersen and Sakmann, 2000;Schubert et al., 2001;Feldmeyer et al., 2002;Feldmeyer et al., 2005;Shepherd and Svoboda, 2005;Lefort et al., 2009). Layer 2/3 pyramidal cells project both within their own barrel column as well as over long distances across barrel columns (Lübke and Feldmeyer, 2007). They contact cells within all layers except layer 4, with a particularly strong connection to other layer 2/3 pyramidal neurons and to thick-tufted layer 5b pyramidal cells (Reyes and Sakmann, 1999;Schubert et al., 2001;Lefort et al., 2009;Petreanu et al., 2009). Layer 5a neurons, which are the main recipients of the paralemniscal pathway, project strongly within their own barrel column to other pyramidal cells across layer 5 (Lefort et al., 2009), and to layer 2 cells distributed across multiple columns and preferentially located above the septa (in rats, but not in mice) (Shepherd and Svoboda, 2005;Bureau et al., 2006). Layer 2 neurons receive additional inputs from layer 3 neurons located above barrels (Bureau et al., 2006), providing one of several possible points of convergence for the lemniscal and paralemniscal pathways (Lübke and Feldmeyer, 2007). Inhibitory input to excitatory neurons is derived from cells within the same cortical layer as well as from cells from other cortical layers (Helmstaedter et al., 2009;Kätzel et al., 2011). In addition to the aforementioned intracolumnar connections within wS1, intracortical projections extend throughout much of wS1 and its dysgranular zone (Chapin et al., 1987;Hoeflinger et al., 1995;Kim and Ebner, 1999;Aronoff et al., 2010).

wS1 forms reciprocal connections with several other cortical areas, including the whisker part of the secondary somatosensory cortex (wS2), wM1, insular cortex and perirhinal cortex (White and DeAmicis, 1977;Welker et al., 1988;Fabri and Burton, 1991;Cauller et al., 1998;Aronoff et al., 2010). The contralateral wS1 is targeted via callosal projections (Larsen et al., 2007;Petreanu et al., 2007). Axonal projections to wS2 originate from the infragranular and supragranular layers of wS1 and arborize across all layers in wS2 (Welker et al., 1988;Fabri and Burton, 1991;Cauller et al., 1998;Chakrabarti and Alloway, 2006;Aronoff et al., 2010). The wS1 to wM1 projection is somatotopically arranged such that a column in wS1 connects to a column of the same whisker in wM1 (Izraeli and Porter, 1995;Hoffer et al., 2003;Ferezou et al., 2007). Layer 2/3 pyramidal cells of wS1 densely innervate layers 5/6 of wM1, while those of layers 5/6 preferentially innervate layers 1 and 2/3 in wM1 (Porter and White, 1983;Miyashita et al., 1994;Aronoff et al., 2010). The majority of connections to wM1 arises from neurons located in septal columns (Crandall et al., 1986;Alloway et al., 2004;Chakrabarti et al., 2008). The reciprocal projection, from wM1 to wS1, innervates mainly layers 5/6 and 1 (Cauller et al., 1998;Veinante and Deschênes, 2003;Matyas et al., 2010).

Cortico-thalamic projections originate in layer 5/6 and target relay cells in VPM and Pom, as well as GABAergic neurons in RT (Hoogland et al., 1987;Welker et al., 1988;Chmielowska et al., 1989;Bourassa et al., 1995;Deschênes et al., 1998;Veinante et al., 2000b;Killackey and Sherman, 2003). The projections to VPM originate from layer 6a pyramidal neurons (located below both the barrels and the septa) and target the barreloid of the corresponding principal whisker as well as those of several whiskers located within the same arc (Hoogland et al., 1987;Bourassa et al., 1995). VPMvl, which is the thalamic relay station for the extralemniscal pathway, receives cortical input from layer 6 pyramidal cells, both from wS1 and from wS2 (Bokor et al., 2008). The heads of the barreloids in VPM, which participate in a multi-whisker lemniscal pathway, receive collaterals from layer 6b pyramidal cells projecting to Pom (Bourassa et al., 1995;Deschênes et al., 1998). The relay cells of Pom also receive input from layer 6a pyramidal cells (located below the septa) and layer 5b tall-tufted pyramidal cells (located below both the barrels and the septa), whose axons form large and powerful synapses that can drive Pom neurons (Hoogland et al., 1991;Killackey and Sherman, 2003;Larsen et al., 2007;Groh et al., 2008). These relay cells project to wS2, forming a cortico-thalamo-cortical pathway (Theyel et al., 2010). Layer 5b neurons also project to the zona incerta (Bourassa et al., 1995;Mitrofanis and Mikuletic, 1999;Veinante et al., 2000b;Barthó et al., 2007), which is involved in state-dependent suppression of whisker sensory responses in Pom (see 4.7.2). RT cells are innervated by collaterals of cortico-thalamic axons from layer 6 cells, but not layer 5 cells (Bourassa et al., 1995), which strongly activate RT cells and evoke disynaptic inhibition in thalamo-cortical relay cells (Cruikshank et al., 2010;Lam and Sherman, 2010). Other projections of wS1 include projections from layer 5a pyramidal cells to the striatum (see 4.3) and from layer 5b pyramidal cells to the anterior pretectal nucleus (Aronoff et al., 2010), the superior colliculus (see 4.4), the red nucleus (see 4.7.3), the pontine nuclei (see 4.5.1) and the sensory trigeminal nuclei (see 3.2).

### 3.5. Secondary somatosensory cortex (S2)

S2 contains a highly organized somatotopic representation of the whiskers (wS2) located in the parietal cortex, lateral to wS1 (Carvell and Simons, 1986;Koralek et al., 1990;Fabri and Burton, 1991;Hoffer et al., 2003;Benison et al., 2007). The whisker receptive fields in wS2 are larger than in wS1; wS2 neurons generally respond equally well to several adjacent whiskers (Welker and Sinha, 1972;Carvell and Simons, 1986;Kwegyir-Afful and Keller, 2004). Responses in wS2 to single whisker deflections are weaker than those in wS1, but they display stronger direction selectivity, while the onset latencies are comparable (Kwegyir-Afful and Keller, 2004). The local connections within wS2 are similar to those within wS1. However, in contrast to wS1, the projections from layer 2/3 to layer 5 are stronger than those from layer 4 to layer 3 (Hooks et al., 2011). Furthermore, the reciprocal connections between layers 5 and 6, which are weak in wS1, are more pronounced in wS2 (Hooks et al., 2011). Whisker input reaches wS2 via the extralemniscal pathway through VPMvl (Pierret et al., 2000;Bokor et al., 2008), but also via Pom (Carvell and Simons, 1987;Spreafico et al., 1987;Alloway et al., 2000;Theyel et al., 2010) and from both the barrel and septal columns of wS1 (Kim and Ebner, 1999;Chakrabarti and Alloway, 2006). The connections between wS1 and wS2 are reciprocal (Carvell and Simons, 1987;Aronoff et al., 2010). In addition, there are reciprocal connections between wS2 and wM1 (Porter and White, 1983;Miyashita et al., 1994). wS2 also receives cholinergic input from the nucleus basalis magnocellularis (Deurveilher and Semba, 2011). Finally, there are projections from wS2 to the striatum (see 4.3) and the pontine nuclei (see 4.5.1).

## 4. Whisker motor control

Rhythmic whisker movements increase the acuity of the whisker system (Szwed et al., 2003;Knutsen et al., 2006). Whisker movements are generated in the facial nucleus, whose activity is affected by a large number of brain regions. It has been proposed that higher-order areas can initiate movement, but that the rhythmicity of the whiskers is caused by a brainstem central pattern generator (see 6.2).

### 4.1. Facial nucleus

The motor neurons of both the intrinsic and the extrinsic muscles of the whisker pad are located in the lateral facial nucleus (Ashwell, 1982;Klein and Rhoades, 1985;Herfst and Brecht, 2008). Of the lateral facial nucleus neurons that evoke whisker movements, about 80% induce the protraction of a single whisker and about 20% the retraction of multiple whiskers (Herfst and Brecht, 2008). Each intrinsic capsular muscle has about 25-50 motoneurons in the lateral facial nucleus (Klein and Rhoades, 1985). The motor commands are forwarded to the whisker muscles via the facial nerve (Fig. 2A) (Dörfl, 1985;Haidarliu et al., 2010). In addition, there is sparse innervation of the extrinsic muscles by the hypoglossal nucleus via the infraorbital branch of the trigeminal nerve (Mameli et al., 2008).

Single motor neurons in the lateral facial nucleus evoke fast, short and stereotypic whisker movements, whereas single neurons in wM1 evoke slow, small and long-lasting rhythmic movements (Brecht et al., 2004b;Herfst and Brecht, 2008). This discrepancy makes it unlikely that wM1 directly commands activity of the lateral facial nucleus, despite the possible existence of a sparse monosynaptic projection from wM1 to the contralateral lateral facial nucleus (Grinevich et al., 2005). Instead, wM1 may induce rhythmic whisker movements via oligosynaptic pathways to the lateral facial nucleus. Remarkably, rhythmic whisker movements persist in the absence of wM1 (Welker, 1964;Semba and Komisaruk, 1984;Gao et al., 2003). Hence, it has been proposed that wM1 projects to a central pattern generator (CPG) in the brainstem, possibly the dorsal raphe nucleus, that in turn activates the lateral facial nucleus (Hattox et al., 2003) (see 6.2). In addition, the lateral facial nucleus receives input from several other subcortical structures, all of which are directly or indirectly innervated by wM1. These afferent regions include the ipsilateral sensory trigeminal nuclei (Nguyen and Kleinfeld, 2005), the ipsilateral pontomedullary reticular formation (RF) (Zerari-Mailly et al., 2001) and the contralateral superior colliculus (Miyashita and Mori, 1995;Hattox et al., 2002). In addition, the lateral facial nucleus is targeted by cholinergic, histaminergic and noradrenergic connections, which may set the overall activity level of the whisker movements (see section 6). Altogether, there is a strong convergence of inputs at the level of the lateral facial nucleus, allowing the integration of whisker movements and other forms of behavior.

## 4.2. Cerebral cortex

### 4.2.1. Primary motor cortex (M1)

The primary motor cortex (M1) is a large area in the frontal cortex involved in movement. M1 has an agranular appearance, low stimulation thresholds for evoking movements, and a topographic and complete representation of the body muscles (Gioanni and Lamarche, 1985;Brecht et al., 2004a). M1 can be divided into the agranular medial field (AGm), the agranular lateral field (AGl) and the cingulate area (Cg1). The topographic representation of whiskers is almost exclusively located in AGm (Brecht et al., 2004a). Sensory input from the whiskers to whisker M1 (wM1) comes predominantly from wS1 (Armstrong-James and Fox, 1987), but also directly from Pom (Deschênes et al., 1998). The latencies to whisker stimulation are 10-20 ms longer in wM1 than in wS1 (Fig. 4D) (Ferezou et al., 2007). Microstimulation of wM1 can generate whisker motion that strongly resembles natural exploratory whisking (Berg and Kleinfeld, 2003b;Brecht et al., 2004b;Haiss and Schwarz, 2005;Matyas et al., 2010). During a training paradigm, mice can learn to protract their whiskers following an auditory conditioned stimulus (Troncoso et al., 2004). Such associative learning probably involves synaptic plasticity of layer 5 pyramidal cells in wM1 (Troncoso et al., 2007). This suggests that whisker movements are subject to change following long-term synaptic plasticity in wM1. Although complete ablation of wM1 does not abolish whisking, it does disrupt whisking kinematics, coordination, and temporal organization such as whisking synchrony (Gao et al., 2003). There are several indirect routes from wM1 to the lateral facial nucleus, for example via the superior colliculus (see 4.4) or the pontomedullary reticular formation (see 4.7.1) and wS1 (see 4.2.2). In addition, wM1 is involved in several feedback loops, including reciprocal connections with wS1 (Aronoff et al., 2010), thalamus (Cicirata et al., 1986;Colechio and Alloway, 2009) and loops involving the basal ganglia (see 4.3), the cerebellum (see 4.5) and the claustrum (see 5). Finally, wM1 projects to the deep mesencephalic nucleus, the periaqueductal gray and the red nucleus (Alloway et al., 2010). This network of inputs and outputs enables wM1 to adjust whisker movements both to sensory input and to the general behavior.

The output of wM1 is not uniform. Layer 5 pyramidal cells project to cells around the facial nucleus while those of layer 6 project to the thalamus. Evidence for strong myelinization and an expanded layer 5 in AGm points to the possible contribution to high speed whisking (Brecht et al., 2004b). Layer 5 output may correspond with timing of individual whisking movements and may be able to reset these rhythms, while layer 6 output may correspond with grouping of multiple whisking movement bursts where action potential frequency determines movement direction and amplitude (Brecht et al., 2004b).

### 4.2.2. Somatosensory cortex as a premotor area

Microstimulation of wM1 can induce both whisker protraction and retraction depending on the location of stimulation in wM1 (Gioanni and Lamarche, 1985;Haiss and Schwarz, 2005;Matyas et al., 2010). A recent study found that stimulation of wS1 induces whisker retraction at shorter latencies than wM1 stimulation. In fact, the wM1-induced whisker retraction can be mediated by synaptic activation in wS1 (Matyas et al., 2010). Contrary to stimulation of wM1, stimulation of wS1 does not evoke whisker protraction (Matyas et al., 2010). In the same study, the authors suggest that wS1 exerts its effect on whisker movement by a disynaptic pathway via SpV to the facial nucleus. Thus, wM1 and wS1 could together form an additional source of rhythmic whisker movements, alongside the putative brainstem pattern generators (see 6.2). Such an organization is in line with the idea that wM1 specifies motor programs rather than simple muscle activity (Brecht et al., 2004b).

### 4.3. Basal ganglia

The first somatosensory feedback system to be discussed involves the basal ganglia, which are important for a wide variety of (sensori-)motor functions. In the oculomotor system, the basal ganglia have been associated with orienting saccadic eye movements based on reward expectancy (Hikosaka et al., 2006). A similar function for the whisker system could very well be possible. The basal ganglia are a heterogeneous group of brain regions, whose main components are the striatum, the globus pallidus (GP), the substantia nigra (SN) and the subthalamic nucleus (STN). The GP consists of two parts: an external (GPe) and an internal part (GPi). In rodents, GPi is commonly referred to as the entopeduncular nucleus (EPN) (Nambu, 2007). SN is composed of a pars compacta (SNc) and a pars reticulata (SNr). In general, the information from the cerebral cortex enters the striatum, is forwarded to other parts of the basal ganglia and the output to the thalamus and superior colliculus is eventually generated by EPN and SNr (Fig. 5A).

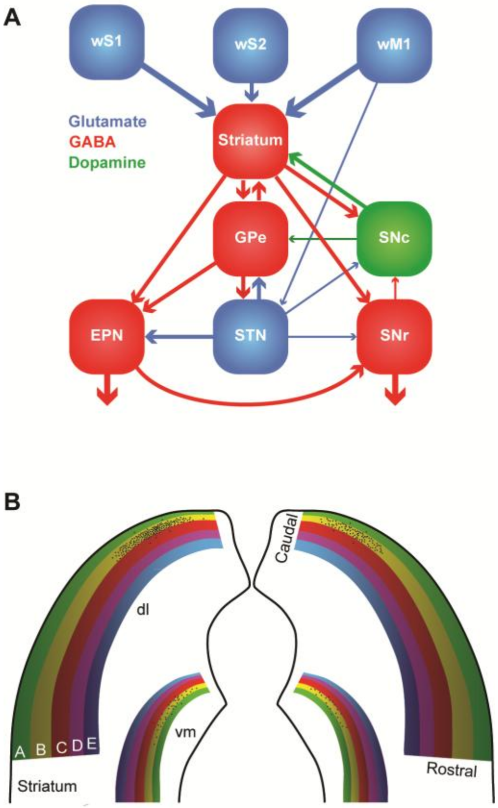

***Figure 5 – The basal ganglia***
***A** | The major connections between the components of the basal ganglia. Most of the input comes from the cerebral cortex (in this case: wS1, wS2 and wM1), and is directed to the striatum. GABAergic medium-spiny neurons of the striatum project to the external part of the globus pallidus (GPe), the entopeduncular nucleus (EPN) and the reticular (SNr) and compact (SNc) parts of the substantia nigra. SNc provides dopaminergic input to the striatum, and the subthalamic nucleus (STN) glutamatergic input to GPe, EPN and SNr. The main output of the basal ganglia is directed to the thalamus, via GPe and SNr, and the superior colliculus, via SNr. The line thickness indicates the relative importance for the whisker system. **B** | Whisker responses in the dorsolateral (dl) striatum follow a loose somatotopy, which is mainly organized according to whisker rows. The black dots indicate schematically the projections of the layer 5 pyramidal cells in the B2 barrel of left wS1. The projection is mainly, but not exclusively, ipsilateral, and largely within the “B row” area in the striatum. There is considerable overlap, however, with the projection areas of other B row whiskers. “Rostral” and “caudal” refer to the positions of the whiskers on the mystacial pad. A smaller and less characterized projection area is also present in the ventromedial (vm) striatum.*

The striatum, or “neostriatum”, is a single area in rodents, but in higher mammals it is composed of two nuclei: the caudate and the putamen (Tepper et al., 2007). Based on function and connectivity, the striatum can be divided into a dorsolateral and a ventromedial part (Voorn et al., 2004). The striatum is involved in the acquisition of habits, goal-directed behaviors and in the motivation to perform. The whisker receptive fields of the dorsolateral striatum are organized in a loosely somatotopic manner: dorsal whiskers project laterally and caudal whiskers project dorsally (Fig. 5B) (Alloway et al., 1999;Wright et al., 1999). There is much overlap between the projection areas of whiskers from a single row, but hardly any from whiskers in different rows. There is also a weaker whisker representation in the ventromedial striatum (Alloway et al., 1999;Wright et al., 1999). The cortico-striatal projections are predominantly ipsilateral and originate from layer 5 pyramidal cells in both barrels and septa

(Alloway et al., 2006). Thus, cortico-striatal projections serve to integrate rather than segregate input from different whiskers. In addition, the striatum receives input from wS2, wM1 and other cortical areas, including motor, cognitive and other sensory areas (Wright et al., 2001;Alloway et al., 2006;Tepper et al., 2007). Hence, the striatum can integrate the whiskers and general behavior.

Apart from the extensive input from the cerebral cortex, the striatum also receives direct input from the thalamus. The thalamo-striatal connections originate mainly in the intralaminar nuclei of the thalamus (Smith et al., 2004;Tepper et al., 2007) and in Pom (Alloway et al., 2006). During whisker stimulation at low frequencies, the responses of the medium spiny neurons in the dorsolateral striatum are approximately 5 ms later than in wS1 (Mowery et al., 2011;Pidoux et al., 2011;Syed et al., 2011). However, during repeated whisker stimulation at 5-8 Hz, striatal responses actually preceded those in wS1 (Mowery et al., 2011). In addition, the striatal responses showed less adaptation to repeated whisker stimulation as responses in wS1 (Mowery et al., 2011). The latter findings support an important role for the direct thalamo-striatal pathway, in addition to the well-established thalamo-cortico-striatal route. The thalamo-striatal pathway conveying whisker information originates mainly in Pom (Alloway et al., 2006). Relay cells in Pom are inhibited during rest and become disinhibited during periods of activity (see 4.7.2 and 4.7.3). Although the disinhibition of Pom has been predominantly linked to active whisking (Bokor et al., 2005;Lavallée et al., 2005;Urbain and Deschênes, 2007a), it might also be evoked by repeated, passive whisker input. Other inputs to the striatum come from the amygdala (Kelley et al., 1982;Popescu et al., 2009), the dorsal raphe nuclei (Di Matteo et al., 2008), GP and SN (Tepper et al., 2007). The main output of the striatum is composed of GABAergic projections to GP and SN.

The GABAergic output of the striatum is the dominant input to SNc, but SNc also receives GABAergic input from SNr and glutamatergic input from the amygdala, and to a lesser extent also from STN (Kita and Kitai, 1987;Gonzales and Chesselet, 1990;Misgeld, 2004). SNc also receives histaminergic input from the tuberomammillary nuclei (Lee et al., 2008b). SNc forms dopaminergic connections to the striatum and is implicated in the reward system (Hikosaka et al., 2006;Redgrave et al., 2008). Its degeneration is an important cause of the motor problems associated with Parkinson’s disease (Gibb and Lees, 1988;Esposito et al., 2007). SNr receives GABAergic input from the striatum and, to a lesser extent also glutamatergic input from STN and the cerebral cortex (Kita and Kitai, 1987;Naito and Kita, 1994;Tepper et al., 2007). SNr sends GABAergic projections to the ventromedial thalamus and the superior colliculus (Beckstead et al., 1979;Di Chiara et al., 1979;Grofova et al., 1982). Activation of the nociceptin/orphanin FQ (N/OFQ) receptors in SNr modulates whisker motor output (Marti et al., 2009).

GPe receives GABAergic input from the striatum and glutamatergic input from STN. Sparse innervation comes from the cerebral cortex, the intralaminar nuclei of the thalamus, SNc, the dorsal raphe nuclei and the pedunculopontine tegmental nuclei (Kita, 2007). The main output areas of GPe are EPN, STN and the striatum (Kita, 2007). EPN receives GABAergic input from GPe and the striatum, and glutamatergic input from STN (Nambu, 2007). In turn, EPN projects to the ventrolateral thalamic nucleus (VL) (Nambu, 2007). To our knowledge, no systematic study of the role of GP in the rodent whisker system has been undertaken. However, GP neurons in cats show responses to vibrissal stimulation, whereby the response depends on the direction of vibrissal movement (Schneider et al., 1982).

The lateral half of STN shows responses to contralateral whisker stimulation. Interestingly, each neuron that responds to contralateral whisker stimulation, also responds to somatosensory stimulation of another area, e.g. forepaw or ipsilateral whisker stimulation (Hammond et al., 1978). This is in line with the putative role of the basal ganglia in bringing different behavioral aspects together. STN receives input from the cerebral cortex, predominantly wM1, and GPe, and projects to GPe, EPN and SNr (Kita and Kitai, 1987;Joel and Weiner, 1997).

### 4.4. Superior colliculus

The second sensorimotor feedback system involves the superior colliculus (SC), which is also known as the "tectum". The upper layers of SC process sensory information, the intermediate layers sensorimotor information, and the lower layers motor information. SC receives sensory input via direct connections from all four parts of the sensory trigeminal nuclei (Steindler, 1985;Cohen et al., 2008), and provides a direct output to the facial nucleus. However, the SC neurons that receive trigeminal input are not the same as those that innervate the facial nucleus (Hemelt and Keller, 2008). Hence, SC does not function as a simple, "reflexive" relay station between the trigeminal nuclei and the facial nucleus. Similarly, the input to SC from wM1 is also not directly relayed to the facial nucleus, since microstimulation of wM1 and SC show qualitatively and quantitatively different whisker responses (Hemelt and Keller, 2008). Instead, the main function of SC for the whisker system may be closely related to its best known function, which is to control saccadic eye movements and direct the gaze direction towards an interesting visual cue (Boehnke and Munoz, 2008;Gandhi and Katnani, 2011). SC can direct all mobile senses towards an object of interest. Microstimulation at a single spot in the intermediate or deep layers of SC can induce coherent movements of the eyes, the auricles and the whiskers together (McHaffie and Stein, 1982). While microstimulation within wM1 induces rhythmic whisker movements (Brecht et al., 2004b;Matyas et al., 2010), microstimulation in SC causes sustained whisker protraction (Hemelt and Keller, 2008), which is in accordance with its putative function in the direction of the whiskers. In addition, SC also responds to whisker input. Passive touch (air puff) as well as whisking in air and active touch (surface contact during whisking) evoked SC neuronal responses which were subject to strong adaptation. Passive and active touch evoked stronger responses than whisking in air. As a consequence, whisking in air at 10 Hz hardly evokes any response in SC, but active touch does (Bezdudnaya and Castro-Alamancos, 2011). SC responses can have different latencies. Fast responses (<10 ms) are probably due to the direct trigemino-tectal input and slow responses are likely mediated by wS1 (Bezdudnaya and Castro-Alamancos, 2011).

SC receives strong input from ipsilateral wM1 (Miyashita et al., 1994;Alloway et al., 2010), wS1 (Wise and Jones, 1977;Cohen et al., 2008;Aronoff et al., 2010) and the cerebellar nuclei, mainly the dentate and interpositus nucleus, and to a lesser extent also from the fastigial nucleus (May, 2006). Other inputs come, as mentioned before, from the trigeminal nuclei (Steindler, 1985;Cohen et al., 2008), and also from the zona incerta, which supplies both glutamatergic and GABAergic efferents (Beitz, 1989;Kim et al., 1992), from SNr (Beckstead et al., 1979;Kaneda et al., 2008) as well as from the visual cortex (Boehnke and Munoz, 2008). There is also input from the thalamus, but this seems to relate more to the visual than to the whisker system (Cosenza and Moore, 1984;Taylor and Lieberman, 1987). SC projects to the lateral facial nucleus. This connection is mainly ipsilateral, but there are distinct patches of neurons within SC that project to the contralateral lateral facial nucleus (Hemelt and Keller, 2008). SC also projects to the contralateral nucleus reticularis tegmenti pontis (NRTP) (Westby et al., 1993;May, 2006), which provides mossy fiber input to the cerebellar cortex and cerebellar nuclei (Mihailoff, 1993). There is also a projection from SC to the contralateral medial accessory olive (Huerta et al., 1983;May, 2006), which is a source of climbing fibers to the cerebellar cortex. Thus, there are two disynaptic pathways from SC to the cerebellar cortex, which projects back to SC via the cerebellar nuclei.

### 4.5. The cerebellar system

The third somatosensory feedback system is that of the cerebellum, which receives most of its mossy fiber afferents from the pons and all its climbing fiber afferents from the inferior olive (Fig. 6).

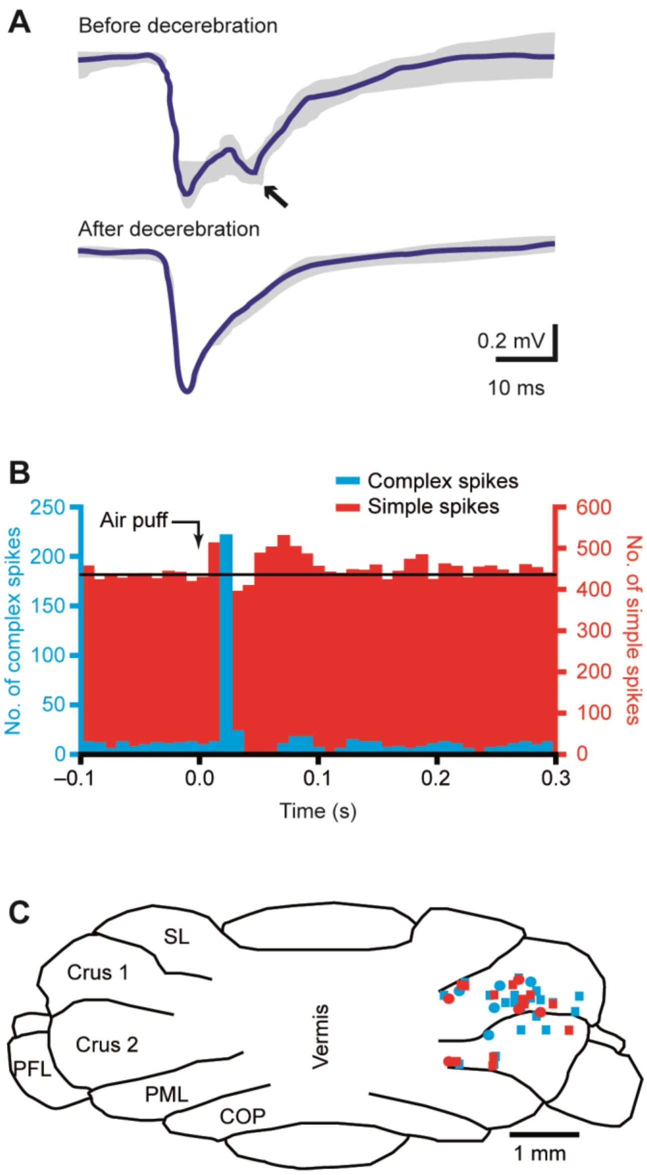

***Figure 6 – The cerebellum***
***A** | Tactile stimulation of the upper lip evokes a bi-phasic response in the cerebellar cortex, as measured with field potential recordings in the granule cell layer in crus 2 of adult rats. Complete midcollicular decerebration abolished the late phase response, indicating that the late phase response (arrow) is induced by the cerebral cortex, while the early phase is not. Schematic drawing based on Morisette and Bower (1996). **B** | Peri-stimulus time histograms of complex spike (blue) and simple spike (red) responses to ipsilateral air puff stimulation of the whiskers in a Purkinje cell in crus 1 of an awake mouse. The complex spike response is uni-phasic, while clear early and late phase simple spike responses can be observed. Reproduced with permission from Bosman et al. (2010). **C** | Cross section of the cerebellar cortex, showing the locations were Purkinje cell responses to ipsilateral stimulation of whisker from the C row were observed in crus 1 and crus 2. COP = copula pyramidis, PFL = paraflocculus, PML = paramedian lobule, SL = simple lobule. Modified with permission from Bosman et al. (2010).*

### 4.5.1. The pontine nucleus and the nucleus reticularis tegmenti pontis

The pontine nucleus (or “basal pons”) forms the main gateway to the cerebellum for efferents from the cerebral cortex. The main input to the pontine nucleus comes from layer 5 neurons throughout the entire ipsilateral cerebral cortex, and the efferents all go to the cerebellum (Legg et al., 1989;Brodal and Bjaalie, 1992). Cerebral cortical inputs are mapped multiply and in different combinations to the pontine nucleus (Schwarz and Möck, 2001;Leergaard et al., 2004;Leergaard et al., 2006). In general, cortico-pontine projections from different cortical regions do not overlap. This seems to hold true also for the barrels of wS1, implying that the pontine nucleus may receive single-whisker input (Schwarz and Möck, 2001). Nevertheless, the whisker-related parts of wS1, wS2 and wM1, sometimes project to adjacent, or even partially overlapping regions (Leergaard et al., 2004). Thus, the somatotopy in the pontine nucleus is somewhat intermediate between the continuous somatotopy of the cerebral cortex and the fractured somatotopy of the cerebellum.

The pontine nucleus sends bilateral (but mainly contralateral) mossy fiber connections to the cerebellar cortex, which give off collaterals to the cerebellar nuclei (Eller and Chan-

Palay, 1976;Parenti et al., 2002;Leergaard et al., 2006). The cerebellar cortex also projects to the cerebellar nuclei. This feedback loop is completed by afferents from the cerebellar nuclei back to the pontine nucleus (De Zeeuw et al., 2011;Ruigrok, in press). In addition to the input from the cerebral cortex, which is the dominant input, and of the cerebellar nuclei, the pontine nucleus also receives inputs from dozens of other brain regions (Mihailoff et al., 1989). The functional relevance of these other inputs is not very clear, and their specific functions for the whisker system are currently unknown. The inputs that could be of importance for the whisker system include projections from the sensory trigeminal nuclei (mainly SpVi) (Swenson et al., 1984;Mihailoff et al., 1989), SC (Burne et al., 1981;Mihailoff et al., 1989), the zona incerta (Ricardo, 1981;Mihailoff, 1995), the dorsal raphe nuclei (Mihailoff et al., 1989), the pedunculopontine tegmental nucleus (Mihailoff et al., 1989) and the tuberomammillary nuclei (Pillot et al., 2002). Recently, a direct connection from STN to the pontine nuclei has been described in cebus monkeys (Bostan et al., 2010). This could underlie a direct coupling between the basal ganglia and the cerebellar system.

Immediately dorsal of the pontine nucleus is the nucleus reticularis tegmenti pontis (NRTP). The main input to NRTP comes from the cerebellar nuclei (Torigoe et al., 1986b;Brodal and Bjaalie, 1992). Other inputs come from SC and the pontomedullary reticular formation (Torigoe et al., 1986b). NRTP also receives input from layer 5 pyramidal cells of the cerebral cortex, mainly bilaterally from the cingulate cortex and to a lesser extent also ipsilaterally from motor areas (Brodal, 1980;Torigoe et al., 1986a). NRTP projects, amongst others, ipsilaterally to the cerebellar cortex and the cerebellar nuclei (Mihailoff, 1993;Parenti et al., 2002) and bilaterally to the lateral facial nucleus (Isokawa-Akesson and Komisaruk, 1987;Hattox et al., 2002). Hence, NRTP may be a relay station between the cerebellar nuclei and the lateral facial nucleus, but whether it has a role in the whisker system is not clear yet.

#### 4.5.2. Cerebellum and inferior olive

The cerebellum has a central role in sensorimotor integration and motor learning (Ito, 2000;De Zeeuw and Yeo, 2005;Krakauer and Shadmehr, 2006). It receives sensory input from the whiskers (Fig. 6B) (Axelrad and Crepel, 1977;Brown and Bower, 2001;Loewenstein et al., 2005;Bosman et al., 2010;Chu et al., 2011) and its activity can affect whisker movements (Esakov and Pronichev, 2001;Lang et al., 2006). The cerebellar cortex has two afferent pathways, the climbing fiber and mossy fiber/parallel fiber pathway, that converge on the cerebellar Purkinje cells, which form the sole efferent projection to the cerebellar and vestibular nuclei (De Zeeuw et al., 2011).

Each adult Purkinje cell is innervated by a single climbing fiber only, with the climbing fiber-to-Purkinje cells synapse being extraordinarily strong (Eccles et al., 1964;Bosman et al., 2008;Davie et al., 2008). Thus, climbing fiber activity reliably evokes postsynaptic spikes, which are, due to their complex waveforms, called “complex spikes” (Davie et al., 2008;De Zeeuw et al., 2011). Climbing fibers originate exclusively from the contralateral inferior olive (IO). The IO comprises three main nuclei, all of which receive input from SpV, but not from PrV (Molinari et al., 1996;Yatim et al., 1996). Trigemino-olivary connections originate from all three compartments of SpV and target mainly the contralateral rostromedial part of the dorsal accessory olive (DAO) and the adjacent dorsal leaf of the principal olive (PO), and to a lesser extent the ventral leaf of the PO and the caudal part of the medial accessory olive (MAO) (Huerta et al., 1983;Molinari et al., 1996;Yatim et al., 1996). Ipsilateral trigemino-olivary projections mirror the contralateral ones, but are relatively sparse (Molinari et al., 1996;Yatim et al., 1996). Altogether, most IO neurons react to somatosensory input (Gellman et al., 1985;Gibson et al., 2004). The IO also receives input from many other regions. These include direct and indirect spinal projections (Miskolczy, 1931;Swenson and Castro, 1983), as well as projections from SC (Akaike, 1992), the zona incerta (Brown et al., 1977), the raphe nuclei (Brown et al., 1977) and the ipsilateral cerebral cortex, both from somatosensory and motor areas (Swenson et al., 1989). As a consequence, Purkinje cells fire complex spikes in response to stimulation of wM1 (Lang, 2002;Lang et al., 2006).

The subnuclei of the IO project to specific parasagittal zones of the cerebellar cortex (Voogd and Glickstein, 1998;Apps and Hawkes, 2009). The IO area with the strongest trigeminal input, the rostromedial DAO and dorsal PO, projects to the C3 and D zones, while the other areas project mainly to the A zones (Yatim et al., 1996;Apps and Hawkes, 2009). Indeed, most Purkinje cells showing complex spike responses to whisker stimulation were found in the C3 and D zones in lobule crus 1, and to a lesser extent also in crus 2 (Fig. 6C) (Bosman et al., 2010). Climbing fiber responses have also been found in the A zones of lobule VII (Thomson et al., 1989). In lobule IX, mossy fiber whisker responses have been reported, but climbing fiber responses were not evaluated (Joseph et al., 1978).

Climbing fiber input to the cerebellar cortex does not follow a somatotopic organization on single whisker level. For most Purkinje cells, the receptive field of the climbing fiber input is restricted to a single whisker, where nearby Purkinje cells may receive inputs from totally unrelated whiskers (Axelrad and Crepel, 1977;Bosman et al., 2010). In the rare cases where a Purkinje cell received input from multiple whiskers, these whiskers were located within the same row (Bosman et al., 2010). Complex spike responses to whisker stimulation are relatively sparse, encoding typically about 10% of the stimuli in responsive Purkinje cells, show a large jitter in the latencies and depend on the direction of whisker movement (Thomson et al., 1989;Bosman et al., 2010).

Mossy fibers terminate at the cerebellar granule cells, whose axons form the parallel fibers, that run transversely over a long distance, innervating numerous Purkinje cells on their way, but with each parallel fiber-to-Purkinje cell synapse being only very weak (De Zeeuw et al., 2011). There are two main mossy fiber routes via which whisker sensory information reaches the cerebellar cortex. First, there is a direct mossy fiber projection from the trigeminal nuclei to the cerebellar cortex. The trigemino-cerebellar mossy fibers originate from ipsilateral PrV, SpVo and SpVi, and to a lesser extent from SpVc (Yatim et al., 1996). This direct pathway can evoke Purkinje cell simple spike responses with a short latency. The second main mossy fiber input originates in the pontine nucleus, which in turn is activated by wS1. This cerebro-cerebellar pathway evokes Purkinje cell simple spike responses with a long latency. Lesioning of the cerebral cortex abolishes the long-latency response, while leaving the short-latency responses in tact (Fig. 6A) (Kennedy et al., 1966;Morisette and Bower, 1996). There is also a direct, trigemino-pontine connection from SpVi, but its relevance for the whisker system is not clear (Swenson et al., 1984;Mihailoff et al., 1989).

Whisker input can also inhibit Purkinje cell simple spike firing, with the inhibitory response having a longer latency than the excitatory response (Fig. 6B) (Bosman et al., 2010;Chu et al., 2011). This reflects most likely the feedforward inhibition by molecular layer interneurons within the cerebellar cortex (Chu et al., 2011;De Zeeuw et al., 2011). The complex spike and simple spike responses of an individual Purkinje cell are largely uncorrelated, both at the level of the receptive field and on the level of individual trials (Bosman et al., 2010). Simple spikes receptive fields usually involve multiple whiskers, without any obvious somatotopic ordering. And, also in contrast to complex spike responses, simple spike responses are not affected by the direction of whisker stimulation (Bosman et al., 2010). Mossy fiber-mediated whisker input seems to be strongest in crus 1, strong in crus 2 and lobules VII and IX in the vermis, and sparse in the simplex and paramedian lobules (Joseph et al., 1978;Shambes et al., 1978;Thomson et al., 1989;Bosman et al., 2010).

Thus, large parts of the cerebellar cortex receive whisker input. The output of the

GABAergic Purkinje cells in the whisker-sensitive regions is fully directed to the cerebellar nuclei. From there, the cerebellar output to the whisker system mainly follows three pathways: (i) to the inferior olive, where it closes the olivo-cortico-nuclear feedback loop (Voogd and Glickstein, 1998;De Zeeuw et al., 2011); (ii) to the VL nucleus of the thalamus (Aumann et al., 1994) to provide feedback to the cerebral cortex (Aumann et al., 1994), and possibly also to the basal ganglia (Hoshi et al., 2005); and (iii) to regions that directly project to the lateral facial nucleus, such as SC (Westby et al., 1993) and NRTP (Torigoe et al., 1986b). So these latter routes may allow the cerebellum to directly affect motor output.

Both the striatum and the pontine nuclei receive input from the cerebral cortex. Interestingly, the cortico-pontine pathway has a stronger convergence of inputs from related regions in wS1 and wS2 than the cortico-striatal pathway (Leergaard et al., 2004). This could imply that the cerebellar system is especially suited for the processing of sensory data. Recent findings in primates link the cerebellar system and the basal ganglia via reciprocal disynaptic pathways. The dentate nucleus projects via the thalamus to the striatum (Hoshi et al., 2005) and STN projects via the pontine nuclei to the cerebellar cortex (Bostan et al., 2010).

### 4.6 Ventrolateral nucleus of the thalamus

Both the basal ganglia and the cerebellum have an ascending projection to wM1 via the ventrolateral nucleus (VL) of the thalamus. VL incorporates input from EPN (Nambu, 2007), the cerebellar nuclei (Aumann et al., 1994) and wM1 (Miyashita et al., 1994;Alloway et al., 2008). VL itself has a somatotopic representation, including a separate area related to the whiskers (Tlamsa and Brumberg, 2010). Thus, VL is a crucial part of the central motor control system.

### 4.7. Other structures projecting to the facial nucleus

#### 4.7.1 Pontomedullary reticular formation

The pontomedullary reticular formation (RF) is a premotor area, whose activation can cause widespread movements (Quessy and Freedman, 2004;Stapley and Drew, 2009). Within RF, several distinct regions can be discriminated. Of these, the dorsal medullary reticular field and the parvocellular reticular nucleus receive strong input from SpVi and SpVc, while the gigantocellular reticular nucleus receives moderate input from SpVo (Zerari-Mailly et al., 2001). Relatively weak inputs from SpV to the other parts of RF can also be found, as well as a few connections between PrV and RF (Zerari-Mailly et al., 2001). The dorsal reticular nucleus (DRN) is probably a pain modulating area (Villanueva et al., 1988;Bouhassira et al., 1992). DRN forms, as other parts of RF, strong bilateral connections to the facial nucleus (Hattox et al., 2002;Leite-Almeida et al., 2006). Indeed, mice move their whiskers, as well as other parts of the face, in response to pain (Langford et al., 2010). In addition, DRN projects to dozens of other brain structures, including other parts of RF, the ipsilateral amygdala, periaqueductal gray, red nucleus, and SpV, as well as the contralateral inferior olive, SC, zona incerta and several nuclei of the thalamus, including Pom and to a lesser extent VPM (Leite-Almeida et al., 2006). Apart from a role in pain transmission, RF is also involved in “normal” whisker movements. RF neurons receiving trigeminal input project to the lateral facial and hypoglossal nuclei (Dauvergne et al., 2001). In addition, RF receives direct input from wM1, and RF stimulation causes whisker retraction (Matyas et al., 2010). RF also receives cholinergic input from the pedunculopontine tegmental nuclei (Jones, 1990) and noradrenergic input from the locus coeruleus (Jones, 1991), indicating that RF activity is strongly modulated by the general state of alertness.

#### 4.7.2. Zona incerta

The zona incerta (ZI) can be functionally divided into rostral (ZIr), dorsal (ZId), ventral (ZIv) and caudal (ZIc) sectors (Kim et al., 1992;Ma et al., 1992;Nicolelis et al., 1992; 1995b) and contributes to the whisker paralemniscal somatosensory pathway (Urbain and Deschênes, 2007a). It has been said to have connections with almost every center in the neuraxis (Mitrofanis, 2005). Multiple whisker receptive fields have been found in both ZId and ZIv. A somatotopic map was found to be partial in ZId and complete in ZIv. The ZId somatotopic map was characterized by large facial receptive fields including the whiskers (Nicolelis et al., 1992;Simpson et al., 2008). Direct whisker input reaches ZI mainly from both PrV and SpVi (Lin et al., 1990;Kolmac et al., 1998;Lavallée et al., 2005), but also via wS1 (Lin et al., 1990;Aronoff et al., 2010). Most likely, the main impact of ZI on the whisker system is by its GABAergic output to Pom. The thalamus can be divided into first order and higher order nuclei where the latter can be defined by different coding strategies, receptive field properties and cortical layer 5 input (Diamond et al., 1992a;Ojima, 1994;Ahissar et al., 2000). ZI forms GABAergic projections that terminate on such higher order thalamic nuclei (Barthó et al., 2002). During rest, ZIv inhibits whisker sensory transmission via Pom (Lavallée et al., 2005). However, wM1 input to the motor subsector of ZI can induce GABAergic interneurons that inhibit the whisker sensory subsector of ZI, which in turn disinhibits the relay cells of Pom, providing a mechanism of lateral inhibition in ZI (Urbain and Deschênes, 2007b). Thus, during active whisker movements, wM1 activity releases the inhibition on sensory gating in Pom. This implies that Pom transmits more details on whisker input during active movement than during periods of rest. Apart from wM1, also cholinergic input from the pedunculopontine tegmental nucleus and the laterodorsal tegmental nucleus can reduce the inhibitory output of ZIv to Pom (Trageser et al., 2006). Since the cholinergic input to ZI is highest during active states (Trageser et al., 2006), this is a possible second form of gating of the whisker input to wS1 under control of the ZI. ZI forms also GABAergic projections to the intermediate and deep layers of the SC, that in turn project back to ZI (Roger and Cadusseau, 1985;May, 2006). In addition, ZId has glutamatergic projections to the basal ganglia (Heise and Mitrofanis, 2004).

#### 4.7.3. Anterior pretectal nucleus

Like ZI, the anterior pretectal nucleus (APT) provides strong GABAergic inhibition in Pom. The morphology of the projections to Pom from ZI and APT are similar, forming multiple synapses on the thick dendrites of relay cells, and different from RT projections that form single synapses on the thin, distal dendrites of relay cells (Bokor et al., 2005;Wanaverbecq et al., 2008). Input from APT strongly suppresses whisker responses in Pom (Murray et al., 2010). In view of the heterogeneity in firing patterns of APT neurons observed *in vivo*, it has been suggested that APT, like ZI, controls the thalamo-cortical output in a state-dependent manner (Bokor et al., 2005). ZI and APT are reciprocally connected. There is a strong projection of both GABAergic and non-GABAergic APT neurons to ZIv, from where the thalamic projections originate (May et al., 1997). The reciprocal connection from ZIv to APT is relatively sparse (May et al., 1997;Giber et al., 2008). Thus, ZI and APT may cooperate in controlling the flow of information from Pom to the cerebral cortex in a state-dependent manner.

Apart from ZI and Pom, APT also targets a large number of brain regions. The functional relevance of these other outputs for the whisker system is still unclear, but potentially relevant target areas are SC, the pontomedullary reticular formation, the pontine nucleus, red nucleus and (dorsal) inferior olive (Cadusseau and Roger, 1991;Terenzi et al., 1995;Zagon et al., 1995). In turn, APT receives strong input from amongst others wS1, SC, the deep mesencephalic nucleus and the pedunculopontine tegmental nucleus, as well as sparse input from the locus coeruleus and the periaqueductal gray (Foster et al., 1989;Cadusseau and Roger, 1991).

### 4.7.4. Red nucleus

The red nucleus is closely associated with limb movements (Massion, 1988;Muir and Whishaw, 2000) and is composed of two parts. The magnocellular part receives input from the cerebral cortex, including wS1 and wM1 (Alloway et al., 2010), as well as from the cerebellar interposed nucleus (Teune et al., 2000), and sends its output to the contralateral limbs via the rubrospinal tract (ten Donkelaar, 1988;Paul and Gould, 2010). The parvocellular part receives its input from the cerebellar dentate nucleus (Teune et al., 2000) and sends its output to the contralateral facial nucleus (Hattox et al., 2002). Thus, from an anatomical point of view, the red nucleus is strongly implicated in the whisker system. However, electrical stimulation of the red nucleus did not evoke whisker movements in a consistent way (Isokawa-Akesson and Komisaruk, 1987).

### 4.7.5. Pontine respiratory group

The parabrachial complex and the Kölliker-Fuse nucleus, both part of the pontine respiratory group, provide strong, ipsilateral projections to the lateral facial nucleus (Isokawa-Akesson and Komisaruk, 1987;Hattox et al., 2002). The pontine respiratory group projects to several areas of the medullar respiratory group, and may therefore affect the respiratory rhythm (Smith et al., 2009). Thus, the connection between the pontine respiratory group and the lateral facial nucleus may facilitate the synchronization of sniffing and whisking. Such coupling is prominent during exploratory whisking (Welker, 1964).

### 4.7.6. Ambiguus nucleus

The ambiguus nucleus has a dense projection to the ipsilateral lateral facial nucleus (Isokawa-Akesson and Komisaruk, 1987;Hattox et al., 2002). Electrical stimulation of the ambiguus nucleus could evoke ipsilateral, rhythmic whisker movements with a remarkably low stimulation threshold (Isokawa-Akesson and Komisaruk, 1987). Since the ambiguus nucleus is mainly involved in respiration (Delgado-García et al., 1983) and swallowing (Broussard and Altschuler, 2000), it could serve to synchronize whisker movements to respiration and swallowing.

### 4.7.7. Other brain regions

This list of brain regions is incomplete since we lack sufficient knowledge of other brain regions which might be involved in the whisker system. Potentially important areas include the deep mesencephalic nucleus and the periaqueductal gray. The deep mesencephalic nucleus receives a strong, ipsilateral input from wM1, and forms dense projections to the lateral facial nucleus (Hattox et al., 2002;Alloway et al., 2010). Yet, its function for the whisker system is not clear. The periaqueductal gray is, amongst others, important for pain transmission and integrating defensive behavior (Behbehani, 1995;Graeff, 2004). Stimulating the periaqueductal gray results in whisker twitches (Verberne and Struyker Boudier, 1991). The periaqueductal gray receives serotonergic input from the dorsal raphe nucleus (Graeff, 2004), strong input from ipsilateral wM1 (Alloway et al., 2010), and forms relatively sparse, bilateral connections to the lateral facial nucleus (Hattox et al., 2002). For further connections of the periaqueductal gray, see Vianno and Brandão (2003).

## 5. Bilateral coordination of whisker movements

In the absence of object contact and head movements, whisker movements on both sides of the head tend to be symmetric. However, during active exploration, in particular involving head movements, whisker movements are often asymmetric (Towal and Hartmann, 2006;Mitchinson et al., 2007;Towal and Hartmann, 2008). This implies that both hemispheres are interconnected, but can be decoupled if the actual behavior requires to do so. In line with this, many, if not most, of the connections discussed in this review are actually bilateral, although the strengths of the ipsi- and contralateral projections are often quite different (see also Alloway et al. (2010)). Putative candidates for the modification of interhemispheric connections, especially involving wM1, are the feedback loops with the thalamus, the basal ganglia and the claustrum (Alloway et al., 2008;Alloway et al., 2009;Alloway et al., 2010). Particularly the claustrum has been proposed to facilitate interhemispheric communication of wM1 (Alloway et al., 2009;Smith and Alloway, 2010). wM1 targets the claustrum mainly contralaterally, and the claustrum projects mainly ipsilaterally to wM1. These projections are highly specific: the cortico-claustro-cortical projections connect the same whisker fields in wM1 of both hemispheres (Smith and Alloway, 2010).

## 6. Arousal, alertness and attention

Whisker movements and the processing of whisker input depend on the general state of alertness. For instance, stimulation of wM1 leads to larger whisker movements in aroused rather than in awake, but sessile rats (Berg et al., 2005). Furthermore, whisker stimuli evoke smaller responses in wS1 showing less spreading during whisking than during rest (Ferezou et al., 2007). The neural systems that control the general state of alertness affect many brain regions and are not specific for the whisker system. We discuss here those systems of which clear effects on the whisker system have been documented or can be expected based on anatomical connections.

### 6.1. Acetylcholine

Central cholinergic projections, mainly originating from the basal forebrain and the tegmentum, affect the whisker system at different levels (Woolf, 1991;Dani and Bertrand, 2007). Roughly, the basal forebrain targets wS1 and wM1, while the tegmentum targets several subcortical areas. The basal forebrain is composed of several areas that provide cholinergic output, including the nucleus basalis magnocellularis (NBM; known as the Meynert nucleus in primates) of the substantia innominata. NBM is active during waking and REM sleep, but not during slow-wave sleep (Lee et al., 2005). The main projection areas of the cholinergic neurons of NBM are the entire cerebral cortex and the amygdala (Wenk, 1997;Deurveilher and Semba, 2011). Electrical stimulation of the cholinergic neurons of the NBM leads to an increased effect of wM1 stimulation on whisker movements. This effect of NBM stimulation is only observed in sessile, but less so in aroused rats (Berg et al., 2005). This could indicate that NBM is already endogenously active in aroused rats.

In addition to enhancing motor performance, cholinergic afferents also increase the sensitivity to sensory stimuli. The response to whisker stimulation in wS1 is increased due to acetylcholine (ACh) (Oldford and Castro-Alamancos, 2003;Constantinople and Bruno, 2011). This effect is partly due to stimulation of the basal forebrain, which enhances especially the responses to non-dominant whiskers (Kuo et al., 2009). In addition, cholinergic projections from the pedunculopontine tegmental nucleus (PPTg) and the laterodorsal tegmental nucleus (LDTg), increase the responses to whisker stimulation in VPM, and consequently also in wS1 (Hirata and Castro-Alamancos, 2010; 2011). Furthermore, the responsiveness to whisker input of Pom is increased by cholinergic input from PPTg as well as from LDTg, due to both direct connections to Pom, where the cholinergic fibers suppress the release of GABA from projections originating in the zona incerta (Masri et al., 2006), as well as indirectly by decreasing the neuronal activity of GABAergic projection neurons in the zona incerta (Trageser et al., 2006). In SpVi, a similar phenomenon occurs as in wS1: activity of the cholinergic input from PPTg increases the responsivity of sensory neurons to inputs from adjacent whiskers (Timofeeva et al., 2005). Finally, there are also cholinergic projections from

PPTg and LDTg to SC, PrV and the lateral facial nucleus (Satoh and Fibiger, 1986;Beak et al., 2010), but their specific functions for the whisker system are currently unknown.

NBM receives strong input from the amygdala, the hypothalamus and the thalamus, as well as from specific areas of the cerebral cortex, probably including the prefrontal and motor cortex (Haring and Wang, 1986;Irle and Markowitsch, 1986). In addition, there are weaker inputs from many other (subcortical) regions (Haring and Wang, 1986;Irle and Markowitsch, 1986). Inputs to PPTg and LDTg come from a wide range of brain regions, including the medial prefrontal and cingulate cortex (but not wS1, wS2 and wM1), the thalamus, the hypothalamus, the zona incerta, the periaqueductal gray, SC, the pontomedullary reticular formation, the dorsal raphe nuclei as well as from many other regions not directly involved in the whisker system (Semba and Fibiger, 1992). The input from the trigeminal and cerebellar nuclei is relatively weak (Semba and Fibiger, 1992).

In conclusion, when the cholinergic system is quiet, as during slow wave sleep (Lee et al., 2005), whisker sensitivity is reduced, and primarily focused on the dominant whiskers. During more attentive states, input from non-dominant whiskers is processed, yielding a more detailed impression of the environment. At the same time, the cholinergic system facilitates whisker movements during arousal, which increases the sensitivity of the whisker system even further.

### 6.2. Noradrenaline

Noradrenergic projections have similar effects on the sensitivity to whisker stimulation as cholinergic projections. The origin of noradrenaline is the locus coeruleus and adjacent brainstem regions (Aston-Jones and Cohen, 2005). Noradrenaline suppresses spontaneous activity of VPM via RT. As a consequence, sensory input is passed on to wS1 with a higher signal-to-noise ratio (Hirata et al., 2006;Hirata and Castro-Alamancos, 2011). In addition, the locus coeruleus can directly modulate the network dynamics of wS1 (Constantinople and Bruno, 2011). Activity of the locus coeruleus is closely related to awakeness and alertness (Aston-Jones and Cohen, 2005). Indeed, a novel environment can stimulate activity of the locus coeruleus and the anterior cingulate cortex, and thus keep the animal fully awake (Gompf et al., 2010). The main inputs to the locus coeruleus come from RF and the hypoglossal nucleus (Jones, 1991). Other relevant outputs are directed to RF, the facial nucleus, the zona incerta and NBM (Jones, 1991). Thus, although noradrenaline works via different mechanisms than ACh, both increase the level of arousal as well as the sensitivity towards whisker input.

### 6.3. Histamine

Histamine is also only released during wakefulness (Takahashi et al., 2006). It promotes, amongst others, vigilance (Anaclet et al., 2009;Thakkar, 2011) and the coordination of goal-directed behaviors (Valdés et al., 2010). The sole source of histamine in the brain is the hypothalamus, most notably the tuberomammillary nuclei and perhaps also the surrounding tissue (Wouterlood et al., 1986;Passani and Blandina, 2011). The tuberomammillary nuclei project to almost all brain regions, including cerebral cortex, thalamus, brainstem and cerebellum (Pillot et al., 2002). Histaminergic connections of particular importance for the whisker system include ipsilateral projections from the ventrolateral tuberomammillary nucleus to wS1 and wM1 (Hong et al., 2010). The dorsomedial tuberomammillary nucleus projects bilaterally to PrV and the lateral facial nucleus (Hong et al., 2010). In addition, all layers of SC, but mainly the superficial ones, receive histaminergic input (Manning et al., 1996). Thus, there are histaminergic connections to many of the important whisker regions, and although the specific functions of these connections are currently unknown, it seems likely that histamine has a general, stimulating effect on the whisker system, comparable to that of acetylcholine and noradrenaline.

### 6.4. Serotonin

The activity of most serotonergic neurons of the dorsal raphe nucleus is strongly affected by the sleep/wake rhythm. In the awake state, they fire at very regular intervals (McGinty and Harper, 1976;Kocsis et al., 2006;Urbain et al., 2006). The dorsal raphe nucleus projects to the lateral facial nucleus (Hattox et al., 2003;Cramer and Keller, 2006;Lee et al., 2008c), where serotonin facilitates a persistent inward current (PIC) in the whisker motor neurons. This lowers their activation thresholds (Cramer et al., 2007). Indeed, spontaneous as well as wM1-induced whisker movements are largely abolished following block of serotonin receptors (Fig. 7B) (Hattox et al., 2003;Cramer and Keller, 2006). Thus, serotonin is both required and sufficient to generate a rhythmic whisker movement pattern, and it also modulates inputs from wM1. That makes the serotonergic system a fourth system that modulates the whisker system according to the state of alertness of the animal, together with the cholinergic, noradrenergic and histaminergic systems.

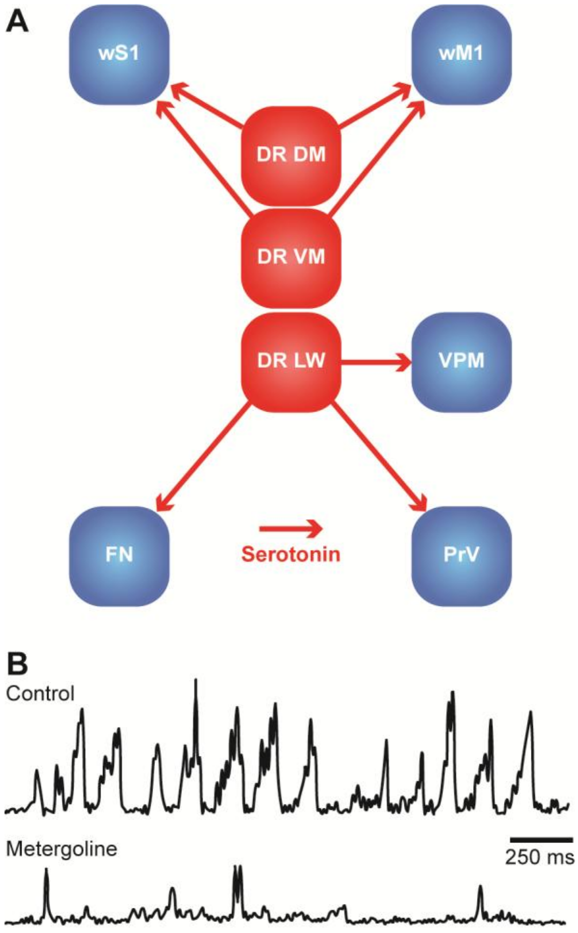

***Figure 7 – The dorsal raphe nuclei as central pattern generator***

***A*** *| Schematic overview of the main serotonergic connections from the dorsal raphe nuclei to the brain regions of the whisker system. DR DM = dorsomedial dorsal raphe nucleus, DR LW = lateral wing division of the dorsal raphe nucleus, DR VM = ventromedial dorsal raphe nucleus, FN = facial nucleus, PrV = principal trigeminal nucleus, VPM = medial ventroposterior nucleus, wM1 = whisker motor cortex, wS1 = barrel cortex.* ***B*** *| During exploratory whisking, rhythmic whisker movements occur, as shown here by EMG recordings of rat whisker muscles. Application of metergoline, an antagonist for the serotonin receptors* $5\text{-}HT_1$ *and* $5\text{-}HT_2$*, in the facial nucleus abolishes the rhythmicity of whisker movements unilaterally at the side of injection. Most likely, the dorsal raphe nuclei are the source of serotonin. This indicates that the dorsal raphe nuclei may act as central pattern generator for whisker movements. Reproduced with permission from Hattox et al. (2003).*

The dorsal raphe nucleus receives inputs from wM1, but also from a wide range of cortical and subcortical areas. Particularly strong inputs come from regions with an emotional and/or cognitive function, such as the medial prefrontal cortex and the amygdala (Lee et al., 2003;Hale and Lowry, 2011). The regular spiking patterns of the dorsal raphe nucleus are in line with its putative function as central pattern generator for rhythmic whisker movements (Hattox et al., 2003). The spiking pattern of the dorsal raphe nucleus can be perturbed by, amongst others, whisker touch and, to a lesser extent, free whisking in air (Waterhouse et al., 2004). The dorsal raphe nucleus projects to the prefrontal cortex and many regions directly involved in the whisker system. The midline region projects to ipsilateral wS1 and wM1, and the lateral wing division to ipsilateral VPMvl, PrV and facial nucleus (Fig. 7A) (Kirifides et al., 2001;Sheibani and Farazifard, 2006;Lee et al., 2008c). Thus, next to being a central pattern generator for rhythmic whisker movements via its direct connection to the lateral facial nucleus, the dorsal raphe nucleus affects several other regions of the whisker system.

## 7. Timing in the whisker system

Timing is essential for the whisker system. During active touch, rats move their whiskers rhythmically over an object. Irregularities in the surface texture cause small disruptions in the whisker movements, which evoke neuronal responses (Fig. 1B-C) (Szwed et al., 2003;Hartmann, 2009;Jadhav and Feldman, 2010). Active touch can be instrumental for several forms of behavior. For instance, Etruscan shrews use their whiskers to locate prey. On average, they initiate an attack on average 179 ms after the first whisker contact, but this interval can be as short as 53 ms (Munz et al., 2010). Indeed, the vibrissae can be used experimentally to explore interval timing. Stimulation of the vibrissae can act as a conditioned stimulus (CS) in eyeblink conditioning (Das et al., 2001;Leal-Campanario et al., 2006;Galvez et al., 2009). In addition, the reverse is possible: to evoke vibrissal movements as an unconditioned response (UR) (Troncoso et al., 2004).

Whisker responses are rapidly distributed over the brain. Many brain regions receive direct input from the trigeminal nuclei, often in addition to input from wS1 (Fig. 8). As a consequence, the whisker responses in the cerebellum (Bosman et al., 2010) and SC (Bezdudnaya and Castro-Alamancos, 2011) are bi-phasic. Fast, direct whisker responses are followed by wS1-mediated responses with longer latencies. This allows for fast, multi-center processing of whisker data.

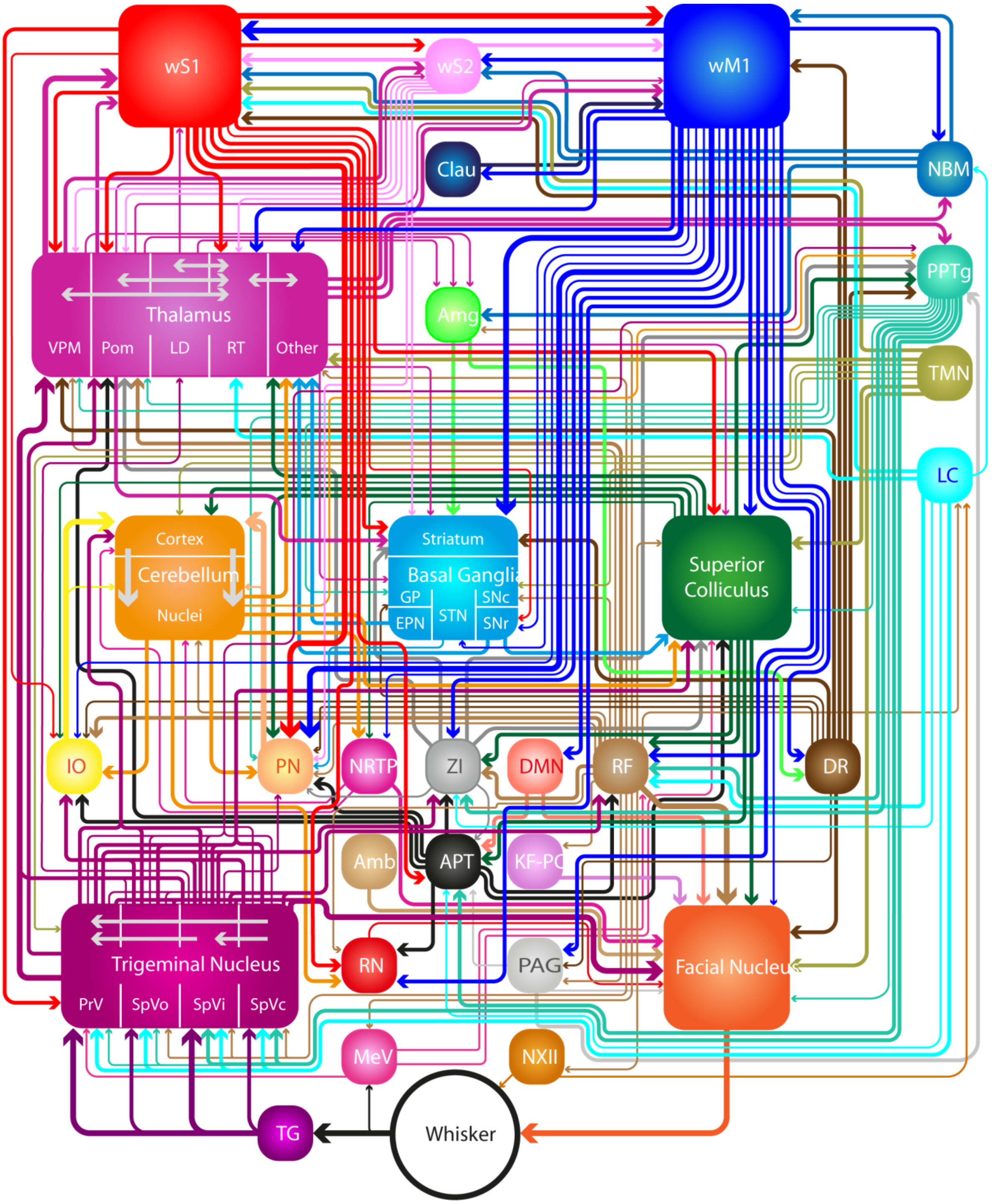
wS1
wS2
wM1
Clau
NBM
Thalamus
VPM
Pom
LD
RT
Other
Amg
PPTg
TMN
LC
Cortex
Cerebellum
Nuclei
Striatum
Basal Ganglia
GP
SNc
EPN
STN
SNr
Superior Colliculus
IO
PN
NRTP
ZI
DMN
RF
DR
Amb
APT
KF-PC
Trigeminal Nucleus
PrV
SpVo
SpVi
SpVc
RN
PAG
Facial Nucleus
MeV
NXII
TG
Whisker

***Figure 8 – Neuronal connections in the whisker system***
*Many brain regions are involved in controlling the whiskers. Schematic representation of the connections discussed in the main text. Thickness of the arrows corresponds to the robustness of the connection involved (divided among three different levels). Some local connections are indicated, but for the connections between the nuclei of the basal ganglia, see Fig. 5A. Amb = ambiguus nucleus, Amg = amygdala, APT = anterior pretectal nucleus, Clau = claustrum, DMN = deep mesencephalic nucleus, DR = dorsal raphe nucleus, EPN = entopeduncular nucleus, GP = globus pallidus, IO = inferior olive, KF-PC = Kölliker-Fuse nucleus and parabrachial complex, LC = locus coeruleus, LD = laterodorsal nucleus, MeV = mesencephalic trigeminal nucleus, NBM = nucleus basalis magnocellularis, NRTP = nucleus reticularis tegmenti pontis, NXII = hypoglossal nucleus, PAG = periaqueductal gray, PN = pontine nucleus, Pom = medial posterior nucleus, PPTg = pedunculopontine tegmental nucleus and the laterodorsal tegmental nucleus, PrV = principal trigeminal nucleus, RF = pontomedullar reticular formation, RN = red nucleus,*

*RT = reticular nucleus, SNc = substantia nigra pars compacta, SNr = substantia nigra pars reticulata, SpVc = spinal trigeminal nucleus pars caudalis, SpVi = spinal trigeminal nucleus pars interpolaris, SpVo = spinal trigeminal nucleus pars oralis, STN = subthalamic nucleus, TG = trigeminal ganglion, TMN = tuberomammillary nucleus, VPM = medial venteroposterior nucleus, wM1 = whisker motor cortex, wS1 = barrel cortex, wS2 = whisker part of the secondary somatosensory cortex, ZI = zona incerta.*

Although wM1 is able to evoke, on a cycle-by-cycle base, rhythmic whisker movements under experimental conditions involving artificial disinhibition (Castro-Alamancos, 2006), under more physiological conditions, the frequency of microstimulation in wM1 does not necessarily correspond to the frequency of the evoked whisker movements (Berg and Kleinfeld, 2003b;Haiss and Schwarz, 2005). However, widespread rhythmic activity (at 7-12 Hz) involving cerebral cortex, thalamus and brainstem often precedes the onset of rhythmic whisker movements, which is then phase-locked to the brain oscillations (Nicolelis et al., 1995a). Nevertheless, it is likely that subcortical structures critically participate in the generation of rhythmicity of the whisker movements. The serotonergic projection from the dorsal raphe nuclei to the facial nucleus has especially been found to be effective in generation rhythmic whisker movements (Hattox et al., 2003). But also the cerebellum and the inferior olive may be involved. After blocking the inferior olive pharmacologically, as well as following cerebellectomy, the frequency-dependence of whisker movements following wM1 stimulation was altered (Lang et al., 2006). In contrast, the superior colliculus does not seem to be involved in the generation of rhythmic movements, as its activity causes prolonged whisker protractions (Hemelt and Keller, 2008).

## 8. Conclusions

Whiskers play a central role in the lives and loves of rodents. Accordingly, many brain regions can affect whisker movements. Whisker movements depend on the general state of arousal, they are coupled to the movements of other mobile senses, like the eyes and the auricles, and integrated with other forms of behavior, like sniffing, swallowing and locomotion. Animals orient their whiskers based on reward expectancy, for instance when searching for food. With respect to whisker input, the level of detail that is transmitted to higher brain areas depends on the general state of arousal as well as on the activity of the whisker motor cortex, and the context of the animal’s environment. The sensory and motor systems of the whiskers are coupled by a number of sensorimotor feedback loops, allowing the animals to adjust whisker movements to sensory input. Unfortunately, many of the brain regions involved in these feedback loops have received relatively little attention with respect to the whisker system. Hence, our knowledge on the relative importance of these areas and interconnections is incomplete. Yet, based on the current data available to us, we present a scheme of the relevant anatomical connections in Fig. 8. Although these brain structures have many more connections, we have attempted to highlight the most prominent ones. However, the complexity of the whisker system seems to depend on the behavioral state; the more active an animal is, the more complex it’s whisker movements are and therefore a greater level of detail results during sensory and motor information processing.

## Conflict of interests

The authors declare that there are no conflicts of interest.

## Acknowledgements

The authors thank Drs. Frank Rice and Hans Dringenberg for their comments on a previous version of the manuscript and Dr. Reha Erzurumlu for contributing an unpublished photomicrograph. We kindly thank the Dutch Organization for Medical Sciences (ZonMw;

CIDZ), Life Sciences (ALW; CIDZ, AH), Senter (Neuro-Bsik; CIDZ), Prinses Beatrix Fonds (CIDZ), and the SENSOPAC, CEREBNET and C7 programs of the European Community (CIDZ) for their financial support. We also thank our lab members for valuable discussions.

## References

*Ahissar, E., Sosnik, R., and Haidarliu, S. (2000). Transformation from temporal to rate coding in a somatosensory thalamocortical pathway. Nature 406***,** *302-306.*

*Ahl, A.S. (1982). Evidence of use of vibrissae in swimming in Sigmodon fulviventer. Anim Behav 30***,** *1203-1206.*

*Ahl, A.S. (1986). The role of vibrissae in behavior: a status review. Vet Res Commun 10***,** *245-268.*

*Akaike, T. (1992). The tectorecipient zone in the inferior olivary nucleus in the rat. J Comp Neurol 320***,** *398-414.*

*Alloway, K.D. (2008). Information processing streams in rodent barrel cortex: the differential functions of barrel and septal circuits. Cereb Cortex 18***,** *979-989.*

*Alloway, K.D., Crist, J., Mutic, J.J., and Roy, S.A. (1999). Corticostriatal projections from rat barrel cortex have an anisotropic organization that correlates with vibrissal whisking behavior. J Neurosci 19***,** *10908-10922.*

*Alloway, K.D., Lou, L., Nwabueze-Ogbo, F., and Chakrabarti, S. (2006). Topography of cortical projections to the dorsolateral neostriatum in rats: multiple overlapping sensorimotor pathways. J Comp Neurol 499***,** *33-48.*

*Alloway, K.D., Mutic, J.J., Hoffer, Z.S., and Hoover, J.E. (2000). Overlapping corticostriatal projections from the rodent vibrissal representations in primary and secondary somatosensory cortex. J Comp Neurol 428***,** *51-67.*

*Alloway, K.D., Olson, M.L., and Smith, J.B. (2008). Contralateral corticothalamic projections from MI whisker cortex: potential route for modulating hemispheric interactions. J Comp Neurol 510***,** *100-116.*

*Alloway, K.D., Smith, J.B., and Beauchemin, K.J. (2010). Quantitative analysis of the bilateral brainstem projections from the whisker and forepaw regions in rat primary motor cortex. J Comp Neurol 518***,** *4546-4566.*

*Alloway, K.D., Smith, J.B., Beauchemin, K.J., and Olson, M.L. (2009). Bilateral projections from rat MI whisker cortex to the neostriatum, thalamus, and claustrum: forebrain circuits for modulating whisking behavior. J Comp Neurol 515***,** *548-564.*

*Alloway, K.D., Zhang, M., and Chakrabarti, S. (2004). Septal columns in rodent barrel cortex: functional circuits for modulating whisking behavior. J Comp Neurol 480***,** *299-309.*

*Anaclet, C., Parmentier, R., Ouk, K., Guidon, G., Buda, C., Sastre, J.P., Akaoka, H., Sergeeva, O.A., Yanagisawa, M., Ohtsu, H., Franco, P., Haas, H.L., and Lin, J.S. (2009). Orexin/hypocretin and histamine: distinct roles in the control of wakefulness demonstrated using knock-out mouse models. J Neurosci 29***,** *14423-14438.*

*Andermann, M.L., and Moore, C.I. (2006). A somatotopic map of vibrissa motion direction within a barrel column. Nat Neurosci 9***,** *543-551.*

*Anjum, F., Turni, H., Mulder, P.G.H., van der Burg, J., and Brecht, M. (2006). Tactile guidance of prey capture in Etruscan shrews. Proc Natl Acad Sci U S A 103***,** *16544-16549.*

*Apps, R., and Hawkes, R. (2009). Cerebellar cortical organization: a one-map hypothesis. Nat Rev Neurosci 10***,** *670-681.*

*Arabzadeh, E., Zorzin, E., and Diamond, M.E. (2005). Neuronal encoding of texture in the whisker sensory pathway. PLoS Biol 3***,** *e17.*

*Armstrong-James, M., and Callahan, C.A. (1991). Thalamo-cortical processing of vibrissal information in the rat. II. spatiotemporal convergence in the thalamic ventroposterior medial nucleus (VPm) and its relevance to generation of receptive fields of S1 cortical "barrel" neurones. J Comp Neurol 303***,** *211-224.*

*Armstrong-James, M., and Fox, K. (1987). Spatiotemporal convergence and divergence in the rat S1 "barrel" cortex. J Comp Neurol 263***,** *265-281.*

*Aronoff, R., Matyas, F., Mateo, C., Ciron, C., Schneider, B., and Petersen, C.C.H. (2010).*

*Long-range connectivity of mouse primary somatosensory barrel cortex. Eur J Neurosci 31*, *2221-2233.*

*Ashwell, K.W. (1982). The adult mouse facial nerve nucleus: morphology and musculotopic organization. J Anat 135*, *531-538.*

*Aston-Jones, G., and Cohen, J.D. (2005). An integrative theory of locus coeruleus-norepinephrine function: adaptive gain and optimal performance. Annu Rev Neurosci 28*, *403-450.*

*Aumann, T.D., Rawson, J.A., Finkelstein, D.I., and Horne, M.K. (1994). Projections from the lateral and interposed cerebellar nuclei to the thalamus of the rat: a light and electron microscopic study using single and double anterograde labelling. J Comp Neurol 349*, *165-181.*

*Axelrad, H., and Crepel, F. (1977). Représentation sélective des vibrisses mystaciales au niveau des cellules de Purkinje du cervelet par la voie des fibres grimpantes chez le rat. C R Acad Sci Hebd Seances Acad Sci D 284*, *1321-1324.*

*Barthó, P., Freund, T.F., and Acsády, L. (2002). Selective GABAergic innervation of thalamic nuclei from zona incerta. Eur J Neurosci 16*, *999-1014.*

*Barthó, P., Slézia, A., Varga, V., Bokor, H., Pinault, D., Buzsáki, G., and Acsády, L. (2007). Cortical control of zona incerta. J Neurosci 27*, *1670-1681.*

*Beak, S.K., Hong, E.Y., and Lee, H.S. (2010). Collateral projection from the forebrain and mesopontine cholinergic neurons to whisker-related, sensory and motor regions of the rat. Brain Res 1336*, *30-45.*

*Beckstead, R.M., Domesick, V.B., and Nauta, W.J.H. (1979). Efferent connections of the substantia nigra and ventral tegmental area in the rat. Brain Res 175*, *191-217.*

*Behbehani, M.M. (1995). Functional characteristics of the midbrain periaqueductal gray. Prog Neurobiol 46*, *575-605.*

*Beitz, A.J. (1989). Possible origin of glutamatergic projections to the midbrain periaqueductal gray and deep layer of the superior colliculus of the rat. Brain Res Bull 23*, *25-35.*

*Belford, G.R., and Killackey, H.P. (1979). Vibrissae representation in subcortical trigeminal centers of the neonatal rat. J Comp Neurol 183*, *305-321.*

*Benison, A.M., Rector, D.M., and Barth, D.S. (2007). Hemispheric mapping of secondary somatosensory cortex in the rat. J Neurophysiol 97*, *200-207.*

*Berg, R.W., Friedman, B., Schroeder, L.F., and Kleinfeld, D. (2005). Activation of nucleus basalis facilitates cortical control of a brain stem motor program. J Neurophysiol 94*, *699-711.*

*Berg, R.W., and Kleinfeld, D. (2003a). Rhythmic whisking by rat: retraction as well as protraction of the vibrissae is under active muscular control. J Neurophysiol 89*, *104-117.*

*Berg, R.W., and Kleinfeld, D. (2003b). Vibrissa movement elicited by rhythmic electrical microstimulation to motor cortex in the aroused rat mimics exploratory whisking. J Neurophysiol 90*, *2950-2963.*

*Bermejo, R., Friedman, W., and Zeigler, H.P. (2005). Topography of whisking II: interaction of whisker and pad. Somatosens Mot Res 22*, *213-220.*

*Bermejo, R., Vyas, A., and Zeigler, H.P. (2002). Topography of rodent whisking-I. Two-dimensional monitoring of whisker movements. Somatosens Mot Res 19*, *341-346.*

*Bezdudnaya, T., and Castro-Alamancos, M.A. (2011). Superior colliculus cells sensitive to active touch and texture during whisking. J Neurophysiol 106*, *332-346.*

*Bezdudnaya, T., and Keller, A. (2008). Laterodorsal nucleus of the thalamus: A processor of somatosensory inputs. J Comp Neurol 507*, *1979-1989.*

*Blanchard, R.J., Takahashi, L.K., Fukunaga, K.K., and Blanchard, D.C. (1977). Functions of the vibrissae in the defensive and aggressive behavior of the rat. Aggress Behav 3*, *231-240.*

*Boehnke, S.E., and Munoz, D.P. (2008). On the importance of the transient visual response in* *the superior colliculus. Curr Opin Neurobiol 18, 544-551.*

*Bokor, H., Acsády, L., and Deschênes, M. (2008). Vibrissal responses of thalamic cells that project to the septal columns of the barrel cortex and to the second somatosensory area. J Neurosci 28, 5169-5177.*

*Bokor, H., Frère, S.G.A., Eyre, M.D., Slézia, A., Ulbert, I., Lüthi, A., and Acsády, L. (2005). Selective GABAergic control of higher-order thalamic relays. Neuron 45, 929-940.*

*Bosman, L.W.J., Koekkoek, S.K.E., Shapiro, J., Rijken, B.F.M., Zandstra, F., van der Ende, B., Owens, C.B., Potters, J.W., de Gruijl, J.R., Ruigrok, T.J.H., and De Zeeuw, C.I. (2010). Encoding of whisker input by cerebellar Purkinje cells. J Physiol 588, 3757-3783.*

*Bosman, L.W.J., Takechi, H., Hartmann, J., Eilers, J., and Konnerth, A. (2008). Homosynaptic LTP of the "winner" climbing fiber synapse in developing Purkinje cells. J Neurosci 28, 798-807.*

*Bostan, A.C., Dum, R.P., and Strick, P.L. (2010). The basal ganglia communicate with the cerebellum. Proc Natl Acad Sci U S A 107, 8452-8456.*

*Bouhassira, D., Villanueva, L., Bing, Z., and le Bars, D. (1992). Involvement of the subnucleus reticularis dorsalis in diffuse noxious inhibitory controls in the rat. Brain Res 595, 353-357.*

*Bourassa, J., Pinault, D., and Deschênes, M. (1995). Corticothalamic projections from the cortical barrel field to the somatosensory thalamus in rats: a single-fibre study using biocytin as an anterograde tracer. Eur J Neurosci 7, 19-30.*

*Brecht, M. (2007). Barrel cortex and whisker-mediated behaviors. Curr Opin Neurobiol 17, 408-416.*

*Brecht, M., Krauss, A., Muhammad, S., Sinai-Esfahani, L., Bellanca, S., and Margrie, T.W. (2004a). Organization of rat vibrissa motor cortex and adjacent areas according to cytoarchitectonics, microstimulation, and intracellular stimulation of identified cells. J Comp Neurol 479, 360-373.*

*Brecht, M., Preilowski, B., and Merzenich, M.M. (1997). Functional architecture of the mystacial vibrissae. Behav Brain Res 84, 81-97.*

*Brecht, M., Roth, A., and Sakmann, B. (2003). Dynamic receptive fields of reconstructed pyramidal cells in layers 3 and 2 of rat somatosensory barrel cortex. J Physiol 553, 243-265.*

*Brecht, M., and Sakmann, B. (2002a). Dynamic representation of whisker deflection by synaptic potentials in spiny stellate and pyramidal cells in the barrels and septa of layer 4 rat somatosensory cortex. J Physiol 543, 49-70.*

*Brecht, M., and Sakmann, B. (2002b). Whisker maps of neuronal subclasses of the rat ventral posterior medial thalamus, identified by whole-cell voltage recording and morphological reconstruction. J Physiol 538, 495-515.*

*Brecht, M., Schneider, M., Sakmann, B., and Margrie, T.W. (2004b). Whisker movements evoked by stimulation of single pyramidal cells in rat motor cortex. Nature 427, 704-710.*

*Brodal, P. (1980). The cortical projection to the nucleus reticularis tegmenti pontis in the rhesus monkey. Exp Brain Res 38, 19-27.*

*Brodal, P., and Bjaalie, J.G. (1992). Organization of the pontine nuclei. Neurosci Res 13, 83-118.*

*Broussard, D.L., and Altschuler, S.M. (2000). Brainstem viscerotopic organization of afferents and efferents involved in the control of swallowing. Am J Med 108 Suppl 4a, 79S-86S.*

*Brown, I.E., and Bower, J.M. (2001). Congruence of mossy fiber and climbing fiber tactile projections in the lateral hemispheres of the rat cerebellum. J Comp Neurol 429, 59-70.*

*Brown, J.T., Chan-Palay, V., and Palay, S.L. (1977). A study of afferent input to the inferior olivary complex in the rat by retrograde axonal transport of horseradish peroxidase. J Comp Neurol 176, 1-22.*

*Brumberg, J.C., Pinto, D.J., and Simons, D.J. (1999). Cortical columnar processing in the rat*

*whisker-to-barrel system. J Neurophysiol 82, 1808-1817.*
*Bruno, R.M., Khatri, V., Land, P.W., and Simons, D.J. (2003). Thalamocortical angular tuning domains within individual barrels of rat somatosensory cortex. J Neurosci 23, 9565-9574.*
*Bureau, I., von Saint Paul, F., and Svoboda, K. (2006). Interdigitated paralemniscal and lemniscal pathways in the mouse barrel cortex. PLoS Biol 4, e382.*
*Burne, R.A., Azizi, S.A., Mihailoff, G.A., and Woodward, D.J. (1981). The tectopontine projection the the rat with comments on visual pathways to the basilar pons. J Comp Neurol 202, 287-307.*
*Cadusseau, J., and Roger, M. (1991). Cortical and subcortical connections of the pars compacta of the anterior pretectal nucleus in the rat. Neurosci Res 12, 83-100.*
*Carvell, G.E., and Simons, D.J. (1986). Somatotopic organization of the second somatosensory area (SII) in the cerebral cortex of the mouse. Somatosens Res 3, 213-237.*
*Carvell, G.E., and Simons, D.J. (1987). Thalamic and corticocortical connections of the second somatic sensory area of the mouse. J Comp Neurol 265, 409-427.*
*Carvell, G.E., and Simons, D.J. (1990). Biometric analyses of vibrissal tactile discrimination in the rat. J Neurosci 10, 2638-2648.*
*Carvell, G.E., and Simons, D.J. (1995). Task- and subject-related differences in sensorimotor behavior during active touch. Somatosens Mot Res 12, 1-9.*
*Castro-Alamancos, M.A. (2006). Vibrissa myoclonus (rhythmic retractions) driven by resonance of excitatory networks in motor cortex. J Neurophysiol 96, 1691-1698.*
*Cauller, L.J., Clancy, B., and Connors, B.W. (1998). Backward cortical projections to primary somatosensory cortex in rats extend long horizontal axons in layer I. J Comp Neurol 390, 297-310.*
*Chakrabarti, S., and Alloway, K.D. (2006). Differential origin of projections from SI barrel cortex to the whisker representations in SII and MI. J Comp Neurol 498, 624-636.*
*Chakrabarti, S., Zhang, M., and Alloway, K.D. (2008). MI neuronal responses to peripheral whisker stimulation: relationship to neuronal activity in si barrels and septa. J Neurophysiol 100, 50-63.*
*Chapin, J.K., Sadeq, M., and Guise, J.L.U. (1987). Corticocortical connections within the primary somatosensory cortex of the rat. J Comp Neurol 263, 326-346.*
*Chernova, O.F. (2006). Evolutionary aspects of hair polymorphism. Biol Bull 33, 43-52.*
*Chmielowska, J., Carvell, G.E., and Simons, D.J. (1989). Spatial organization of thalamocortical and corticothalamic projection systems in the rat SmI barrel cortex. J Comp Neurol 285, 325-338.*
*Chu, C.P., Bing, Y.H., and Qiu, D.L. (2011). Sensory stimulus evokes inhibition rather than excitation in cerebellar Purkinje cells in vivo in mice. Neurosci Lett 487, 182-186.*
*Cicirata, F., Angaut, P., Cioni, M., Serapide, M.F., and Papale, A. (1986). Functional organization of thalamic projections to the motor cortex. An anatomical and electrophysiological study in the rat. Neuroscience 19, 81-99.*
*Cohen, J.D., Hirata, A., and Castro-Alamancos, M.A. (2008). Vibrissa sensation in superior colliculus: wide-field sensitivity and state-dependent cortical feedback. J Neurosci 28, 11205-11220.*
*Colechio, E.M., and Alloway, K.D. (2009). Differential topography of the bilateral cortical projections to the whisker and forepaw regions in rat motor cortex. Brain Struct Funct 213, 423-439.*
*Constantinople, C.M., and Bruno, R.M. (2011). Effects and mechanisms of wakefulness on local cortical networks. Neuron 69, 1061-1068.*
*Cosenza, R.M., and Moore, R.Y. (1984). Afferent connections of the ventral lateral geniculate nucleus in the rat: an HRP study. Brain Res 310, 367-370.*
*Cox, C.L., Huguenard, J.R., and Prince, D.A. (1997). Nucleus reticularis neurons mediate*

*diverse inhibitory effects in thalamus. Proc Natl Acad Sci U S A 94, 8854-8859.*

*Crabtree, J.W., Collingridge, G.L., and Isaac, J.T.R. (1998). A new intrathalamic pathway linking modality-related nuclei in the dorsal thalamus. Nat Neurosci 1, 389-394.*

*Cramer, N.P., and Keller, A. (2006). Cortical control of a whisking central pattern generator. J Neurophysiol 96, 209-217.*

*Cramer, N.P., Li, Y., and Keller, A. (2007). The whisking rhythm generator: a novel mammalian network for the generation of movement. J Neurophysiol 97, 2148-2158.*

*Crandall, J.E., Korde, M., and Caviness, V.S., Jr. (1986). Somata of layer V projection neurons in the mouse barrelfield cortex are in preferential register with the sides and septa of the barrels. Neurosci Lett 67, 19-24.*

*Crochet, S., and Petersen, C.C.H. (2006). Correlating whisker behavior with membrane potential in barrel cortex of awake mice. Nat Neurosci 9, 608-610.*

*Crochet, S., Poulet, J.F.A., Kremer, Y., and Petersen, C.C.H. (2011). Synaptic mechanisms underlying sparse coding of active touch. Neuron 69, 1160-1175.*

*Cruikshank, S.J., Lewis, T.J., and Connors, B.W. (2007). Synaptic basis for intense thalamocortical activation of feedforward inhibitory cells in neocortex. Nat Neurosci 10, 462-468.*

*Cruikshank, S.J., Urabe, H., Nurmikko, A.V., and Connors, B.W. (2010). Pathway-specific feedforward circuits between thalamus and neocortex revealed by selective optical stimulation of axons. Neuron 65, 230-245.*

*Curtis, J.C., and Kleinfeld, D. (2009). Phase-to-rate transformations encode touch in cortical neurons of a scanning sensorimotor system. Nat Neurosci 12, 492-501.*

*Dani, J.A., and Bertrand, D. (2007). Nicotinic acetylcholine receptors and nicotinic cholinergic mechanisms of the central nervous system. Annu Rev Pharmacol Toxicol 47, 699-729.*

*Das, S., Weiss, C., and Disterhoft, J.F. (2001). Eyeblink conditioning in the rabbit (Oryctolagus cuniculus) with stimulation of the mystacial vibrissae as a conditioned stimulus. Behav Neurosci 115, 731-736.*

*Dauvergne, C., Pinganaud, G., Buisseret, P., Buisseret-Delmas, C., and Zerari-Mailly, F. (2001). Reticular premotor neurons projecting to both facial and hypoglossal nuclei receive trigeminal afferents in rats. Neurosci Lett 311, 109-112.*

*Davie, J.T., Clark, B.A., and Häusser, M. (2008). The origin of the complex spike in cerebellar Purkinje cells. J Neurosci 28, 7599-7609.*

*De Kock, C.P.J., Bruno, R.M., Spors, H., and Sakmann, B. (2007). Layer and cell type specific suprathreshold stimulus representation in primary somatosensory cortex. J Physiol 581, 139.*

*De Kock, C.P.J., and Sakmann, B. (2009). Spiking in primary somatosensory cortex during natural whisking in awake head-restrained rats is cell-type specific. Proc Natl Acad Sci U S A 106, 16446-16450.*

*De Zeeuw, C.I., Hoebeek, F.E., Bosman, L.W.J., Schonewille, M., Witter, L., and Koekkoek, S.K. (2011). Spatiotemporal firing patterns in the cerebellum. Nat Rev Neurosci 12, 327-344.*

*De Zeeuw, C.I., and Yeo, C.H. (2005). Time and tide in cerebellar memory formation. Curr Opin Neurobiol 15, 667-674.*

*Dehnhardt, G., Hyvärinen, H., Palviainen, A., and Klauer, G. (1999). Structure and innervation of the vibrissal follicle-sinus complex in the Australian water rat, Hydromys chrysogaster. J Comp Neurol 411, 550-562.*

*Dehnhardt, G., and Kaminski, A. (1995). Sensitivity of the mystacial vibrissae of harbour seals (Phoca vitulina) for size differences of actively touched objects. J Exp Biol 198, 2317-2323.*

*Dehnhardt, G., Mauck, B., Hanke, W., and Bleckmann, H. (2001). Hydrodynamic trail-following in harbor seals (Phoca vitulina). Science 293, 102-104.*

*Dehnhardt, G., Mauck, B., and Hyvärinen, H. (1998). Ambient temperature does not affect the tactile sensitivity of mystacial vibrissae in harbour seals. J Exp Biol 201***,** *3023-3029.*
*Delgado-García, J.M., López-Barneo, J., Serra, R., and González-Barón, S. (1983). Electrophysiological and functional identification of different neuronal types within the nucleus ambiguus in the cat. Brain Res 277***,** *231-240.*
*Deschênes, M., Timofeeva, E., Lavallée, P., and Dufresne, C. (2005). The vibrissal system as a model of thalamic operations. Prog Brain Res 149***,** *31-40.*
*Deschênes, M., Veinante, P., and Zhang, Z.W. (1998). The organization of corticothalamic projections: reciprocity versus parity. Brain Res Brain Res Rev 28***,** *286-308.*
*Desilets-Roy, B., Varga, C., Lavallée, P., and Deschênes, M. (2002). Substrate for cross-talk inhibition between thalamic barreloids. J Neurosci 22***,** *RC218.*
*Deurveilher, S., and Semba, K. (2011). Basal forebrain regulation of cortical activity and sleep-wake states: Roles of cholinergic and non-cholinergic neurons. Sleep Biol Rhythms 9***,** *65-70.*
*Di Chiara, G., Porceddu, M.L., Morelli, M., Mulas, M.L., and Gessa, G.L. (1979). Evidence for a GABAergic projection from the substantia nigra to the ventromedial thalamus and to the superior colliculus of the rat. Brain Res 176***,** *273-284.*
*Di Matteo, V., Pierucci, M., Esposito, E., Crescimanno, G., Benigno, A., and Di Giovanni, G. (2008). Serotonin modulation of the basal ganglia circuitry: therapeutic implication for Parkinson's disease and other motor disorders. Prog Brain Res 172***,** *423-463.*
*Diamond, M.E., Armstrong-James, M., Budway, M.J., and Ebner, F.F. (1992a). Somatic sensory responses in the rostral sector of the posterior group (POm) and in the ventral posterior medial nucleus (VPM) of the rat thalamus: dependence on the barrel field cortex. J Comp Neurol 319***,** *66-84.*
*Diamond, M.E., Armstrong-James, M., and Ebner, F.F. (1992b). Somatic sensory responses in the rostral sector of the posterior group (POm) and in the ventral posterior medial nucleus (VPM) of the rat thalamus. J Comp Neurol 318***,** *462-476.*
*Diamond, M.E., von Heimendahl, M., Knutsen, P.M., Kleinfeld, D., and Ahissar, E. (2008). 'Where' and 'what' in the whisker sensorimotor system. Nat Rev Neurosci 9***,** *601-612.*
*Dörfl, J. (1982). The musculature of the mystacial vibrissae of the white mouse. J Anat 135***,** *147-154.*
*Dörfl, J. (1985). The innervation of the mystacial region of the white mouse: A topographical study. J Anat 142***,** *173-184.*
*Ebara, S., Kumamoto, K., Matsuura, T., Mazurkiewicz, J.E., and Rice, F.L. (2002). Similarities and differences in the innervation of mystacial vibrissal follicle-sinus complexes in the rat and cat: a confocal microscopic study. J Comp Neurol 449***,** *103-119.*
*Eccles, J., Llinás, R., and Sasaki, K. (1964). Excitation of cerebellar Purkinje cells by the climbing fibres. Nature 203***,** *245-246.*
*Eller, T., and Chan-Palay, V. (1976). Afferents to the cerebellar lateral nucleus. Evidence from retrograde transport of horseradish peroxidase after pressure injections through micropipettes. J Comp Neurol 166***,** *285-301.*
*Erzurumlu, R.S., Bates, C.A., and Killackey, H.P. (1980). Differential organization of thalamic projection cells in the brain stem trigeminal complex of the rat. Brain Res 198***,** *427-433.*
*Erzurumlu, R.S., and Killackey, H.P. (1979). Efferent connections of the brainstem trigeminal complex with the facial nucleus of the rat. J Comp Neurol 188***,** *75-86.*
*Erzurumlu, R.S., and Killackey, H.P. (1980). Diencephalic projections of the subnucleus interpolaris of the brainstem trigeminal complex in the rat. Neuroscience 5***,** *1891-1901.*
*Erzurumlu, R.S., and Killackey, H.P. (1983). Development of order in the rat trigeminal system. J Comp Neurol 213***,** *365-380.*
*Erzurumlu, R.S., Murakami, Y., and Rijli, F.M. (2010). Mapping the face in the somatosensory*

*brainstem. Nat Rev Neurosci 11, 252-263.*

*Esakov, S.A., and Pronichev, I.V. (2001). Movement representations of facial muscles and vibrissae in cerebellar cortex of the white mouse Mus musculus. J Evol Biochem Phys 37, 642-647.*

*Esposito, E., Di Matteo, V., and Di Giovanni, G. (2007). Death in the substantia nigra: a motor tragedy. Expert Rev Neurother 7, 677-697.*

*Fabri, M., and Burton, H. (1991). Ipsilateral cortical connections of primary somatic sensory cortex in rats. J Comp Neurol 311, 405-424.*

*Favaro, P.D.N., Gouvêa, T.S., de Oliveira, S.R., Vautrelle, N., Redgrave, P., and Comoli, E. (2011). The influence of vibrissal somatosensory processing in rat superior colliculus on prey capture. Neuroscience 176, 318-327.*

*Fee, M.S., Mitra, P.P., and Kleinfeld, D. (1997). Central versus peripheral determinants of patterned spike activity in rat vibrissa cortex during whisking. J Neurophysiol 78, 1144-1149.*

*Feldmeyer, D., Lübke, J., Silver, R.A., and Sakmann, B. (2002). Synaptic connections between layer 4 spiny neurone-layer 2/3 pyramidal cell pairs in juvenile rat barrel cortex: physiology and anatomy of interlaminar signalling within a cortical column. J Physiol 538, 803-822.*

*Feldmeyer, D., Roth, A., and Sakmann, B. (2005). Monosynaptic connections between pairs of spiny stellate cells in layer 4 and pyramidal cells in layer 5A indicate that lemniscal and paralemniscal afferent pathways converge in the infragranular somatosensory cortex. J Neurosci 25, 3423-3431.*

*Ferezou, I., Haiss, F., Gentet, L.J., Aronoff, R., Weber, B., and Petersen, C.C.H. (2007). Spatiotemporal dynamics of cortical sensorimotor integration in behaving mice. Neuron 56, 907-923.*

*Fitzgerald, O. (1940). Discharges from the sensory organs of the cat's vibrissae and the modification in their activity by ions. J Physiol 98, 163-178.*

*Foster, G.A., Sizer, A.R., Rees, H., and Roberts, M.H.T. (1989). Afferent projections to the rostral anterior pretectal nucleus of the rat: a possible role in the processing of noxious stimuli. Neuroscience 29, 685-694.*

*Fundin, B.T., Rice, F.L., Pfaller, K., and Arvidsson, J. (1994). The innervation of the mystacial pad in the adult rat studied by anterograde transport of HRP conjugates. Exp Brain Res 99, 233-246.*

*Furuta, T., Kaneko, T., and Deschênes, M. (2009). Septal neurons in barrel cortex derive their receptive field input from the lemniscal pathway. J Neurosci 29, 4089-4095.*

*Furuta, T., Timofeeva, E., Nakamura, K., Okamoto-Furuta, K., Togo, M., Kaneko, T., and Deschenes, M. (2008). Inhibitory gating of vibrissal inputs in the brainstem. J Neurosci 28, 1789-1797.*

*Furuta, T., Urbain, N., Kaneko, T., and Deschênes, M. (2010). Corticofugal control of vibrissa-sensitive neurons in the interpolaris nucleus of the trigeminal complex. J Neurosci 30, 1832-1838.*

*Gabernet, L., Jadhav, S.P., Feldman, D.E., Carandini, M., and Scanziani, M. (2005). Somatosensory integration controlled by dynamic thalamocortical feed-forward inhibition. Neuron 48, 315-327.*

*Galvez, R., Weiss, C., Cua, S., and Disterhoft, J. (2009). A novel method for precisely timed stimulation of mouse whiskers in a freely moving preparation: application for delivery of the conditioned stimulus in trace eyeblink conditioning. J Neurosci Methods 177, 434-439.*

*Gandhi, N.J., and Katnani, H.A. (2011). Motor functions of the superior colliculus. Annu Rev Neurosci 34, 205-231.*

*Ganmor, E., Katz, Y., and Lampl, I. (2010). Intensity-dependent adaptation of cortical and thalamic neurons is controlled by brainstem circuits of the sensory pathway. Neuron 66, 273-286.*

*Gao, P., Hattox, A.M., Jones, L.M., Keller, A., and Zeigler, H.P. (2003). Whisker motor cortex ablation and whisker movement patterns. Somatosens Mot Res 20***,** *191-198.*

*Gellman, R., Gibson, A.R., and Houk, J.C. (1985). Inferior olivary neurons in the awake cat: detection of contact and passive body displacement. J Neurophysiol 54***,** *40-60.*

*Gentet, L.J., Avermann, M., Matyas, F., Staiger, J.F., and Petersen, C.C.H. (2010). Membrane potential dynamics of GABAergic neurons in the barrel cortex of behaving mice. Neuron 65***,** *422-435.*

*Gerdjikov, T.V., Bergner, C.G., Stüttgen, M.C., Waiblinger, C., and Schwarz, C. (2010). Discrimination of vibrotactile stimuli in the rat whisker system: behavior and neurometrics. Neuron 65***,** *530-540.*

*Gibb, W.R.G., and Lees, A.J. (1988). The relevance of the Lewy body to the pathogenesis of idiopathic Parkinson's disease. J Neurol Neurosurg Psychiatry 51***,** *745-752.*

*Giber, K., Slézia, A., Bokor, H., Bodor, A.L., Ludányi, A., Katona, I., and Acsády, L. (2008). Heterogeneous output pathways link the anterior pretectal nucleus with the zona incerta and the thalamus in rat. J Comp Neurol 506***,** *122-140.*

*Gibson, A.R., Horn, K.M., and Pong, M. (2004). Activation of climbing fibers. Cerebellum 3***,** *212-221.*

*Gibson, J.M., and Welker, W.I. (1983). Quantitative studies of stimulus coding in first-order vibrissa afferents of rats. 1. Receptive field properties and threshold distributions. Somatosens Mot Res 1***,** *51-67.*

*Gioanni, Y., and Lamarche, M. (1985). A reappraisal of rat motor cortex organization by intracortical microstimulation. Brain Res 344***,** *49-61.*

*Gogan, P., Guéritaud, J.P., Horcholle-Bossavit, G., and Tyc-Dumont, S. (1981). The vibrissal pad as a source of sensory information for the oculomotor system of the cat. Exp Brain Res 44***,** *409-418.*

*Gompf, H.S., Mathai, C., Fuller, P.M., Wood, D.A., Pedersen, N.P., Saper, C.B., and Lu, J. (2010). Locus ceruleus and anterior cingulate cortex sustain wakefulness in a novel environment. J Neurosci 30***,** *14543-14551.*

*Gonzales, C., and Chesselet, M.F. (1990). Amygdalonigral pathway: an anterograde study in the rat with Phaseolus vulgaris leucoagglutinin (PHA-L). J Comp Neurol 297***,** *182-200.*

*Gottschaldt, K.M., Iggo, A., and Young, D.W. (1973). Functional characteristics of mechanoreceptors in sinus hair follicles of the cat. J Physiol 235***,** *287-315.*

*Graeff, F.G. (2004). Serotonin, the periaqueductal gray and panic. Neurosci Biobehav Rev 28***,** *239-259.*

*Grant, R.A., Mitchinson, B., Fox, C.W., and Prescott, T.J. (2009). Active touch sensing in the rat: anticipatory and regulatory control of whisker movements during surface exploration. J Neurophysiol 101***,** *862-874.*

*Grinevich, V., Brecht, M., and Osten, P. (2005). Monosynaptic pathway from rat vibrissa motor cortex to facial motor neurons revealed by lentivirus-based axonal tracing. J Neurosci 25***,** *8250-8258.*

*Groenewegen, H.J., and Witter, M.P. (2004). "Thalamus," in The rat nervous system, ed. P. G. Third ed (Sydney: Academic Press), 407-453.*

*Grofova, I., Deniau, J.M., and Kitai, S.T. (1982). Morphology of the substantia nigra pars reticulata projection neurons intracellularly labeled with HRP. J Comp Neurol 208***,** *352-368.*

*Groh, A., de Kock, C.P.J., Wimmer, V.C., Sakmann, B., and Kuner, T. (2008). Driver or coincidence detector: modal switch of a corticothalamic giant synapse controlled by spontaneous activity and short-term depression. J Neurosci 28***,** *9652-9663.*

*Guillery, R.W., and Harting, J.K. (2003). Structure and connections of the thalamic reticular nucleus: Advancing views over half a century. J Comp Neurol 463***,** *360-371.*

*Haidarliu, S., and Ahissar, E. (2001). Size gradients of barreloids in the rat thalamus. J Comp*

*Neurol 429, 372-387.*

*Haidarliu, S., Simony, E., Golomb, D., and Ahissar, E. (2010). Muscle architecture in the mystacial pad of the rat. Anat Rec (Hoboken) 293, 1192-1206.*

*Haiss, F., and Schwarz, C. (2005). Spatial segregation of different modes of movement control in the whisker representation of rat primary motor cortex. J Neurosci 25, 1579-1587.*

*Halata, Z., Grim, M., and Baumann, K.I. (2010). Current understanding of Merkel cells, touch reception and the skin. Exp Rev Dermatol 5, 109-116.*

*Hale, M.W., and Lowry, C.A. (2011). Functional topography of midbrain and pontine serotonergic systems: implications for synaptic regulation of serotonergic circuits. Psychopharmacology (Berl) 213, 243-264.*

*Hammond, C., Deniau, J.M., Rouzaire-Dubois, B., and Feger, J. (1978). Pepipheral input to the rat subthalamic nucleus, an electrophysiological study. Neurosci Lett 9, 171-176.*

*Haring, J.H., and Wang, R.Y. (1986). The identification of some sources of afferent input to the rat nucleus basalis magnocellularis by retrograde transport of horseradish peroxidase. Brain Res 366, 152-158.*

*Hartings, J.A., Temereanca, S., and Simons, D.J. (2003). Processing of periodic whisker deflections by neurons in the ventroposterior medial and thalamic reticular nuclei. J Neurophysiol 90, 3087-3094.*

*Hartmann, M.J.Z. (2009). Active touch, exploratory movements, and sensory prediction. Integr Comp Biol 49, 681-690.*

*Hartmann, M.J.Z. (2011). A night in the life of a rat: vibrissal mechanics and tactile exploration. Ann N Y Acad Sci 1225, 110-118.*

*Harvey, M.A., Bermejo, R., and Zeigler, H.P. (2001). Discriminative whisking in the head-fixed rat: optoelectronic monitoring during tactile detection and discrimination tasks. Somatosens Mot Res 18, 211-222.*

*Hattox, A., Li, Y., and Keller, A. (2003). Serotonin regulates rhythmic whisking. Neuron 39, 343-352.*

*Hattox, A.M., Priest, C.A., and Keller, A. (2002). Functional circuitry involved in the regulation of whisker movements. J Comp Neurol 442, 266-276.*

*Hayashi, H. (1980). Distributions of vibrissae afferent fiber collaterals in the trigeminal nuclei as revealed by intra-axonal injection of horseradish peroxidase. Brain Res 183, 442-446.*

*Heise, C.E., and Mitrofanis, J. (2004). Evidence for a glutamatergic projection from the zona incerta to the basal ganglia of rats. J Comp Neurol 468, 482-495.*

*Helmstaedter, M., Sakmann, B., and Feldmeyer, D. (2009). Neuronal correlates of local, lateral, and translaminar inhibition with reference to cortical columns. Cereb Cortex 19, 926-937.*

*Hemelt, M.E., and Keller, A. (2008). Superior colliculus control of vibrissa movements. J Neurophysiol 100, 1245-1254.*

*Herfst, L.J., and Brecht, M. (2008). Whisker movements evoked by stimulation of single motor neurons in the facial nucleus of the rat. J Neurophysiol 99, 2821-2832.*

*Hikosaka, O., Nakamura, K., and Nakahara, H. (2006). Basal ganglia orient eyes to reward. J Neurophysiol 95, 567-584.*

*Hill, D.N., Bermejo, R., Zeigler, H.P., and Kleinfeld, D. (2008). Biomechanics of the vibrissa motor plant in rat: rhythmic whisking consists of triphasic neuromuscular activity. J Neurosci 28, 3438-3455.*

*Hirata, A., Aguilar, J., and Castro-Alamancos, M.A. (2006). Noradrenergic activation amplifies bottom-up and top-down signal-to-noise ratios in sensory thalamus. J Neurosci 26, 4426-4436.*

*Hirata, A., and Castro-Alamancos, M.A. (2010). Neocortex network activation and* *deactivation states controlled by the thalamus. J Neurophysiol 103, 1147-1157.*

*Hirata, A., and Castro-Alamancos, M.A. (2011). Effects of cortical activation on sensory responses in barrel cortex. J Neurophysiol 105, 1495-1505.*

*Hoeflinger, B.F., Bennett-Clarke, C.A., Chiaia, N.L., Killackey, H.P., and Rhoades, R.W. (1995). Patterning of local intracortical projections within the vibrissae representation of rat primary somatosensory cortex. J Comp Neurol 354, 551-563.*

*Hoffer, Z.S., Hoover, J.E., and Alloway, K.D. (2003). Sensorimotor corticocortical projections from rat barrel cortex have an anisotropic organization that facilitates integration of inputs from whiskers in the same row. J Comp Neurol 466, 525-544.*

*Hollis, D.E., and Lyne, A.G. (1974). Innervation of vibrissa follicles in the marsupial Trichosurus vulpecula. Austr J Zool 22, 263-276.*

*Hong, E.Y., Beak, S.K., and Lee, H.S. (2010). Dual projections of tuberomammillary neurons to whisker-related, sensory and motor regions of the rat. Brain Res 1354, 64-73.*

*Hoogland, P.V., Welker, E., and Van der Loos, H. (1987). Organization of the projections from barrel cortex to thalamus in mice studied with Phaseolus vulgaris-leucoagglutinin and HRP. Exp Brain Res 68, 73-87.*

*Hoogland, P.V., Wouterlood, F.G., Welker, E., and Van der Loos, H. (1991). Ultrastructure of giant and small thalamic terminals of cortical origin: a study of the projections from the barrel cortex in mice using Phaseolus vulgaris leuco-agglutinin (PHA-L). Exp Brain Res 87, 159-172.*

*Hooks, B.M., Hires, S.A., Zhang, Y.X., Huber, D., Petreanu, L., Svoboda, K., and Shepherd, G.M.G. (2011). Laminar analysis of excitatory local circuits in vibrissal motor and sensory cortical areas. PLoS Biol 9, e1000572.*

*Hoshi, E., Tremblay, L., Féger, J., Carras, P.L., and Strick, P.L. (2005). The cerebellum communicates with the basal ganglia. Nat Neurosci 8, 1491-1493.*

*Huber, D., Petreanu, L., Ghitani, N., Ranade, S., Hromádka, T., Mainen, Z., and Svoboda, K. (2008). Sparse optical microstimulation in barrel cortex drives learned behaviour in freely moving mice. Nature 451, 61-64.*

*Huerta, M.F., Frankfurter, A., and Harting, J.K. (1983). Studies of the principal sensory and spinal trigeminal nuclei of the rat: projections to the superior colliculus, inferior olive, and cerebellum. J Comp Neurol 220, 147-167.*

*Hutson, K.A., and Masterton, R.B. (1986). The sensory contribution of a single vibrissa's cortical barrel. J Neurophysiol 56, 1196-1223.*

*Hyvärinen, H., Palviainen, A., Strandberg, U., and Holopainen, I.J. (2009). Aquatic environment and differentiation of vibrissae: comparison of sinus hair systems of ringed seal, otter and pole cat. Brain Behav Evol 74, 268-279.*

*Irle, E., and Markowitsch, H.J. (1986). Afferent connections of the substantia innominata/basal nucleus of Meynert in carnivores and primates. J Hirnforsch 27, 343-367.*

*Isokawa-Akesson, M., and Komisaruk, B.R. (1987). Difference in projections to the lateral and medial facial nucleus: anatomically separate pathways for rhythmical vibrissa movement in rats. Exp Brain Res 65, 385-398.*

*Ito, M. (1988). Response properties and topography of vibrissa-sensitive VPM neurons in the rat. J Neurophysiol 60, 1181-1197.*

*Ito, M. (2000). Mechanisms of motor learning in the cerebellum. Brain Res 886, 237-245.*

*Izraeli, R., and Porter, L.L. (1995). Vibrissal motor cortex in the rat: connections with the barrel field. Exp Brain Res 104, 41-54.*

*Jacquin, M.F., Barcia, M., and Rhoades, R.W. (1989a). Structure-function relationships in rat brainstem subnucleus interpolaris: IV. Projection neurons. J Comp Neurol 282, 45-62.*

*Jacquin, M.F., Golden, J., and Rhoades, R.W. (1989b). Structure-function relationships in rat brainstem subnucleus interpolaris: III. Local circuit neurons. J Comp Neurol 282, 24-44.*

*Jacquin, M.F., and Rhoades, R.W. (1990). Cell structure and response properties in the trigeminal subnucleus oralis. Somatosens Mot Res 7***,** *265-288.*

*Jadhav, S.P., and Feldman, D.E. (2010). Texture coding in the whisker system. Curr Opin Neurobiol 20***,** *313-318.*

*Jadhav, S.P., Wolfe, J., and Feldman, D.E. (2009). Sparse temporal coding of elementary tactile features during active whisker sensation. Nat Neurosci 12***,** *792-800.*

*Jin, T.E., Witzemann, V., and Brecht, M. (2004). Fiber types of the intrinsic whisker muscle and whisking behavior. J Neurosci 24***,** *3386-3393.*

*Joel, D., and Weiner, I. (1997). The connections of the primate subthalamic nucleus: indirect pathways and the open-interconnected scheme of basal ganglia-thalamocortical circuitry. Brain Res Brain Res Rev 23***,** *62-78.*

*Jones, B.E. (1990). Immunohistochemical study of choline acetyltransferase-immunoreactive processes and cells innervating the pontomedullary reticular formation in the rat. J Comp Neurol 295***,** *485-514.*

*Jones, B.E. (1991). Noradrenergic locus coeruleus neurons: their distant connections and their relationship to neighboring (including cholinergic and GABAergic) neurons of the central gray and reticular formation. Prog Brain Res 88***,** *15-30.*

*Jones, L.M., Depireux, D.A., Simons, D.J., and Keller, A. (2004). Robust temporal coding in the trigeminal system. Science 304***,** *1986-1989.*

*Joseph, J.W., Shambes, G.M., Gibson, J.M., and Welker, W. (1978). Tactile projections to granule cells in caudal vermis of the rat's cerebellum. Brain Behav Evol 15***,** *141-149.*

*Kaneda, K., Isa, K., Yanagawa, Y., and Isa, T. (2008). Nigral inhibition of GABAergic neurons in mouse superior colliculus. J Neurosci 28***,** *11071-11078.*

*Kätzel, D., Zemelman, B.V., Buetfering, C., Wölfel, M., and Miesenböck, G. (2011). The columnar and laminar organization of inhibitory connections to neocortical excitatory cells. Nat Neurosci 14***,** *100-107.*

*Kelley, A.E., Domesick, V.B., and Nauta, W.J.H. (1982). The amygdalostriatal projection in the rat--an anatomical study by anterograde and retrograde tracing methods. Neuroscience 7***,** *615-630.*

*Kennedy, T.T., Grimm, R.J., and Towe, A.L. (1966). The role of cerebral cortex in evoked somatosensory activity in cat cerebellum. Exp Neurol 14***,** *13-32.*

*Kerr, F.W.L., and Lysak, W.R. (1964). Somatotopic organization of trigeminal-ganglion neurones. Arch Neurol 11***,** *593-602.*

*Kerr, J.N.D., De Kock, C.P.J., Greenberg, D.S., Bruno, R.M., Sakmann, B., and Helmchen, F. (2007). Spatial organization of neuronal population responses in layer 2/3 of rat barrel cortex. J Neurosci 27***,** *13316-13328.*

*Khatri, V., Bermejo, R., Brumberg, J.C., Keller, A., and Zeigler, H.P. (2009). Whisking in air: Encoding of kinematics by trigeminal ganglion neurons in awake rats. J Neurophysiol 101***,** *1836-1846.*

*Killackey, H.P. (1973). Anatomical evidence for cortical subdivisions based on vertically discrete thalamic projections from the ventral posterior nucleus to cortical barrels in the rat. Brain Res 51***,** *326-331.*

*Killackey, H.P., and Sherman, S.M. (2003). Corticothalamic projections from the rat primary somatosensory cortex. J Neurosci 23***,** *7381-7384.*

*Kim, J.N., Koh, K.S., Lee, E., Park, S.C., and Song, W.C. (2011). The morphology of the rat vibrissal follicle-sinus complex revealed by three-dimensional computer-aided reconstruction. Cells Tissues Organs 193***,** *207-214.*

*Kim, U., and Ebner, F.F. (1999). Barrels and septa: separate circuits in rat barrels field cortex. J Comp Neurol 408***,** *489-505.*

*Kim, U., Gregory, E., and Hall, W.C. (1992). Pathway from the zona incerta to the superior* *colliculus in the rat. J Comp Neurol 321, 555-575.*

*Kirifides, M.L., Simpson, K.L., Lin, R.C.S., and Waterhouse, B.D. (2001). Topographic organization and neurochemical identity of dorsal raphe neurons that project to the trigeminal somatosensory pathway in the rat. J Comp Neurol 435, 325-340.*

*Kita, H. (2007). Globus pallidus external segment. Prog Brain Res 160, 111-133.*

*Kita, H., and Kitai, S.T. (1987). Efferent projections of the subthalamic nucleus in the rat: light and electron microscopic analysis with the PHA-L method. J Comp Neurol 260, 435-452.*

*Klein, B.G., and Rhoades, R.W. (1985). Representation of whisker follicle intrinsic musculature in the facial motor nucleus of the rat. J Comp Neurol 232, 55-69.*

*Kleinfeld, D., Berg, R.W., and O'Connor, S.M. (1999). Anatomical loops and their electrical dynamics in relation to whisking by rat. Somatosens Mot Res 16, 69-88.*

*Knutsen, P.M., Pietr, M., and Ahissar, E. (2006). Haptic object localization in the vibrissal system: behavior and performance. J Neurosci 26, 8451-8464.*

*Kocsis, B., Varga, V., Dahan, L., and Sik, A. (2006). Serotonergic neuron diversity: identification of raphe neurons with discharges time-locked to the hippocampal theta rhythm. Proc Natl Acad Sci U S A 103, 1059-1064.*

*Kolmac, C.I., Power, B.D., and Mitrofanis, J. (1998). Patterns of connections between zona incerta and brainstem in rats. J Comp Neurol 396, 544-555.*

*Koralek, K.A., Jensen, K.F., and Killackey, H.P. (1988). Evidence for two complementary patterns of thalamic input to the rat somatosensory cortex. Brain Res 463, 346-351.*

*Koralek, K.A., Olavarria, J., and Killackey, H.P. (1990). Areal and laminar organization of corticocortical projections in the rat somatosensory cortex. J Comp Neurol 299, 133-150.*

*Krakauer, J.W., and Shadmehr, R. (2006). Consolidation of motor memory. Trends Neurosci 29, 58-64.*

*Krupa, D.J., Matell, M.S., Brisben, A.J., Oliveira, L.M., and Nicolelis, M.A.L. (2001). Behavioral properties of the trigeminal somatosensory system in rats performing whisker-dependent tactile discriminations. J Neurosci 21, 5752-5763.*

*Krupa, D.J., Wiest, M.C., Shuler, M.G., Laubach, M., and Nicolelis, M.A.L. (2004). Layer-specific somatosensory cortical activation during active tactile discrimination. Science 304, 1989-1992.*

*Kuo, M.C., Rasmusson, D.D., and Dringenberg, H.C. (2009). Input-selective potentiation and rebalancing of primary sensory cortex afferents by endogenous acetylcholine. Neuroscience 163, 430-441.*

*Kwegyir-Afful, E.E., and Keller, A. (2004). Response properties of whisker-related neurons in rat second somatosensory cortex. J Neurophysiol 92, 2083-2092.*

*Lam, Y.W., and Sherman, S.M. (2010). Functional organization of the somatosensory cortical layer 6 feedback to the thalamus. Cereb Cortex 20, 13-24.*

*Lam, Y.W., and Sherman, S.M. (2011). Functional organization of the thalamic input to the thalamic reticular nucleus. J Neurosci 31, 6791-6799.*

*Land, P.W., Buffer, S.A., Jr., and Yaskosky, J.D. (1995). Barreloids in adult rat thalamus: three-dimensional architecture and relationship to somatosensory cortical barrels. J Comp Neurol 355, 573-588.*

*Lang, E.J. (2002). GABAergic and glutamatergic modulation of spontaneous and motor-cortex-evoked complex spike activity. J Neurophysiol 87, 1993-2008.*

*Lang, E.J., Sugihara, I., and Llinás, R. (2006). Olivocerebellar modulation of motor cortex ability to generate vibrissal movements in rat. J Physiol 571, 101-120.*

*Langford, D.J., Bailey, A.L., Chanda, M.L., Clarke, S.E., Drummond, T.E., Echols, S., Glick, S., Ingrao, J., Klassen-Ross, T., Lacroix-Fralish, M.L., Matsumiya, L., Sorge, R.E., Sotocinal, S.G., Tabaka, J.M., Wong, D., van den Maagdenberg, A.M.J.M., Ferrari, M.D., Craig, K.D., and Mogil, J.S. (2010). Coding of facial expressions of pain in the laboratory mouse. Nat*

Methods 7, 447-449.

Larsen, D.D., Wickersham, I.R., and Callaway, E.M. (2007). Retrograde tracing with recombinant rabies virus reveals correlations between projection targets and dendritic architecture in layer 5 of mouse barrel cortex. Front Neural Circuits 1, 5.

Lavallée, P., Urbain, N., Dufresne, C., Bokor, H., Acsády, L., and Deschênes, M. (2005). Feedforward inhibitory control of sensory information in higher-order thalamic nuclei. J Neurosci 25, 7489-7498.

Lazarov, N.E. (2002). Comparative analysis of the chemical neuroanatomy of the mammalian trigeminal ganglion and mesencephalic trigeminal nucleus. Prog Neurobiol 66, 19-59.

Leal-Campanario, R., Delgado-García, J.M., and Gruart, A. (2006). Microstimulation of the somatosensory cortex can substitute for vibrissa stimulation during Pavlovian conditioning. Proc Natl Acad Sci U S A 103, 10052-10057.

Lee, H.S., Kim, M.A., Valentino, R.J., and Waterhouse, B.D. (2003). Glutamatergic afferent projections to the dorsal raphe nucleus of the rat. Brain Res 963, 57-71.

Lee, M.G., Hassani, O.K., Alonso, A., and Jones, B.E. (2005). Cholinergic basal forebrain neurons burst with theta during waking and paradoxical sleep. J Neurosci 25, 4365-4369.

Lee, S., Carvell, G.E., and Simons, D.J. (2008a). Motor modulation of afferent somatosensory circuits. Nat Neurosci 11, 1430-1438.

Lee, S.B., Chang, B.J., and Lee, H.S. (2008b). Organization of histamine-immunoreactive, tuberomammillary neurons projecting to the dorsal tier of the substantia nigra compacta in the rat. Brain Res 1203, 79-88.

Lee, S.B., Lee, H.S., and Waterhouse, B.D. (2008c). The collateral projection from the dorsal raphe nucleus to whisker-related, trigeminal sensory and facial motor systems in the rat. Brain Res 1214, 11-22.

Leergaard, T.B., Alloway, K.D., Pham, T.A.T., Bolstad, I., Hoffer, Z.S., Pettersen, C., and Bjaalie, J.G. (2004). Three-dimensional topography of corticopontine projections from rat sensorimotor cortex: comparisons with corticostriatal projections reveal diverse integrative organization. J Comp Neurol 478, 306-322.

Leergaard, T.B., Lillehaug, S., De Schutter, E., Bower, J.M., and Bjaalie, J.G. (2006). Topographical organization of pathways from somatosensory cortex through the pontine nuclei to tactile regions of the rat cerebellar hemispheres. Eur J Neurosci 24, 2801-2812.

Lefort, S., Tomm, C., Floyd Sarria, J.C., and Petersen, C.C.H. (2009). The excitatory neuronal network of the C2 barrel column in mouse primary somatosensory cortex. Neuron 61, 301-316.

Legg, C.R., Mercier, B., and Glickstein, M. (1989). Corticopontine projection in the rat: the distribution of labelled cortical cells after large injections of horseradish peroxidase in the pontine nuclei. J Comp Neurol 286, 427-441.

Leiser, S.C., and Moxon, K.A. (2006). Relationship between physiological response type (RA and SA) and vibrissal receptive field of neurons within the rat trigeminal ganglion. J Neurophysiol 95, 3129-3145.

Leiser, S.C., and Moxon, K.A. (2007). Responses of trigeminal ganglion neurons during natural whisking behaviors in the awake rat. Neuron 53, 117-133.

Leite-Almeida, H., Valle-Fernandes, A., and Almeida, A. (2006). Brain projections from the medullary dorsal reticular nucleus: an anterograde and retrograde tracing study in the rat. Neuroscience 140, 577-595.

Li, Y., Erzurumlu, R.S., Chen, C., Jhaveri, S., and Tonegawa, S. (1994). Whisker-related neuronal patterns fail to develop in the trigeminal brainstem nuclei of NMDAR1 knockout mice. Cell 76, 427-437.

Lichtenstein, S.H., Carvell, G.E., and Simons, D.J. (1990). Responses of rat trigeminal ganglion neurons to movements of vibrissae in different directions. Somatosens Mot Res 7, *47-65.*

*Lin, C.S., Nicolelis, M.A.L., Schneider, J.S., and Chapin, J.K. (1990). A major direct GABAergic pathway from zona incerta to neocortex. Science 248, 1553-1556.*

*Loewenstein, Y., Mahon, S., Chadderton, P., Kitamura, K., Sompolinsky, H., Yarom, Y., and Häusser, M. (2005). Bistability of cerebellar Purkinje cells modulated by sensory stimulation. Nat Neurosci 8, 202-211.*

*Lu, S.M., and Lin, R.C.S. (1993). Thalamic afferents of the rat barrel cortex: a light- and electron-microscopic study using Phaseolus vulgaris leucoagglutinin as an anterograde tracer. Somatosens Mot Res 10, 1-16.*

*Lübke, J., Egger, V., Sakmann, B., and Feldmeyer, D. (2000). Columnar organization of dendrites and axons of single and synaptically coupled excitatory spiny neurons in layer 4 of the rat barrel cortex. J Neurosci 20, 5300-5311.*

*Lübke, J., and Feldmeyer, D. (2007). Excitatory signal flow and connectivity in a cortical column: focus on barrel cortex. Brain Struct Funct 212, 3-17.*

*Lumpkin, E.A., Marshall, K.L., and Nelson, A.M. (2010). The cell biology of touch. J Cell Biol 191, 237-248.*

*Ma, P.M. (1991). The barrelettes--architectonic vibrissal representations in the brainstem trigeminal complex of the mouse. I. Normal structural organization. J Comp Neurol 309, 161-199.*

*Ma, T.P., Hu, X.J., Anavi, Y., and Rafols, J.A. (1992). Organization of the zona incerta in the macaque: a Nissl and Golgi study. J Comp Neurol 320, 273-290.*

*Mameli, O., Stanzani, S., Mulliri, G., Pellitteri, R., Caria, M.A., Russo, A., and De Riu, P. (2010). Role of the trigeminal mesencephalic nucleus in rat whisker pad proprioception. Behav Brain Funct 6, 69.*

*Mameli, O., Stanzani, S., Russo, A., Romeo, R., Pellitteri, R., Spatuzza, M., Caria, M.A., and De Riu, P.L. (2008). Hypoglossal nuclei participation in rat mystacial pad control. Pflügers Arch 456, 1189-1198.*

*Manning, K.A., Wilson, J.R., and Uhlrich, D.J. (1996). Histamine-immunoreactive neurons and their innervation of visual regions in the cortex, tectum, and thalamus in the primate Macaca mulatta. J Comp Neurol 373, 271-282.*

*Manns, I.D., Sakmann, B., and Brecht, M. (2004). Sub- and suprathreshold receptive field properties of pyramidal neurones in layers 5A and 5B of rat somatosensory barrel cortex. J Physiol 556, 601-622.*

*Marotte, L.R., Rice, F.L., and Waite, P.M.E. (1992). The morphology and innervation of facial vibrissae in the tammar wallaby, Macropus eugenii. J Anat 180, 401-417.*

*Marti, M., Viaro, R., Guerrini, R., Franchi, G., and Morari, M. (2009). Nociceptin/orphanin FQ modulates motor behavior and primary motor cortex output through receptors located in substantia nigra reticulata. Neuropsychopharmacology 34, 341-355.*

*Masri, R., Trageser, J.C., Bezdudnaya, T., Li, Y., and Keller, A. (2006). Cholinergic regulation of the posterior medial thalamic nucleus. J Neurophysiol 96, 2265-2273.*

*Massion, J. (1988). Red nucleus: past and future. Behav Brain Res 28, 1-8.*

*Matesz, C. (1981). Peripheral and central distribution of fibres of the mesencephalic trigeminal root in the rat. Neurosci Lett 27, 13-17.*

*Matyas, F., Sreenivasan, V., Marbach, F., Wacongne, C., Barsy, B., Mateo, C., Aronoff, R., and Petersen, C.C.H. (2010). Motor control by sensory cortex. Science 330, 1240-1243.*

*May, P.J. (2006). The mammalian superior colliculus: laminar structure and connections. Prog Brain Res 151, 321-378.*

*May, P.J., Sun, W., and Hall, W.C. (1997). Reciprocal connections between the zona incerta and the pretectum and superior colliculus of the cat. Neuroscience 77, 1091-1114.*

*McGinty, D.J., and Harper, R.M. (1976). Dorsal raphe neurons: depression of firing during* *sleep in cats. Brain Res 101, 569-575.*

*McHaffie, J.G., and Stein, B.E. (1982). Eye movements evoked by electrical stimulation in the superior colliculus of rats and hamsters. Brain Res 247, 243-253.*

*McMullen, N.T., Smelser, C.B., and Rice, F.L. (1994). Parvalbumin expression reveals a vibrissa-related pattern in rabbit SI cortex. Brain Res 660, 225-231.*

*Meyer, H.S., Wimmer, V.C., Hemberger, M., Bruno, R.M., de Kock, C.P.J., Frick, A., Sakmann, B., and Helmstaedter, M. (2010a). Cell type-specific thalamic innervation in a column of rat vibrissal cortex. Cereb Cortex 20, 2287-2303.*

*Meyer, H.S., Wimmer, V.C., Oberlaender, M., de Kock, C.P.J., Sakmann, B., and Helmstaedter, M. (2010b). Number and laminar distribution of neurons in a thalamocortical projection column of rat vibrissal cortex. Cereb Cortex 20, 2277-2286.*

*Mihailoff, G.A. (1993). Cerebellar nuclear projections from the basilar pontine nuclei and nucleus reticularis tegmenti pontis as demonstrated with PHA-L tracing in the rat. J Comp Neurol 330, 130-146.*

*Mihailoff, G.A. (1995). Orthograde axonal transport studies of projections from the zona incerta and pretectum to the basilar pontine nuclei in the rat. J Comp Neurol 360, 301-318.*

*Mihailoff, G.A., Kosinski, R.J., Azizi, S.A., and Border, B.G. (1989). Survey of noncortical afferent projections to the basilar pontine nuclei: a retrograde tracing study in the rat. J Comp Neurol 282, 617-643.*

*Miller, E.H. (1975). A comparative study of facial expressions of two species of pinnipeds. Behaviour 53, 268-284.*

*Misgeld, U. (2004). Innervation of the substantia nigra. Cell Tissue Res 318, 107-114.*

*Miskolczy, D. (1931). Über die Endigungsweise der spino-cerebellaren Bahnen. Z Anat Entwicklungsgesch 96, 537-542.*

*Mitchinson, B., Martin, C.J., Grant, R.A., and Prescott, T.J. (2007). Feedback control in active sensing: rat exploratory whisking is modulated by environmental contact. Proc Biol Sci 274, 1035-1041.*

*Mitrofanis, J. (2005). Some certainty for the "zone of uncertainty"? Exploring the function of the zona incerta. Neuroscience 130, 1-15.*

*Mitrofanis, J., and Mikuletic, L. (1999). Organisation of the cortical projection to the zona incerta of the thalamus. J Comp Neurol 412, 173-185.*

*Miyashita, E., Keller, A., and Asanuma, H. (1994). Input-output organization of the rat vibrissal motor cortex. Exp Brain Res 99, 223-232.*

*Miyashita, E., and Mori, S. (1995). The superior colliculus relays signals descending from the vibrissal motor cortex to the facial nerve nucleus in the rat. Neurosci Lett 195, 69-71.*

*Molinari, H.H., Schultze, K.E., and Strominger, N.L. (1996). Gracile, cuneate, and spinal trigeminal projections to inferior olive in rat and monkey. J Comp Neurol 375, 467-480.*

*Moore, R.Y., and Bloom, F.E. (1979). Central catecholamine neuron systems: anatomy and physiology of the norepinephrine and epinephrine systems. Annu Rev Neurosci 2, 113-168.*

*Morisette, J., and Bower, J.M. (1996). Contribution of somatosensory cortex to responses in the rat cerebellar granule cell layer following peripheral tactile stimulation Exp Brain Res 109, 240-250.*

*Mowery, T.M., Harrold, J.B., and Alloway, K.D. (2011). Repeated whisker stimulation evokes invariant neuronal responses in the dorsolateral striatum of anesthetized rats: a potential correlate of sensorimotor habits. J Neurophysiol 105, 2225-2238.*

*Muchlinski, M.N. (2010). A comparative analysis of vibrissa count and infraorbital foramen area in primates and other mammals. J Hum Evol 58, 447-473.*

*Muir, G.D., and Whishaw, I.Q. (2000). Red nucleus lesions impair overground locomotion in rats: a kinetic analysis. Eur J Neurosci 12, 1113-1122.*

*Munz, M., Brecht, M., and Wolfe, J. (2010). Active touch during shrew prey capture. Front*

*Behav Neurosci 4, 191.*

*Murray, P.D., Masri, R., and Keller, A. (2010). Abnormal anterior pretectal nucleus activity contributes to central pain syndrome. J Neurophysiol 103, 3044-3053.*

*Naito, A., and Kita, H. (1994). The cortico-nigral projection in the rat: an anterograde tracing study with biotinylated dextran amine. Brain Res 637, 317-322.*

*Nambu, A. (2007). Globus pallidus internal segment. Prog Brain Res 160, 135-150.*

*Ndiaye, A., Pinganaud, G., VanderWerf, F., Buisseret-Delmas, C., and Buisseret, P. (2000). Connections between the trigeminal mesencephalic nucleus and the superior colliculus in the rat. Neurosci Lett 294, 17-20.*

*Neimark, M.A., Andermann, M.L., Hopfield, J.J., and Moore, C.I. (2003). Vibrissa resonance as a transduction mechanism for tactile encoding. J Neurosci 23, 6499-6509.*

*Nguyen, Q.T., and Kleinfeld, D. (2005). Positive feedback in a brainstem tactile sensorimotor loop. Neuron 45, 447-457.*

*Nicolelis, M.A.L., Baccala, L.A., Lin, R.C.S., and Chapin, J.K. (1995a). Sensorimotor encoding by synchronous neural ensemble activity at multiple levels of the somatosensory system. Science 268, 1353-1358.*

*Nicolelis, M.A.L., Chapin, J.K., and Lin, R.C.S. (1992). Somatotopic maps within the zona incerta relay parallel GABAergic somatosensory pathways to the neocortex, superior colliculus, and brainstem. Brain Res 577, 134-141.*

*Nicolelis, M.A.L., Chapin, J.K., and Lin, R.C.S. (1995b). Development of direct GABAergic projections from the zona incerta to the somatosensory cortex of the rat. Neuroscience 65, 609-631.*

*Nilsson, B.Y. (1969). Structure and function of the tactile hair receptors on the cat's foreleg. Acta Physiol Scand 77, 396-416.*

*O'Connor, D.H., Clack, N.G., Huber, D., Komiyama, T., Myers, E.W., and Svoboda, K. (2010a). Vibrissa-based object localization in head-fixed mice. J Neurosci 30, 1947-1967.*

*O'Connor, D.H., Peron, S.P., Huber, D., and Svoboda, K. (2010b). Neural activity in barrel cortex underlying vibrissa-based object localization in mice. Neuron 67, 1048-1061.*

*Ojima, H. (1994). Terminal morphology and distribution of corticothalamic fibers originating from layers 5 and 6 of cat primary auditory cortex. Cereb Cortex 4, 646-663.*

*Oldford, E., and Castro-Alamancos, M.A. (2003). Input-specific effects of acetylcholine on sensory and intracortical evoked responses in the "barrel cortex" in vivo. Neuroscience 117, 769-778.*

*Parenti, R., Zappalà, A., Serapide, M.F., Pantò, M.R., and Cicirata, F. (2002). Projections of the basilar pontine nuclei and nucleus reticularis tegmenti pontis to the cerebellar nuclei of the rat. J Comp Neurol 452, 115-127.*

*Passani, M.B., and Blandina, P. (2011). Histamine receptors in the CNS as targets for therapeutic intervention. Trends Pharmacol Sci 32, 242-249.*

*Paul, G., and Gould, D.J. (2010). The red nucleus: Past, present, and future. Neuroanatomy 9, 1-3.*

*Peschanski, M. (1984). Trigeminal afferents to the diencephalon in the rat. Neuroscience 12, 465-487.*

*Petersen, C.C.H. (2007). The functional organization of the barrel cortex. Neuron 56, 339-355.*

*Petersen, C.C.H., and Sakmann, B. (2000). The excitatory neuronal network of rat layer 4 barrel cortex. J Neurosci 20, 7579-7586.*

*Petreanu, L., Huber, D., Sobczyk, A., and Svoboda, K. (2007). Channelrhodopsin-2-assisted circuit mapping of long-range callosal projections. Nat Neurosci 10, 663-668.*

*Petreanu, L., Mao, T., Sternson, S.M., and Svoboda, K. (2009). The subcellular organization of neocortical excitatory connections. Nature 457, 1142-1145.*

*Pidoux, M., Mahon, S., Deniau, J.M., and Charpier, S. (2011). Integration and propagation of somatosensory responses in the corticostriatal pathway: an intracellular study in vivo. J Physiol 589, 263-281.*

*Pierret, T., Lavallée, P., and Deschênes, M. (2000). Parallel streams for the relay of vibrissal information through thalamic barreloids. J Neurosci 20, 7455-7462.*

*Pillot, C., Heron, A., Cochois, V., Tardivel-Lacombe, J., Ligneau, X., Schwartz, J.C., and Arrang, J.M. (2002). A detailed mapping of the histamine H(3) receptor and its gene transcripts in rat brain. Neuroscience 114, 173-193.*

*Pinault, D. (2004). The thalamic reticular nucleus: structure, function and concept. Brain Res Brain Res Rev 46, 1-31.*

*Pinault, D., Bourassa, J., and Deschênes, M. (1995). The axonal arborization of single thalamic reticular neurons in the somatosensory thalamus of the rat. Eur J Neurosci 7, 31-40.*

*Pinganaud, G., Bernat, I., Buisseret, P., and Buisseret-Delmas, C. (1999). Trigeminal projections to hypoglossal and facial motor nuclei in the rat. J Comp Neurol 415, 91-104.*

*Popescu, A.T., Popa, D., and Paré, D. (2009). Coherent gamma oscillations couple the amygdala and striatum during learning. Nat Neurosci 12, 801-807.*

*Porter, L.L., and White, E.L. (1983). Afferent and efferent pathways of the vibrissal region of primary motor cortex in the mouse. J Comp Neurol 214, 279-289.*

*Quessy, S., and Freedman, E.G. (2004). Electrical stimulation of rhesus monkey nucleus reticularis gigantocellularis. I. Characteristics of evoked head movements. Exp Brain Res 156, 342-356.*

*Redgrave, P., Gurney, K., and Reynolds, J. (2008). What is reinforced by phasic dopamine signals? Brain Res Rev 58, 322-339.*

*Reep, R.L., Stoll, M.L., Marshall, C.D., Homer, B.L., and Samuelson, D.A. (2001). Microanatomy of facial vibrissae in the Florida manatee: the basis for specialized sensory function and oripulation. Brain Behav Evol 58, 1-14.*

*Reyes, A., and Sakmann, B. (1999). Developmental switch in the short-term modification of unitary EPSPs evoked in layer 2/3 and layer 5 pyramidal neurons of rat neocortex. J Neurosci 19, 3827-3835.*

*Ricardo, J.A. (1981). Efferent connections of the subthalamic region in the rat. II. The zona incerta. Brain Res 214, 43-60.*

*Rice, F.L. (1985). An attempt to find vibrissa-related barrels in the primary somatosensory cortex of the cat. Neurosci Lett 53, 169-172.*

*Rice, F.L. (1993). Structure, vascularization, and innervation of the mystacial pad of the rat as revealed by the lectin Griffonia simplicifolia. J Comp Neurol 337, 386-399.*

*Rice, F.L., Mance, A., and Munger, B.L. (1986). A comparative light microscopic analysis of the sensory innervation of the mystacial pad. I. Innervation of vibrissal follicle-sinus complexes. J Comp Neurol 252, 154-174.*

*Ritt, J.T., Andermann, M.L., and Moore, C.I. (2008). Embodied information processing: vibrissa mechanics and texture features shape micromotions in actively sensing rats. Neuron 57, 599-613.*

*Roger, M., and Cadusseau, J. (1985). Afferents to the zona incerta in the rat: a combined retrograde and anterograde study. J Comp Neurol 241, 480-492.*

*Ruigrok, T.J.H. (in press). Ins and outs of cerebellar modules. Cerebellum DOI 10.1007/s12311-010-0164-y.*

*Sarko, D.K., Reep, R.L., Mazurkiewicz, J.E., and Rice, F.L. (2007). Adaptations in the structure and innervation of follicle-sinus complexes to an aquatic environment as seen in the Florida manatee (Trichechus manatus latirostris). J Comp Neurol 504, 217-237.*

*Sarko, D.K., Rice, F.L., and Reep, R.L. (2011). Mammalian tactile hair: divergence from a limited distribution. Ann N Y Acad Sci 1225, 90-100.*

*Satoh, K., and Fibiger, H.C. (1986). Cholinergic neurons of the laterodorsal tegmental nucleus: efferent and afferent connections. J Comp Neurol 253***,** *277-302.*

*Schneider, J.S., Morse, J.R., and Lidsky, T.I. (1982). Somatosensory properties of globus pallidus neurons in awake cats. Exp Brain Res 46***,** *311-314.*

*Schubert, D., Kötter, R., and Staiger, J.F. (2007). Mapping functional connectivity in barrel-related columns reveals layer- and cell type-specific microcircuits. Brain Struct Funct 212***,** *107-119.*

*Schubert, D., Staiger, J.F., Cho, N., Kötter, R., Zilles, K., and Luhmann, H.J. (2001). Layer-specific intracolumnar and transcolumnar functional connectivity of layer V pyramidal cells in rat barrel cortex. J Neurosci 21***,** *3580-3592.*

*Schwarz, C., and Möck, M. (2001). Spatial arrangement of cerebro-pontine terminals. J Comp Neurol 435***,** *418-432.*

*Semba, K., and Fibiger, H.C. (1992). Afferent connections of the laterodorsal and the pedunculopontine tegmental nuclei in the rat: a retro- and antero-grade transport and immunohistochemical study. J Comp Neurol 323***,** *387-410.*

*Semba, K., and Komisaruk, B.R. (1984). Neural substrates of two different rhythmical vibrissal movements in the rat. Neuroscience 12***,** *761-774.*

*Shambes, G.M., Gibson, J.M., and Welker, W. (1978). Fractured somatotopy in granule cell tactile areas of rat cerebellar hemispheres revealed by micromapping. Brain Behav Evol 15***,** *94-140.*

*Sheibani, V., and Farazifard, R. (2006). Dorsal raphe nucleus stimulation modulates the response of layers IV and V barrel cortical neurons in rat. Brain Res Bull 68***,** *430-435.*

*Shepherd, G.M.G., and Svoboda, K. (2005). Laminar and columnar organization of ascending excitatory projections to layer 2/3 pyramidal neurons in rat barrel cortex. J Neurosci 25***,** *5670-5679.*

*Shosaku, A., Kayama, Y., and Sumitomo, I. (1984). Somatotopic organization in the rat thalamic reticular nucleus. Brain Res 311***,** *57-63.*

*Simons, D.J. (1978). Response properties of vibrissa units in rat SI somatosensory neocortex. J Neurophysiol 41***,** *798-820.*

*Simons, D.J. (1985). Temporal and spatial integration in the rat SI vibrissa cortex. J Neurophysiol 54***,** *615-635.*

*Simons, D.J., and Carvell, G.E. (1989). Thalamocortical response transformation in the rat vibrissa/barrel system. J Neurophysiol 61***,** *311-330.*

*Simony, E., Bagdasarian, K., Herfst, L., Brecht, M., Ahissar, E., and Golomb, D. (2010). Temporal and spatial characteristics of vibrissa responses to motor commands. J Neurosci 30***,** *8935-8952.*

*Simpson, K., Wang, Y., and Lin, R.C.S. (2008). Patterns of convergence in rat zona incerta from the trigeminal nuclear complex: light and electron microscopic study. J Comp Neurol 507***,** *1521-1541.*

*Smith, J.B., and Alloway, K.D. (2010). Functional specificity of claustrum connections in the rat: interhemispheric communication between specific parts of motor cortex. J Neurosci 30***,** *16832-16844.*

*Smith, J.C., Abdala, A.P.L., Rybak, I.A., and Paton, J.F.R. (2009). Structural and functional architecture of respiratory networks in the mammalian brainstem. Philos Trans R Soc Lond B Biol Sci 364***,** *2577-2587.*

*Smith, Y., Raju, D.V., Pare, J.F., and Sidibe, M. (2004). The thalamostriatal system: a highly specific network of the basal ganglia circuitry. Trends Neurosci 27***,** *520-527.*

*Spreafico, R., Barbaresi, P., Weinberg, R.J., and Rustioni, A. (1987). SII-projecting neurons in the rat thalamus: a single- and double-retrograde-tracing study. Somatosens Res 4***,** *359-375.*

*Stapley, P.J., and Drew, T. (2009). The pontomedullary reticular formation contributes to the* *compensatory postural responses observed following removal of the support surface in the standing cat. J Neurophysiol 101, 1334-1350.*

*Steindler, D.A. (1985). Trigeminocerebellar, trigeminotectal, and trigeminothalamic projections: a double retrograde axonal tracing study in the mouse. J Comp Neurol 237, 155-175.*

*Stephens, R.J., Beebe, I.J., and Poulter, T.C. (1973). Innervation of the vibrissae of the California sea lion, Zalophus californianus. Anat Rec 176, 421-441.*

*Stüttgen, M.C., and Schwarz, C. (2008). Psychophysical and neurometric detection performance under stimulus uncertainty. Nat Neurosci 11, 1091-1099.*

*Sun, Q.Q., Huguenard, J.R., and Prince, D.A. (2006). Barrel cortex microcircuits: thalamocortical feedforward inhibition in spiny stellate cells is mediated by a small number of fast-spiking interneurons. J Neurosci 26, 1219-1230.*

*Swadlow, H.A. (2002). Thalamocortical control of feed-forward inhibition in awake somatosensory 'barrel' cortex. Philos Trans R Soc Lond B Biol Sci 357, 1717-1727.*

*Swenson, R.S., and Castro, A.J. (1983). The afferent connections of the inferior olivary complex in rats. An anterograde study using autoradiographic and axonal degeneration techniques. Neuroscience 8, 259-275.*

*Swenson, R.S., Kosinski, R.J., and Castro, A.J. (1984). Topography of spinal, dorsal column nuclear, and spinal trigeminal projections to the pontine gray in rats. J Comp Neurol 222, 301-311.*

*Swenson, R.S., Sievert, C.F., Terreberry, R.R., Neafsey, E.J., and Castro, A.J. (1989). Organization of cerebral cortico-olivary projections in the rat. Neurosci Res 7, 43-54.*

*Syed, E.C.J., Sharott, A., Moll, C.K.E., Engel, A.K., and Kral, A. (2011). Effect of sensory stimulation in rat barrel cortex, dorsolateral striatum and on corticostriatal functional connectivity. Eur J Neurosci 33, 461-470.*

*Szwed, M., Bagdasarian, K., and Ahissar, E. (2003). Encoding of vibrissal active touch. Neuron 40, 621-630.*

*Szymonowicz, W. (1895). Beiträge zur Kentniss der Nervenendigungen in Hautgebilden. Arch Mikr Anat 45, 624-654.*

*Takahashi, K., Lin, J.S., and Sakai, K. (2006). Neuronal activity of histaminergic tuberomammillary neurons during wake-sleep states in the mouse. J Neurosci 26, 10292-10298.*

*Taylor, A.M., and Lieberman, A.R. (1987). Ultrastructural organisation of the projection from the superior colliculus to the ventral lateral geniculate nucleus of the rat. J Comp Neurol 256, 454-462.*

*ten Donkelaar, H.J. (1988). Evolution of the red nucleus and rubrospinal tract. Behav Brain Res 28, 9-20.*

*Tepper, J.M., Abercrombie, E.D., and Bolam, J.P. (2007). Basal ganglia macrocircuits. Prog Brain Res 160, 3-7.*

*Terenzi, M.G., Zagon, A., and Roberts, M.H.T. (1995). Efferent connections from the anterior pretectal nucleus to the diencephalon and mesencephalon in the rat. Brain Res 701, 183-191.*

*Teune, T.M., van der Burg, J., van der Moer, J., Voogd, J., and Ruigrok, T.J. (2000). Topography of cerebellar nuclear projections to the brain stem in the rat. Prog Brain Res 124, 141-172.*

*Thakkar, M.M. (2011). Histamine in the regulation of wakefulness. Sleep Med Rev 15, 65-74.*

*Theyel, B.B., Llano, D.A., and Sherman, S.M. (2010). The corticothalamocortical circuit drives higher-order cortex in the mouse. Nat Neurosci 13, 84-88.*

*Thomson, M.A., Piat, G., Cordonnier, V., Ellouze-Kallel, L., Delhaye-Bouchaud, N., and Mariani, J. (1989). Representation of vibrissae inputs through the climbing fiber pathway in lobule VII of the adult rat cerebellar vermis. Brain Res 488, 241-252.*

*Timofeeva, E., Dufresne, C., Sik, A., Zhang, Z.W., and Deschênes, M. (2005). Cholinergic modulation of vibrissal receptive fields in trigeminal nuclei. J Neurosci 25*, *9135-9143.*

*Timofeeva, E., Mérette, C., Émond, C., Lavallée, P., and Deschénes, M. (2003). A map of angular tuning preference in thalamic barreloids. J Neurosci 23*, *10717-10723.*

*Tlamsa, A.P., and Brumberg, J.C. (2010). Organization and morphology of thalamocortical neurons of mouse ventral lateral thalamus. Somatosens Mot Res 27*, *34-43.*

*Torigoe, Y., Blanks, R.H., and Precht, W. (1986a). Anatomical studies on the nucleus reticularis tegmenti pontis in the pigmented rat. I. Cytoarchitecture, topography, and cerebral cortical afferents. J Comp Neurol 243*, *71-87.*

*Torigoe, Y., Blanks, R.H., and Precht, W. (1986b). Anatomical studies on the nucleus reticularis tegmenti pontis in the pigmented rat. II. Subcortical afferents demonstrated by the retrograde transport of horseradish peroxidase. J Comp Neurol 243*, *88-105.*

*Towal, R.B., and Hartmann, M.J. (2006). Right-left asymmetries in the whisking behavior of rats anticipate head movements. J Neurosci 26*, *8838-8846.*

*Towal, R.B., and Hartmann, M.J. (2008). Variability in velocity profiles during free-air whisking behavior of unrestrained rats. J Neurophysiol 100*, *740-752.*

*Towal, R.B., Quist, B.W., Gopal, V., Solomon, J.H., and Hartmann, M.J.Z. (2011). The morphology of the rat vibrissal array: A model for quantifying spatiotemporal patterns of whisker-object contact. PLoS Comput Biol 7*, *e1001120.*

*Trageser, J.C., Burke, K.A., Masri, R., Li, Y., Sellers, L., and Keller, A. (2006). State-dependent gating of sensory inputs by zona incerta. J Neurophysiol 96*, *1456-1463.*

*Trageser, J.C., and Keller, A. (2004). Reducing the uncertainty: gating of peripheral inputs by zona incerta. J Neurosci 24*, *8911-8915.*

*Troncoso, J., Múnera, A., and Delgado-García, J.M. (2004). Classical conditioning of eyelid and mystacial vibrissae responses in conscious mice. Learn Mem 11*, *724-726.*

*Troncoso, J., Múnera, A., and Delgado-García, J.M. (2007). Learning-dependent potentiation in the vibrissal motor cortex is closely related to the acquisition of conditioned whisker responses in behaving mice. Learn Mem 14*, *84-93.*

*Urbain, N., Creamer, K., and Debonnel, G. (2006). Electrophysiological diversity of the dorsal raphe cells across the sleep-wake cycle of the rat. J Physiol 573*, *679-695.*

*Urbain, N., and Deschênes, M. (2007a). Motor cortex gates vibrissal responses in a thalamocortical projection pathway. Neuron 56*, *714-725.*

*Urbain, N., and Deschênes, M. (2007b). A new thalamic pathway of vibrissal information modulated by the motor cortex. J Neurosci 27*, *12407-12412.*

*Valdés, J.L., Sánchez, C., Riveros, M.E., Blandina, P., Contreras, M., Farías, P., and Torrealba, F. (2010). The histaminergic tuberomammillary nucleus is critical for motivated arousal. Eur J Neurosci 31*, *2073-2085.*

*Van der Loos, H. (1976). Barreloids in mouse somatosensory thalamus. Neurosci Lett 2*, *1-6.*

*Van Horn, R.N. (1970). Vibrissae structure in the rhesus monkey. Folia Primatol (Basel) 13*, *241-285.*

*Veinante, P., and Deschênes, M. (1999). Single- and multi-whisker channels in the ascending projections from the principal trigeminal nucleus in the rat. J Neurosci 19*, *5085-5095.*

*Veinante, P., and Deschênes, M. (2003). Single-cell study of motor cortex projections to the barrel field in rats. J Comp Neurol 464*, *98-103.*

*Veinante, P., Jacquin, M.F., and Deschênes, M. (2000a). Thalamic projections from the whisker-sensitive regions of the spinal trigeminal complex in the rat. J Comp Neurol 420*, *233-243.*

*Veinante, P., Lavallée, P., and Deschênes, M. (2000b). Corticothalamic projections from layer 5 of the vibrissal barrel cortex in the rat. J Comp Neurol 424*, *197-204.*

*Verberne, A.J.M., and Struyker Boudier, H.A.J. (1991). Midbrain central grey: regional* *haemodynamic control and excitatory amino acidergic mechanisms. Brain Res 550, 86-94.*

*Vianna, D.M.L., and Brandao, M.L. (2003). Anatomical connections of the periaqueductal gray: specific neural substrates for different kinds of fear. Braz J Med Biol Res 36, 557-566.*

*Villanueva, L., Bouhassira, D., Bing, Z., and Le Bars, D. (1988). Convergence of heterotopic nociceptive information onto subnucleus reticularis dorsalis neurons in the rat medulla. J Neurophysiol 60, 980-1009.*

*Vincent, S.B. (1913). The tactile hair of the white rat. J Comp Neurol 23, 1-36.*

*von Heimendahl, M., Itskov, P.M., Arabzadeh, E., and Diamond, M.E. (2007). Neuronal activity in rat barrel cortex underlying texture discrimination. PLoS Biol 5, e305.*

*Voogd, J., and Glickstein, M. (1998). The anatomy of the cerebellum. Trends Neurosci 21, 370-375.*

*Voorn, P., Vanderschuren, L.J.M.J., Groenewegen, H.J., Robbins, T.W., and Pennartz, C.M.A. (2004). Putting a spin on the dorsal-ventral divide of the striatum. Trends Neurosci 27, 468-474.*

*Waite, P.M.E., and Jacquin, M.F. (1992). Dual innervation of the rat vibrissa: responses of trigeminal ganglion cells projecting through deep or superficial nerves. J Comp Neurol 322, 233-245.*

*Wanaverbecq, N., Bodor, A.L., Bokor, H., Slézia, A., Lüthi, A., and Acsády, L. (2008). Contrasting the functional properties of GABAergic axon terminals with single and multiple synapses in the thalamus. J Neurosci 28, 11848-11861.*

*Waterhouse, B.D., Devilbiss, D., Seiple, S., and Markowitz, R. (2004). Sensorimotor-related discharge of simultaneously recorded, single neurons in the dorsal raphe nucleus of the awake, unrestrained rat. Brain Res 1000, 183-191.*

*Welker, C. (1971). Microelectrode delineation of fine grain somatotopic organization of (SmI) cerebral neocortex in albino rat. Brain Res 26, 259-275.*

*Welker, C., and Sinha, M.M. (1972). Somatotopic organization of Smll cerebral neocortex in albino rat. Brain Res 37, 132-136.*

*Welker, C., and Woolsey, T.A. (1974). Structure of layer IV in the somatosensory neocortex of the rat: description and comparison with the mouse. J Comp Neurol 158, 437-453.*

*Welker, E., Hoogland, P.V., and Van der Loos, H. (1988). Organization of feedback and feedforward projections of the barrel cortex: a PHA-L study in the mouse. Exp Brain Res 73, 411-435.*

*Welker, W.I. (1964). Analysis of sniffing of the albino rat. Behaviour 22, 223-244.*

*Wenk, G.L. (1997). The nucleus basalis magnocellularis cholinergic system: one hundred years of progress. Neurobiol Learn Mem 67, 85-95.*

*Westby, G.W.M., Collinson, C., and Dean, P. (1993). Excitatory drive from deep cerebellar neurons to the superior colliculus in the rat: an electrophysiological mapping study. Eur J Neurosci 5, 1378-1388.*

*White, E.L., and DeAmicis, R.A. (1977). Afferent and efferent projections of the region in mouse SmL cortex which contains the posteromedial barrel subfield. J Comp Neurol 175, 455-481.*

*Williams, M.N., Zahm, D.S., and Jacquin, M.F. (1994). Differential foci and synaptic organization of the principal and spinal trigeminal projections to the thalamus in the rat. Eur J Neurosci 6, 429-453.*

*Wimmer, V.C., Bruno, R.M., de Kock, C.P.J., Kuner, T., and Sakmann, B. (2010). Dimensions of a projection column and architecture of VPM and POm axons in rat vibrissal cortex. Cereb Cortex 20, 2265-2276.*

*Wineski, L.E. (1985). Facial morphology and vibrissal movement in the golden hamster. J Morphol 183, 199-217.*

*Wise, S.P., and Jones, E.G. (1977). Somatotopic and columnar organization in the* *corticotectal projection of the rat somatic sensory cortex. Brain Res 133, 223-235.*

*Wolfe, J., Hill, D.N., Pahlavan, S., Drew, P.J., Kleinfeld, D., and Feldman, D.E. (2008). Texture coding in the rat whisker system: slip-stick versus differential resonance. PLoS Biol 6, e215.*

*Woolf, N.J. (1991). Cholinergic systems in mammalian brain and spinal cord. Prog Neurobiol 37, 475-524.*

*Woolsey, T.A., and Van der Loos, H. (1970). The structural organization of layer IV in the somatosensory region (SI) of mouse cerebral cortex. The description of a cortical field composed of discrete cytoarchitectonic units. Brain Res 17, 205-242.*

*Woolsey, T.A., Welker, C., and Schwartz, R.H. (1975). Comparative anatomical studies of the SmI face cortex with special reference to the occurrence of "barrels" in layer IV. J Comp Neurol 164, 79-94.*

*Woolston, D.C., La Londe, J.R., and Gibson, J.M. (1983). Corticofugal influences in the rat on responses of neurons in the trigeminal nucleus interpolaris to mechanical stimulation. Neurosci Lett 36, 43-48.*

*Wouterlood, F.G., Sauren, Y.M.H.F., and Steinbusch, H.W.M. (1986). Histaminergic neurons in the rat brain: correlative immunocytochemistry, Golgi impregnation, and electron microscopy. J Comp Neurol 252, 227-244.*

*Wright, A.K., Norrie, L., Ingham, C.A., Hutton, E.A.M., and Arbuthnott, G.W. (1999). Double anterograde tracing of outputs from adjacent "barrel columns" of rat somatosensory cortex. Neostriatal projection patterns and terminal ultrastructure. Neuroscience 88, 119-133.*

*Wright, A.K., Ramanathan, S., and Arbuthnott, G.W. (2001). Identification of the source of the bilateral projection system from cortex to somatosensory neostriatum and an exploration of its physiological actions. Neuroscience 103, 87-96.*

*Yatim, N., Billig, I., Compoint, C., Buisseret, P., and Buisseret-Delmas, C. (1996). Trigeminocerebellar and trigemino-olivary projections in rats. Neurosci Res 25, 267-283.*

*Yohro, T. (1977). Structure of the sinus hair follicle in the big-clawed shrew, Sorex unguiculatus. J Morphol 153, 333-353.*

*Yu, C., Derdikman, D., Haidarliu, S., and Ahissar, E. (2006). Parallel thalamic pathways for whisking and touch signals in the rat. PLoS Biol 4, e124.*

*Zagon, A., Terenzi, M.G., and Roberts, M.H.T. (1995). Direct projections from the anterior pretectal nucleus to the ventral medulla oblongata in rats. Neuroscience 65, 253-272.*

*Zerari-Mailly, F., Pinganaud, G., Dauvergne, C., Buisseret, P., and Buisseret-Delmas, C. (2001). Trigemino-reticulo-facial and trigemino-reticulo-hypoglossal pathways in the rat. J Comp Neurol 429, 80-93.*

*Zucker, E., and Welker, W.I. (1969). Coding of somatic sensory input by vibrissae neurons in the rat's trigeminal ganglion. Brain Res 12, 138-156.*

## 1.6 *Scope of the thesis*

The cerebellum is considered as a modulator for smooth movement. It fulfills this task by integrating sensory and motor information. We know the basic construction plan of the cerebellum in great detail, but how the sensory and motor related information integrates within the cerebellum is still an open question. The regularity of the cellular organization of the cerebellar cortex has long been considered as a sign of structural homogeneity, where all parts perform a similar type of information processing on different types of data streams. In contrast to the structural homogeneity of the neuronal network, the inputs to the cerebellar cortex are not homogeneously distributed. Instead, they project to distinct parasagittal zones based on their origin. The zones can be observed in the patterning of the climbing fiber projections from the inferior olive to the cerebellar cortex and in that of the projections from the cerebellar cortex to the nuclei. The parasagittal zones can be recognized, apart from by its connections, by their alternating expression patterns of the protein “zebrin II”.The parasagittal zones can be subdivided into smaller “microbands” that could function as synchronized ensembles. For this thesis, we first investigated the basic electrophysiological properties of Purkinje cells with different zebrin identities. Then we zoomed in to single cell resolution to observe the responses of Purkinje cells to different sensory inputs via climbing fiber projections.

In chapter2, we compared, using single unit recordings across the whole cerebellar cortex, the spontaneous firing rates of Purkinje cells in zebrin-positive and -negative bands.

In chapter 3, we studied the distribution of pauses in Purkinje cell simple spike firing in awake mice.

In chapter 4, using the two photon $Ca^{2+}$ imaging technique, we mapped tactile, auditory and visual responses of lobule crus 1 Purkinje cells.

In chapter 5, we mapped, using the whisker system as a reliable and precise source of tactile inputs, the single whisker sensory projections to lobule crus 1.

## Reference

Braitenberg, V., and R. P. Atwood. 1958. “Morphological Observations on the Cerebellar Cortex.” *The Journal of Comparative Neurology* 109 (1): 1–33.

Brochu, Gino, Leonard Maler, and Richard Hawkes. 1990. “Zebrin II: A Polypeptide Antigen Expressed Selectively by Purkinje Cells Reveals Compartments in Rat and Fish Cerebellum.” *The Journal of Comparative Neurology* 291 (4): 538–52. doi:10.1002/cne.902910405.

Devor, A., and Y. Yarom. 2002. “Coherence of Subthreshold Activity in Coupled Inferior Olivary Neurons.” *Annals of the New York Academy of Sciences* 978 (December): 508.

De Zeeuw, C. I., and A. S. Berrebi. 1995. “Postsynaptic Targets of Purkinje Cell Terminals in the Cerebellar and Vestibular Nuclei of the Rat.” *The European Journal of Neuroscience* 7 (11): 2322–33.

Gauck, V., and D. Jaeger. 2000. “The Control of Rate and Timing of Spikes in the Deep Cerebellar Nuclei by Inhibition.” *The Journal of Neuroscience: The Official Journal of the Society for Neuroscience* 20 (8): 3006–16.

Groenewegen, H. J., and J. Voogd. 1977. “The Parasagittal Zonation within the Olivocerebellar Projection. I. Climbing Fiber Distribution in the Vermis of Cat Cerebellum.” *The Journal of Comparative Neurology* 174 (3): 417–88. doi:10.1002/cne.901740304.

Groenewegen, H. J., J. Voogd, and S. L. Freedman. 1979. “The Parasagittal Zonation within the Olivocerebellar Projection. II. Climbing Fiber Distribution in the Intermediate and Hemispheric Parts of Cat Cerebellum.” *The Journal of Comparative Neurology* 183 (3): 551–601. doi:10.1002/cne.901830307.

Hawkes, Richard, Marc Colonnier, and Nicole Leclerc. 1985. “Monoclonal Antibodies Reveal Sagittal Banding in the Rodent Cerebellar Cortex.” *Brain Research* 333 (2): 359–65. doi:10.1016/0006-8993(85)91593-8.

Hawkes, R., and N. Leclerc. 1987. “Antigenic Map of the Rat Cerebellar Cortex: The Distribution of Parasagittal Bands as Revealed by Monoclonal Anti-Purkinje Cell Antibody mabQ113.” *The Journal of Comparative Neurology* 256 (1): 29–41. doi:10.1002/cne.902560104.

Jörntell, Henrik, and Carl-Fredrik Ekerot. 2002. “Reciprocal Bidirectional Plasticity of Parallel Fiber Receptive Fields in Cerebellar Purkinje Cells and Their Afferent Interneurons.” *Neuron* 34 (5): 797–806.

Kleinfeld, D., R. W. Berg, and S. M. O’Connor. 1999. “Anatomical Loops and Their Electrical Dynamics in Relation to Whisking by Rat.” *Somatosensory & Motor Research* 16 (2): 69–88.

Latham, R. A. 1971. “Growth Mechanism of the Human Face with Special Reference to Cleft Lip and Palate Conditions.” *Annals of the Royal College of Surgeons of England* 48 (1): 30–31.

Llinas, R., R. Baker, and C. Sotelo. 1974. “Electrotonic Coupling between Neurons in Cat Inferior Olive.” *Journal of Neurophysiology* 37 (3): 560–71.

Loewenstein, Yonatan, Séverine Mahon, Paul Chadderton, Kazuo Kitamura, Haim Sompolinsky, Yosef Yarom, and Michael Häusser. 2005. “Bistability of Cerebellar Purkinje Cells Modulated by Sensory Stimulation.” *Nature Neuroscience* 8 (2): 202–11. doi:10.1038/nn1393.

Matsushita, M., H. Yaginuma, and T. Tanami. 1992. “Somatotopic Termination of the Spino-Olivary Fibers in the Cat, Studied with the Wheat Germ Agglutinin-Horseradish Peroxidase Technique.” *Experimental Brain Research* 89 (2): 397–407.

Nelson, B. J., and E. Mugnaini. 1988. “The Rat Inferior Olive as Seen with Immunostaining for Glutamate Decarboxylase.” *Anatomy and Embryology* 179 (2): 109–27.

Palkovits, M., E. Mezey, J. Hámori, and J. Szentágothai. 1977. “Quantitative Histological

Analysis of the Cerebellar Nuclei in the Cat. I. Numerical Data on Cells and on Synapses.” *Experimental Brain Research* 28 (1-2): 189–209.

Robertson, L. T. 1984. “Topographic Features of Climbing Fiber Input in the Rostral Vermal Cortex of the Cat Cerebellum.” *Experimental Brain Research* 55 (3): 445–54.

Saint-Cyr, Jean A., and Jacques Courville. 1981. “Sources of Descending Afferents to the Inferior Olive from the Upper Brain Stem in the Cat as Revealed by the Retrograde Transport of Horseradish Peroxidase.” *The Journal of Comparative Neurology* 198 (4): 567–81. doi:10.1002/cne.901980403.

Scheibel, M. E., and A. B. Scheibel. 1975. “Dendrite Bundles, Central Programs and the Olfactory Bulb.” *Brain Research* 95 (2-3): 407–21.

Shambes, Georgia M., John M. Gibson, and Wally Welker. 1978. “Fractured Somatotopy in Granule Cell Tactile Areas of Rat Cerebellar Hemispheres Revealed by Micromapping; Pp. 106–115.” *Brain, Behavior and Evolution* 15 (2): 106–15. doi:10.1159/000315982.

Sultan, Fahad, and Mitchel Glickstein. 2007. “The Cerebellum: Comparative and Animal Studies.” *The Cerebellum* 6 (3): 168–76. doi:10.1080/14734220701332486.

Van Ham, Jacqueline J., and Christopher H. Yeo. 1992. “Somatosensory Trigeminal Projections to the Inferior Olive, Cerebellum and Other Precerebellar Nuclei in Rabbits.” *The European Journal of Neuroscience* 4 (4): 302–17.

Walberg, F., and O. P. Ottersen. 1989. “Demonstration of GABA Immunoreactive Cells in the Inferior Olive of Baboons (Papio Papio and Papio Anubis).” *Neuroscience Letters* 101 (2): 149–55.

Zagon, I. S., P. J. McLaughlin, and S. Smith. 1977. “Neural Populations in the Human Cerebellum: Estimations from Isolated Cell Nuclei.” *Brain Research* 127 (2): 279–82.

# Chapter 2

# Cerebellar modules operate at different frequencies

Haibo Zhou[1]*, Zhanmin Lin[1]*, Kai Voges[1], Chiheng Ju[1], Zhenyu Gao[1], Laurens W.J. Bosman[1], Tom J. Ruigrok[1], Freek E. Hoebeek[1], Chris I. De Zeeuw[1,2#] and Martijn Schonewille[1#]

**Elife. 2014**

## Abstract

Due to the uniform cyto-architecture of the cerebellar cortex, its overall physiological characteristics have traditionally been considered to be homogeneous. Here we show in awake mice at rest that spiking activity of Purkinje cells, the sole output cells of the cerebellar cortex, differs between cerebellar modules and correlates with their expression of the glycolytic enzyme aldolase C or zebrin. Simple spike and complex spike frequencies were significantly higher in Purkinje cells located in zebrin-negative than zebrin-positive modules. The difference in simple spike frequency persisted when the synaptic input to, but not intrinsic activity of, Purkinje cells was manipulated. Blocking TRPC3, the effector channel of a cascade of proteins that have zebrin-like distribution patterns, attenuated the simple spike frequency difference. Our results indicate that zebrin-discriminated cerebellar modules operate at different frequencies, which depends on activation of TRPC3, and that this property is relevant for all cerebellar functions.

## Introduction

Resolving structure - function relations remains one of the main challenges of modern neuroscience. The unique cyto-architecture of the cerebellum is characterized by the crystalline matrix of its sagittally oriented PC dendrites and climbing fibers and its orthogonally running parallel fibers[1,2]. The ubiquitous nature of this relatively simple matrix throughout all lobules and modules of the cerebellar cortex made scientists predict in 1967 that this neuronal machine was probably the first to be elucidated[3]. Yet, about half a century later, we have collected a wealth of information about the molecular and physiological identity of the various cell types in the cerebellum[4], but gross structure - function relations are still largely lacking. For example, the amount of evidence for physiological differences within the cerebellar cortex is limited and there is little comparative analysis of spiking activity throughout the cerebellar cortex in adult awake animals. In fact, even most slice physiology studies do not discriminate between lobules or modules, indicative of the fact that the cerebellum is still considered physiologically homogeneous.

At the same time, several molecular markers have been identified that can subdivide the cerebellar cortex into distinct bands[5]. The best-known of these molecules are the zebrins, which are highly expressed by specific bands of Purkinje cells (PCs), i.e. the sole output of the cerebellar cortex. Immunostainings for both zebrin I and II give rise to symmetric stripes that are oriented perpendicular to the cerebellar folds[6,7]. The combined presence of zebrin positive and negative PCs can be found in all vertebrate classes, and zebra-like patterns are present in the cerebellum of birds and mammals, varying from pigeons and mice up to monkeys and humans[7-10]. In most cases, adjacent PCs with zebrin II (from hereon refered to as zebrin) are located in the same bands, receive CF inputs from the same part of the inferior olive, and project their axons to the same part of the cerebellar nuclei[5,11-15]. Moreover, although their various terminal rosettes may be located in different parts of the cerebellar cortex, individual mossy fibers often also adhere to the same zebrin signature[11]. As such zebrin may be regarded as a biomarker linking different cerebellar cortical zones, potentially binding activity of different olivo-cerebellar modules and mossy fiber systems[11,13,16]. However, what the basic characteristics of this zebrin related activity might be is unknown. Since zebrin has been identified as the glycolytic enzyme aldolase C, its presence might in principle be linked to the level of metabolic and/or electrophysiological activity. Indeed, the distribution of zebrin in the cerebellum is similar to that of the excitatory amino acid transporter 4 (EAAT4) and complementary to splice variant b of the metabotropic glutamate receptor 1 (mGluR1b)[17-

[19]. Intracellularly, several proteins in a molecular cascade linked to mGluR1 are also expressed in zebrin-like bands, including the IP3-receptor[20], PLCβ3/4[21], PKCδ[22] and NCS-1[23]. This cascade controls the activity of the transient receptor potential cation channel type C3 (TRPC3)[24], which in turn can influence the firing activity of PCs[25]. We hypothesized that differential activity of this cascade of proteins with zebrin-related expression might lead to differential activity of their effector channel, TRPC3, and thereby to differences in simple spike (SS) firing frequency between modules[26,27].

To test this hypothesis, we investigated the activity of PCs in awake mice at rest in relation to the zebrin-identity of their module. We demonstrate that there are zebrin-related differences in firing frequency of both SSs and complex spikes (CSs), that these differences are intrinsically driven, and that they are consistently present throughout the cerebellar cortex contributing to all its functions.

## Results

### Simple spike firing activity differs between Purkinje cell populations

We performed extracellular recordings from PCs in the cerebellar cortex of awake, restrained C57Bl/6 mice at rest with the use of double-barrel electrodes marking the recording location with Alcian Blue (**Fig. 1A-B**). Purkinje cells were identified by the presence of SSs and CSs and the consistent presence of a pause in SS firing after a CS (i.e. climbing fiber pause) (**Fig. 1C-F**). Recordings that were used for analysis had to meet several criteria including a minimum duration of 120 sec, stable spike amplitude over the whole recording period and no detectable tissue damage in a 400 μm radius (see also **Figure 1-figure supplement 1**). Following perfusion of the animals and processing of their cerebella, the zebrin-negative (Z−) and zebrin-positive (Z+) zones were identified by immunostaining. Of the 104 PCs included in the analysis (50 mice), 47 and 57 cells were located in Z− and Z+ zones, respectively (**Fig. 1G**, plot adapted from[28]). The SS firing frequency was significantly higher in Z− zones than in Z+ zones (Z−: 96.1 ± 15.4 Hz, Z+: 61.4 ± 19.3 Hz, $t = 9.942$, $p < 0.001$) (**Fig. 1H**). In line with this the climbing fiber pause was also significantly longer ($t = -7.482$, $p < 0.001$) in Z+ zones (**Fig. 1I**) (see also [29]). Both the SS firing frequency, SS regularity and CS firing frequency were stable over time (**Figure 1-figure supplement 2**). In contrast to the SS firing frequency and climbing fiber pause, the waveform and regularity of SSs did not consistently depend on zebrin identity in that average half-width and mean coefficient of variation for adjacent intervals (CV2) were not significantly different between Z− and Z+ PCs (half-width: $t = -1.133$, $p = 0.260$, data not shown; CV2: $t = 1.197$, $p = 0.234$) (**Fig. 1F-J**).

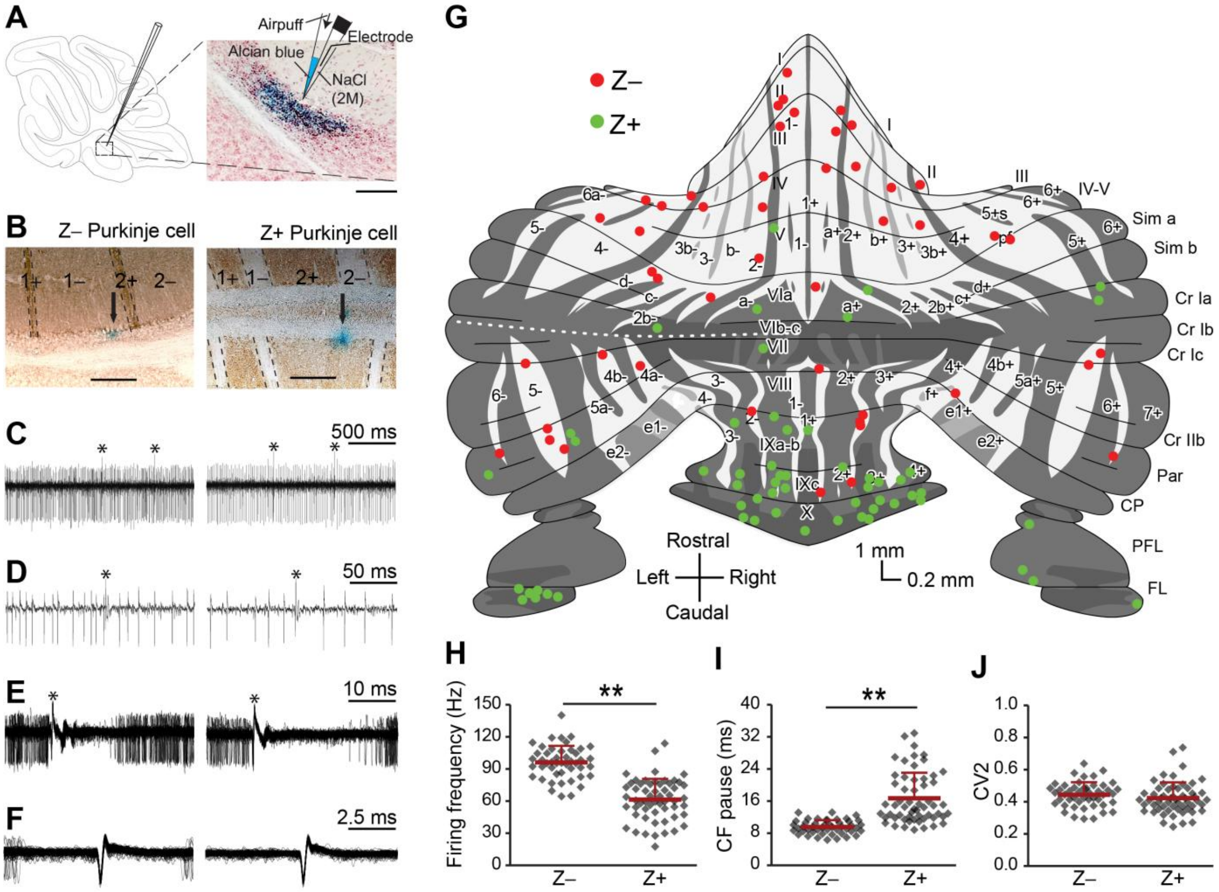

***Figure 1. Simple spike firing activity differs between Purkinje cell populations.***
***A**, Extracellular recordings were made from PCs in the cerebellar cortex of awake mice, using double barrel glass electrodes (right). Dye injections were placed to histologically identify the recording location. **B**, Photomicrographs of coronal sections with examples of zebrin-negative (Z−, left) and -positive (Z+, right) identified Purkinje cells in lobule II and lobule IX, respectively. Cells are marked by dye injections (blue, indicated by arrows), zebrin is stained brown, dotted lines demark zebrin borders. Note that Z+ stripes in lobules I-III are very narrow. **C**, **D**, Example trace of Z− and Z+ Purkinje cell recordings identified by its hallmark feature, the occurrence of complex spikes (asterisk) and simple spikes. **E**, Recordings were confirmed to be from a single neuron by the consistent pause in simple spike firing following each complex spike, in the overlay. **F**, Overlay of simple spikes. **G**, Distribution of recorded Z− and Z+ cells throughout the unfolded cerebellar cortex based on zebrin II compartments. **H**, Simple spike firing frequency is significantly lower in identified Z+ PCs compared to Z− PCs (Z−: n = 47 cells, 26 mice; Z+: n = 57 cells, 34 mice; t = 9.942, p < 0.001). **I**, In line with the lower simple spike firing frequency, the climbing fiber pause was longer in identified Z+ Purkinje cells (CF pause; t = -7.482, p < 0.001). **J**, Simple spike regularity is not different between Z+ and Z− PCs (CV2: t = 1.147, p = 0.234). Error bars represent s.d., * p < 0.05, ** p < 0.001. Schematic drawing in A was adapted from [28] with permission. Scale bars in A and B indicate 100 and 200 µm, respectively.*

### Simple spike firing frequency correlates with the zebrin identity of Purkinje cells

Due to the heterogeneous distribution of Z+ vs. Z− Purkinje cells over the cerebellar cortex, the majority of the Z+ cells were recorded in the posterior half, whereas the Z− cells were predominantly from the anterior half. Hence, one could argue that the difference between Z+ and Z− is related to location, rather than directly linked with zebrin identity. Re-plotting the results, but now color-coded for simple spike frequency to facilitate individual comparisons, seems to largely contradict this possibility (**Figure 2-figure supplement 1**). To more thoroughly test our hypothesis that differences are indeed related to zebrin identity, we also attempted to record neighboring, online identified, Z+ and Z− PCs in a single experiment. To this end, we performed two-photon imaging *in vivo* in awake, head-fixed mice that express enhanced green fluorescent protein (eGFP) under the EAAT4 promoter in a pattern similar to that of zebrin[30]. In the dorsal layer of lobule V, VI and Crus I we identified adjacent Z+ and Z− bands and recorded PCs in adjacent zebrin bands (**Fig. 2A-B**). In line with our hypothesis, we observed higher simple spike activity in Z− than in Z+ Purkinje cells (Z+: 36.0 ± 15.5 Hz, n = 8; Z−: 75.8 ± 19.5 Hz, n = 9; $t = 4.618$, $p < 0.001$) and concommitant longer climbing fiber pause (**Fig. 2C**). In contrast to the immuno-histochemically subdivided PC dataset (**Fig. 1)**, that covers the entire cerebellar cortex, this spatially restricted dataset did show a difference in simple spike regularity, suggesting that variations in regularity may occur more locally.

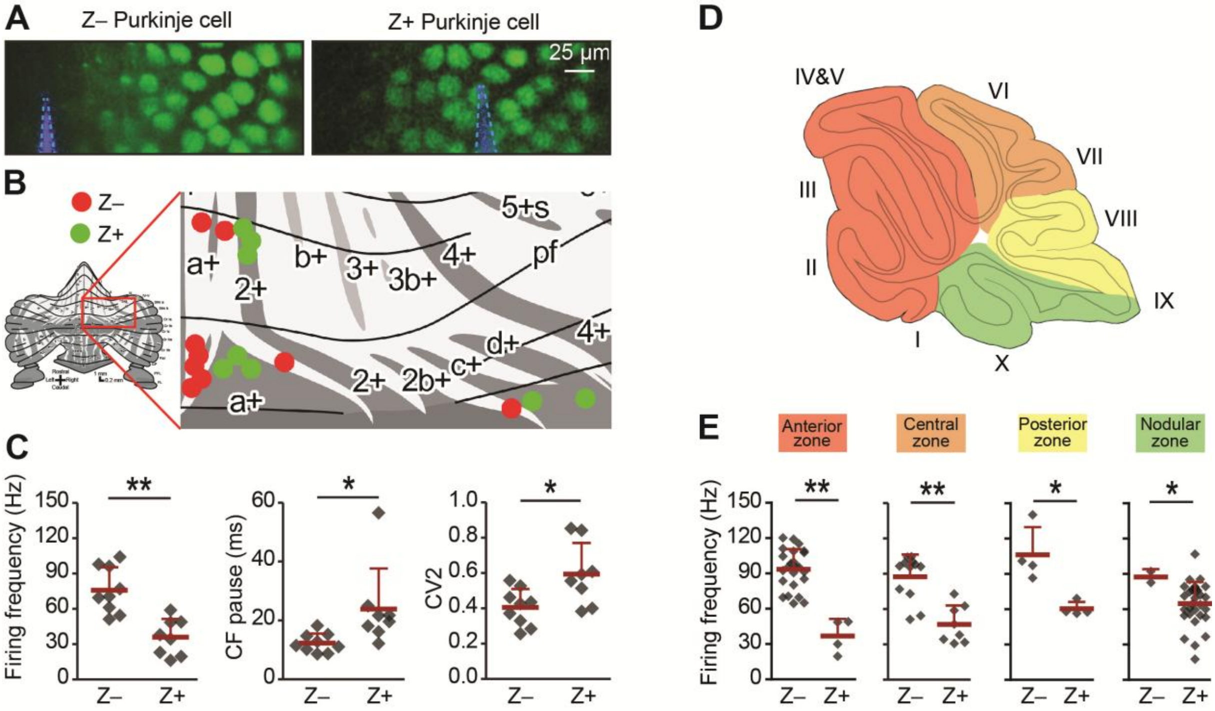

***Figure 2. Simple spike firing frequency correlates with the zebrin identity of Purkinje cells.*** *To determine of the differences in simple spike activity are related to the location of the Purkinje cells, or to their zebrin identity, we compared PC activity of Z+ against Z– Purkinje cells in various smaller areas of the cerebellar cortex.* ***A****, To more directly test the link with zebrin, we used EAAT4-eGFP mice that express eGFP in a pattern similar to that of zebrin. Two-photon images show an EAAT4+/Z+ band (green) in lobule V of an EAAT4-eGFP mouse: left, electrode (blue) positioned in the adjacent negative band; right, electrode (blue) in the positive band.* ***B****, The activity of 17 zebrin-identity determined PCs (Z+, n = 8; Z–, n = 9, 5 mice) from lobule V, VI and Crus I was recorded.* ***C****, The difference in simple spike firing frequency was pertained in this subset of Purkinje cell recordings (Z+: 36.0 ± 15.5 Hz; Z−: 75.8 ± 19.5 Hz; $t = 4.618$, $p < 0.001$), indicating that this difference is linked to zebrin identity, rather than lobular location. In contrast to data obtained with immunostaining for zebrin, the regularity of simple spikes also differs in this subpopulation ($t = -2.715$, $p < 0.016$).* ***D****, Cerebellar Purkinje cells can be subdivided based on the input they receive into four transverse zones: the anterior (red), central (orange), posterior (yellow) and nodular (green) zone.* ***E****, The difference in simple spike firing frequency between Z+ and Z– Purkinje cells is consistently present throughout all transverse zones. In each of the four transverse zones the simple spike rate was significantly lower in Z+ compared to Z– Purkinje cells (all $p < 0.05$, One-tailed Students t-test). Note that simple spike frequency within different Z+ subgroups was also variable, in that the frequency in the anterior zone was lower than that in the nodular zone ($p = 0.018$, One-way ANOVA, followed by Bonferroni's posthoc test). Error bars represent s.d., * $p < 0.05$, ** $p < 0.001$.*

Finally, to extend this analysis over the entire cortex, we compared Z+ vs. Z− PC activity per transverse zone. Along the rostro-caudal axis the cerebellum can be subdivided into four transverse zones: the anterior, central, posterior and nodular zone[31]. We consistently observed a similar difference in simple spike activity between Z+ and Z− PCs in each zone, independent of the location within the cerebellar cortex (**Figure 2D-E**). This approach also revealed a difference within the population of Z+ PCs. Whereas the simple spike firing frequency of Z− PCs is comparable over different transverse zones, Z+ PCs firing rate is lower in the anterior zone when compared to the nodular zone ($p = 0.018$, One-way ANOVA followed by Tukey’s post-hoc test).

If the SS activity of PCs depends on the presence of zebrin, one should also observe differences between lobules, as there is a gradual increase in zebrin positive modules and, thus, average zebrin intensity from lobule I to lobule X in the vermis as well as in the corresponding lobules in the hemispheres[32] (**Fig. 1G** and **Fig. 3A**). Indeed, when we extend the immunohistochemically analyzed dataset with recordings from all lobules in which the zebrin identity was not determined to generate one large, randomly sampled dataset (combined n = 245), our prediction is confirmed. Both the firing frequency and climbing fiber pause of SS activity, among the different lobules in the vermis as well as the hemispheres, show robust and consistent correlations with the averaged intensity of zebrin staining (for firing frequency, vermis: $r = 0.893$, $p = 0.007$; hemisphere: $r = 1.000$, $p < 0.001$; for climbing fiber pause, vermis: $r = -0.929$, $p = 0.003$; hemisphere: $r = -1.000$, $p < 0.001$) (**Fig. 3A-C** and **Figure 3-figure supplement 1**). In contrast, the CV2 of SSs could not be consistently related to the zebrin intensity in the vermis and hemispheres (vermis: $r = 0.929$, $p = 0.003$; hemisphere: $r = -0.300$, $p = 0.624$) (**Fig. 3D**).

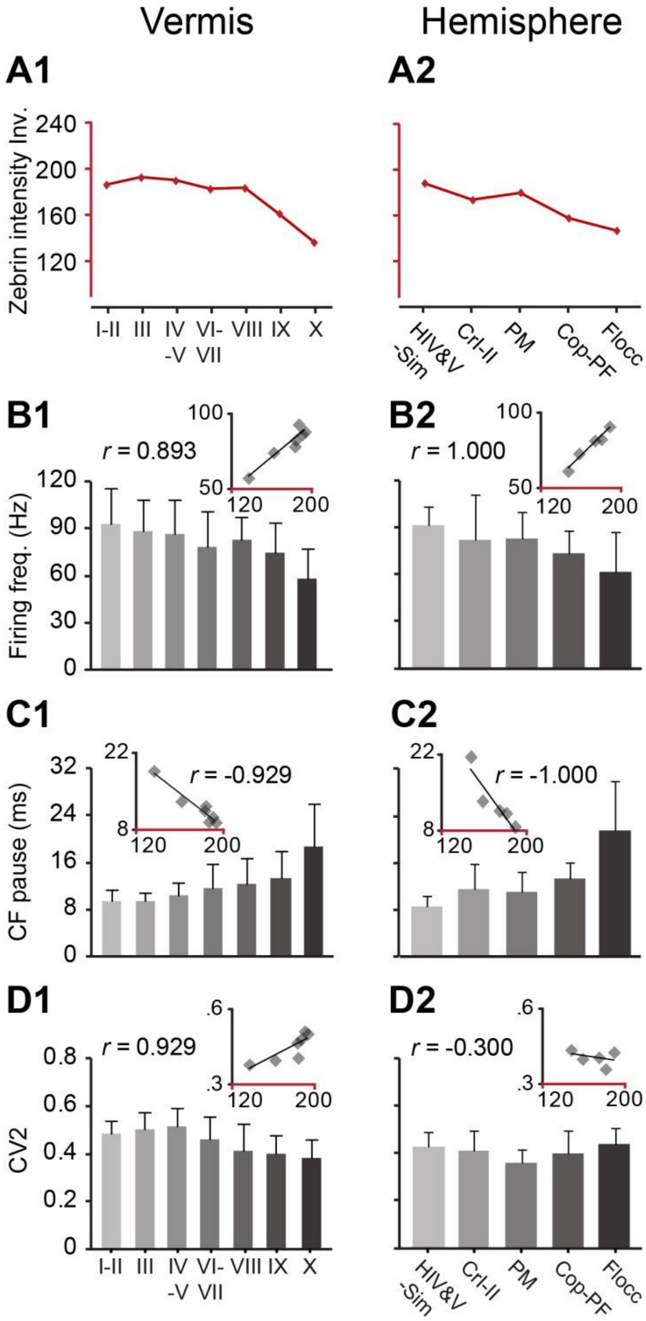

***Figure 3. Zebrin staining intensity and simple spike frequency are inversely correlated.*** *To test the correlation to zebrin identity of modules throughout the cerebellar cortex, Purkinje cell activity was recorded from all parts of the cerebellar cortex, each followed by dye injection to identify the lobule.* ***A1-2****, The average zebrin staining intensities of Purkinje cell somata in vermis and hemispheres were obtained from the sagittal sections of three mice. Note that high intensity values equal weak staining, and vice versa.* ***B1-2, C1-2****, The average simple spike firing frequency (vermis: n = 192 cells, 70 mice, r = 0.893, p = 0.007; hemisphere: n = 53 cells, 30 mice, r = 1.000, p < 0.001) and CF pause (vermis: r = -0.929, p = 0.003; hemisphere: r = -1.000, p < 0.001) show significant correlation with zebrin intensity over different parts of vermis and hemisphere.* ***D1-2****, The CV2 of SSs could not be consistently related with zebrin intensity (vermis: r = 0.929, p = 0.003; hemisphere: r = -0.300, p = 0.624). Error bars represent s.d.. Figure 2 – figure supplement 1. Statistical analysis of PC spiking characteristics per lobule. Statistical comparisons of the Purkinje cell recordings presented in Figure 2 and 3, obtained from identified parts of the vermis and hemispheres. Error bars represent s.d.*

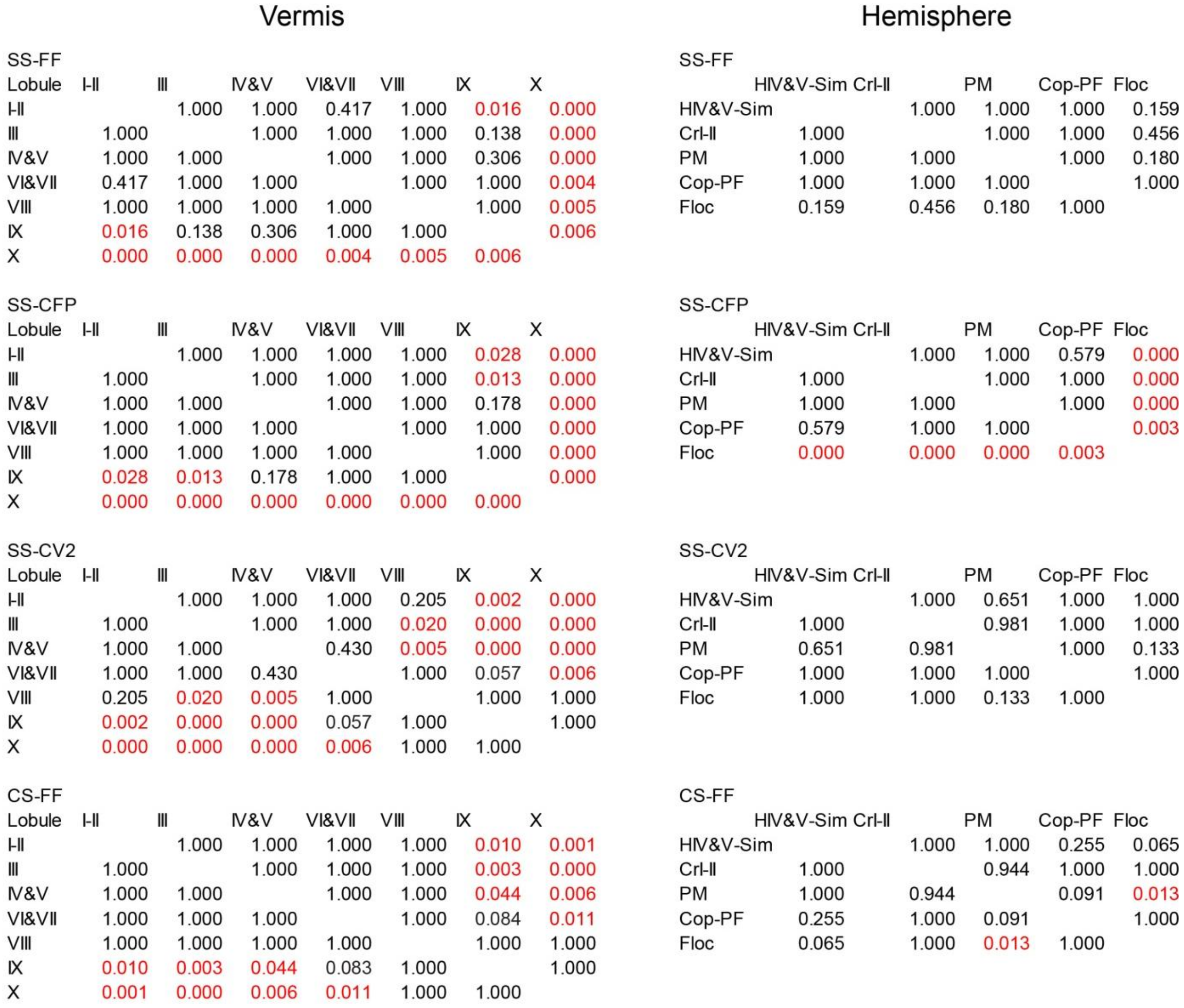

Vermis

SS-FF

| Lobule | I-II | III | IV&V | VI&VII | VIII | IX | X |
|---|---|---|---|---|---|---|---|
| I-II | | 1.000 | 1.000 | 0.417 | 1.000 | 0.016 | 0.000 |
| III | 1.000 | | 1.000 | 1.000 | 1.000 | 0.138 | 0.000 |
| IV&V | 1.000 | 1.000 | | 1.000 | 1.000 | 0.306 | 0.000 |
| VI&VII | 0.417 | 1.000 | 1.000 | | 1.000 | 1.000 | 0.004 |
| VIII | 1.000 | 1.000 | 1.000 | 1.000 | | 1.000 | 0.005 |
| IX | 0.016 | 0.138 | 0.306 | 1.000 | 1.000 | | 0.006 |
| X | 0.000 | 0.000 | 0.000 | 0.004 | 0.005 | 0.006 | |

SS-CFP

| Lobule | I-II | III | IV&V | VI&VII | VIII | IX | X |
|---|---|---|---|---|---|---|---|
| I-II | | 1.000 | 1.000 | 1.000 | 1.000 | 0.028 | 0.000 |
| III | 1.000 | | 1.000 | 1.000 | 1.000 | 0.013 | 0.000 |
| IV&V | 1.000 | 1.000 | | 1.000 | 1.000 | 0.178 | 0.000 |
| VI&VII | 1.000 | 1.000 | 1.000 | | 1.000 | 1.000 | 0.000 |
| VIII | 1.000 | 1.000 | 1.000 | 1.000 | | 1.000 | 0.000 |
| IX | 0.028 | 0.013 | 0.178 | 1.000 | 1.000 | | 0.000 |
| X | 0.000 | 0.000 | 0.000 | 0.000 | 0.000 | 0.000 | |

SS-CV2

| Lobule | I-II | III | IV&V | VI&VII | VIII | IX | X |
|---|---|---|---|---|---|---|---|
| I-II | | 1.000 | 1.000 | 1.000 | 0.205 | 0.002 | 0.000 |
| III | 1.000 | | 1.000 | 1.000 | 0.020 | 0.000 | 0.000 |
| IV&V | 1.000 | 1.000 | | 0.430 | 0.005 | 0.000 | 0.000 |
| VI&VII | 1.000 | 1.000 | 0.430 | | 1.000 | 0.057 | 0.006 |
| VIII | 0.205 | 0.020 | 0.005 | 1.000 | | 1.000 | 1.000 |
| IX | 0.002 | 0.000 | 0.000 | 0.057 | 1.000 | | 1.000 |
| X | 0.000 | 0.000 | 0.000 | 0.006 | 1.000 | 1.000 | |

CS-FF

| Lobule | I-II | III | IV&V | VI&VII | VIII | IX | X |
|---|---|---|---|---|---|---|---|
| I-II | | 1.000 | 1.000 | 1.000 | 1.000 | 0.010 | 0.001 |
| III | 1.000 | | 1.000 | 1.000 | 1.000 | 0.003 | 0.000 |
| IV&V | 1.000 | 1.000 | | 1.000 | 1.000 | 0.044 | 0.006 |
| VI&VII | 1.000 | 1.000 | 1.000 | | 1.000 | 0.084 | 0.011 |
| VIII | 1.000 | 1.000 | 1.000 | 1.000 | | 1.000 | 1.000 |
| IX | 0.010 | 0.003 | 0.044 | 0.083 | 1.000 | | 1.000 |
| X | 0.001 | 0.000 | 0.006 | 0.011 | 1.000 | 1.000 | |

Hemisphere

SS-FF

| | HIV&V-Sim | CrI-II | PM | Cop-PF | Floc |
|---|---|---|---|---|---|
| HIV&V-Sim | | 1.000 | 1.000 | 1.000 | 0.159 |
| CrI-II | 1.000 | | 1.000 | 1.000 | 0.456 |
| PM | 1.000 | 1.000 | | 1.000 | 0.180 |
| Cop-PF | 1.000 | 1.000 | 1.000 | | 1.000 |
| Floc | 0.159 | 0.456 | 0.180 | 1.000 | |

SS-CFP

| | HIV&V-Sim | CrI-II | PM | Cop-PF | Floc |
|---|---|---|---|---|---|
| HIV&V-Sim | | 1.000 | 1.000 | 0.579 | 0.000 |
| CrI-II | 1.000 | | 1.000 | 1.000 | 0.000 |
| PM | 1.000 | 1.000 | | 1.000 | 0.000 |
| Cop-PF | 0.579 | 1.000 | 1.000 | | 0.003 |
| Floc | 0.000 | 0.000 | 0.000 | 0.003 | |

SS-CV2

| | HIV&V-Sim | CrI-II | PM | Cop-PF | Floc |
|---|---|---|---|---|---|
| HIV&V-Sim | | 1.000 | 0.651 | 1.000 | 1.000 |
| CrI-II | 1.000 | | 0.981 | 1.000 | 1.000 |
| PM | 0.651 | 0.981 | | 1.000 | 0.133 |
| Cop-PF | 1.000 | 1.000 | 1.000 | | 1.000 |
| Floc | 1.000 | 1.000 | 0.133 | 1.000 | |

CS-FF

| | HIV&V-Sim | CrI-II | PM | Cop-PF | Floc |
|---|---|---|---|---|---|
| HIV&V-Sim | | 1.000 | 1.000 | 0.255 | 0.065 |
| CrI-II | 1.000 | | 0.944 | 1.000 | 1.000 |
| PM | 1.000 | 0.944 | | 0.091 | 0.013 |
| Cop-PF | 0.255 | 1.000 | 0.091 | | 1.000 |
| Floc | 0.065 | 1.000 | 0.013 | 1.000 | |

***Figure 3 – figure supplement 1. Statistical analysis of PC spiking characteristics per lobule.*** *Statistical comparisons of all recorded Purkinje cells, as presented in **Figure 3** and **4C.** These comparisons include all Purkinje cells from the vermis and hemispheres of which the location was determined based on dye injection (One-way ANOVA, followed by Bonferroni's posthoc test). FF, firing frequency; CFP, climbing fiber pause.*

## Complex spike characteristics depend on the zebrin identity

Reduced tonic SS activity of PCs at rest, as observed in Z+ modules, will lead to enhanced activity of the GABAergic neurons in the cerebellar nuclei that inhibit inferior olivary neurons[33,34]. Therefore one can expect the CS activity that results from activity in the climbing fibers originating in the inferior olive to be reduced as well. This prediction indeed holds (**Fig. 4A**). The CS activity of immunostaining identified Z+ PCs was significantly lower than that in Z− PCs (same PCs as described in **Fig. 1G-J**; Z−: 1.13 ± 0.25 Hz, Z+: 0.92 ± 0.28 Hz, $t$ = 3.926, $p$ < 0.001). This difference persisted in the subset of two-photon imaging identified Z+ and Z− PCs recorded in lobule V-VI and Crus I, supporting the link to zebrin-identity, rather than cortical location (**Fig. 4B**). Moreover, the gradual trend that we observed for SS firing frequency, but not for CV2, in the different lobules in both the vermis and hemispheres was also observed for CS activity (**Fig. 4C** and **Figure 3-figure supplement 1**).

Since climbing fibers evoked prolonged EPSCs in Z+ Purkinje cells[29], we also investigated the half-width of the first upward deflection in potential and the integrated deviation of the CS potential from zero. Both parameters were significantly higher in immunostaining identified Z+ PCs (half-width: $t = -3.269$, $p = 0.001$, spike area: $t = -2.523$, $p = 0.013$) (**Fig. 4D**). Given that SS activity as well as the wave of CS activity correlated with zebrin, the distribution of post-CS configurations of SS activity might in principle also be affected[35]. Based on the peri-CS time histograms, we could distinguish 4 different types of SS responses following the climbing fiber pause. These included a neutral pattern (i.e. normal type), a pattern with increased SS activity (i.e. facilitation type), and two patterns with decreased SS activity, one without and one with a superimposed oscillatory effect (i.e. suppression and oscillation type, respectively) (**Fig. 4E**). Thus, if there is a relation with zebrin expression, one could predict that the facilitation type of cells prevail in the Z− zones, whereas the suppression and oscillation type of cells occur predominantly in the Z+ zones. This prediction did hold. Even though the normal type dominated in both Z− and Z+ PCs, the suppression and oscillation types only occurred in Z+ PCs. The facilitation type occurred in both Z− and Z+ PCs, but significantly more in the Z− areas (Z−: 17 / 47, Z+: 6 / 57; $\chi^2 = 9.835$, $p = 0.002$, Pearson's Chi-squared test) (**Fig. 4F**). Attempts to find other parameters correlating with the response type were largely unsuccessful, except for the oscillation type, which showed a combination of low SS frequency and low CV (**Fig. 4G**).

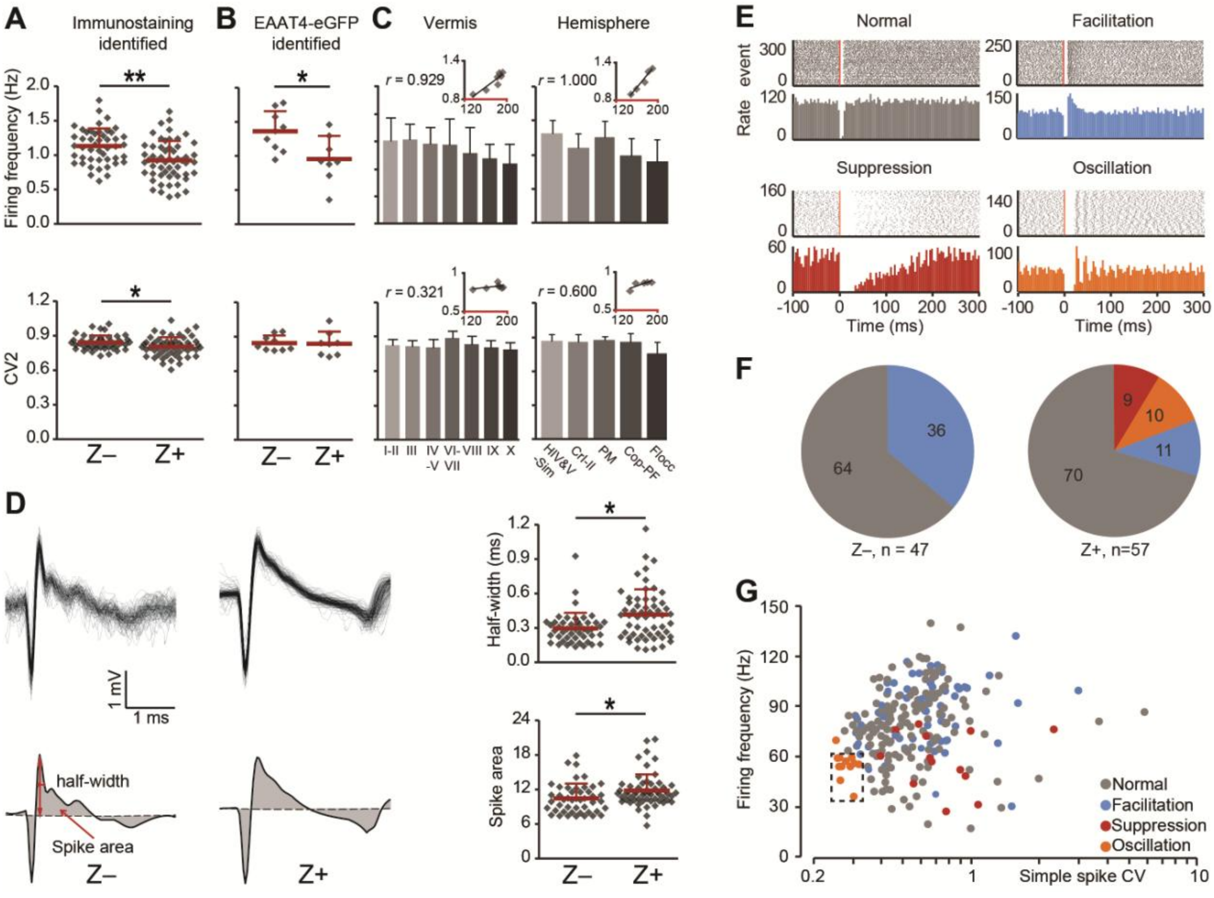

***Figure 4. Complex spike characteristics depend on zebrin identitiy. A**, Similar to simple spike frequency, complex spike frequency differs between immunostaining identified Z+ and Z− PCs (data from zebrin-identified PCs shown in Figure 1; t = 3.926, p < 0.001), **B**, This difference is confirmed in the sample of Z+ and Z− PCs obtained by two-photon imaging in EAAT4-eGFP mice, in that Z+ Purkinje cells have a lower complex spike firing frequency here too (t = 2.692, p = 0.017). **C**, Moreover, complex spikes frequency*

]

*shows significant correlation with zebrin intensity in vermis and hemisphere (vermis: $r = 0.929$, $p = 0.003$; hemisphere: $r = 1.000$, $p < 0.001$). Even though the regularity of CSs differs between immunostaining identified Z− and Z+ PCs (**A**, bottom), this was not reproduced in the other two experimental datasets (**B**-**C**, bottom). **D**, Typical Z− and Z+ CS shapes (–0.5 to +3 ms) showing the characteristics analyzed: half-width and spike area (left). Z+ PCs have a longer half-width and bigger spike area than Z− cells (right). **E**, Raster plots of simple spike activity around complex spikes (event, -100 ms till +300 ms) were converted in peri complex-spike time histograms. Based on these histograms, we could distinguish four different types of simple spike response types among the Purkinje cells recorded in all areas: normal, facilitation, suppression and oscillation. **F**, The percentage of different types in Z− and Z+ PCs (values indicate percentage). The facilitation type occurs predominantly in Z− PCs, whereas the suppression and oscillation type are restricted to the Z+ PCs. **G**, Attempts to find other parameters correlating in all recorded cells (n = 243 cells) with the response type were largely unsuccessful. The exception is the oscillation type, which has a signature combination of simple spike frequency and CV (11 out of 13, SS freq. range 35-60 Hz and CV < 0.32). Two-photon imaging data are only included in panel B; panels D-F are based on immunostaining identified Z+ and Z− PCs only and panels C and G on all recorded PCs. Error bars represent s.d., * $p < 0.05$, ** $p < 0.001$.*

## Z+ and Z− Purkinje cells differ in intrinsic spiking activity

In general, SS activity of PCs results from the integration of their excitatory input, inhibitory input and intrinsic pace-making activity[33]. This raises the question as to what extent the difference in SS firing frequency between Z+ and Z− PCs results from differences in input or intrinsic activity. We used two approaches to tackle this question. First, we completely removed the impact of external inputs onto the PCs using blockers for AMPA, NMDA and $GABA_A$ receptors during cell-attached recordings from sagittal slices (**Fig. 5A**). The average SS firing frequency was, on average, 22 ± 7 % lower over all lobules *in vitro* than that *in vivo* indicating that the larger part of SS activity is internally driven by PCs. The dominant impact of intrinsic PC activity was also reflected by the finding that the differential firing frequency pattern over all lobules *in vitro* correlated with that *in vivo* ($r = 0.916$, $p = 0.010$, Pearson's correlation) (**Fig. 5B**). For example, the *in vitro* SS firing frequency of PCs in lobules III, which are predominantly Z−, was alike the *in vivo* recordings significantly higher than that in lobule X, where PCs are Z+ ($t = 2.844$, $p = 0.007$). This higher firing frequency in lobule III was associated with a higher intrinsic excitability in lobule III compared to lobule X, reinforcing the interpretation that the difference is predominantly intrinsic to Purkinje cells (**Figure 5-figure supplement 1**) (see also [27]). To confirm that under these *in vitro* conditions, without excitatory or inhibitory input, the difference in simple spike firing frequency still correlates with zebrin identity, we also recorded the activity of fluorescence-identified Z+ and Z− PCs in adjacent bands in slices from the EAAT4-eGFP mice. Comparison of sets from lobules II-V and lobule VIII-IX confirmed this presumption (II-V: $t = 2.910$, $p = 0.017$; VIII-IX: $t = 2.352$, $p = 0.043$) (**Fig. 5C**).

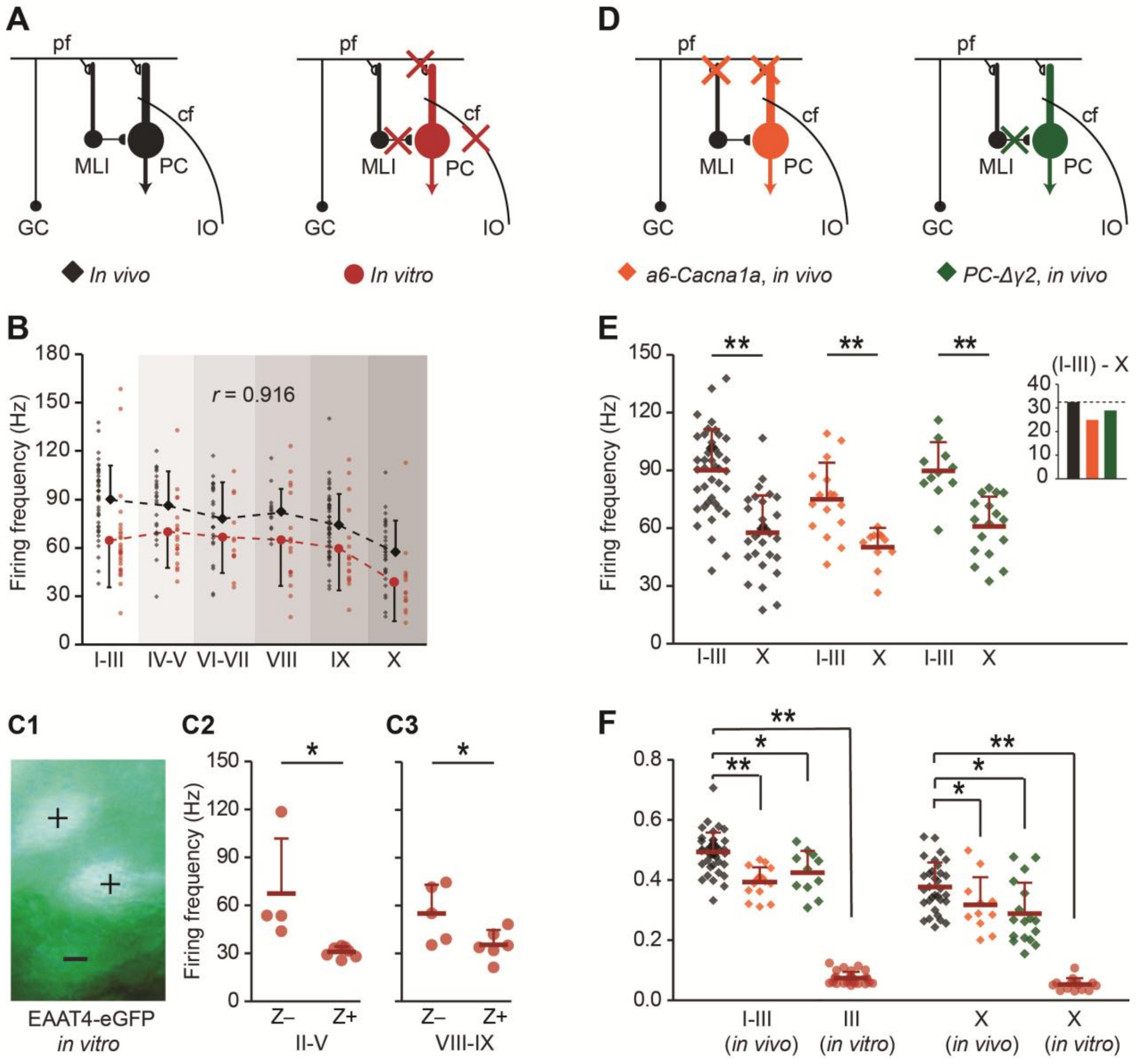

***Figure 5. Zebrin-related differences are present in the intrinsic activity of Purkinje cells.*** *To test if intrinsic or input-related differences underly the difference in simple spike frequency we recorded PC activity in conditions of limited or no synaptic input.* ***A****, PC activity was recorded in vitro ($n = 107$ cells, 15 mice) under complete block of synaptic inputs.* ***B****, Spiking frequency in vitro (red) was lower than that in vivo (black) over the range of lobules, but the shape of the curve was similar ($r = 0.916$, $p = 0.010$, Pearson's correlation).* ***C1-3****, To verify the correlation with zebrin, we recorded activity of EAAT4/zebrin-positive and negative PCs in slices of EAAT4-eGFP mice. Both in lobules II-V (Z+: $n = 7$ cells, Z−: $n = 4$; 3 mice; $t = 2.910$, $p = 0.017$) and lobules VIII-IX (Z+: $n = 6$, Z−: $n = 5$; 2 mice; $t = 2.352$, $p = 0.043$) the difference in simple spike firing frequency was present, further confirming the link with zebrin.* ***D****, Next, extracellular recordings were made in vivo in a6-Cacna1a and PC-Δγ2 mutant mice that have minimized excitatory and no synaptic inhibitory inputs to their PCs, respectively.* ***E****, PC activity in Z+ lobule X of both mutants was lower than that in the predominantly Z− lobules I-III (normal, lobules I-III: $n = 43$ cells, 18 mice, lobule X: $n = 32$ cells, 25 mice, $t = 6.808$, $p < 0.001$; a6-Cacna1a, I-III: $n = 16$ cells, 2 mice; X: $n = 10$ cells, 2 mice; $t = 3.988$, $p < 0.001$; PC-Δγ2, I-III: $n = 11$ cells, 3 mice; X: $n = 17$ cells, 3 mice; $t = 4.876$, $p < 0.001$). Inset compares the absolute differences in firing frequency between lobules I-III and X.* ***F****, CV2 values of Z− and Z+ SS activity from in vitro recordings (lobules I-III and X: both $p < 0.001$) and in vivo recordings of both a6-Cacna1a mutants (lobule I-III: $t = 5.613$, $p < 0.001$; lobule X: $t = 1.864$, $p = 0.070$) and PC-Δγ2 mutants (lobules I-III and X: both $p < 0.005$) were signifcantly lower than the wild type recordings. Abbreviations: cf, climbing fiber; GC, granule cell; IO, inferior olive; MLI, molecular layer interneuron; PC, Purkinje cell; pf, parallel fiber. Error bars represent s.d., * $p < 0.05$, ** $p < 0.001$.*

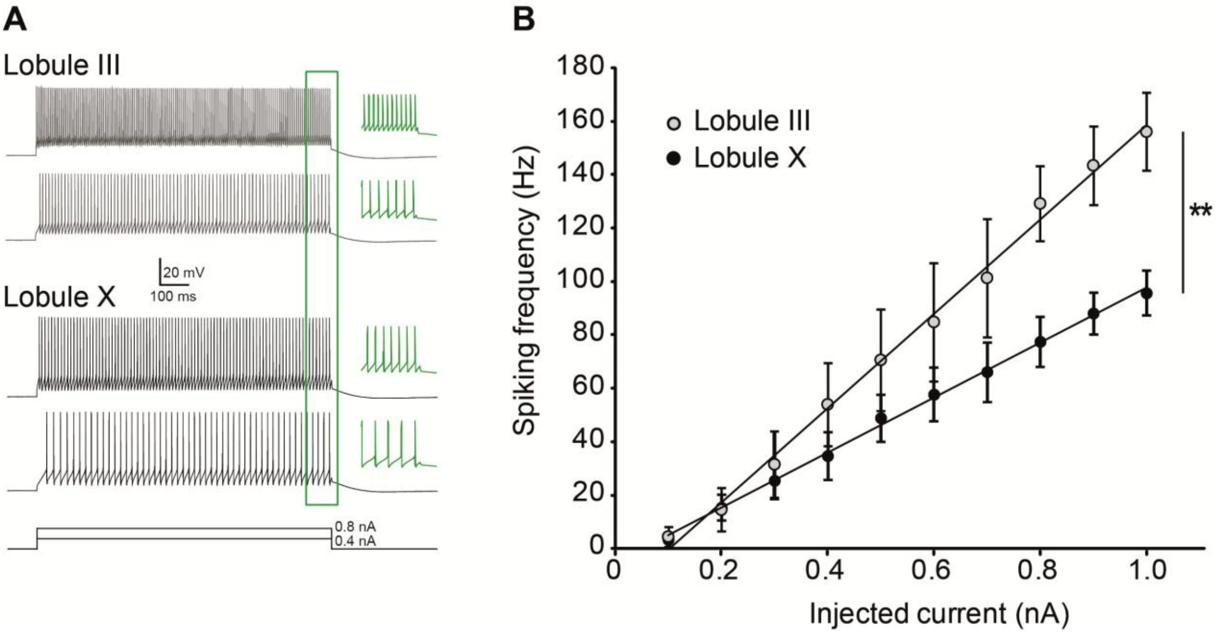

***Figure 5 – figure supplement 1. Purkinje cell intrinsic excitability is higher in lobule III than in X.*** *To test intrinsic excitability, Purkinje cells were current clamped at –65 mV, 1 s current steps were injected increasing from 0.1 to 1.0 nA and the response frequencies were determined.* ***A****, Example traces with insets (green) showing a magnification of the last 100 ms.* ***B****, Response frequency was determined for the entire range, and the slope was calculated. The slope of the input-output curves was significantly higher in Purkinje cells from lobule III compared to lobule X (III: mean ± s.e.m. 226.0 ± 14.5 spk/nA, n = 7; X: 124.1 ± 20.6 spk/nA, n = 9; t = 4.311, p < 0.001). Error bars denote s.e.m, ** p < 0.001.*

To further assess the impact of excitatory and inhibitory inputs, we investigated the *in vivo* SS activity in mouse mutants, in which either the glutamatergic input (*a6-Cacna1a* mutants) or the GABAergic input (*PC-Δγ2* mutants) to PCs was affected. The *a6-Cacna1a* mutants are characterized by a silenced parallel fiber output in the vast majority of their granule cells due to a lack of voltage gated calcium channels required for neurotransmission[36], while the *PC-Δγ2* mutants are characterized by the absence of synaptic inhibition from the molecular layer interneurons through ablation of the γ2 subunit of the $\text{GABA}_\text{A}$-receptor in PCs[37] (**Fig. 5D**). In both *a6-Cacna1a* and *PC-Δγ2* mutant mice the differences *in vivo* in SS firing frequency between lobules I-III and lobule X were still significant, analogous to that in normal mice (*a6-Cacna1a*, I-III: 75.1 ± 19.0 Hz, X: 49.1 ± 9.9 Hz, $t = 3.988$, $p < 0.001$; *PC-Δγ2*, I-III: 89.8 ± 14.9 Hz, X: 60.9 ± 15.6 Hz, $t = 4.876$, $p < 0.001$) (**Fig. 5E**). In contrast, the CV2 values of SS activity were significantly reduced not only *in vitro*, but also *in vivo* in both *a6-Cacna1a* and *PC-Δγ2* mutants as compared to wild-types (**Fig. 5F**). These differences held true for lobules I-III (*in vitro*: $t = 32.647$; *a6-Cacna1a*: $t = 5.613$, $p < 0.001$; *PC-Δγ2*: $t = 3.068$, $p = 0.003$ vs. *in vivo* wild-types), as well as in 2 out of 3 cases for lobule X (*in vitro*: $t = 14.593$, $p < 0.001$; *a6-Cacna1a*: $t = 1.864$, $p = 0.070$; *PC-Δγ2*: $t = 3.292$, $p = 0.002$). Together, these data suggest that the SS firing frequency is largely determined by intrinsic properties of PCs, whereas the level of regularity appears to be predominantly determined by external inputs.

### Activation of TRPC3 contributes to increase in SS activity in Z− Purkinje cells

The finding that the difference in firing frequency between Z+ and Z− PCs must predominantly reflect their different intrinsic properties raises the question whether PC proteins other than zebrin also play a mechanistic role. This may be particular relevant as zebrin, or aldolase C, is a glycolytic enzyme and probably plays a secondary role via energy consumption without a direct impact on the electrophysiological properties of PCs. In fact, when the products of aldolase C, i.e. glyceraldehyde-3-phosphate (GAP) and dihydroxyacetone phosphate (DHAP), were introduced to the ACSF in our *in vitro* recordings, SS firing increased in both the largely zebrin-negative lobule III and zebrin-positive lobule X (**Figure 6-figure supplement 1**), arguing against the possibility that aldolase C's enzymatic function directly contributes to a lower SS firing frequency in Z+ PCs. Hence, we shifted our focus to TRPC3, which can be associated with zebrin-negative PCs[19,24,26], and underlies the mGluR1-mediated slow EPSCs[24] and mGluR1-agonist (DHPG) induced currents[38], that have been shown to affect SS activity even in the absence of synaptic input[39-41]. We first tested the effect of blocking TRPC3 on the activity of PCs *in vitro* in lobules III and X, in the absence of synaptic input, using two blockers, genistein and Pyr3[26,42]. Both TRPC3 blockers had a significant impact on PC activity reducing the firing frequency in lobule III (genistein, $p < 0.001$; Pyr3, $p < 0.001$ vs. vehicle control, **One-Way ANOVA** followed by **Tukey's post-hoc** test) without a significant effect in lobule X ($p = 0.271$ and $p = 1.000$ vs. vehicle respectively, **One-Way ANOVA** followed by **Tukey's post-hoc** test) (**Fig. 6A-B**), an effect that is in line with that of blocking mGluR1[39-41]. To more directly compare the effect of blocking TRPC3 between lobule III and X, we recorded PC activity during wash-in of the blockers (**Fig. 6C**). Wash-in of Pyr3 had a robust effect on SS firing frequency of PCs in lobule III (pre: 49.9 ± 7.9 Hz; post: 25.5 ± 9.9 Hz; $t = 5.412$, $p = 0.002$, paired Student's $t$-test) and this effect was significantly larger than that in lobule X (% reduction, lobule III: 48.2 ± 19.7%; lobule X: 8.5 ± 16.6%; $t = 4.069$, $p = 0.002$) (**Fig. 6D-E**).

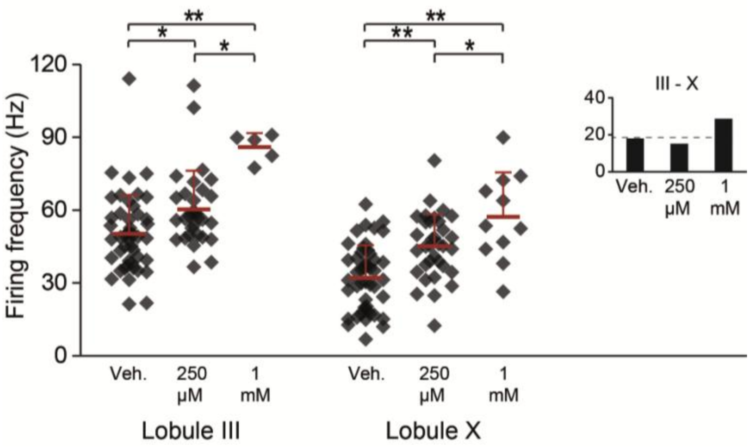

***Figure 6 – figure supplement 1. Aldolase C enzymatic reaction products GAP and DHAP increase the activity in lobules III and X.*** *To test the possibility that zebrin, or aldolase c, is responsible for the difference in simple spike activity due to its enzymatic activity, we bath-applied its reaction products. If this difference in enzymatic activity is responsible for the difference in simple spike activity between Z+ and Z– Purkinje cells, addition of the reaction products of zebrin should decrease the activity of Zebrin negative Purkinje cells in lobule III. Simultaneous application of 250 µM of glyceraldehyde-3-phosphate (GAP) and dihydroxyacetone phosphate (DHAP) caused a subtle but significant increase in simple spike activity in both lobule X and lobule III (X: p < 0.001; III: p = 0.019 vs. vehicle, One-Way ANOVA followed by Bonferroni's post-hoc tests). This increase was even more pronounced when we increased the concentration to 1 mM of each (X: p < 0.001; III: p < 0.001 vs. vehicle, One-Way ANOVA followed by Bonferroni's post-hoc tests). The increase of activity, particularly in lobule III, and the persistence of the difference between lobule III and X, argue against a role for aldolase c in generating the difference in simple spike activity between Z+ and Z– Purkinje cells. Minimum recording duration was 60 s. Error bars represent s.d., * p < 0.05, ** p < 0.001.*

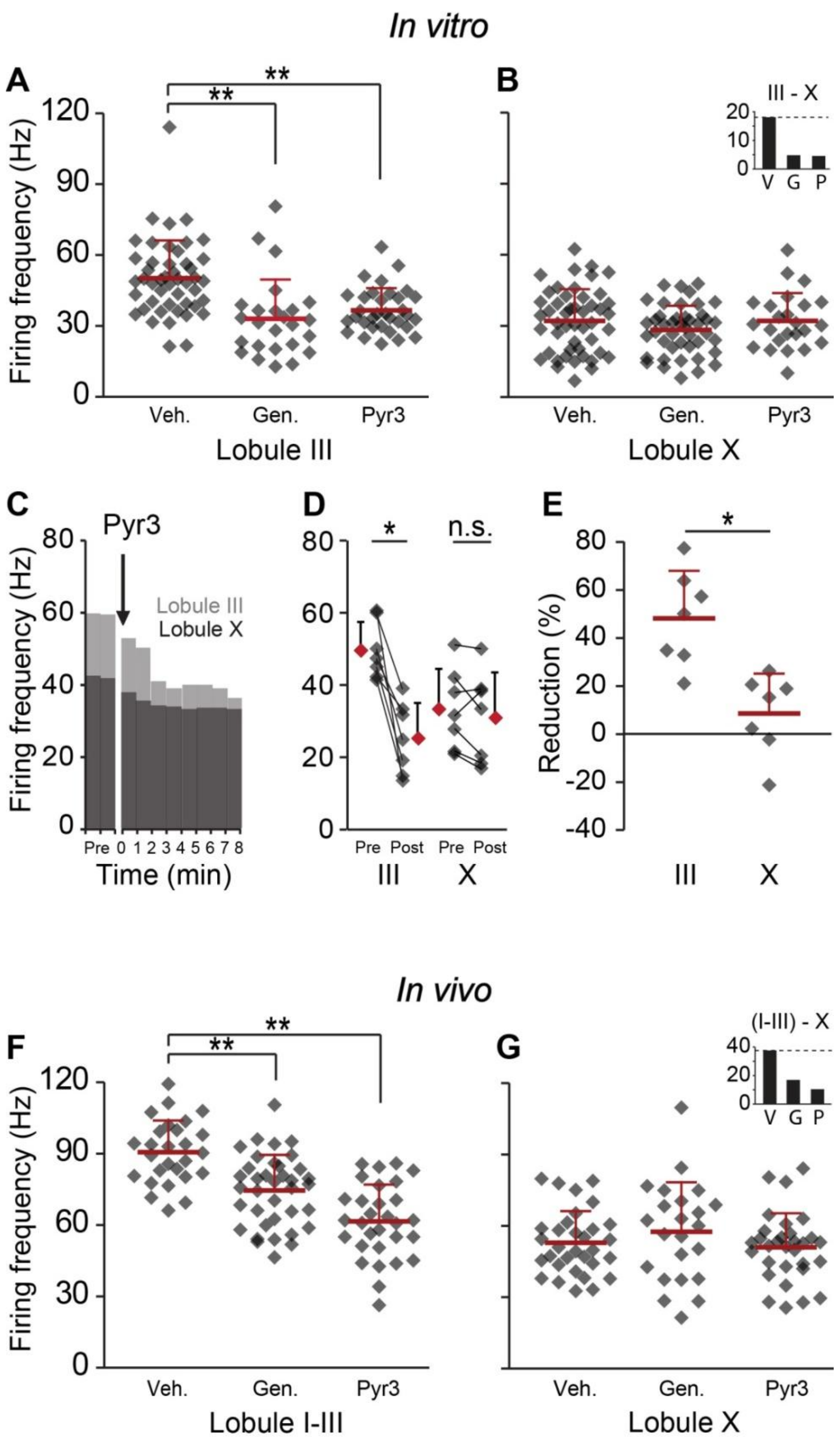

***Figure 6. Blocking TRPC3 attenuates the simple spike frequency difference.*** *In search for the underlying mechanism, we tested the contribution of TRPC3, which can be indirectly linked to zebrin-like expression.* ***A-B****, The presence of TRPC3 blocker genistein (10 μM) or the more selective Pyr3 (100 μM) reduced Purkinje cell firing frequency in lobule III (vehicle: $n = 47$ cells, 6 mice; genistein: $n = 25$ cells, 7 mice; Pyr3: $n = 33$ cells, 7 mice; both $p < 0.001$ vs. vehicle, One-Way ANOVA followed by Tukey's post-hoc test), but not in lobule X (vehicle: $n = 48$ cells, 6 mice; genistein: $n = 44$ cells, 7 mice; Pyr3, $n = 24$ cells, 7 mice; $p = 0.271$ and $p = 1.000$ vs. vehicle, respectively, One-Way ANOVA followed by Tukey's post-hoc test), virtually eliminating the difference between averages for lobule III-X (inset). To more directly quantify the effect of blocking TRPC3 we washed-in Pyr3 during the recording of Purkinje cells in lobule III and X.* ***C-E****, Pyr3 wash-in significantly decreased the simple spike firing frequency in lobule III ($n = 7$ cells, 7 mice; $t = 5.412$, $p = 0.002$, paired Student's t-test), and this decrease was larger in lobule III than in lobule X ($t = 4.069$; $p = 0.002$).* ***F-G****, In line with the in vitro data, in vivo blocking of TRPC3 by application of genistein (240 mg/kg, i.p.) or Pyr3 (200 μg, i.c.v.) decreased simple spike firing in lobule I-III (vehicle: $n = 27$ cells, 3 mice; genistein: $n = 37$ cells, 3 mice and Pyr3: $n = 30$ cells, 2 mice; both $p < 0.001$ vs. vehicle, One-Way ANOVA followed by Tukey's post-hoc test), but had no effect in lobule X (vehicle: $n = 32$ cells, 3 mice; genistein: $n = 23$ cells, 4 mice and Pyr3: $n = 31$ cells, 4 mice; $p = 0.546$ and $p = 0.887$ vs. vehicle, respectively One-Way ANOVA followed by Tukey's post-hoc test), resulting in a pronounced reduction of the difference (inset). Error bars represent s.d., * $p < 0.05$, ** $p < 0.001$.*

An alternative candidate protein that has a zebrin-related expression in adult animals and could potentially influence spiking activity is EAAT4, a glutamate transporter that is expressed in a zebrin-like pattern and carries a depolarizing current[18]. Based on the higher expression of EAAT4 in Z+ Purkinje cells, blocking EAAT4 would arguably affect lobule X more than lobule III, but the general EAAT blocker DL-TBOA had no significant effect on the activity of Purkinje cells in either lobule (**Figure 6-figure supplement 2A-B**) (lobule III: $t = 1.219$, $p = 0.227$; lobule X: $t = -0.597$, $p = 0.533$), maintaining the difference between lobule III and X (inset, $t = 3.641$, $p < 0.001$). Wash-in of DL-TBOA did also not affect activity in lobule III or X (lobule III: 2.0 ± 10.8%; lobule X: -3.6 ± 3.4%; $t = 0.982$, $p = 0.352$) (**Figure 6-figure supplement 2C-E**).

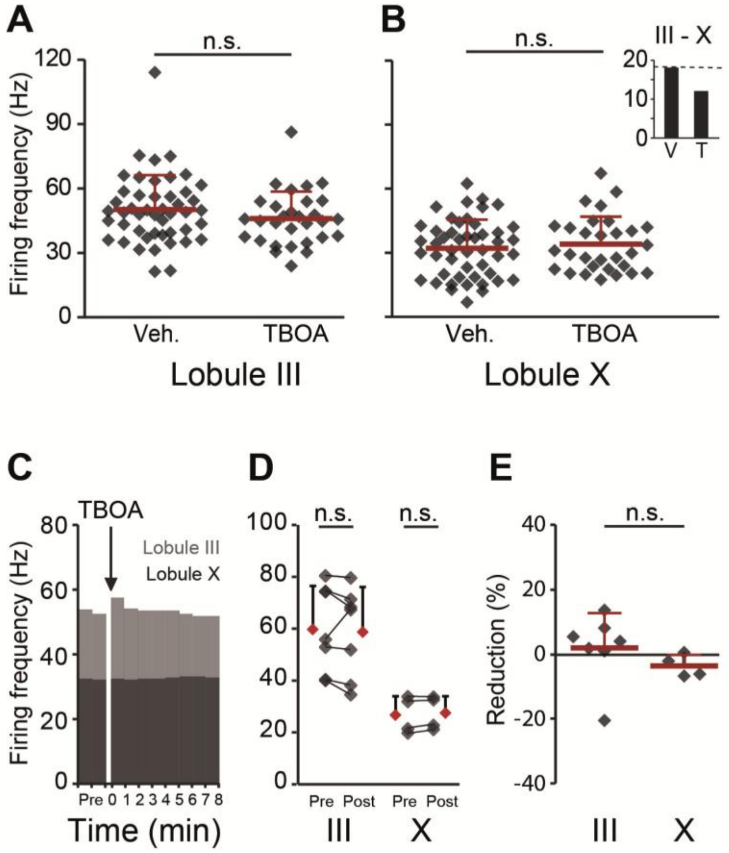

***Figure 6 – figure supplement 2. Effects of blocking EAAT4 on Purkinje cell activity in lobule III and X in vitro.*** *In search for the underlying mechanism, we tested the contribution of EAAT4, which is expressed in a pattern similar to that of zebrin, to Purkinje cell activity in vitro.* ***A-B****, EAAT4 blocker TBOA (25 µM) did not affect the firing frequency of Purkinje cells in lobule III (vehicle: $n = 47$ cells, 6 mice; DL-TBOA: $n = 30$ cells, 5 mice; $t = 1.219$, $p = 0.227$), or those in lobule X (vehicle: $n = 48$ cells, 6 mice; DL-TBOA: $n = 30$ cells, 5 mice; $t = -0.597$, $p = 0.553$), largely maintaining the difference between averages for lobule III-X (inset).* ***C-E****, Wash-in of DL-TBOA had no significant effect (III: $n = 7$ cells, 6 mice; $t = 0.457$, $p = 0.664$, X: $n = 4$ cells, 4 mice; $t = -2.202$, $p = 0.115$, paired Student's t-test). Error bars represent s.d..*

Next, we studied whether the effects of TRPC3 blockers were sufficiently robust to also induce measurable effects *in vivo*. In line with the *in vitro* data, both genistein and Pyr3 (i.p. and i.c.v., 240 mg/kg and 200 µg, respectively) caused a decrease in SS activity in lobules I-III, lasting for several hours (vehicle: 90.6 ± 13.3 Hz; genistein: 74.6 ± 14.9 Hz; Pyr3: 61.6 ± 15.5 Hz; both $p < 0.001$ vs. vehicle, **One-way ANOVA** followed by **Tukey's post-hoc** test), while no significant effect was recorded in lobule X (vehicle: 52.9 ± 13.3 Hz; genistein: 57.5 ± 20.8 Hz,; Pyr3: 51.1 ± 14.3 Hz, $p = 0.546$ and $p = 0.887$ vs. vehicle, **One-way ANOVA** followed by **Tukey's post-hoc** test) (**Fig. 6F,G**). Together with changes in simple spike frequency, several other parameters, related to the complex spike of Purkinje cells in lobule I-III shifted, upon Pyr3 application, towards the values for lobule X with or without drugs. These included including climbing fiber pause, complex spike frequency and width and type of simple spike response following complex spikes (**Figure 6-figure**

**supplement 3**). Effects of genistein were less consistent, probably due to its less selective nature. Together, these data suggest that TRPC3 contributes to the elevated SS activity in zebrin-negative PC zones.

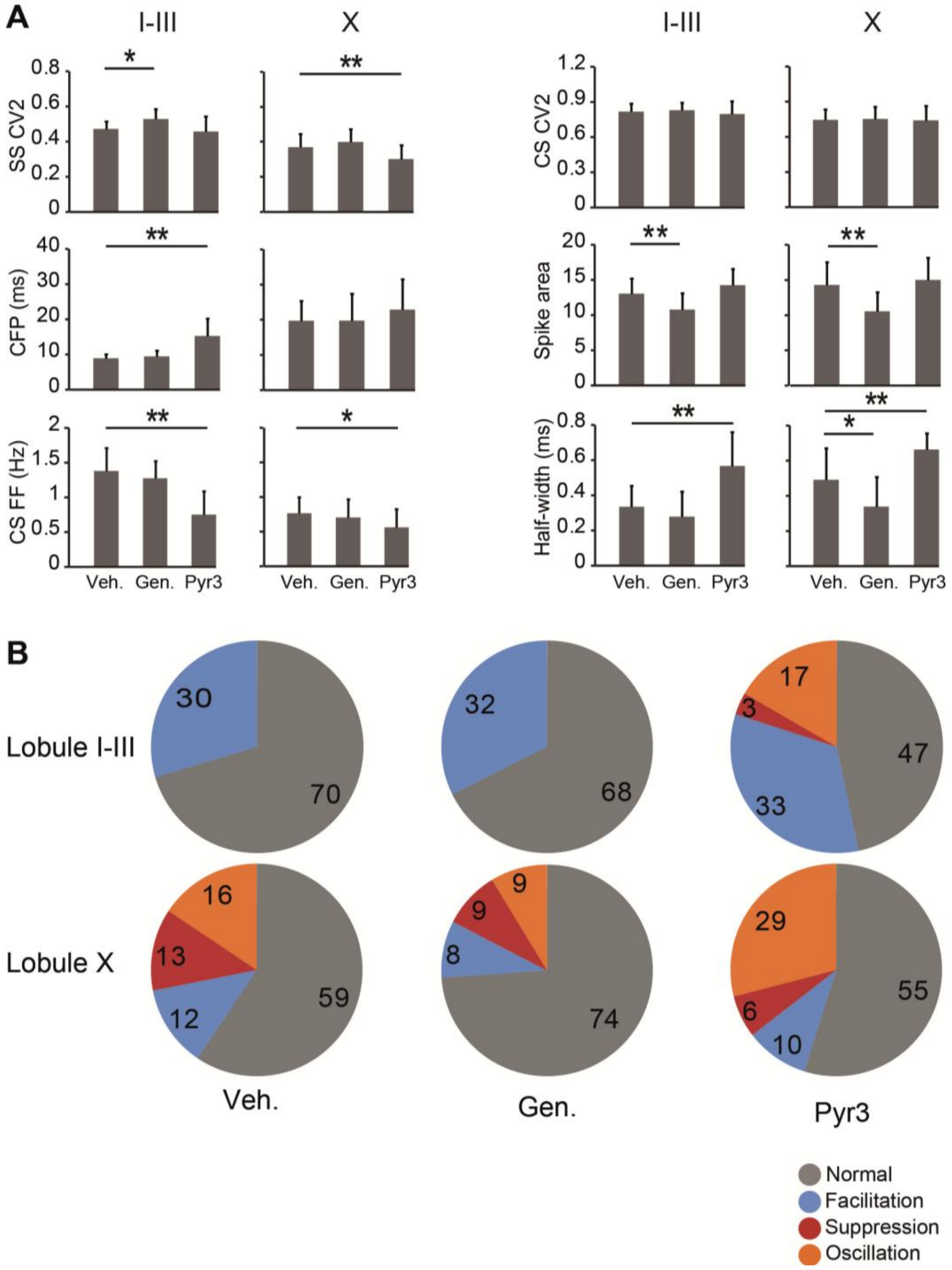

*Figure 6 – figure supplement 3.* ***Effects of TRPC3 blockers on other PC activity parameters.*** *Application of TRPC3 blockers genistein and Pyr3 affected, apart from simple spike firing frequency, several other characteristics of Purkinje cell activity.* ***A****, Whereas effects of TRPC3 blockers on simple and complex spike regularity were subtle or absent, Pyr3 increased the climbing fiber pause and decreased the complex spikes firing frequency in lobules I-III towards levels comparable to those found in lobule X, suggesting that the differences in these parameters between the predominantly zebrin-negative lobules I-III and zebrin-positive lobule X are also, at least in part, dependent on the activity of TRPC3. The effects of Pyr3 on complex spike half width appears to be comparable, in that it increases half-width towards levels observed in lobule X, while genistein predominantly has an attenuating effect on half-width and spike area, possibly due to its*

*less selective nature.* ***B****, Interestingly, blocking TRPC3 with Pyr3 induces the occurence of the suppression and oscillation response types in the post complex spike simple spikes activity. These types are under normal and vehicle conditions restricted to PCs in lobule X, suggesting a role for TRPC3 in the post complex spike activity. Error bars represent s.d. * $p < 0.05$, ** $p < 0.001$.*

## *Discussion*

This study provides, to our knowledge, the first evidence for ubiquitously organized differences in cerebellar Purkinje cell firing activity *in vivo* and for the correlation of these differences to a marker protein, zebrin II. As zebrin, as a biomarker, can be associated with the modular organization of the olivo-cortico-nuclear circuit[7,11,12,43], our results indicate that Purkinje cells within the same module operate around a preferred range of intrinsically determined SS firing frequencies and that this activity is different from modules with a different zebrin identity. Moreover, presumably as a secondary effect, CS activity is also altered. Since the differences were consistently found throughout the entire cerebellar cortex, these findings have direct consequences for all cerebellar functions and the coding schemes they can engage.

### Difference in SS activity and underlying factors

The difference in SS firing frequency between zebrin-positive and zebrin-negative PCs *in vivo* was robust (i.e. approximately 60 Hz versus 90 Hz) and highly significant, present throughout the cerebellar cortex and could be reproduced by directly comparing the activity of Purkinje cells in adjacent modules. Although we cannot exclude the possibility that lobule-specific effects contribute to the observed differences in simple and complex spike firing frequency, the results obtained in EAAT4-eGFP mice *in vivo* and *in vitro* argue against a contribution of their rostro-caudal or lobular location. The difference in SS firing frequency is probably largely determined by the intrinsic properties of PCs, as this difference was maintained in the reduced slice preparation, in which the inputs are blocked, as well as in mouse mutants, in which the excitatory (*a6-Cacna1a* mice) or inhibitory (*PC-Δγ2* mice) inputs are attenuated. Comparing the PC activity in zebrin-positive and negative PCs per transverse zone confirmed its link to zebrin-identity, but also revealed a more subtle difference within the population of zebrin-positive PCs. These differences could be lobule-specific and/or originate from differences in input, in more subtle variations in zebrin or its related proteins or even in the expression pattern of other proteins. It should be noted, however, that blocking TRPC3 shifts the activity of Z− PCs towards that of Z+ PCs, indicating that the potential differences within the group of Z+ PCs do not affect our conclusions.

In contrast, the level of regularity of firing (i.e. CV2) was not consistently dependent on zebrin identity, but significantly altered by impairing the excitatory and/or inhibitory inputs. In line with the notion that reduced SS activity of PCs, as observed in the zebrin-positive modules, should lead to enhanced firing of the GABAergic neurons in the cerebellar nuclei and thereby to reduced activity in the inferior olivary neurons[33,34], we found that CS activity induced by activity of olivary climbing fibers was reduced in zebrin-positive PCs. In fact, reduction of simple spike frequency in lobule III *in vivo* for several minutes to hours by Pyr3 application also reduced complex spike frequency, supporting the indirect control of simple spikes on complex spike activity. Interestingly, temporary increases in climbing fiber evoked CS activity suppresses SS frequency providing a homeostatic control mechanism within an olivocerebellar module[44,45]. Thus, whereas the external inputs to PCs may control the precise temporal coding of SS activity at rest as well as the firing frequency and dynamic range during natural sensory stimulation[36,46], their intrinsic properties appear to determine the baseline frequencies of SSs as well as CSs at rest, around which they can operate.

These findings raise the question which proteins in the zebrin-positive and zebrin-negative zones may actually determine the difference in intrinsic firing frequencies of their PCs. Since zebrin's enzymatic reaction products did not underly the differences in SS firing frequency, we shifted attention to other proteins that are expressed in pattern similar or complementary to that of zebrin. We targeted EAAT4, which is expressed in a pattern similar to that of zebrin, and TRPC3, the effector channel of a cascade of proteins that have zebrin-like expression patterns[17-19]. Whereas blocking EAAT4 *in vitro* had no detectable effect on SS firing frequency, blocking TRPC3 reduced SS activity in lobule III (largely zebrin-negative), but not in lobule X (zebrin-positive), both *in vitro* and *in vivo*. It should be noted that, although TRPC3 gene expression appears to vary from anterior to posterior with higher levels in the anterior, largely zebrin-negative, lobules (Allen Brain Atlas, www.brain-map.org), there is no immunohistochemical evidence for differences in protein levels available[24,25,47]. If the expression of TRPC3 is indeed homogeneous throughout the cerebellum, the differential effect of blocking TRPC3 suggests that its activity might be higher in Z− PCs. Two mutually non-exclusive mechanisms could contribute to this difference in activity. First, several proteins in the molecular cascade related to TRPC3 are expressed in zebrin-like bands, including the IP3-receptor[20] (TRPC3 modulator[26]), PLCβ3/4[21] (TRPC3 activator[26]), PKCδ[22] and NCS-1[23]. In fact, zebrin II, or aldolase C, which is not likely to be involved via its enzymatic function, bears the capacity to bind IP3[48], and thus could potentially reduce the activation of TRPC3 in Z+ PCs, through IP3R1. At the same time, mGluR1 subtype b is expressed in a pattern complementary to that of zebrin[19], and it has been shown that mGluR1 can be tonically activated, that mGlurR1 blockers can reduce SS firing frequency[39-41], and that mGluR1-evoked depolarizing currents can be blocked with TRPC3-selective blockers[26,42]. However, the possibility that an alternative pathway, independent of mGluR1, leads to TRPC3 activition cannot be excluded. Knowledge of this pathway of proteins and their exact interactions is at current presumably incomplete and beyond the scope of this study. The findings that the expression patterns of mGluR1b, PLCβ, PKCδ and IP3R1, all of which are key proteins in calcium release from intracellular calcium stores, are linked to cerebellar modules[19] and intimately connected with TRPC3, provokes the speculation that this entire pathway contributes to the difference in SS activity between zebrin-positive and zebrin-negative PCs (see also [24,47]).

### General functional implications

Our finding that SS activity and indirectly also CS activity at rest are determined by the intrinsic properties of PCs implies that they operate around these baseline frequencies during natural stimulation and behaviour. Interestingly, the low and high baseline frequencies of zebrin-positive and zebrin-negative PCs also appear to be in line with their propensities for induction of long-term potentiation (LTP) and long-term depression (LTD), respectively[18,49]. Thus, PCs operating at lower frequencies may be preferentially potentiated, whereas PCs with higher SS firing frequency may have less 'space' for increasing the firing rate and may be more prone to express LTD. Likewise, entrainment of cerebellar nuclei neurons by synchronized SS input from PCs, which results in phase-locking of connected neurons, may occur at 50 - 80 Hz, but is impaired at 100 Hz[50]. If correct, this mechanism predicts that the phase-locking mechanism is engaged in contacts between zebrin-positive PCs and cerebellar nuclei neurons, whereas those involved in zebrin-negative zones may be more prone for rebound excitation, which follows strong forms of inhibition[33,50].

The cerebellar nuclei can also be divided based on the zebrin expression pattern, with a rostral half that receives predominantly input from zebrin-negative PC's and a caudal part that mostly receives zebrin-positive inputs[12,14,15]. This implies that PC input to cerebellar nuclei neurons may be segregated on the basis of frequency, and that as a consequence the output of cerebellar nuclei neurons located within zebrin-positive and -negative territories may be distinctly different. Although this remains speculative at this stage, similar phenomena have been described for highly active neurons in cerebral cortex[51] and hyperpolarization-activated currents in affiliated olfactory bulb mitral neurons[52]. Combined with the zebrin- or lobule-related prevalence of plasticity mechanisms[18,49], our results suggest that the biochemically identified bands in the structurally homogenous cerebellar cortex are physiologically different with distinct biophysical signatures that probably have significant implications downstream in the cerebellar nuclei and thereby on motor behaviour and cognition.

## Materials and Methods

### *In vivo* extracellular recordings

We recorded *in vivo* single-unit Purkinje cell activity in adult male C57Bl/6 mice (C57Bl/6J, Charles River), aged 10 to 35 weeks. Mice were prepared for recordings by placing an immobilizing construct (pedestal) and a craniotomy on their skulls[46]. In short, the skin over the skull was shaven, and opened along the rostro-caudal midline. Using Optibond (Kerr, Salerno, Italy) and Charisma (Heraeus Kulzer, Hesse, **Germany**) a U-shaped holder (6 x 4 mm) with a magnet inside (4 x 4 mm, MTG, Weilbach, Germany) was fixed on the skull, overlying the frontal and parietal bones. Next, the medial neck muscles overlying the occipital bone were removed, a craniotomy was made over the interparietal or occipital bone and a recording chamber was placed around it, allowing *in vivo* electrophysiological recordings throughout different areas in the cerebellum of awake mice. The exact location of the craniotomy depended on the target area, see **Figure 1-figure supplement 1** for details. After recovery of > 24 hrs, mice were head-fixed to a bar, their bodies restrained in a custom-made plastic tube and the dura was opened to facilitate the recording of extracellular Purkinje cell activity, as previously described[53]. Electrophysiological activity in the cerebellar cortex was recorded using double barrel borosilicate glass pipettes (theta septum, 1.5 OD, 1.02 ID, WPI, FL, USA). To do so, one of the barrels was opened laterally, approx. 10 mm from the taper, to allow entrance of the electrode wire and sealed with glass glue at the back. The other barrel was filled with a blue dye (Alcian Blue, 0.1-0.2 % solution in saline, **Sigma-Aldrich**, St. Louis, MO, USA). The recording half of the double barrel pipettes were filled with 2 M NaCl-solution, and had a tip size of 3-6 μm, respectively. Pipettes were advanced into the cerebellum with an oil micro-drive (Narishige, Tokyo, Japan) and signals were pre-amplified (custom-made preamplifier, 1000x DC), filtered (CyberAmp 320, Axon, Molecular Devices, Sunnyvale, CA, USA), digitized (Power1401, CED, Cambridge, UK) and stored for offline analysis. After successful recordings, brief pressure pulses were delivered through the other barrel of the electrode, using a custom-built device, to mark the recording site. To obtain *a6-Cacna1a* and *PC-Δγ2* mice, we used the Cre/loxP system to delete exon 4 of the gene coding for the P/Q-type voltage-gated calcium channel (*Cacna1a*) selectively from granule cells and exon 4 of the $GABA_A$ receptor γ2 subunit gene (*Gabrg2*) selectively from PCs, respectively, as described previously[36,37]. In short, we crossed $\textit{Cacna1a}^{lox/lox}$ mice with Gabra6::Cre (or Δa6::cre) mice[54] and $\textit{Gabrg2}^{lox/lox}$ mice with Pcp2::Cre (or L7::Cre) mice[55], respectively. From the offspring, that was heterozygous for the floxed genes (i.e. $\textit{Cacna1a}^{lox/+}$ and $\textit{Gabrg2}^{lox/+}$), Cre-negative males were crossed with Cre-positive females to generate, amongst others, $\Delta a6::cre;Cacna1a^{lox/lox}$ (or $\textit{Cacna1a}^{\Delta/\Delta}$, here named *a6-Cacna1a*) and $Pcp2::cre;gabrg2^{lox/lox}$ (or $\textit{Gabrg2}^{\Delta/\Delta}$, here named *PC-Δγ2*) mice, respectively. Both lines were maintained in a C57Bl6 background. In the experiments with mutant mice and blocker injections, double and single barrel (2.0 mm OD, 1.16 mm ID, Harvard Apparatus, MA, USA) borosilicate glass pipettes were used, and alcian blue was injected to confirm that the recordings were from lobules I-III or X.

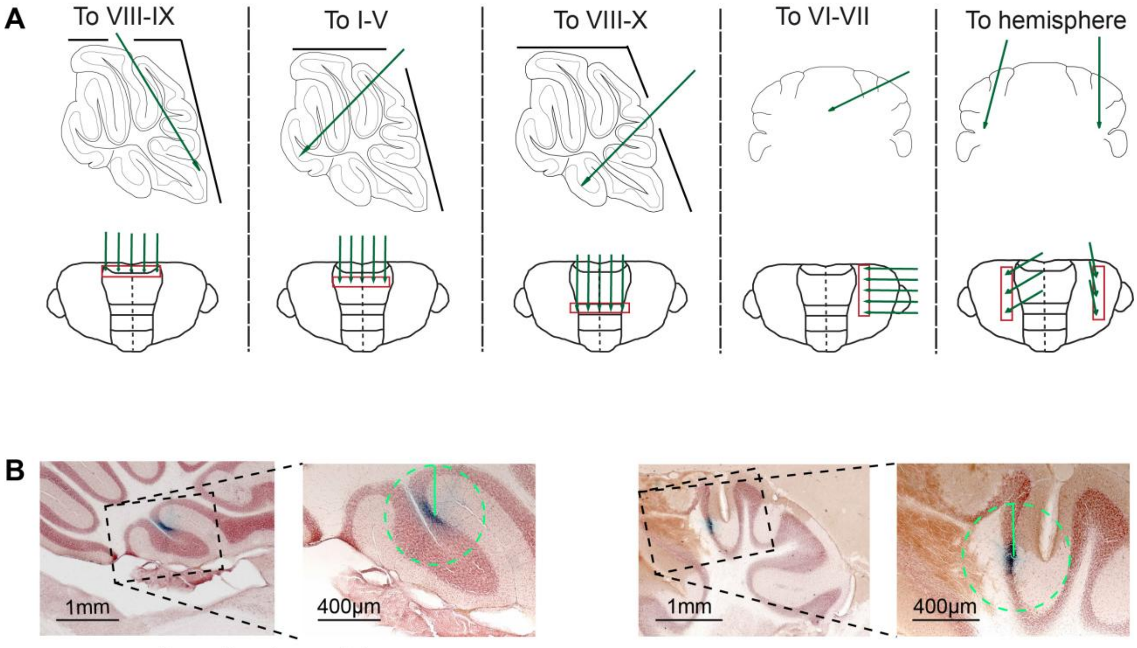

Recording in good tissue

Recording in damaged tissue

***Figure 1 – figure supplement 1. Experimental approach and histological verification.***
*A, In order to obtain recordings from all cerebellar areas in vivo, we placed craniotomies in different locations. We avoided recording close to the craniotomy to decrease the chance of having to exclude the cells due to tissue damage (see B). Five different approaches (top row) were used to cover all cerebellar areas, and recordings were done in a straight line running in either mediolateral or rostrocaudal direction, to assure reliable retrieval after histology. B, To minimize the potential influence of tissue disruption on the recording results, we excluded all Purkinje cells that showed clear damage to the tissue, visible by light microscope, in a 400 µm radius circle around the dye identified recording location. Cells without detectable damage in surrounding tissue (left) were included, and those with clear damage (right) were excluded. Also, we did not observed obvious cell death in the Z– areas[56].*

## *In vivo* two-photon imaging of EAAT4-eGFP mice

EAAT4-eGFP mice express enhanced green fluorescent protein (eGFP) under control of the EAAT4 promoter, and were generated using the bacterial artificial chromosome (BAC)[30]. Targeted recordings of eGFP-positive and -negative Purkinje cells were made after visualizing the eGFP-positive bands using *in vivo* two-photon imaging of 5 awake EAAT4-eGFP mice (3 females, 2 males, 10-26 wks old). Images were acquired using a TriM Scope II (LaVision BioTec, Bielefeld, Germany) attached to an upright microscope with a 40x/0.8 NA water-immersion objective (Olympus, Tokyo, Japan). Laser illumination was provided by a Chameleon Ultra titanium sapphire laser (Coherent, Santa Clara, CA). We aimed to image Purkinje cells in the superficial layer of a restricted part of the cortex (lobules V-VI and Crus I) at a depth of ~250 µm using an excitation wavelength of 920 nm, and their location in relation to zebrin bands was determined online. The recording pipette was filled with Alexa-594 (10 µM in 2 M NaCl; Life Technologies, Carlsbad, CA) and visualized with an excitation wavelength of 800 nm, the minimum recording duration was 30 seconds. Images from eGFP and Alexa-594 were filtered using a Gaussian kernel, contrast-optimized and subsequently merged in Photoshop (Adobe, San Jose, CA). Purkinje cells recorded *in vivo* from EAAT4-eGFP mice are included in **Figure 2, Figure 2-figure supplement 1** and **Figure 4B**.

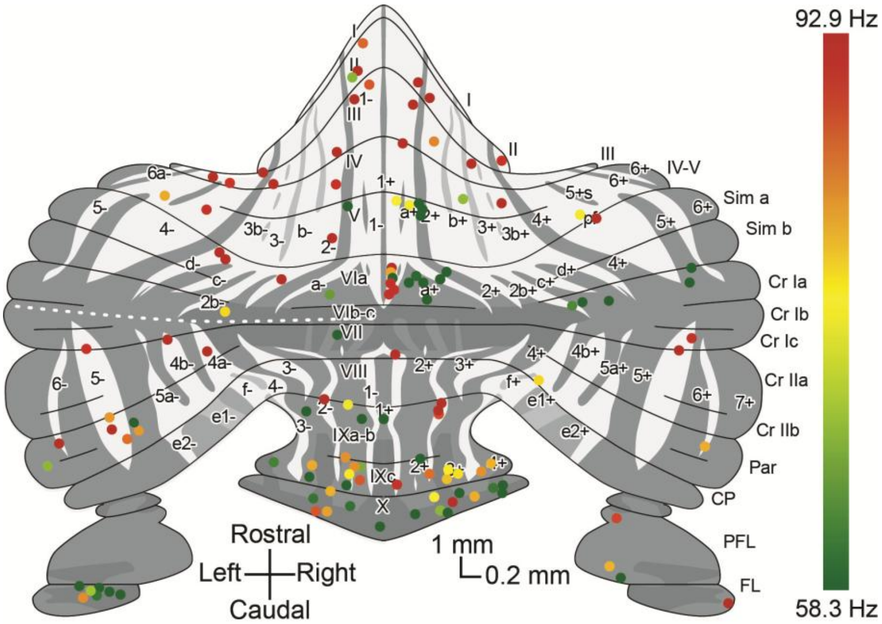

*Figure 2 - figure supplement 1.* ***Overview with color-coded simple spike frequency for all identified Z+ and Z− Purkinje cells.*** *Overview on plot of the unfolded cerebellar cortex depicting all Purkinje cells for which the activity was recorded and the zebrin identity was determined using either immunostaining or two-photon imaging, with dot color indicating the simple spike firing frequency. Dot color ranges from the combined average simple spike firing frequency for Z+ Purkinje cells, 58.3 Hz, in green to that of Z– Purkinje cells, 92.9 Hz, in red.*

### Analysis of *in vivo* recordings

Purkinje cells were identified by the occurrence of simple and complex spikes and were confirmed to be from a single unit by the presence of a pause in simple spikes after each complex spike. To assure the quality and reliability of the recording the following criteria were imposed: 1) a minimum recording duration of 120 sec, 2) stable simple spike amplitude, 3) no clear signs of tissue damage in a circle with 400 µm radius, around the recording site (see **Figure 1-figure supplement 1B**). All *in vivo* data were analyzed using SpikeTrain (Neurasmus B.V., Rotterdam, The Netherlands, www.neurasmus.com), running under Matlab (Mathworks, MA, USA). SpikeTrain uses wave clustering to identify simple and complex spikes, and in case of doubt manual checking (and correcting) would be performed. For each cell the firing rate, CV and mean CV2 were determined for simple and complex spikes, as well as the climbing fiber pause. CV is the standard deviation of inter-spike intervals (ISI) divided by the mean, the mean CV2 is calculated as the mean of $2\,|(\mathrm{ISI})_{n+1} - \mathrm{ISI}_n|/(\mathrm{ISI}_{n+1} + \mathrm{ISI}_n)$. Both are measures for the regularity of the firing, with CV reflecting that of the entire recording and mean CV2 that of adjacent intervals, making the latter a measure of regularity on small timescales. The climbing fiber pause is determined as the minimum duration between a complex spike and the following simple spike. To extend this analysis we also plotted histograms of simple spike activity time locked on the complex spike, and labelled the shape of this time histogram as normal, facilitation, suppression and oscillation (see Figure 3 for examples). The spike characteristics half maximum width (HMW) and spike area were determined from the normalized average signal of simple and complex spikes of individual recordings. Half-width was calculated as the width of the first peak at half of its maximum amplitude. The spike area was defined as the integral of the rectified complex spike wave form in a time window of 0.5 ms pre and 3 ms post spike onset.

### *In vitro* cell-attached and whole-cell patch recordings

Acute sagittal slices (250 μm thick) were prepared from the cerebellar vermis of 3-5 month old male C57BL/6J mice (Charles River) in ice-cold slicing medium that contains the following (in mM): 240 sucrose, 2.5 KCl, 1.25 $Na_2HPO_4$, 2 $MgSO_4$, 1 $CaCl_2$, 26 $NaHCO_3$, and 10 D-glucose, bubbled with 95% $O_2$ and 5% $CO_2$. Subsequently, slices were incubated in ACSF containing (in mM): 124 NaCl, 2.5 KCl, 1.25 $Na_2HPO_4$, 2 $MgSO_4$, 2 $CaCl_2$, 26 $NaHCO_3$, and 10 D-glucose equilibrated with 95% $O_2$ and 5% $CO_2$ at 34.0 ℃ for 30 min, and then at room temperature. Slices were typically used within 5 h *ex vivo*. NBQX (10 μM), DL-AP5 (50 μM) and picrotoxin (100 μM) were bath-applied to block AMPA-, NMDA-, and GABA subtype A ($GABA_A$)-receptors, respectively. Borosilicate glass pipettes (WPI) were filled with ACSF and had an open pipette resistance of 2-4 MΩ. Purkinje cells were identified using visual guidance by DIC video microscopy and water-immersion 40X objective (Axioskop 2 FS plus; Carl Zeiss, Jena, Germany). Slices were transferred to the recording chamber and incubated for at least 10 min before starting the recordings. We recorded the Purkinje cell activity in cell-attached mode (0 pA injection) at 33.0 ± 1.0 ℃, with a distance of 0.5 cm between temperature probe and slice. Current clamp recordings were performed with the same setting as cell-attached recording, except that pipettes were filled with intracellular solution contains the following (in mM): 120 K-Gluconate, 9 KCl, 10 KOH, 3.48 $MgCl_2$, 4 NaCl, 10 HEPES, 4 $Na_2ATP$, 0.4 $Na_3GTP$, and 17.5 sucrose, pH 7.25.

For experiments in EAAT4-eGFP mice, all experimental conditions were the same as cell-attached experiments above, except that coronal slices (300 μm thick) were used to record from identified EAAT4-positive and -negative Purkinje cells within the same lobules. We first identified the lobules by their locations and band patterns with a 10X objective, and then zoomed in with a 40X objective to proceed to recording.

### *In vitro* data acquisition and analysis

Electrophysiological data were acquired using an EPC9 amplifier (HEKA, Lambrecht, Germany), filtered at 10 kHz and digitized at 25 kHz. Acquisition was controlled using PULSE software (HEKA) and the data were exported and analyzed using Minianalysis (v6.0.3) software (Synaptosoft, Fort Lee, NJ, USA) or Matlab. The typical signal-to-noise ratio was larger than 5:1, and minimum recording duration was 120 s, unless stated otherwise. Cells were included based on the following criteria: 1. the CV over the whole period of recording was < 0.2; 2. the average frequency changed less than 20% between the the first and the last (30 s), except for those in the wash-in experiment. To minimize the day-to-day and slice-to-slice variations, recordings were targeted at different lobules for every slice. For the Pyr3 wash-in experiment, firing frequencies were normalized to the average frequency over the 2-min period before adding the drug to the ACSF (pre). The wash-in effect was determined by calculating the firing frequency in the period of 5 to 7 min after the drug was in the recording chamber (post).

In the whole-cell patch recording, the membrane potential of Purkinje was held at −65 mV using current injection to avoid spontaneous spiking activity (average: -454 ± 38 pA). We recorded the intrinsic excitability by injecting depolarizing currents ranging from 100 to 1000 pA (100 pA steps) relative to the holding current. Data were exported and analysed using threshold search with Clampfit (v10.4, Molecular Devices, Sunnyvale, CA, USA).

### Drugs

DL-TBOA (EAAT blocker, **Tocris**, Ellisville, MO, USA), genistein (TRPC3 blocker, **Sigma-Aldrich**) and Pyr3 (TRPC3 blocker, **Tocris**) were dissolved in dimethyl sulfoxide (DMSO, Carl Roth GmbH, Karlsruhe, Germany) and ACSF. NBQX (10 μM), DL-AP5 (50 μM) and picrotoxin (100 μM) were bath-applied to block AMPA-, NMDA-, and GABA subtype A

($GABA_A$)-receptors, respectively. For *in vivo* recordings, mice were injected with 240 mg/kg genistein (i.p.) and 200 µg Pyr3 (i.c.v) dissolved in saline or DMSO. Vehicle control mice were injected with 100 µl DMSO (i.p.). After injection, extracellular Purkinje cell activity was recorded as described above, and alcian blue was injected to verify that the recordings were from lobules I-III or X. The minimum recording duration was 60 s and recordings were made for up to 4 hours after injection for these experiments. For *in vitro* experiments all blockers were prepared in 1:1000 stock solutions in DMSO, stored at -20℃ and used within 4 weeks after preparation. Blockers were bath applied where indicated in the following concentrations: DL-TBOA (25 µM), genistein (10 µM), and Pyr3 (100 µM). Except for the wash-in experiments, all recordings started after the slice was incubated in the drug-containing ASCF for at least 15 min. In the cases where we observed an effect in the wash-in experiments, the firing frequency of Purkinje cells typically dropped the moment the drug reached the bath, an effect maximizing within a few minutes and sometimes followed by a smaller recovery. The experimenter was blind to the presence and type of drug applied until analysis was completed. The tubing was changed after every blocker experiment.

**Histochemistry**

After recordings, mice were deeply anesthetized with Nembutal and perfused with 75 ml of 4% paraformaldehyde (PFA). The brains were removed from the skull and post-fixed for 1-2 hrs in 4% PFA, and stored in 0.1M PB containing 10% sucrose. After embedding in 10% gelatin and 10% sucrose, blocks were hardened in a solution containing 10% formaldehyde, 30% sucrose for 1-2 hour at room temperature and then stored overnight in 0.1M PB with 30% sucrose at 4℃. To identify if recordings were made in a Z+ or Z− band, coronal sections with a thickness of 40 µm were processed based on a standard immunostaining procedure; next, they were thoroughly rinsed with 0.1M PB. The goat–derived zebrin II antibody (Santa cruz, TX, USA) was diluted at 1:1000 in PBS, pH 7.6, containing 2% normal horse serum and 0.4% Triton. Rabbit anti-goat secondary antibody HRP conjugate diluted at 1:200 was used as a secondary antibody (Dako, Glostrup, Denmark). The sections were thoroughly rinsed 3 times with PBS and PB, followed by diaminobenzidine (DAB) incubation (0.66% DAB, and 0.033% $H_2O_2$ for 10–20 min). The sections were put on glass and then dehydrated by different grades of ethanol (70%, 80%, 90%, 96%, 96%, 100%, 100%, 100%, 2 min per grade), xylene was applied to clean the ethanol, and subsequently the sections were covered with Permount. To only determine the recording sites for recordings throughout the cerebellum, sagittal sections were cut at 80 µm followed by neutral red staining.

**Analysis of immunohistochemistry**

The injection sites were located by the light microscope. If the same injection could be found in several slices, the injection was allocated to the slice with the highest density of Alcian Blue. If the injection site was at the border of two cerebellar lobules, the cell was allocated to the most rostral lobule. Particularly in the hemipsheres, a distinction between positive and lightly positive areas can be made. In this study they were taken together as positive, and compared to the –clearly identifiable- negative bands. Recordings were excluded from further analysis if there was clear tissue damage within a circle with a radius of 400 µm around the injection site. The recording sites of 7 out 8 cells in the flocculus (FL) were confirmed by the response to visual stimulation instead of histology[36]. Example sections and sections used to determine the staining intensity of zebrin II were photographed using a Leica DMRB microscope equipped with Leica DC300 camera. To compare zebrin intensity between lobules the average pixel intensity of the PC somas in each lobule was determined using ImageJ software, based on the average of a total of 3 sections for vermis and 2 sections for the hemisphere per mouse, from 3 mice. Sections compared in the same panel, were processed in parallel. To correct for minor differences in overall staining intensity between vermis and hemispheres, soma intensities were normalized based on background (granule cell layer) intensity.

**Statistics**

All values are shown as mean ± s.d, unless stated otherwise. Unpaired Student's *t*-test were used for comparisons and Spearman's *r*-test for correlations, unless stated otherwise, and $p < 0.05$ was considered to be significant. Comparisons in which at least one of the groups had $n \leq 4$ were re-tested using a Mann-Whitney *U*-test, and in all cases the outcome was confirmed.

All experiments were performed under the GGO license no. IG 04-197, and approved by the Dutch animal ethical committee (DEC, EMC 2168 / 2545 / 2999 / 3002 / 3057).

**Acknowledgements**

The authors want to thank Mandy Rutteman, Erika Goedknegt, Elize Haasdijk, Laura Post and Daphne Groeneveld for technical assistance and Gerard Borst and Jan Voogd for valuable discussion. We thank Jeremy Rothstein for providing the EAAT4-eGFP mice.

**Author information**

The authors declare no financial or non-financial competing interests. Correspondence and requests for materials should be addressed to C.I.D.Z. (c.dezeeuw@erasmusmc.nl) and M.S. (m.schonewille@erasmusmc.nl)

**Reference list**

1 Larsell, O. *The Comparative Anatomy & Histology of the Cerebellum: The Human Cerebellum, Cerebellar Connections, & Cerebellar Cortex*. (The University of Minnesota Press, 1972).

2 Voogd, J. Cerebellar zones: a personal history. *Cerebellum* **10**, 334-350, doi:10.1007/s12311-010-0221-6 (2011).

3 Eccles, J. C. Circuits in the cerebellar control of movement. *Proc Natl Acad Sci U S A* **58**, 336-343 (1967).

4 Gao, Z., van Beugen, B. J. & De Zeeuw, C. I. Distributed synergistic plasticity and cerebellar learning. *Nat Rev Neurosci* **13**, 619-635, doi:nrn3312 [pii]

10.1038/nrn3312 (2012).

5 Apps, R. & Hawkes, R. Cerebellar cortical organization: a one-map hypothesis. *Nat Rev Neurosci* **10**, 670-681, doi:nrn2698 [pii]

10.1038/nrn2698 (2009).

6 Leclerc, N., Dore, L., Parent, A. & Hawkes, R. The compartmentalization of the monkey and rat cerebellar cortex: zebrin I and cytochrome oxidase. *Brain Res* **506**, 70-78, doi:0006-8993(90)91200-Z [pii] (1990).

7 Brochu, G., Maler, L. & Hawkes, R. Zebrin II: a polypeptide antigen expressed selectively by Purkinje cells reveals compartments in rat and fish cerebellum. *J Comp Neurol* **291**, 538-552, doi:10.1002/cne.902910405 (1990).

8 Graham, D. J. & Wylie, D. R. Zebrin-immunopositive and -immunonegative stripe pairs represent functional units in the pigeon vestibulocerebellum. *J Neurosci* **32**, 12769-12779, doi:32/37/12769 [pii]

10.1523/JNEUROSCI.0197-12.2012 (2012).

9 Sillitoe, R. V., Kunzle, H. & Hawkes, R. Zebrin II compartmentation of the cerebellum in a basal insectivore, the Madagascan hedgehog tenrec Echinops telfairi. *J Anat* **203**, 283-296 (2003).

10 Marzban, H. & Hawkes, R. On the architecture of the posterior zone of the cerebellum. *Cerebellum* **10**, 422-434, doi:10.1007/s12311-010-0208-3 (2011).

11 Pijpers, A., Apps, R., Pardoe, J., Voogd, J. & Ruigrok, T. J. Precise spatial relationships between mossy fibers and climbing fibers in rat cerebellar cortical zones. *J Neurosci* **26**, 12067-12080, doi:26/46/12067 [pii]

10.1523/JNEUROSCI.2905-06.2006 (2006).

12 Sugihara, I. & Shinoda, Y. Molecular, topographic, and functional organization of the cerebellar nuclei: analysis by three-dimensional mapping of the olivonuclear projection and aldolase C labeling. *J Neurosci* **27**, 9696-9710, doi:27/36/9696 [pii]

10.1523/JNEUROSCI.1579-07.2007 (2007).

13 Voogd, J. & Ruigrok, T. J. The organization of the corticonuclear and olivocerebellar climbing fiber projections to the rat cerebellar vermis: the congruence of projection zones and the zebrin pattern. *J Neurocytol* **33**, 5-21, doi:10.1023/B:NEUR.0000029645.72074.2b

5271056 [pii] (2004).

14 Sugihara, I. Compartmentalization of the deep cerebellar nuclei based on afferent projections and aldolase C expression. *Cerebellum* **10**, 449-463, doi:10.1007/s12311-010-0226-1 (2011).

15 Sugihara, I. *et al.* Projection of reconstructed single Purkinje cell axons in relation to the cortical and nuclear aldolase C compartments of the rat cerebellum. *J Comp Neurol* **512**, 282-304, doi:10.1002/cne.21889 (2009).

16 Ruigrok, T. J. Ins and outs of cerebellar modules. *Cerebellum* **10**, 464-474, doi:10.1007/s12311-010-0164-y (2011).

17 Dehnes, Y. *et al.* The glutamate transporter EAAT4 in rat cerebellar Purkinje cells: a glutamate-gated chloride channel concentrated near the synapse in parts of the dendritic membrane facing astroglia. *J Neurosci* **18**, 3606-3619 (1998).

18 Wadiche, J. I. & Jahr, C. E. Patterned expression of Purkinje cell glutamate transporters controls synaptic plasticity. *Nat Neurosci* **8**, 1329-1334, doi:nn1539 [pii]

10.1038/nn1539 (2005).

19 Mateos, J. M. *et al.* Parasagittal compartmentalization of the metabotropic glutamate receptor mGluR1b in the cerebellar cortex. *Eur J Anat* **5**, 15-21 (2001).

20 Furutama, D. *et al.* Expression of the IP3R1 promoter-driven nls-lacZ transgene in Purkinje cell parasagittal arrays of developing mouse cerebellum. *J Neurosci Res* **88**, 2810-2825, doi:10.1002/jnr.22451 (2010).

21 Sarna, J. R., Marzban, H., Watanabe, M. & Hawkes, R. Complementary stripes of phospholipase Cbeta3 and Cbeta4 expression by Purkinje cell subsets in the mouse cerebellum. *J Comp Neurol* **496**, 303-313, doi:10.1002/cne.20912 (2006).

22 Barmack, N. H., Qian, Z. & Yoshimura, J. Regional and cellular distribution of protein kinase C in rat cerebellar Purkinje cells. *J Comp Neurol* **427**, 235-254, doi:10.1002/1096-9861(20001113)427:2<235::AID-CNE6>3.0.CO;2-6 [pii] (2000).

23 Jinno, S., Jeromin, A., Roder, J. & Kosaka, T. Compartmentation of the mouse cerebellar cortex by neuronal calcium sensor-1. *J Comp Neurol* **458**, 412-424, doi:10.1002/cne.10585 (2003).

24 Hartmann, J. *et al.* TRPC3 channels are required for synaptic transmission and motor coordination. *Neuron* **59**, 392-398, doi:S0896-6273(08)00502-3 [pii]

10.1016/j.neuron.2008.06.009 (2008).

25 Sekerkova, G. *et al.* Early onset of ataxia in moonwalker mice is accompanied by complete ablation of type II unipolar brush cells and Purkinje cell dysfunction. *J Neurosci* **33**, 19689-19694, doi:10.1523/JNEUROSCI.2294-13.2013 (2013).

26 Kim, Y. *et al.* Alternative splicing of the TRPC3 ion channel calmodulin/IP3 receptor-binding domain in the hindbrain enhances cation flux. *J Neurosci* **32**, 11414-11423, doi:32/33/11414 [pii]

10.1523/JNEUROSCI.6446-11.2012 (2012).

27 Kim, C. H. *et al.* Lobule-specific membrane excitability of cerebellar Purkinje cells. *J Physiol* **590**, 273-288, doi:jphysiol.2011.221846 [pii]

10.1113/jphysiol.2011.221846 (2012).

28 Sugihara, I. & Quy, P. N. Identification of aldolase C compartments in the mouse cerebellar cortex by olivocerebellar labeling. *J Comp Neurol* **500**, 1076-1092, doi:10.1002/cne.21219 (2007).

29 Paukert, M., Huang, Y. H., Tanaka, K., Rothstein, J. D. & Bergles, D. E. Zones of enhanced glutamate release from climbing fibers in the mammalian cerebellum. *J Neurosci* **30**, 7290-7299, doi:30/21/7290 [pii]

10.1523/JNEUROSCI.5118-09.2010 (2010).

30 Gincel, D. *et al.* Analysis of cerebellar Purkinje cells using EAAT4 glutamate transporter promoter reporter in mice generated via bacterial artificial chromosome-mediated transgenesis. *Exp Neurol* **203**, 205-212, doi:S0014-4886(06)00474-2 [pii]

10.1016/j.expneurol.2006.08.016 (2007).

31 Ozol, K., Hayden, J. M., Oberdick, J. & Hawkes, R. Transverse zones in the vermis of the mouse cerebellum. *J Comp Neurol* **412**, 95-111 (1999).

32 Sugihara, I. & Shinoda, Y. Molecular, topographic, and functional organization of the cerebellar cortex: a study with combined aldolase C and olivocerebellar labeling. *J Neurosci* **24**, 8771-8785, doi:24/40/8771 [pii]

10.1523/JNEUROSCI.1961-04.2004 (2004).

33 De Zeeuw, C. I. *et al.* Spatiotemporal firing patterns in the cerebellum. *Nat Rev Neurosci* **12**, 327-344, doi:nrn3011 [pii]

10.1038/nrn3011 (2011).

34 Chen, X. *et al.* Disruption of the olivo-cerebellar circuit by Purkinje neuron-specific ablation of BK channels. *Proc Natl Acad Sci U S A* **107**, 12323-12328, doi:1001745107 [pii]

10.1073/pnas.1001745107 (2010).

35 Simpson, J. I., Wylie, D. R. & De Zeeuw, C. I. On climbing fiber signals and their consequence(s). *Beh.Brain Sciences* **19**, 380-394 (1996).

36 Galliano, E. *et al.* Silencing the majority of cerebellar granule cells uncovers their essential role in motor learning and consolidation. *Cell Rep* **3**, 1239-1251, doi:S2211-1247(13)00130-7 [pii]

10.1016/j.celrep.2013.03.023 (2013).

37 Wulff, P. *et al.* Synaptic inhibition of Purkinje cells mediates consolidation of vestibulo-cerebellar motor learning. *Nat Neurosci* **12**, 1042-1049, doi:nn.2348 [pii]

10.1038/nn.2348 (2009).

38 Nelson, C. & Glitsch, M. D. Lack of kinase regulation of canonical transient receptor potential 3 (TRPC3) channel-dependent currents in cerebellar Purkinje cells. *J Biol Chem* **287**, 6326-6335, doi:M111.246553 [pii]

10.1074/jbc.M111.246553 (2012).

39 Chanda, S. & Xu-Friedman, M. A. Excitatory modulation in the cochlear nucleus through group I metabotropic glutamate receptor activation. *J Neurosci* **31**, 7450-7455, doi:31/20/7450 [pii]

10.1523/JNEUROSCI.1193-11.2011 (2011).

40 Coesmans, M. *et al.* Mechanisms underlying cerebellar motor deficits due to mGluR1-autoantibodies. *Ann Neurol* **53**, 325-336, doi:10.1002/ana.10451 (2003).

41 Yamakawa, Y. & Hirano, T. Contribution of mGluR1 to the basal activity of a mouse cerebellar Purkinje neuron. *Neurosci Lett* **277**, 103-106, doi:S0304-3940(99)00852-6 [pii] (1999).

42 Kiyonaka, S. *et al.* Selective and direct inhibition of TRPC3 channels underlies biological activities of a pyrazole compound. *Proc Natl Acad Sci U S A* **106**, 5400-5405, doi:0808793106 [pii]

10.1073/pnas.0808793106 (2009).

43 Voogd, J., Pardoe, J., Ruigrok, T. J. & Apps, R. The distribution of climbing and mossy fiber collateral branches from the copula pyramidis and the paramedian lobule: congruence of climbing fiber cortical zones and the pattern of zebrin banding within the rat cerebellum. *J Neurosci* **23**, 4645-4656, doi:23/11/4645 [pii] (2003).

44 Mathews, P. J., Lee, K. H., Peng, Z., Houser, C. R. & Otis, T. S. Effects of climbing fiber driven inhibition on Purkinje neuron spiking. *J Neurosci* **32**, 17988-17997, doi:32/50/17988 [pii]

10.1523/JNEUROSCI.3916-12.2012 (2012).

45 Coddington, L. T., Rudolph, S., Vande Lune, P., Overstreet-Wadiche, L. & Wadiche, J. I. Spillover-mediated feedforward inhibition functionally segregates interneuron activity. *Neuron* **78**, 1050-1062, doi:S0896-6273(13)00321-8 [pii]

10.1016/j.neuron.2013.04.019 (2013).

46 Badura, A. *et al.* Climbing fiber input shapes reciprocity of Purkinje cell firing. *Neuron* (2013).

47 Becker, E. B. *et al.* A point mutation in TRPC3 causes abnormal Purkinje cell development and cerebellar ataxia in moonwalker mice. *Proc Natl Acad Sci U S A* **106**, 6706-6711, doi:0810599106 [pii]

10.1073/pnas.0810599106 (2009).

48 Baron, C. B., Tolan, D. R., Choi, K. H. & Coburn, R. F. Aldolase A Ins(1,4,5)P3-binding domains as determined by site-directed mutagenesis. *Biochem J* **341 ( Pt 3)**, 805-812 (1999).

49 Wang, X., Chen, G., Gao, W. & Ebner, T. J. Parasagittally aligned, mGluR1-dependent patches are evoked at long latencies by parallel fiber stimulation in the mouse cerebellar cortex in vivo. *J Neurophysiol* **105**, 1732-1746, doi:jn.00717.2010 [pii]

10.1152/jn.00717.2010 (2011).

50 Person, A. L. & Raman, I. M. Purkinje neuron synchrony elicits time-locked spiking in the cerebellar nuclei. *Nature* **481**, 502-505, doi:nature10732 [pii]

10.1038/nature10732 (2012).

51 Yassin, L. *et al.* An embedded subnetwork of highly active neurons in the neocortex. *Neuron* **68**, 1043-1050, doi:S0896-6273(10)00971-2 [pii]

10.1016/j.neuron.2010.11.029 (2010).

52 Angelo, K. *et al.* A biophysical signature of network affiliation and sensory processing in mitral cells. *Nature* **488**, 375-378, doi:nature11291 [pii]

10.1038/nature11291 (2012).

53 Hoebeek, F. E. *et al.* Increased noise level of purkinje cell activities minimizes impact of their modulation during sensorimotor control. *Neuron* **45**, 953-965, doi:S0896-6273(05)00129-7 [pii]

10.1016/j.neuron.2005.02.012 (2005).

54 Aller, M. I. *et al.* Cerebellar granule cell Cre recombinase expression. *Genesis* **36**, 97-103, doi:10.1002/gene.10204 (2003).

55 Oberdick, J., Smeyne, R. J., Mann, J. R., Zackson, S. & Morgan, J. I. A promoter that drives transgene expression in cerebellar Purkinje and retinal bipolar neurons. *Science* **248**, 223-226 (1990).

56 Welsh, J. P. *et al.* Why do Purkinje cells die so easily after global brain ischemia? Aldolase C, EAAT4, and the cerebellar contribution to posthypoxic myoclonus. *Adv Neurol* **89**, 331-359 (2002).

# Chapter 3

# Differential Purkinje cell simple spike activity and pausing behavior related to cerebellar modules

Haibo Zhou[1], Kai Voges[1], Zhanmin Lin[1], Chiheng Ju[1], Martijn Schonewille[1#]

[1] Department of Neuroscience, Erasmus MC, Rotterdam, The Netherlands
[#] Correspondence to: m.schonewille@erasmusmc.nl (MS)

**J Neurophysiol. 2015**

## Abstract:

The massive computational capacity of the cerebellar cortex is conveyed by Purkinje cells onto cerebellar and vestibular nuclei neurons through their GABAergic, inhibitory output. This implies that pauses in Purkinje cell simple spike activity are potentially instrumental in cerebellar information processing, but their occurrence and extent are still heavily debated. The cerebellar cortex, although often treated as such, is not homogeneous. Cerebellar modules with distinct anatomical connectivity and gene expression have been described and Purkinje cells in these modules also differ in firing rate of simple and complex spikes. In this study we systematically correlate, in awake mice, the pausing in simple spike activity of Purkinje cells recorded throughout the entire cerebellum, with their location in terms of lobule, transverse zone and zebrin-identified cerebellar module. A subset of Purkinje cells displayed long (>500 ms) pauses, but we found that their occurrence correlated with tissue damage and lower temperature. In contrast to long pauses, short pauses (<500 ms) and the shape of the inter spike interval (ISI) distributions can differ between Purkinje cells of different lobules and cerebellar modules. In fact, the ISI distributions can differ both between and within populations of Purkinje cells with the same zebrin-identity and these differences are at least in part caused by differential synaptic inputs. Our results suggest that long pauses are rare, but that there are differences related to shorter inter simple spike intervals between and within specific subsets of Purkinje cells, indicating a potential further segregation in the activity of cerebellar Purkinje cells.

## Introduction

As one of the largest integrators in the brain, the cerebellar Purkinje cell is contacted by tens of thousands of -predominantly excitatory- synaptic inputs which it, combined with intrinsic pacemaker activity, converges into the sole output of the cerebellar cortex. Hence, and in contrast to neurons in the cerebral cortex, Purkinje cells in the cerebellar cortex commonly operate in the upstate and have a high firing rate, even at rest (Crunelli and Hughes 2009; McCormick 2005; Thach 1968; Zhou et al. 2014). In addition to their alternative preferred state of membrane potential, Purkinje cells also have an alternative output, in that they inhibit their target neurons in the cerebellar nuclei. How Purkinje cells use their inhibitory control to convey their information onto the downstream targets remains enigmatic, even to-date. Despite several lines of evidence identifying possible methods of information transfer, including those based on rate coding, spatio-temporal coding or a combination of both (De Zeeuw et al. 2011; Jirenhed et al. 2007; Medina and Lisberger 2009; Person and Raman 2011; Shin et al. 2007), there is to date no consensus regarding the patterns of activity required for proper behavior or learning.

The occurrence of two different states of membrane potential was already observed in the first intracellular recordings of cerebellar Purkinje cells (Llinas and Sugimori 1980a; b). Subsequent studies have identified several factors that modulate the switch between the two states, including molecular layer interneurons (Oldfield et al. 2010), Bergmann glia cells (Wang et al. 2012), climbing fibers (Libster and Yarom 2013), and the hyperpolarization-activated cation current (Williams et al. 2002). *In vivo,* in anesthetized mammals, the *in vitro* findings were confirmed, in that a significant portion of Purkinje cells switch between upstates with a high simple spike firing rate and downstates with seconds long silence of simple spikes (Loewenstein et al. 2005), and later also replicated in awake cats and mice during chronic recordings (Cheron et al. 2014; Yartsev et al. 2009). Long pauses were suggested to be functionally relevant, as whisker-stimulation induced complex spikes can toggle transitions from up- to downstates and vice versa (Loewenstein et al. 2005). These conclusions were challenged by other studies, which showed that long simple spike pauses are rare in awake behaving mice (Cao et al. 2012; Schonewille et al. 2006), and that the probability is significantly increased by anesthesia (Schonewille et al. 2006). However, the cerebellum is not a homogeneous structure; differences in gene expression, anatomical connectivity and physiological properties have been identified. Parasagittal stripes, or bands, of cerebellar cortex show alternating levels of gene expression for particular genes, most notable of which is aldolase C, typically referred to as zebrin II (Ahn et al. 1994; Brochu et al. 1990). Purkinje cells that have a similar zebrin 'identity', i.e. have a similar expression level of zebrin II (from here on: zebrin), typically receive inputs from the same part of the inferior olive, and project their axons to the same part of the cerebellar nuclei (Apps and Hawkes 2009; Brochu et al. 1990; Pijpers et al. 2006; Sugihara 2011; Sugihara and Quy 2007; Voogd and Ruigrok 2004), creating functional units, or modules. More recently physiological differences between modules have been described in terms of plasticity (Wadiche and Jahr 2005; Wang et al. 2011) and firing dynamics and rates (Kim et al. 2012; Xiao et al. 2014; Zhou et al. 2014). In addition, the cerebellar cortex can also be subdivided in zones on the basis of development and function by borders that run perpendicular to the sagittal bands, i.e. into transverse zones (Ozol et al. 1999; Reeber et al. 2013). Together these subdivisions raise a question that could answer previous discrepancies: How are Purkinje cells with longer or shorter simple spike pauses distributed over the cerebellum?

Here, we show that a fraction of cerebellar Purkinje cells, recorded *in vivo* in awake mice at rest, displays varying degrees of long (> 500 ms) simple spike pausing behavior. We identify nearby tissue damage and local temperature as two important factors affecting Purkinje cell simple spike activity. Moreover, whereas longer pauses do not correlate with cerebellar location, there are difference in the occurrence of shorter pauses (< 500 ms) and the shape of their inter-spike interval distributions between zebrin-identified cerebellar modules and transverse zones. These differences can be ablated by blocking input, suggesting that whereas the firing rate is largely determined by intrinsic differences, the differential input shapes the dynamic range of Purkinje cell activity, creating differences between and within the same functional units.

## **Methods**:

All experiments involving animals were approved by the Dutch Ethical Committee for animal experiments. A large part of the dataset of Purkinje cell recordings used for this study has also been used in a previous study (Zhou et al. 2014), and consequently the methods sections largely overlap.

### ***In vivo* extracellular recordings**

As recently described (Zhou et al. 2014), Purkinje cells were recorded *in vivo* in adult male C57Bl/6 mice (C57Bl/6J, Charles River, Wilmington, MA, USA, 10-35 weeks old). An immobilizing pedestal was constructed on the skull overlying the frontal and parietal bones to enable fixation of the mouse head and a craniotomy was made in the interparietal or occipital bone to allow the entrance of the recording pipettes. The locations of the craniotomy are variable, as illustrated in Figure 1B, allowing recordings in different cerebellar regions. After recovery of at least 24 hrs, mice were ready for *in vivo* recordings. The head of the mouse was fixed to a metal bar and the body supported by a plastic tube. Electrophysiological activity of Purkinje cells was recorded using double barrel borosilicate glass pipettes (theta septum, 1.5 OD, 1.02 ID, WPI, FL, USA), see Figure 1A for details. To do so, one of the barrels was opened laterally to place the recording wire and sealed at the back with glass glue, the other barrel was filled with Alcian Blue to mark the recording sites (0.1-0.2 % solution in saline). The recording signals were pre-amplified (custom-made), filtered (CyberAmp, Axon, USA), digitized (Power1401, CED, UK) and stored for offline analysis. Recording duration was on average 220.41 ± 9.31 s, and at least 120 s for all recordings (except when combined with two-photon imaging, see below). To mark the recording location, brief air pulses were applied to the barrel filled with Alcian Blue after every recording. The temperature for different recording depths was measured by BAT-12 Microprobe Thermometer (Physitemp Instruments, NJ, USA), the tip size of the probe was 200 µm.

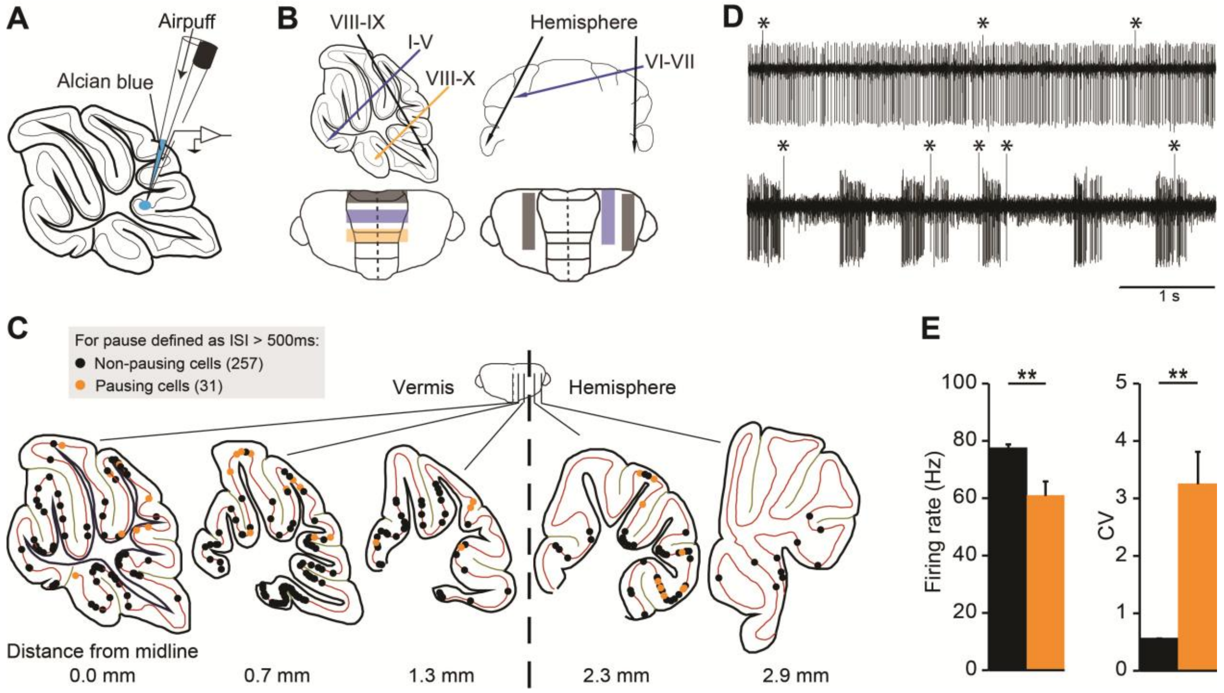

***Figure 1. Distribution of all recorded Purkinje cells in relation to the occurrence of long SS pauses.***
*(**A**) We performed extracellular recordings of Purkinje cell (PC) activity from awake C57Bl/6 mice at rest. After each recording, the recording site was marked by a small injection of Alcian Blue. (**B**) The location of the craniotomy was varied to be able to obtain PCs from different parts of the cerebellum at different recordings depths. (**C**) After histological processing or imaging, the location of 288 cells was successfully determined. The locations of all recording sites were projected on the medio-laterally nearest of five sagittal sections [schematic drawings were adapted from Franklin and Paxinos atlas (Paxinos and Franklin 2001)]. PCs were subdivided based on the presence of a 'long' pause in the recording, i.e. the occurrence of at least one inter spike interval (ISI) with a duration of 500 ms (cells with long pause, orange, n = 31; without, black, n = 257). Note that the recordings obtained in combination with two-photon imaging (n = 17) are located in the superficial layer of lobules IV-V, VI and Crus I. (**D**) Example traces of PC recordings without (top) and with long pauses (bottom). (**E**) PCs with long pauses on average have a lower SS firing rate and higher CV. Error bars represent SEM, ** p < 0.01.*

## Analysis of *in vivo* recordings

Analysis was performed using SpikeTrain (Neurasmus B.V., Rotterdam, www.neurasmus.com) for Matlab (Mathworks, MA, USA). The single unit nature of the recording was confirmed by the occurrence of a pause in simple spike activity following each complex spike, termed the climbing fiber pause. First, the average firing rate, CV (standard deviation divided by the mean per cell) and mean inter spike interval (ISI) were determined for simple spikes. Next, we examined various features of simple spike activity that are independent of the mean ISI, or firing rate, as much as possible. To do so, we first determined the occurrence of pauses, for which there is currently no generally accepted definition (Cao et al. 2012; Schonewille et al. 2006; Shin et al. 2007; Yartsev et al. 2009). Shin and De Schutter (2006) developed formal criteria to identify pauses, based on the climbing fiber pause, in order to study the correlation between pairs of Purkinje cells. This elegant method is less suitable in our study, for instance because the resulting definition of a pause (12 ms in their study) is between the mean ISI of Z+ and Z– PCs (see Figure 5D), and thus would automatically result in more pauses in Z+ PCs. In an attempt to avoid this bias, we considered ISIs pauses when they clearly deviated from the mean. We considered pauses ‘long’ when the ISI exceeded 500 ms in duration, based on previous descriptions of pausing Purkinje cells (Loewenstein et al. 2005; Yartsev et al. 2009). Pauses were considered short if the interval between simple spikes clearly deviated from the average or ‘normal’ ISIs. To determine a standard value we calculated, based on the entire dataset, the mean ISI plus 3 standard deviations, which gave 14.8 + (3 * 11.9) = 50.8 ms, rounded to 50 ms. To evaluate if differences between groups are dependent on the pause length that was chosen, we tested for pauses longer than an ISI duration of 50, 100, 200, 500, 1000 and 2000 ms, termed ‘pause length’ in figures. Cells were labelled ‘pausing cell’ if at least one interval of the indicated pause length was present in the recorded period. ‘Pause time’ refers to the cumulative time of all pauses longer than indicated pause length, divided by the total recording length.

To further analyse the simple spike activity, independently from the mean ISI, we calculated the median, mode, skewness and kurtosis of ISIs. Skewness (s) was calculated as:

$$s = \frac{E\,(x - \mu\,)^3}{\sigma^3}$$

and kurtosis as:

$$k = \frac{E\,(x - \mu\,)^4}{\sigma^4}$$

where μ is the mean of x, σ is the standard deviation of x, and E is the expectation operator. To prevent bias by long ISIs (>500 ms) these values were excluded for this analysis.

### Immunohistochemistry

Mice were anesthetized and then perfused using 75 ml of 4% paraformaldehyde (PFA). The brains were post-fixed and stored in 0.1M PB with 10% sucrose over night. The brains were embedded in 10% gelatin with 10% sucrose, hardened in 10% formalin with 30% sucrose solution for 1-2 hours and stored overnight in 0.1M PB with 30% sucrose (at 4 ℃). Sagittal sections with a thickness of 80 µm were processed by neutral red staining in experiments in which only the recording sites were determined. Coronal sections were cut at 40 µm followed by standard immunostaining to determine the zebrin identity. Zebrin bands were revealed using goat–derived zebrin II primary antibody (Santa Cruz, TX, USA, diluted at 1:1000) and rabbit anti-goat secondary antibody (Dako, Glostrup, Denmark, diluted at 1:200). After staining, the recording sites were determined by light microscope, and plotted on a 2D schematic drawing of the unfolded cerebellar cortex (adapted from Sugihara and Quy 2007). The injection site was assigned to the section with the highest Alcian Blue density, although the same injection could typically be found in several sections. For those cells that were recorded at the border of two cerebellar lobules, the cells were allocated to the rostral lobule. The locations of 7 out of 9 FL cells were estimated based on their responses to visual stimulation. Recorded Purkinje cells were determined to be from “damaged tissue” if we observed an obvious, i.e. visually identifiable, disruption in the tissue within a circle with a radius of 400 µm. Due to the highly organized, layered structure of the cerebellar cortex, tissue disruptions could be easily identified. Nevertheless, the person assessing the tissue quality was blind for the related Purkinje cell activity, and the reproducibility of the assessment was confirmed by another, blind experimenter.

### *In vivo* two-photon imaging of EAAT4-eGFP mice

Two-photon imaging-based recordings of Purkinje cell activity (included in Figures 1-3) were obtained using EAAT4-eGFP mice (Gincel et al. 2007), which express enhanced green fluorescent protein (eGFP) under the EAAT4 promoter, in a pattern similar to that of zebrin. In 5 awake EAAT4-eGFP mice (3 females, 2 males, 10-26 wks old, zebrin : n = 9 cells, zebrin+: n = 8 cells). Purkinje cell activity was recorded after placing the recording pipette using two-photon imaging. Purkinje cell recordings were aimed at lobule V-VI and Crus I. Purkinje cells were visualized with an excitation wavelength of 920 nm and recorded at a depth around 250 μm with a minimum recording duration of 30 s. The zebrin identity of each recorded cell was determined online. The recording pipettes were filled with 2 M NaCl and 10 μM Alexa-594, which can be visualized using an excitation wavelength of 800 nm.

### *In vitro* cell-attached recordings and data analysis

Acute sagittal slices with the thickness of 250 μm were prepared from the cerebellar vermis (C57BL/6J mice) in ice-cold slicing medium that contains: 240 mM sucrose, 2.5 mM KCl, 1.25 mM $Na_2HPO_4$, 2 mM $MgSO_4$, 1 mM $CaCl_2$, 26 mM $NaHCO_3$, and 10 mM D-glucose, and 95% $O_2$ and 5% $CO_2$ was bubbled into solution. Subsequently, slices were incubated at 34.0 ℃ for 30 min and then at room temperature in ACSF solution, which contains: 124 mM NaCl, 2.5 mM KCl, 1.25 mM $Na_2HPO_4$, 2 mM $MgSO_4$, 2 mM $CaCl_2$, 26 mM $NaHCO_3$, 10 mM D-glucose, 95% $O_2$ and 5% $CO_2$. AMPA-, NMDA-, and GABA subtype A ($GABA_A$)-receptors were blocked by NBQX (10 μM), DL-AP5 (50 μM) and picrotoxin (100 μM) in the bath respectively. Slices were then incubated in the recording chamber for at least 10 min before recordings and Purkinje cells were recorded in cell-attached mode with a temperature at 33.0 ± 1.0 ℃. Electrophysiological recordings, with a minimum recording duration of 120s, were acquired, filtered and digitized. Data were analyzed using Mini-analysis (Synaptosoft, Fort Lee, NJ, USA) or Matlab. Cells were only included if: (1) CV < 0.2; (2) The changes in firing rate between the first and the last 30 s was less than 20%.

### Statistics

All values are shown as mean ± s.e.m, difference were tested for statistical significance by Unpaired Student’s *t*-test, unless stated otherwise, and were considered to be significant if $p < 0.05$.

## Results

### A fraction of Purkinje cells show simple spike pauses longer than 500 ms.

To study the occurrence of long pauses in simple spike activity in relation to the location in the cerebellum, we analyzed extracellular recordings from Purkinje cells (PCs) in awake C57Bl/6 mice at rest, and determined their location using immunohistochemistry or based on two-photon imaging (see Methods). PCs were identified by the occurrence of the characteristic complex spike, and the consistent presence of the climbing fiber pause, a pause in simple spikes following each complex spike, was taken as evidence that the recording was from a single unit. For immunohistochemical analysis, Alcian Blue was injected to identify the recording site after each recording in an attempt to correlate cerebellar subpopulations with the occurrence of pauses (Figure 1A). The craniotomy was rectangular, strip-like shaped to allow access to the different parts of the cerebellar cortex without exposing a large surface (Figure 1B). The location of in total 288 PCs was identified by histological retrieval or imaging (Figure 1C). In a fraction of PCs, in both vermis and hemisphere, we observed at least one prolonged inter-simple spikes interval (ISI), ranging in duration from hundreds milliseconds to seconds (see example in Figure 1D), during the recording period of at least 2 min. Notably, the location of most of these cells was close to the surface of lobules IV/V, VI/VII, Crus I/II and PM, i.e. typically near the craniotomy. When we consider ISIs with a duration longer than 500 ms a ‘long’ pause, 31 out of 288 Purkinje cells are categorized as pausing cells. Not surprisingly, these PCs with long SS pauses show lower SS firing rate and higher CV compared to PCs without long pauses (Figure 1E).

**Percentages of pausing cells and pause time per cell correlate with local tissue damage.** The observation that most PCs with long pauses are located close to the surface of cerebellar cortex, under the craniotomy, suggests that some non-physiological factors may induce the occurrence of SS pauses. To facilitate the entrance of the pipette and record from PCs in the cerebellum, bone and underlying dura were removed (Figure 1A). After each successful recording the recording site was labelled by dye injection, which did not cause damage, and the pipette was moved at least 500 µm away from the recording site. Despite of all precautions, tissue damage did occur, particularly in the, less common, chronic recordings over multiple sessions (Figure 2A). To test the possible influence of tissue damage on the occurrence of pauses, we evaluated the integrity of the tissue surrounding every cell under light microscopy (Figure 2A) in relation to pausing. There is, to our knowledge, no generally accepted ISI duration that constitutes a pause (see e.g. Cao et al. 2012; Loewenstein et al. 2005; Schonewille et al. 2006; Shin and De Schutter 2006; Yartsev et al. 2009). Here, we aimed to identify the ISIs that are decidedly longer than normal ISIs to quantify pausing behavior. Hence, we evaluated pauses in Purkinje cell simple spike activity based on different minimum ISI durations labeled as pause, ranging from 50 to 2000 ms (see Methods for details). Even though, due to the sectioning procedure, we could only identify damage in a single (cutting) plane, we found that cells near damaged tissue showed striking higher incidence of ‘long’ pauses (> 500 ms) compared to cells from intact tissue (11/26, or 42.3% vs. 20/262, or 7.6%, respectively, Figure 2B, C). In fact, this difference was present even when different ISI durations were considered a pause, both in the form of a higher percentage of pausing cells and a longer pause time. In contrast to pausing cells (Fig. 1E), cells near tissue damage on average do not fire simple spikes at a lower rate (Fig. 2D), indicating that these cells are as a population less distinct from the norm and that tissue damage does not, by definition, affect all firing properties.

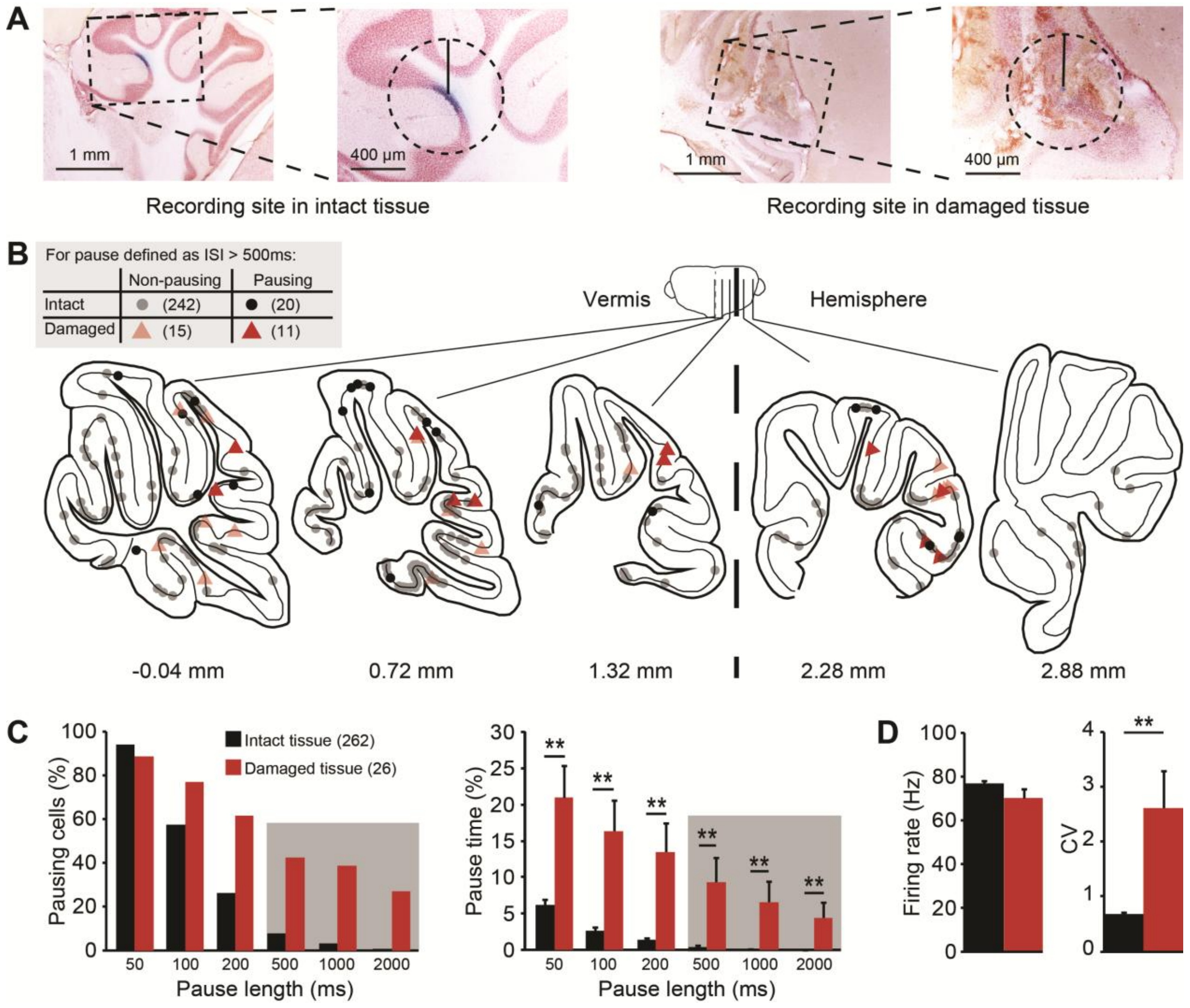

*Figure 2. **Correlating the quality of surrounding tissue with Purkinje cell simple spike pauses.***
*(**A**) Evaluation of the tissue quality under light microscope. Cells are classified as 'intact' if there is no clear tissue damage in a circle with a radius of 400 µm around the injection site (left). If the structure of the surrounding tissue is disrupted, the cell was labeled as 'damaged' (right). (**B**) Distribution of all cells (n = 288) over the cerebellar cortex, with color indicating the quality of surrounding tissue (black circles, intact; red triangle, damaged) and with the presence (light) or absence (dark) of 'long' simple spike pauses (> 500 ms) indicated by transparency. (**C**) Histograms comparing pausing cells, indicating the percentage of cells displaying at least one pause of the indicated length, and pause time, indicating the cumulative time of all pauses longer than indicated pause length divided by the total recording time per cell. Note that long pauses (> 500 ms) are shaded. PCs recorded from damaged tissue show both higher percentages of pausing cells and pause time for different pause lengths than PCs recorded from the intact tissue (all p < 0.001, Mann-Whitney U-test). (**D**) In line with the increased occurrence of pauses, tissue damage also correlates with higher SS CV, whereas simple spike firing rate is not affected. Numbers of cells are indicated between brackets. Error bars represent SEM, ** p < 0.01.*

## Temperature differences correlate with the occurrence of long pauses and a lower firing rate

In addition to possible damage, PCs in the vicinity of the craniotomy can potentially be affected by other non-physiological changes, such as temperature changes. In the neocortex, radiative temperature loss under the craniotomy has been reported to negatively affect the temperature of brain surface, reducing it by several degrees centigrade and altering the up-down transitions and firing rate (Kalmbach and Waters 2012; Long and Fee 2008). Could the proportion of PCs that shows longer simple spike pauses, even though they were recorded from undisrupted tissue, be explained by a correlation with local dysregulation of temperature near the craniotomies? To answer this question, we measured the brain temperature at different recording depths. Repeated measurements show that the temperature difference between the cerebellar surface immediately below a saline-covered craniotomy and the deepest cerebellar parts at about 4 mm in awake mice can be up to 5 ℃. The absolute temperature is relatively low compared to the core temperature of mice (37-38.5 ℃), suggesting a small artifact of the recording method itself. Correlating the local temperature with the occurrence of SS pauses in PCs, excluding the cells near tissue damage, roughly identifies two populations, based on recording depth. PCs recorded < 1 mm from the entrance point show more pauses in general, including long pauses (> 500 ms), whereas the probability of long pauses is minimized in PCs recorded beyond 1 mm depth (Figure 3A). This difference could, at least in part, be the result of a general decrease in simple spike firing rate, as described for the cortex (Kalmbach and Waters 2012; Long and Fee 2008). As the average firing rate differs substantially between zebrin-positive and –negative PCs (Zhou et al. 2014), we subdivived PCs accordingly and analyzed the effect of temperature per group. Independent of their zebrin-identity, PC firing rate correlates with the temperature, in that PCs in the first 0.5 mm of tissue in both subgroups have a significantly lower simple spike firing rate, compared to those at larger depth (Figure 3B1, 2).

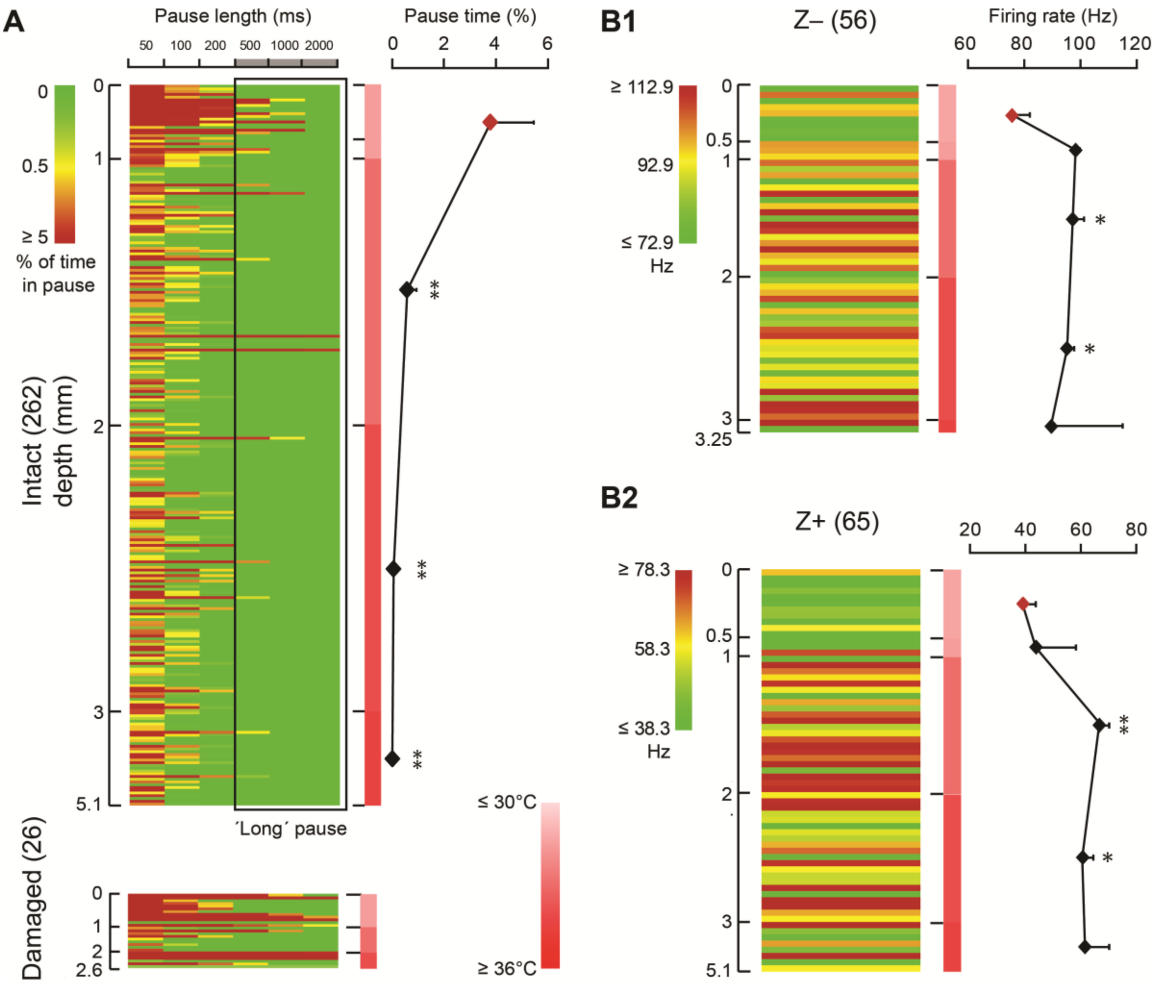

***Figure 3. The potential influence of temperature on the occurrence of long simple spike pauses and firing rate.***

*(**A**) In total 262 cells recorded from intact tissue (see Figure 2B) are presented in a matrix, in which rows*

*represent individual cells ordered based on recording depth, columns represent different pause lengths, and color indicates the percentage of pause time per cell for each pause length. As indicated by the scale bar, the color represent the percentage of the total recording time each cells is pausing, with green indicating no pauses and dark red indicates that the cell was pausing, at the indicated pause length for 5% of the total recording time or more. The scale bar in the middle indicates the temperature from low (light red) to high (dark red). Note that the maximum temperature (35 ℃) we detected is lower than the normal mouse body temperature (~37-38 ℃), which is presumably an artifact induced by the relatively large temperature probe (diameter ~200 µm). Recording depth correlates with pausing behavior in that superficial (depth ≤ 1 mm) PCs in lower temperature have a higher percentage of long pauses than the cells recorded in warmer tissue, at depths deeper than 1 mm (One-way ANOVA followed by Tukey's post-hoc test). PCs from damaged tissue are added for comparison (bottom). (***B1, 2***) Lower temperature also correlates with decreased SS firing rate. To eliminate a possible confounding effect, PCs were subdivided based on zebrin identity; both in zebrin-negative (B1) and zebrin-positive (B2) PCs the SS firing rate was significantly higher in most deeper regions compared those at ≤ 0.5 mm depth (One-way ANOVA followed by Tukey's post-hoc test). Row color is determined by the average simple spike firing rate for Z–and Z+ PCs ± 20 Hz, respectively. Numbers of cells are indicated between brackets. Error bars represent SEM, * $p < 0.05$, ** $p < 0.01$.*

This is, to our knowledge, the first analysis of the effect of a craniotomy on cerebellar temperature and PC activity. Our results suggest that recording conditions can significantly reduce PC simple spike rate and increase the probability of longer pauses.

### Distribution of short pauses over cerebellar lobules and hemispheral parts.

We have demonstrated how tissue damage and reduced temperature can affect PC activity. If long pauses represent a common property of PC firing, one would expect that, even after excluding cells obtained from damaged tissue or near the craniotomy (depth from entrance point < 1.0 mm), long pauses can be readily identified in a significant portion of the recordings, as described before (Cheron et al. 2014; Loewenstein et al. 2005; Yartsev et al. 2009). This was not the case; only 4.3% of PCs (10/234) have one or more pauses of more than 500 ms.

To test if there are any regional differences in the occurrence of pauses, we grouped cells based on their longest ISI, i.e. longest pause length, and determined the percentage of cells per lobule (Figure 4B and 4C, top) and determine the average percentage of total recording time that the cells were pausing at each given pause length (Figure 4C, bottom). Both the percentage of pausing cells and pause time drop off when an ISI duration of longer than 500 ms is taken as the definition of a pause. We consider inter-simple spike intervals of > 500 ms to be a long pause, but as the typical PC fires simple spikes at 50 to 100 Hz, the typical inter-simple spike interval is approx. 10 to 20 ms and thus intervals much shorter than 500 ms could be considered a pause too. Whereas long pauses are rare and are not linked to specific lobules, shorter pauses, i.e. 50 to 500 ms intervals, are more omnipresent and vary more commonly in occurrence between lobules.

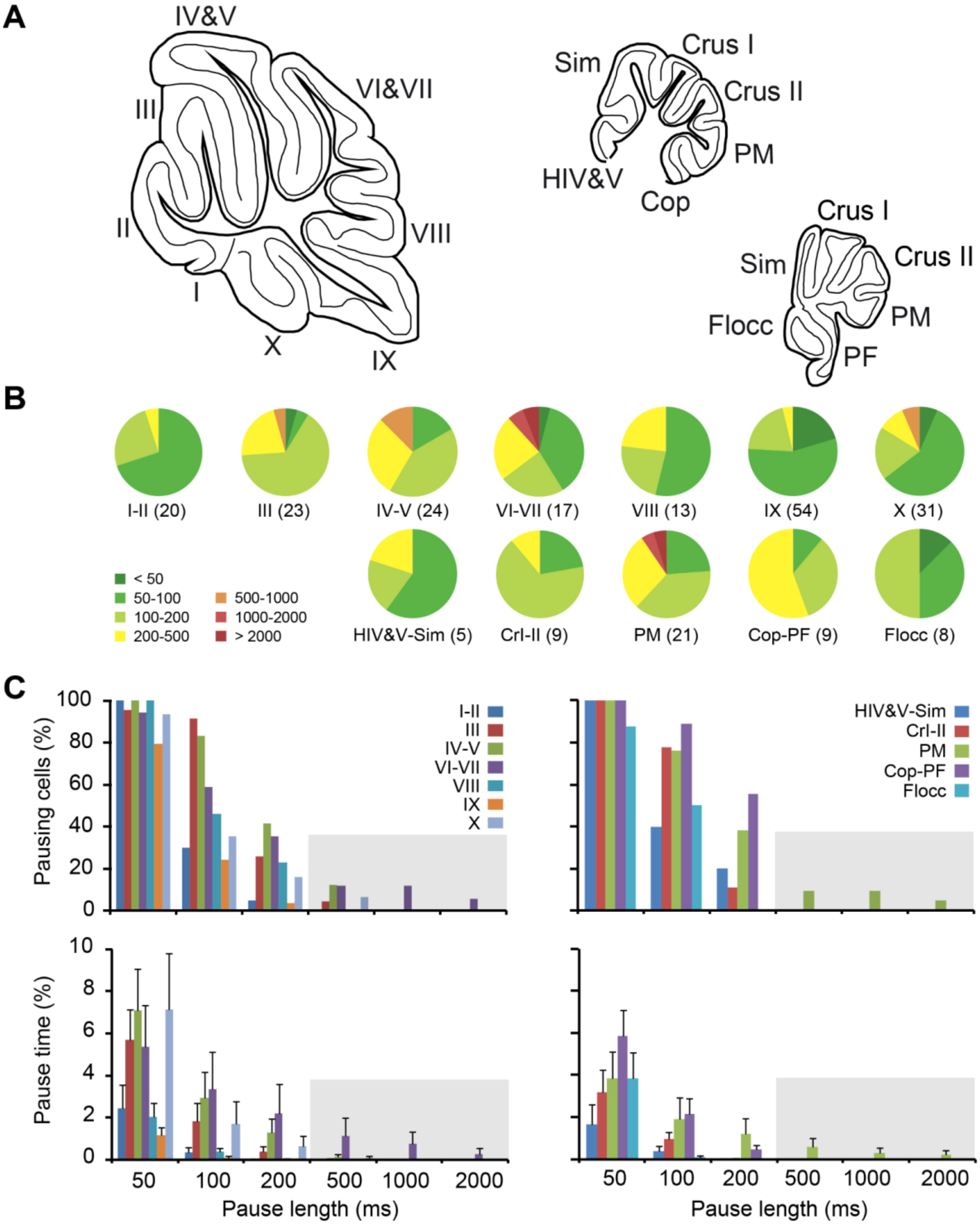

**Figure 4. The occurrence of long pauses throughout the cerebellar cortex.**
*Based on the evidence that firing properties can potentially be affected by non-physiological conditions, we excluded PCs recorded from superficial layers (recording depth ≤ 1 mm) or damaged tissue. (**A**) Schematic drawing of sagittal sections of the vermis and hemisphere (at two levels), indicating the lobules and hemispheral regions. (**B**) Pie charts of the percentages of PCs displaying at least one ISI, or pause length, of the durations indicated by the colors. For example, in lobule III 1 out of 23 PCs (4%) showed at least one ISI of 500 to 1000 ms, indicated in orange, and in 1 out of 23 PCs all ISIs were shorter than 50 ms, indicated in dark green. (**C**) Top, similar to B, but now displayed per pause length. Bottom, the average pause time compared between different lobules and regions of the vermis and hemisphere for different pause lengths. Whereas long pauses (> 500 ms) are rare after imposing the criteria mentioned above, there is little indication of a preferred location of Purkinje cells showing shorter SS pauses. Lobules marked by Roman numbers I to X, hemispheral regions are: HIV-V, hemispheric parts of lobules IV and V; Sim, lobus simplex; PM, paramedian lobule; Cop, copula pyramidis; PF, paraflocculus; Flocc, flocculus. Numbers of cells per area are indicated between brackets.*

These results indicate that long pauses are not a common characteristic of PC firing, and that shorter pauses are not only more common, but also appear to have a more differential distribution across cerebellar lobules.

### Functional modules differ in distribution of short simple spike pauses.

Functionally linked parts of the cerebellar cortex, organized in sagittal bands of cerebellar modules, can be identified based on their expression of zebrin (Apps and Hawkes 2009; Brochu et al. 1990; Sugihara 2011; Voogd 2011; Voogd and Ruigrok 2004). We have previously demonstrated that the firing rate of PCs in zebrin negative (Z–) bands is higher than that of those in positive (Z+) bands (Zhou et al. 2014). To test if pausing behavior is also related to cerebellar modules, we analyzed simple spike activity in a subset of the PCs of which the zebrin identity was determined by immunohistochemistry (n = 95). When we grouped PCs based on their zebrin expression we find that, consistent with Figure 4, only a small percentage of PCs show long pauses (Figure 5A). Moreover, both the percentage of pause time and pausing cells are not different between cerebellar modules, independent of the chosen pause length (Figure 5B). To evaluate whether Z+ and Z– PCs also differ in parameters other than firing rate, we determined several other parameters related to their ISI distributions. Anatomical evidence suggests that in Z+ PCs have thinner axons than Z– cells (Haines and Manto 2011; Voogd 1964). This would be in line with the higher average firing frequency of Z– cells, since thicker axons are capable of sustaining higher firing rates, but also suggests that the maximum instantaneous frequency should be higher in zebrin negative PCs. This prediction holds, as the minimum ISI, i.e. the maximum instantaneous firing rate, of Z– PCs is shorter than that of Z+ cells and correspondingly their maximum firing rate is higher (Figure 5C). Moreover, the fact that the difference in mean ISI, compared to that in median and mode, is relatively small, i.e. that the mode over mean and median over mean ratios are larger in Z+ PCs (Figure 5D), suggests that the proportion of longer ISIs is also relatively larger in Z− PCs. To test this, we calculated the 3rd and 4th moment of distributions, skewness and kurtosis (the 1st and 2nd moment are mean and variance, respectively). Our prediction turned out to be correct; Z− cells have a larger, positive skewness, a signature feature of a larger ‘tail’ to the right in the ISI distribution, causes by relatively less shorter, and more longer ISIs and independent of average firing rate. Kurtosis, or ‘peakedness’, is also larger in Z− PCs, which implicates that Z– PCs, more so than Z+ PCs, fire simple spikes at a ́preferred ́interspike interval, or ́preferred ́firing rate.

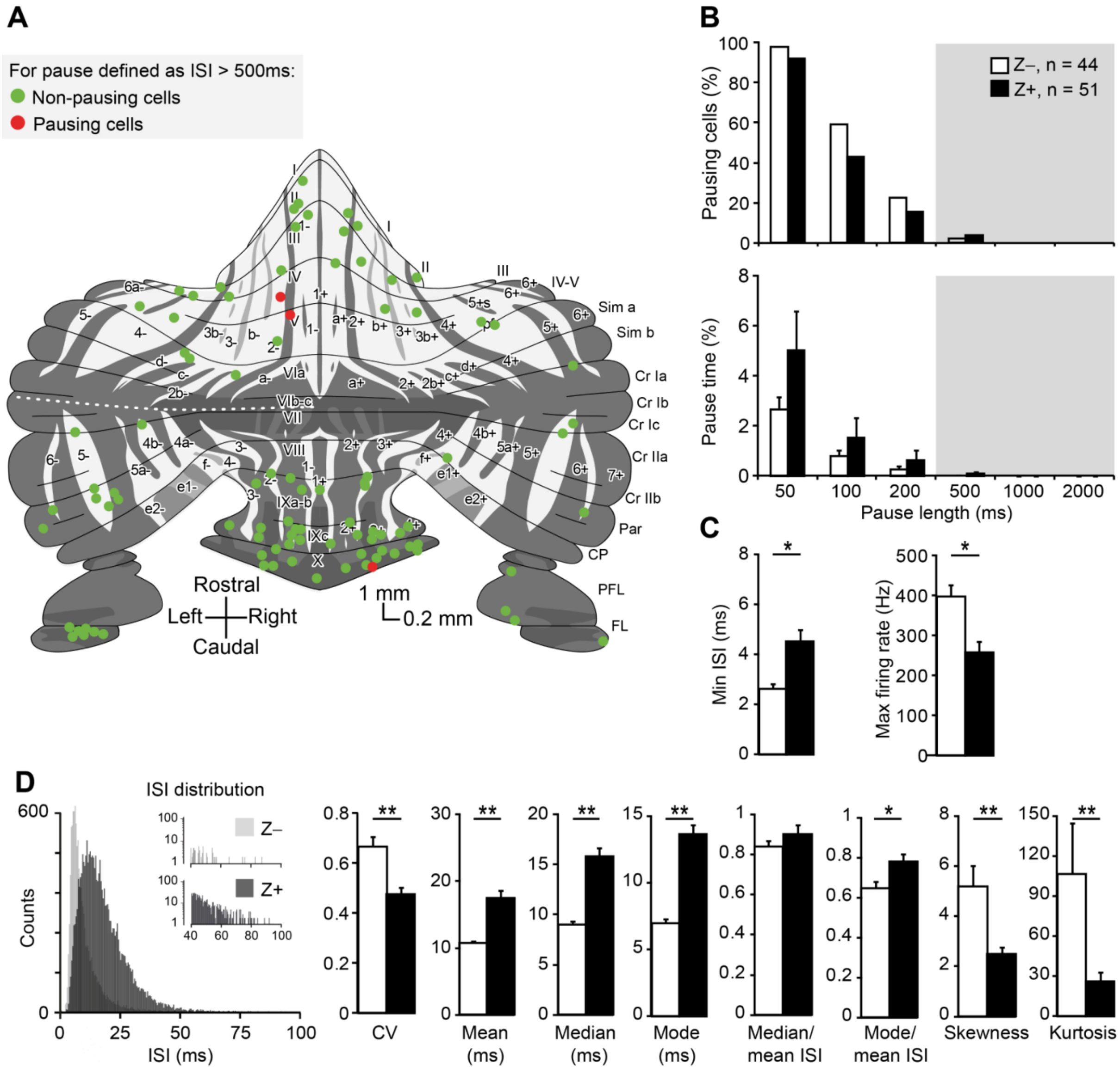

***Figure 5. Simple spike distribution shape and short pauses correlates with functional modules***
*(**A**) Distribution of PCs of which the zebrin-identity and location was determined, throughout the unfolded cerebellum. Note that only 3 out of 95 cells have simple spike pauses longer than 500 ms. Schematic drawing adapted from (Sugihara and Quy 2007; Zhou et al. 2014) (**B**) The percentages of pausing cells and pause time are not different between Z+ and Z– modules (Z–: n = 44, Z+: n = 51 cells; all p > 0.1, Mann-Whitney U-test). (**C**) Z- cells have shorter minimum inter simple spike interval (ISI) and higher maximum firing rate than Z+ cells. (**D**) Left, examples of ISI distributions for a Z+ (dark gray) and Z– (light gray) Purkinje cell. Right, detailed analysis of short simple spike pauses (< 500 ms) based on these ISI distributions revealed differences in most ISI characteristics between Z– and Z+ modules. The differences in median and mode of ISIs are larger than that in mean, suggesting a difference in shape of the ISI distributions. This was confirmed as skewness and kurtosis, the third and the fourth moment describing distributions and measures for asymmetry and 'peakedness' that are independent of the mean, respectively, differed between modules. Both kurtosis and skewness are higher in zebrin-negative PCs, indicating their ISI distributions have a more preferred ISI combined a larger tail to the right, i.e. more short pauses (50-500 ms). Numbers of cells are indicated between brackets. Note that the number of ISIs in the example distributions is higher for the Z+ PC. Error bars represent SEM, * p < 0.05, ** p < 0.01.*

Thus, subdividing PCs based on functional modules marked by zebrin effectively identifies differences in simple spike firing characteristics, including an anatomically correlated maximum firing rate and a relatively higher proportion of short pauses.

### The shape of ISI distributions can differ between subpopulations of PCs with the same zebrin identity.

The zebrin expression pattern subdivides the cerebellar cortex in parasagittal stripes, generally considered to be functional modules based on their anatomical connectivity. In addition to the sagittally oriented subdivision related to zebrin, and also based on the discontinuity of these bands, the cerebellar cortex can also be subdivided horizontally into transverse zones (Ozol et al. 1999; Reeber et al. 2013). Interestingly, PCs with the same zebrin-identity but located in different transverse zones appeared to differ in firing rate too (Zhou et al. 2014), suggesting that perhaps the occurrence of pauses or shape of the ISI distributions could differ within modules too. Indeed, specific characteristics of ISIs vary between transverse zones in that the skewness and kurtosis of Z+ PCs are different between posterior and vestibular zones. In all other comparisons we did not detect significant differences, suggesting that in general PCs with the same zebrin identity are rather similar between transverse zones. Alternatively, PCs can be attributed to the lobule or hemispheral region they are located in. To test the possibility that instead the differences occur within specific subpopulations of the same zebrin-identity in the same transverse zone, we compared Z– PCs from lobules II and III and Z+ PCs from IX and X (Figure 6D), lobules for which we had sufficient numbers of cells to compare. Although the PCs from lobule II and III are confirmed zebrin negative, ISI distribution analysis revealed that skewness and kurtosis are significantly lower in lobule II *in vivo* compared to lobule III, indicating that even within groups with the same zebrin identity from the same transverse zone, there can be subpopulations differing in characteristics.

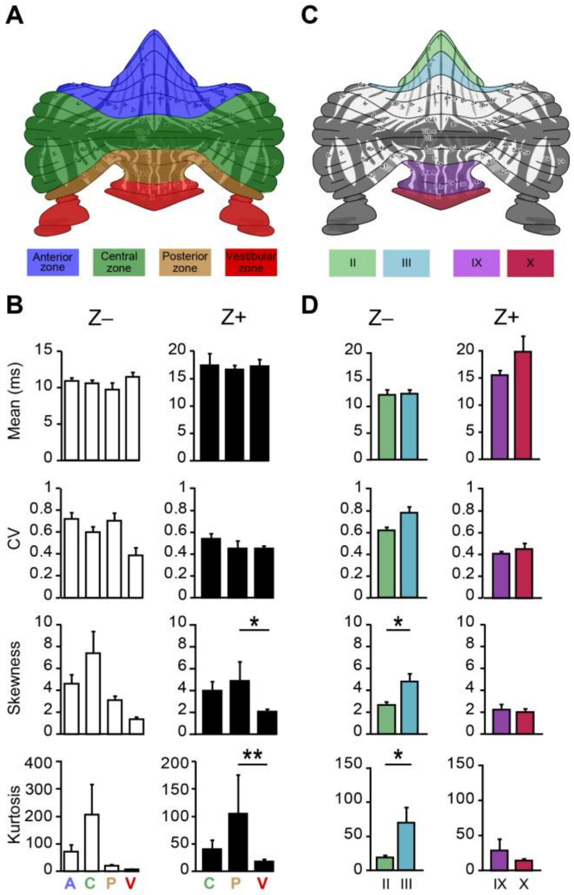

***Figure 6. Differences in spiking activity between Purkinje cells with the same zebrin identity.***
*(**A**) Based on cerebellar development and discontinuity of the zebrin bands, PCs can also be subdivided in four functionally distinct regions, called transverse zones: the anterior (A), central (C), posterior (P) and vestibular (V) zone. (**B**) Analysis of the four moments describing a distribution: mean, variance (here CV), skewness and kurtosis of ISI distributions per transverse zone for Z− and Z+ PCs. Whereas Z− cells in A, C, P and V (n = 24, 14, 4 and 2 cells, respectively) are not significantly different, Z+ cells (C, P and V, n = 4, 4 and 42 cells, respectively) in the posterior zone have a higher skewness and kurtosis of ISI distributions (One-way ANOVA followed by Tukey's post-hoc test), compared to the vestibular transverse zones. (**C**) Similarly, the ISI distribution shapes of PCs with the same zebrin identity, but from different lobules were compared. (**D**) Analysis of recordings from the confirmed Z− PCs of lobules II (n = 6 cells) and III (n = 10), and of the Z+ Purkinje cells of lobules IX (n = 19) versus X (n = 16) revealed that significant differences can occur within subpopulations of PCs with the same zebrin identity, as Z− PCs of lobule III have a higher skewness and kurtosis than those of lobule II.*

The presence of differences in shape of the ISI distributions between subpopulations of PCs with the same zebrin-identity, but located in different transverse zones or lobules, suggests a further segregation in the activity of PCs in addition to that related to zebrin expression.

### Differences between and within populations of zebrin-identified PCs are absent or reversed in vitro.

The difference in firing rate between Z– and Z+ PCs has been determined to be largely the result of intrinsic differences, as it was still present in the absence of synaptic inputs (Zhou et al. 2014). To verify if the differences in higher order properties of ISI distributions, skewness and kurtosis, between and within groups of PCs with the same zebrin-identity are also related to input or depend more on the presence of synaptic inputs, we recorded PC activity *in vitro* in the presence of blockers of synaptic inputs. These conditions have obvious, strong effects on all properties of the ISI distribution, resulting in a lower CV and skewness, and a higher kurtosis. We compared the *in vivo* activity of the confirmed Z– and Z+ PCs from lobules II-III and IX-X, respectively, with that of PCs from these lobules recorded *in vitro* to evaluate the contribution of synaptic inputs to the difference between zebrin-identified cerebellar modules (see Figure 6C). As to be expected, the difference in mean ISI, which is strongly linked to firing rate, persisted *in vitro* (Figure 7A, top). In contrast, the differences in skewness and kurtosis found *in vivo* are no longer present *in vitro*, or even reversed (Figure 7A). As the differences in shape of the ISI distribution between Z+ and Z– modules are absent under conditions of blocked synaptic inputs, one could assume that the differences within subpopulations with the same zebrin-identity are also no longer present *in vitro*. This was found to be true; when comparing the firing characteristics of lobules II vs. III and IX vs. X, the differences observed *in vivo* were no longer present, or even reversed (Figure 6D vs. 7B). Together these results suggest that ISI distribution characteristics are the result of synaptic inputs, and not intrinsic to the PC. If indeed the firing rate and mean ISI are predominantly dependent on intrinsic properties and other ISI distribution features, such as CV, skewness and kurtosis, are more dependent on the synaptic inputs to PCs, there should be no clear correlation between firing rate and the other parameters. This was confirmed, in that we found no significant correlations between firing rate and CV, skewness or kurtosis for Z+ or Z– PCs (Figure 7C).

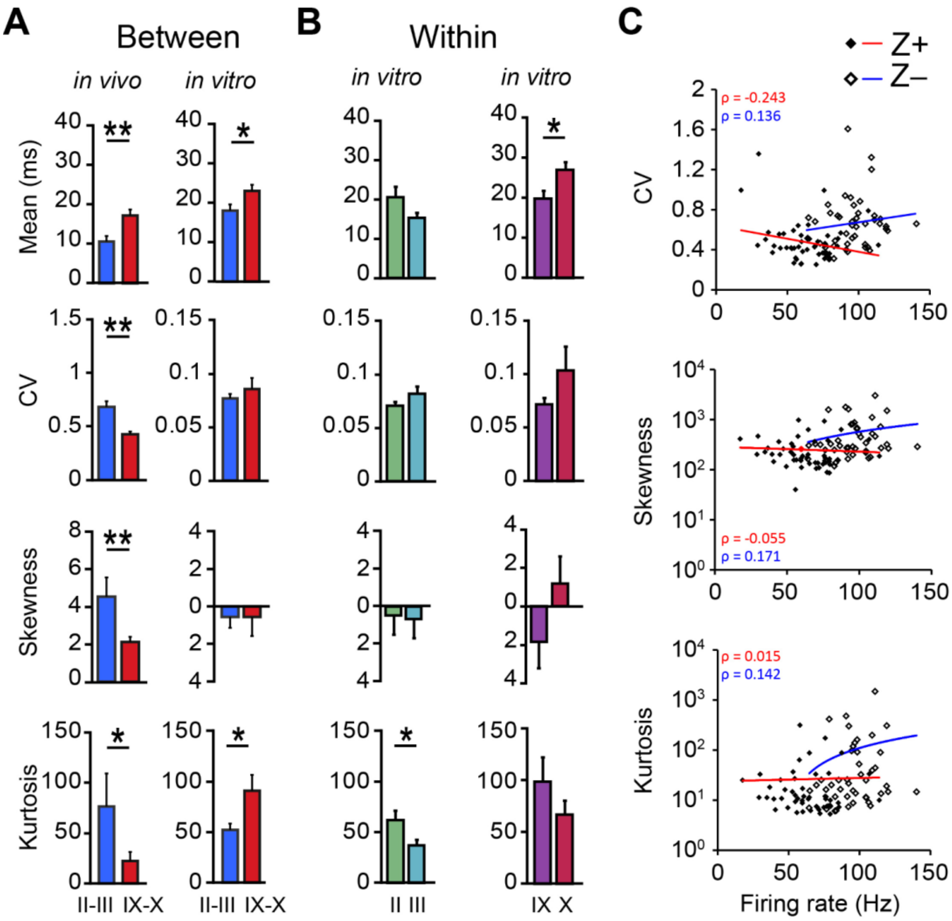

***Figure 7. Differences in the shape of ISI distributions are absent in vitro.***

*(**A**) To test if the differences in the shape of the ISI distributions are intrinsic to PCs or depend on the input PCs receive, we compared all ISI features of the Z− PCs of lobules II and III with the Z+ Purkinje cells of lobules IX and X, recorded in vivo and in vitro (in vivo: $n = 16$ vs. 35 and in vitro: $n = 27$ vs. 33 for Z− and Z+ PCs, respectively). In vitro recordings were performed in the presence of blockers for AMPA, NMDA and GABA, to block synaptic inputs to PCs. As a result, the simple spike activity only reflects intrinsic activity, which is characterized by a higher mean ISI and skewness and a lower CV and kurtosis. Whereas in vivo, in line with the results of Figure 5D, the mean, CV, skewness and kurtosis are all significantly different between Z− and Z+ PCs ($p = 0.003$, $p < 0.001$, $p = 0.004$ and $p = 0.038$, respectively), in vitro only the difference in the mean ISI persisted ($p = 0.027$). The other parameters are no longer different, or the difference is even reversed (kurtosis, $p = 0.039$). (**B**) Moreover, the differences we found in vivo between PCs with the same zebrin identity from different lobules, presented in Figure 6D, are also no longer present in vitro (for II, III, IX and X, $n =$ 13, 14, 19 and 14, respectively). In the absence of synaptic inputs the differences between Z− PCs of lobules II and III are ablated (skewness, $p = 0.87$) or even inverted (kurtosis, $p = 0.029$). Note that for PCs recorded in vitro zebrin identity was not confirmed. (**C**) Whereas the difference between Z− and Z+ PCs was found to be largely dependent on differences in intrinsic activity, the differences in shape of the ISI distribution are absent in vitro. This implicates that firing rate and ISI distribution should be independent factors, and thus not correlate with each other. To evaluate this, we plotted these parameters against each other and determined the correlation coefficients, for in vivo recorded Z− and Z+ PCs. Indeed, we found no significant correlations in any of the plots (with and without log-linear transformations, all $p > 0.05$, Spearman's correlation). Error bars represent SEM, * $p < 0.05$, ** $p < 0.01$.*

Overall we conclude that, whereas the differences in firing rate between functional modules are largely intrinsic, the differences in the shape of ISI distributions between and within subpopulation appear mostly dependent on synaptic inputs.

## Discussion

Neurons commonly confer information by means of action potentials. Whereas in most brain regions the resting activity of neurons is relatively low and thus the information is transferred by action potentials, in the cerebellum there is an alternative configuration. The combination of a high level of activity, even at rest (Zhou et al. 2014), and the fact that their output is inhibitory, make it tempting to assume that Purkinje cells communicate through the absence of action potentials, i.e. pauses (see e.g. De Schutter and Steuber 2009; De Zeeuw et al. 2011). The occurrence and relevance of short (50-500 ms) and long (>500 ms) SS pauses under physiological conditions has been a topic under debate for nearly a decade (Cao et al. 2012; Cheron et al. 2014; Libster and Yarom 2013; Loewenstein et al. 2005; Oldfield et al. 2010; Schonewille et al. 2006; Shin et al. 2007; Wang et al. 2012; Yartsev et al. 2009). Understanding where and under what conditions pauses occur is crucial for evaluating their functional importance. By recording PCs throughout the whole cerebellum in awake mice and marking each recording site, we found that PCs that show long SS pauses were typically close to the brain surface, in the vicinity of the craniotomy. Evaluation of the tissue quality and measurements of the tissue temperature in relation to the recording depth suggests that local disruption of surrounding tissue and drop in temperature can contribute to an increase in the occurrence of long SS pauses. In contrast to long pauses, short pauses are more abundant and differentially distributed between modules and, in some cases, even differs between subpopulations of Purkinje cells with the same zebrin identity. Blocking all synaptic inputs to Purkinje cells *in vitro* ablated the differences between and within subpopulations of Purkinje cells with the same zebrin identity, suggesting that differences in the shape of ISI distributions are related to differential inputs to PCs.

### Methodological considerations

Although intensively studied, previous work has focused on the charaterization and possible role of simple spike pauses, with limited interest in the cerebellar cortical location of the studied Purkinje cells (Kim et al. 2012; Sugihara and Quy 2007; Wadiche and Jahr 2005; Wang et al. 2011; Xiao et al. 2014; Zhou et al. 2014). In the current study, we systemically correlated the locations of PCs with the occurrence of long pauses and found that these cells are often located close to the exposed brain surface, near the craniotomy. Craniotomies are widely used in brain research for probing the neural activity using electrophysiology or imaging. However, creating a cranial window to allow access for an objective or single or multiple pipette can profoundly compromise the physiological conditions especially in the superficial layer (Kalmbach and Waters 2012). Our data show that the brain tissue near a craniotomy which is commonly disrupted, correlates with increased occurrence of long pauses. The tissue temperature in more superficial locations is also affected by the craniotomy, correlating with, and presumably causing, a decrease the firing rate (Kalmbach and Waters 2012; Long and Fee 2008), but may also, more specifically for the cerebellum, induce long SS pauses. Our data are inconsistent with previous reports (Loewenstein et al. 2005; Yartsev et al. 2009), in that the percentage of PCs that fire simple spikes with several hundreds milliseconds or even seconds long pauses, was significantly smaller. We have previously shown that anesthesia can increase the occurrence of long pauses (Schonewille et al. 2006). Yartsev and colleagues (Yartsev et al. 2009) performed 35 recordings sessions in lobule VI of one cat and 17 in crus II of another using one to four glass coated tungsten microelectrodes. This method could be more prone to induce tissue damage, but alternative explanations cannot be excluded. It is, for instance, possible that longer pauses are rare and require either recordings of longer duration, or specific sensory stimulation and/or motor activity to be revealed. This assumption however, does not explain the eminent difference between the various obtained results.

Although other factors, such as species differences, may be at play, the effects of tissue disruption and temperature could also explain the discrepancies between earlier reports on Purkinje cell pausing behavior (Cao et al. 2012; Cheron et al. 2014; Loewenstein et al. 2005; Schonewille et al. 2006; Yartsev et al. 2009; Zhou et al. 2014). Particularly due to the recent developments in two-photon imaging techniques, recording *in vivo* has become increasingly popular. Relating our results to the typical recording depth for two-photon imaging of up to several hunderds of micrometers, suggests these measurements could also be affected by tissue damage and lower temperatures. Future experiments will have to evaluate if keeping the dura in tact together with isolation or perfusion methods will prevent these unfavorable effects. In summary, our results demonstrate that, by opening the skin, bone and/or dura, the local environment is disrupted and thus the biophysical properties of the cell and circuits are affected.

### Purkinje cell simple spike activity

There is currently no consensus on how cerebellar Purkinje cells convey their information onto cerebellar nuclear neurons. Elements of rate coding and spatiotemporal coding have been identified (for review, see De Zeeuw et al. 2011). Analysis of smooth pursuit learning has revealed an important role for rate coding (Medina and Lisberger 2009), whereas similar rate but disrupted regularity impaired cerebellar functioning (Hoebeek et al. 2005; Wulff et al. 2009). At the level of the major output targets of Purkinje cells, the cerebellar nuclei, particular temporal patterns are thought to evoke rebound potentiation (De Zeeuw et al. 2011; Hoebeek et al. 2010), with a role for the rate coding (De Schutter and Steuber 2009). Alternatively, or in addition, the level of synchrony of the inhibitory Purkinje cell inputs is thought to control the cerebellar nuclei neuron output in a temporal manner (Person and Raman 2011; 2012). Independent of the proposed mechanisms, the simple spike pauses will be of relevance, and our data show that there are clear differences in the occurrence and their distribution of these pauses between cerebellar modules. We observed a higher CV, i.e. a lower regularity, in Z− compared to Z+ Purkinje cells, whereas we did not detect a significant difference in CV2 in our previous study (Zhou et al. 2014). Although the datasets are also slightly different, this difference is predominantly related to the difference between the two measures. CV reflects the standard deviation over all ISIs, whereas CV2 is the mean of all CV's for adjacent ISIs. This suggests that the difference is in the range, rather than in the rapid fluctuations in ISI length. Notably, the higher CV is opposite to recently published results by Xiao et al. (2014) who found that Z− PCs are more regular. This discrepancy could be related to the difference in recording locations, but could also be caused by the use of anesthetics in that study, which have been previously shown to affect Purkinje cell regularity (Schonewille et al. 2006).

The combination of a higher skewness and kurtosis in Z− Purkinje cells indicates that these cells commonly operate at a 'preferred' particular interval (high kurtosis), but when deviating from this rate, do so typically with more, longer pauses (high skewness). Conversely, the lower skewness and kurtosis in Z+ PCs suggests that these cells have a less pronounced 'preferred' interval, and fewer longer pauses. This would roughly match with the spiking activity observed in relation to eye blink conditioning and that during compensatory eye movements, which are thought to be predominantly dependent on Z− and Z+ PCs, respectively (Apps and Hawkes 2009; Mostofi et al. 2010; Sugihara and Quy 2007). Eye blink conditioning, i.e. acquiring a new, conditioned response to a previously unrelated stimulus, correlates with a short pause in an otherwise stable simple spike activity rate (Jirenhed et al. 2007). In contrast, compensatory eye movements and their adaptation, i.e. modulating existing reflexes, are typically linked to more gradually changing simple spike firing rates (see e.g. Kimpo et al. 2014; Wulff et al. 2009), in line with a lower CV (Fig. 5D). Together, this suggests that differential information coding principles are used in different cerebellar modules that correlate not only with firing rate, but also result in distinct ISI distributions. Interestingly, even though the SS firing rates of PCs with the same zebrin–identity are quite homogeous, the distributions of short ISIs can also show variations between lobules of the same zebrin-identity, which are probably caused by differential synaptic inputs as they are ablated in conditions without input (Fig. 7B). These differences in pausing behavior between groups of PCs with the same zebrin identity suggest an additional layer of complexity in the physiology of the cerebellar cortex, potentially correlating with the functional requirements of particular subpopulations.

### Functional importance of maintaining the physiological conditions

Previous studies in song production showed that small changes at the brain surface can alter the functional interactions between superficial and deep structures (Long and Fee 2008). Similarly, in the cerebellum changes in biophysical dynamics of PCs near the craniotomy can potentially influence the synchronization of PCs and thereby their control on downstream target neurons in the cerebellar nuclei, ultimately affecting the cerebellar functional output. Unraveling the physiological features of cellular activity in the absence of non-physiological perturbations is crucial for interpretation of experimental data, not only in cerebellar research, but in neuroscience in general. Our current results underline these potentially disruptive effects and identify the physiological characteristics of Purkinje cell activity and how they differ throughout the cerebellar cortex.

## Contributions

H.Z. and M.S. are responsible for conception and design of research; H.Z. performed and analyzed the *in vivo* extracellular recordings; K.V. wrote the analysis software; H.Z., K.V., C.J. and M.S. performed and analyzed the two-photon based extracellular recordings; Z.L. performed the *in vitro* recordings; K.V. and Z.L. commented on the manuscript; H.Z. and M.S. prepared the figures and wrote the manuscript.

## Acknowledgements

The authors want to thank Mandy Rutteman, Erika Goedknegt, Elize Haasdijk, Laura Post and Daphne Groeneveld for technical assistance. We gratefully thank Chris I. De Zeeuw for valuable discussion and Jeremy Rothstein for providing the EAAT4-eGFP mice. This work was supported by Dutch Organization for Life Sciences (MS) and the Erasmus University Rotterdam Fellowship (MS).

## References

*Ahn AH, Dziennis S, Hawkes R, and Herrup K. The cloning of zebrin II reveals its identity with aldolase C. Development 120: 2081-2090, 1994.*

*Apps R, and Hawkes R. Cerebellar cortical organization: a one-map hypothesis. Nat Rev Neurosci 10: 670-681, 2009.*

*Brochu G, Maler L, and Hawkes R. Zebrin II: a polypeptide antigen expressed selectively by Purkinje cells reveals compartments in rat and fish cerebellum. J Comp Neurol 291: 538-552, 1990.*

*Cao Y, Maran SK, Dhamala M, Jaeger D, and Heck DH. Behavior-related pauses in simple-spike activity of mouse Purkinje cells are linked to spike rate modulation. J Neurosci 32: 8678-8685, 2012.*

*Cheron G, Prigogine C, Cheron J, Marquez-Ruiz J, Traub RD, and Dan B. Emergence of a 600-Hz buzz UP state Purkinje cell firing in alert mice. Neuroscience 263: 15-26, 2014.*

*Crunelli V, and Hughes SW. The slow (<1 Hz) rhythm of non-REM sleep: a dialogue between three cardinal oscillators. Nat Neurosci 13: 9-17, 2009.*

*De Schutter E, and Steuber V. Patterns and pauses in Purkinje cell simple spike trains: experiments, modeling and theory. Neuroscience 162: 816-826, 2009.*

*De Zeeuw CI, Hoebeek FE, Bosman LW, Schonewille M, Witter L, and Koekkoek SK. Spatiotemporal firing patterns in the cerebellum. Nat Rev Neurosci 12: 327-344, 2011.*

*Gincel D, Regan MR, Jin L, Watkins AM, Bergles DE, and Rothstein JD. Analysis of cerebellar Purkinje cells using EAAT4 glutamate transporter promoter reporter in mice generated via bacterial artificial chromosome-mediated transgenesis. Exp Neurol 203: 205-212, 2007.*

*Haines DE, and Manto MU. The saga of zones in the cerebellar cortex as reflected in the corticonuclear system: a different approach, a specific hypothesis, and the proof begins (Voogd, 1969). Cerebellum 10: 307-333, 2011.*

*Hoebeek FE, Stahl JS, van Alphen AM, Schonewille M, Luo C, Rutteman M, van den Maagdenberg AM, Molenaar PC, Goossens HH, Frens MA, and De Zeeuw CI. Increased noise level of purkinje cell activities minimizes impact of their modulation during sensorimotor control. Neuron 45: 953-965, 2005.*

*Hoebeek FE, Witter L, Ruigrok TJ, and De Zeeuw CI. Differential olivo-cerebellar cortical control of rebound activity in the cerebellar nuclei. Proc Natl Acad Sci U S A 107: 8410-8415, 2010.*

*Jirenhed DA, Bengtsson F, and Hesslow G. Acquisition, extinction, and reacquisition of a cerebellar cortical memory trace. J Neurosci 27: 2493-2502, 2007.*

*Kalmbach AS, and Waters J. Brain surface temperature under a craniotomy. J Neurophysiol 108: 3138-3146, 2012.*

*Kim CH, Oh SH, Lee JH, Chang SO, Kim J, and Kim SJ. Lobule-specific membrane excitability of cerebellar Purkinje cells. J Physiol 590: 273-288, 2012.*

*Kimpo RR, Rinaldi JM, Kim CK, Payne HL, and Raymond JL. Gating of neural error signals during motor learning. Elife 3: e02076, 2014.*

*Libster AM, and Yarom Y. In and out of the loop: external and internal modulation of the olivo-cerebellar loop. Front Neural Circuits 7: 73, 2013.*

*Llinas R, and Sugimori M. Electrophysiological properties of in vitro Purkinje cell dendrites in mammalian cerebellar slices. J Physiol 305: 197-213, 1980a.*

*Llinas R, and Sugimori M. Electrophysiological properties of in vitro Purkinje cell somata in mammalian cerebellar slices. J Physiol 305: 171-195, 1980b.*

*Loewenstein Y, Mahon S, Chadderton P, Kitamura K, Sompolinsky H, Yarom Y, and Hausser*

*M. Bistability of cerebellar Purkinje cells modulated by sensory stimulation. Nat Neurosci 8: 202-211, 2005.*

*Long MA, and Fee MS. Using temperature to analyse temporal dynamics in the songbird motor pathway. Nature 456: 189-194, 2008.*

*McCormick DA. Neuronal networks: flip-flops in the brain. Curr Biol 15: R294-296, 2005.*

*Medina JF, and Lisberger SG. Encoding and decoding of learned smooth-pursuit eye movements in the floccular complex of the monkey cerebellum. J Neurophysiol 102: 2039-2054, 2009.*

*Mostofi A, Holtzman T, Grout AS, Yeo CH, and Edgley SA. Electrophysiological localization of eyeblink-related microzones in rabbit cerebellar cortex. J Neurosci 30: 8920-8934, 2010.*

*Oldfield CS, Marty A, and Stell BM. Interneurons of the cerebellar cortex toggle Purkinje cells between up and down states. Proc Natl Acad Sci U S A 107: 13153-13158, 2010.*

*Ozol K, Hayden JM, Oberdick J, and Hawkes R. Transverse zones in the vermis of the mouse cerebellum. J Comp Neurol 412: 95-111, 1999.*

*Paxinos G, and Franklin KBJ. The Mouse Brain in Stereotaxic Coordinates. Academic Press, San Diego 2001.*

*Person AL, and Raman IM. Purkinje neuron synchrony elicits time-locked spiking in the cerebellar nuclei. Nature 481: 502-505, 2011.*

*Person AL, and Raman IM. Synchrony and neural coding in cerebellar circuits. Front Neural Circuits 6: 97, 2012.*

*Pijpers A, Apps R, Pardoe J, Voogd J, and Ruigrok TJ. Precise spatial relationships between mossy fibers and climbing fibers in rat cerebellar cortical zones. J Neurosci 26: 12067-12080, 2006.*

*Reeber SL, White JJ, George-Jones NA, and Sillitoe RV. Architecture and development of olivocerebellar circuit topography. Front Neural Circuits 6: 115, 2013.*

*Schonewille M, Khosrovani S, Winkelman BH, Hoebeek FE, De Jeu MT, Larsen IM, Van der Burg J, Schmolesky MT, Frens MA, and De Zeeuw CI. Purkinje cells in awake behaving animals operate at the upstate membrane potential. Nat Neurosci 9: 459-461; author reply 461, 2006.*

*Shin SL, and De Schutter E. Dynamic synchronization of Purkinje cell simple spikes. J Neurophysiol 96: 3485-3491, 2006.*

*Shin SL, Hoebeek FE, Schonewille M, De Zeeuw CI, Aertsen A, and De Schutter E. Regular patterns in cerebellar Purkinje cell simple spike trains. PLoS One 2: e485, 2007.*

*Sugihara I. Compartmentalization of the deep cerebellar nuclei based on afferent projections and aldolase C expression. Cerebellum 10: 449-463, 2011.*

*Sugihara I, and Quy PN. Identification of aldolase C compartments in the mouse cerebellar cortex by olivocerebellar labeling. J Comp Neurol 500: 1076-1092, 2007.*

*Thach WT. Discharge of Purkinje and cerebellar nuclear neurons during rapidly alternating arm movements in the monkey. J Neurophysiol 31: 785-797, 1968.*

*Voogd J. Cerebellar zones: a personal history. Cerebellum 10: 334-350, 2011.*

*Voogd J. The cerebellum of the cat: Structure and fiber connections. Thesis Leiden 1964.*

*Voogd J, and Ruigrok TJ. The organization of the corticonuclear and olivocerebellar climbing fiber projections to the rat cerebellar vermis: the congruence of projection zones and the zebrin pattern. J Neurocytol 33: 5-21, 2004.*

*Wadiche JI, and Jahr CE. Patterned expression of Purkinje cell glutamate transporters controls synaptic plasticity. Nat Neurosci 8: 1329-1334, 2005.*

*Wang F, Xu Q, Wang W, Takano T, and Nedergaard M. Bergmann glia modulate cerebellar Purkinje cell bistability via Ca2+-dependent K+ uptake. Proc Natl Acad Sci U S A 109: 7911-7916, 2012.*

*Wang X, Chen G, Gao W, and Ebner TJ. Parasagittally aligned, mGluR1-dependent patches are evoked at long latencies by parallel fiber stimulation in the mouse cerebellar cortex in vivo. J Neurophysiol 105: 1732-1746, 2011.*

*Williams SR, Christensen SR, Stuart GJ, and Hausser M. Membrane potential bistability is controlled by the hyperpolarization-activated current I(H) in rat cerebellar Purkinje neurons in vitro. J Physiol 539: 469-483, 2002.*

*Wulff P, Schonewille M, Renzi M, Viltono L, Sassoe-Pognetto M, Badura A, Gao Z, Hoebeek FE, van Dorp S, Wisden W, Farrant M, and De Zeeuw CI. Synaptic inhibition of Purkinje cells mediates consolidation of vestibulo-cerebellar motor learning. Nat Neurosci 12: 1042-1049, 2009.*

*Xiao J, Cerminara NL, Kotsurovskyy Y, Aoki H, Burroughs A, Wise AK, Luo Y, Marshall SP, Sugihara I, Apps R, and Lang EJ. Systematic regional variations in purkinje cell spiking patterns. PLoS One 9: e105633, 2014.*

*Yartsev MM, Givon-Mayo R, Maller M, and Donchin O. Pausing purkinje cells in the cerebellum of the awake cat. Front Syst Neurosci 3: 2, 2009.*

*Zhou H, Lin Z, Voges K, Ju C, Gao Z, Bosman LW, Ruigrok TJ, Hoebeek FE, De Zeeuw CI, and Schonewille M. Cerebellar modules operate at different frequencies. Elife 3: e02536, 2014.*

# Chapter 4

# Climbing fiber responses of individual Purkinje cells in crus 1 of the cerebellar cortex to tactile, auditory and visual inputs in awake mice

Chiheng Ju[1], Pascal Warnaar[1], Mario Negrello[1], Tycho Hoogland[2], Laurens W.J. Bosman[1]*
and Chris I. De Zeeuw[1,2]

**in preparation**

.

## Abstract

Climbing fiber afferents originating in the inferior olive have been shown to convey sensorimotor information to Purkinje cells in the cerebellar cortex. At present it is unknown to what extent single Purkinje cells in crus 1 can relay cimbing fiber signals with different sensory modalities. Here, we studied the spatial and temporal patterns of sensory projections via the climbing fiber pathway to crus 1 at single-cell resolution using $Ca^{2+}$ imaging in awake mice. Purkinje cells in crus 1 were found to respond to subtle cutaneous, auditory and/or visual stimulation. A large percentage (37.6%) of the Purkinje cells responded to more than one type of stimulation. We did not find a clear topographical organization but rather an interspersed map of responsive and non-responsive cells. These results indicate that there must be sensory integration either within or upstream of the inferior olive.

## Introduction

The cerebellum is essential for the adaptation of movements to sensory feedback. To this end, the cerebellum receives input originating from among others the spinal cord and the brainstem as well as indirectly from the cerebral cortex. The input to the cerebellum is mainly organized in two excitatory pathways: the mossy fibers and the climbing fibers. Both pathways carry both ascending and descending inputs. Somatosensory input to the cerebellar cortex is organized according to a fractured somatotopy, where body parts have multiple representations that together only loosely represent the structury on the body surface. Such fractured somatotopical maps have been demonstrated both for the mossy fibers (Joseph et al., 1978; Shambes et al., 1978; Kassel et al., 1984) and for the climbing fibers (Miles and Wiesendanger, 1975; Rushmer et al., 1980; Castelfranco et al., 1994). The two maps share similarities, but are not identical (Ekerot and Jörntell, 2001; Bosman et al., 2010). The overlap of different climbing fiber-receptive fields and the correlation with visual and auditory input are largely unknown. In this study, we used two-photon $Ca^{2+}$ imaging in awake mice to study spatial and temporal aspects of tactile inputs from multiple facial areas as well as of auditory and visual inputs in cerebellar lobule crus 1 of mice. This technique has been shown to allow reliable detection of complex spikes in cerebellar Purkinje cells that result from climbing fiber activity (Ozden et al., 2009; Schultz et al., 2009).

The climbing fibers to the cerebellar cortex are organized in parasagittal zones, as has been confirmed by physiological studies using electrical stimulation of the major nerves of the legs and arms of the cat (Oscarsson, 1969; Groenewegen et al., 1979). A strict organization of climbing fiber receptive fields to cutaneous stimulation along these parasagittal zones could not be found, however (Eccles et al., 1968). This implies further differentiation of the parasagittal zones into smaller units or “microzones”, defined as those Purkinje cells that respond to tactile stimulation of a particular spot on the body (Ekerot et al., 1991). It has been proposed that these microzones or “microbands” correspond to groups of Purkinje cells that together form a reliable encoding of sensory input (Ozden et al., 2009; Schultz et al., 2009).

We studied the complex spike responses of Purkinje cells to tactile stimulations of four different facial areas to investigate whether we could indeed identify groups of adjacent Purkinje cells that together encode specific stimuli. The tactile stimuli were compared to auditory and visual input. We found that the receptive fields, independent of the sensory modality, were interspersed rather than clustered, and that Purkinje cells show a tendency to respond to sensory inputs from multiple sources. Taken together, the climbing fiber inputs to cerebellar lobule crus 1 seem to promote sensory integration rather than segregation.

## Materials and Methods

### *Animals and surgery*

All experimental procedures involving animals were in agreement with Dutch and European legislation and guidelines and approved in advance by the institutional animal welfare board (Erasmus MC, Rotterdam, the Netherlands). For this study, we used male C57Bl/6 mice of 4-12 weeks of age (Charles Rivers, Leiden, the Netherlands). Prior to surgery, the mice were anesthetized using isoflurane (initial concentration: 4% V/V in $O_2$, maintenance concentration: ca. 2% V/V) and received Carprofen (Rimadyl, 5 mg/ml subcutaneously) to reduce post-surgical pain. During surgery, we attached a metal head plate to the skull with dental cement (Superbond C&B, Sun Medical Co., Moriyama City, Japan) and made a craniotomy with a diameter of approximately 2 mm centered on the medial part of crus 1 ipsilateral to the side of somatosensory stimulations (Fig. 1A). The dura mater was preserved and the surface of the cerebellar cortex was cleaned with extracellular solution composed of (in mM) 150 NaCl, 2.5 KCl, 2 $CaCl_2$, 1 $MgCl_2$ and 10 HEPES (pH 7.4, adjusted with NaOH). After the surgery, the mice were allowed to recover from anesthesia for at least 30 minutes. Subsequently, the mice were head-fixed in the recording setup and they received a bolus-loading of the $Ca^{2+}$ indicator Cal-520 (0.2 mM; AAT Bioquest, Sunnyvale, CA). The dye was first dissolved with 10% w/V Pluronic F-127 in DMSO (Invitrogen) and diluted in 20x in the extracellular solution. In a subset of experiments, we also added Alexa 594 dye (20 µM; Invitrogen) to visualize the staining procedure. The dye solution was pressure injected into the molecular layer (50–80 µm below the surface) at 0.35 bar for 5 min. Finally, the brain surface was covered with 2% agarose dissolved in saline (0.9% NaCl) in order to reduce motion artifacts and prevent dehydration.

### In vivo *two-photon $Ca^{2+}$ imaging*

Starting at least 30 min after dye injection, *in vivo* two-photon $Ca^{2+}$ imaging was performed of the molecular layer using a setup consisting of a titanium sapphire laser (Chameleon Ultra, Coherent, Santa Clara, CA), a TriM Scope II system (LaVisionBioTec, Bielefeld, Germany) mounted on a BX51 microscope with a 20x 1.0 NA water immersion objective (Olympus, Tokyo, Japan) and GaAsP photomultiplier detectors (Hamamatsu, Iwata City, Japan). A typical recording sampled 40 x 200 µm with a frame rate of approximately 25 Hz.

### *Sensory stimulation*

Cutaneous stimuli were delivered to four defined regions on the left side of the face, ipsilateral to side of the craniotomy. These regions were the whisker pad, the cheek posterior to the whisker pad, the upper lip and the lower lip. Stimuli were applied using a Von Frey filament (Touch Test Sensory Evaluator 2.83, Stoelting Co., IL) attached to a piezo linear drive (M-663, Physik Instrumente, Karlsruhe, Germany). Prior to the set of experiments described in this chapter, we tested a series of 8 Von Frey filaments with a stiffness range from 0.02 g to 1.4 g in awake head-fixed mice to select the optimal force for these experiments. We selected the 0.07 g filament because this filament induced a mild reaction in the mouse, but no signs of a nociceptive response (cf. Chaplan et al. (1994)). The touch time was fixed at 100 ms. As control, we also moved the stimulator without touching the face (“sound only” condition). Visual stimuli were delivered as 10 ms pulses using a 460 nm LED (L-7104QBC-D, Kingbright, CA). The stimulation frequency was fixed at 1 Hz. The different stimuli were applied in a random order.

### *Data analysis*

Image analysis was performed offline using custom made software as described and validated previously (Ozden et al., 2012; De Gruijl et al., 2014). In short, we performed independent component analysis to define the areas of individual Purkinje cell dendrites (Fig. 1B). The fluorescent values of all pixels in each region of interest were averaged per frame. These averages were plotted over time using a high-pass filter. A 8% rolling baseline was subtracted with a time window of 0.5 ms (Ozden et al. 2012). $Ca^{2+}$ transients were detected using template matching (Fig. 1C-D).

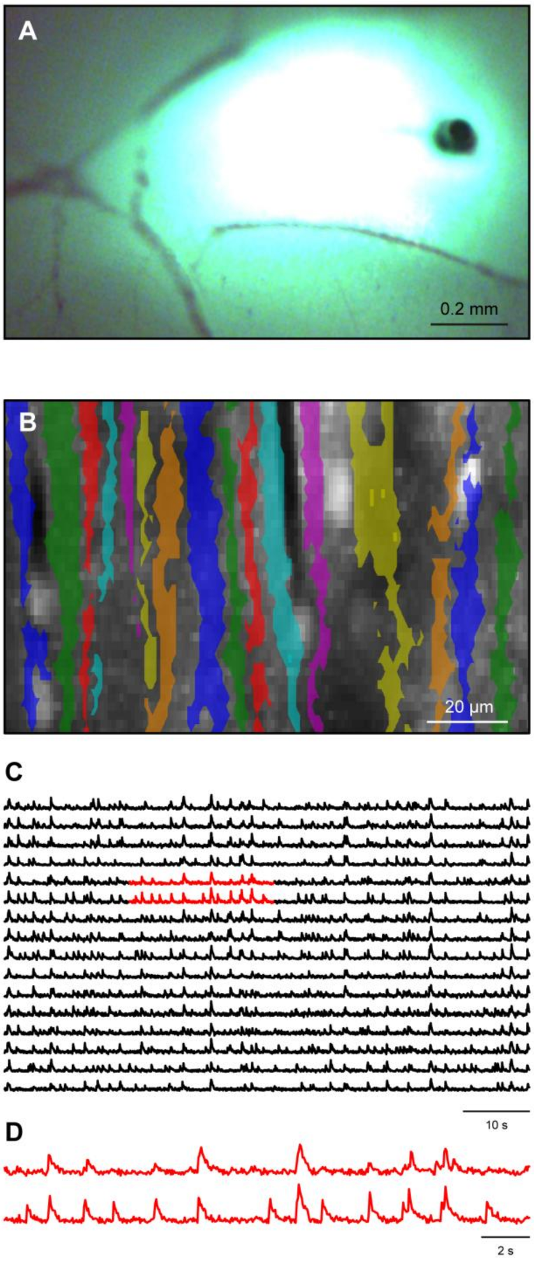

***Figure 1 – Two-photon $Ca^{2+}$ imaging in crus 1 of awake mice***
***A*** *– Bulk-loading of the $Ca^{2+}$-sensitive fluorescent dye Cal-520 in lobule crus 1 enabled the recording of complex spike activity of groups of adjacent Purkinje cells in awake mice. The recording area was verified after each experiment using epifluorescence. In this experiment, the medial part of crus 1 was stained. The exact location of the recording area is marked with a black dot.* ***B*** *– Overview of the recording area (in gray) with superimposed the locations of Purkinje cell dendrites as determined using independent component analysis. Each Purkinje cell is indicated in another color.* ***C*** *– Fluorecent traces obtained from the areas indicates in panel B. The part indicated in red is enlarged in panel D.*

After extracting the time stamps of the $Ca^{2+}$ we constructed peri-stimulus time histograms (PSTHs) using the inter-frame time (approx. 40 ms) as bin size. Significance of responses was tested using a bootstrap method: we shuffled the inter-spike intervals and created artificial PSTHs using the original stimulus times. This procedure was repeated 500x and the resultant bootstrap-PSTHs were averaged (Fig. 2C). As threshold we used the average + 2 sd. Bootstrap methods were also employed to estimate the expected variation in the fraction of Purkinje cells or cell pairs that exhibit responses to a specific stimulation.

Unless specified otherwise, data are represented as mean ± sd.

## Results

### *Climbing fibers mediate tactile input*

The climbing fibers that connect the inferior olive with the cerebellar Purkinje cells are best known for their roles in modulating motor output, but they also carry sensory feedback. Although some studies addressed the gross anatomy of climbing fiber-mediated receptive fields (Rushmer et al., 1980; Castelfranco et al., 1994), the distribution at the level of single cells is not known. In view of the functional anatomy of the cerebellum, whereby many adjacent Purkinje cells project to a single neuron in the cerebellar nuclei, knowledge of the climbing fiber projections at such a detailed level is required for understanding how sensory and sensorimotor integration can take place in the cerebellar cortex. Here we recorded climbing fiber activity as complex spikes in many (up to 26) Purkinje cells simultaneously using two-photon $Ca^{2+}$ imaging in awake mice. As demonstrated previously, complex spikes can be reliably detected as phasic changes in the fluorescent signal (Ozden et al., 2009; Schultz et al., 2009) (Fig. 1). In our hands, we found a spontaneous complex spike firing rate of 0.84 ± 0.42 Hz ($n$ = 340 Purkinje cells in 5 mice).

Next, we characterized the response properties of gentle tactile stimulation at four facial locations: the whisker pad, the cheek posterior to the whisker pad, the upper lip and the lower lip (Fig. 2A). The stimulus strength was carefully calibrated to be of the minimal strength required to evoke a response, but not so strong to induce responses from neighboring skin areas (see Methods). We found that whisker pad and lower lip stimulation were approximately equally effective in triggering Purkinje cell responses (whisker pad: $n$ = 107 out of 295 Purkinje cells (36.3%); lower lip: $n$ = 91 out of 299 cells (30.4%); $p$ = 0.140; Fisher's exact test). Cheek and upper lip stimulation evoked responses in less Purkinje cells than did whisker pad and lower lip stimulation (cheek: $n$ = 51 out of 242 cells (21.1%); upper lip: $n$ = 57 out of 280 cells (20.4%); $p$ = 0.014 (lower lip vs. cheek); $p$ = 0.914 (cheek vs. upper lip); Fisher's exact tests).

Despite the differences in fractions of responsive Purkinje cells between the four stimulation regions, the response properties of responsive Purkinje cells turned out to be rather similar irrespective of the stimulus location. We did not observe a significant difference in the response amplitude ($p$ = 0.369; Kruskal-Wallis test; Fig. 2E) nor in the response latency ($p$ = 0.434; Kruskal-Wallis test; Fig. 2F). Overall, the response amplitudes were rather small (11.5 ± 4.5) and the response latencies rather long (127 ± 2 ms; average ± SEM; $n$ = 236). This is in line with mild stimulations given under anesthesia (Bosman et al., 2010), suggesting that the tactile stimuli were indeed mild enough to avoid indirect stimulation of adjacent areas.

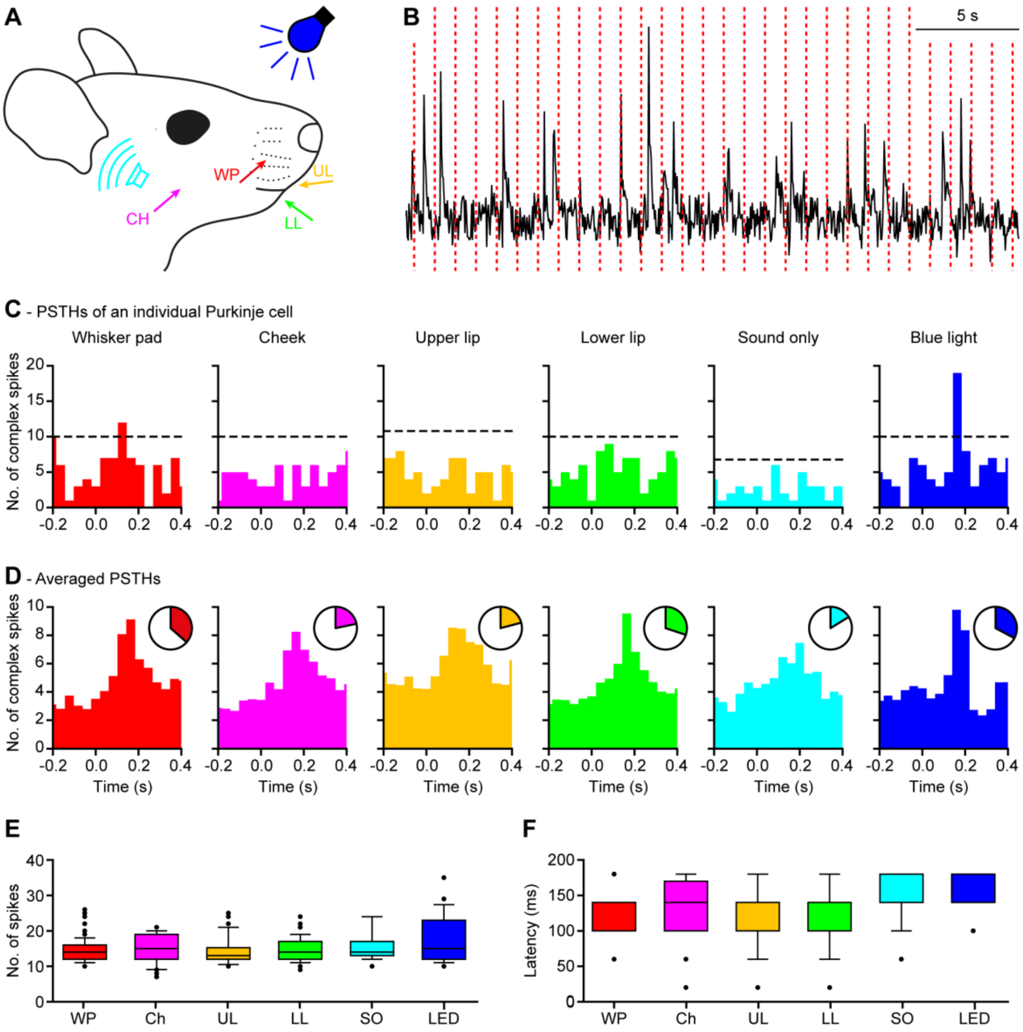

***Figure 2 – Purkinje cells in crus 1 respond to multiple types of sensory input***
***A*** *– Schematic of the locations used for tactile stimulation. WP = whisker pad; CH = cheek; UL = upper lip; LL = lower lip.* ***B*** *– Representative fragment of the* $Ca^{2+}$ *dynamics in a Purkinje cell during whisker pad stimulation (indicated by dashed red lines).* ***C*** *– Peri-stimulus time histograms of a single Purkinje cell to tactile, auditory and visual input. The dashed line indicates the threshold for a statistically significant result (see Methods).* ***D*** *– Average peri-stimulus time histograms for all responsive Purkinje cells. The pie diagrams indicate the fraction of responsive cells. Peak amplitudes (****E****) and response latencies (****F****) for all different stimuli. The peak amplitudes were comparable for all types of stimulation, but the response latencies for auditory and visual input were longer than those for tactile input.*

Finally, we recorded also the Purkinje cell responses to the sound of the stimulation device in the absence of touch. We found Purkinje cell responses to the sound only stimulation in 26 out of 177 Purkinje cells tested (14.7%). Although the sound of the stimulator was present during all tactile stimulations, we found only 1 Purkinje cell (out of 152 cells tested; 0.7%) responding to sound and all four tactile stimuli. This latter finding implies that we were not able to reliably detect auditory responses to the sound of the stimulator in our recording setup. This could be due to the relatively low sound intensity of the stimulator in a noisy environment. This raises the question, however, to what extent the tactile stimulations indeed evoked responses via mechanical stimulation of the skin or via the auditory pathway. The sound only stimuli indicate that we cannot preclude an effect of the sound, but we expect this to be minimal. The main reason for this is that the sound only stimuli had a longer latency than the tactile stimuli (142 ± 7 ms vs. 127 ± 2 ms; average ± SEM; $p$ = 0.031; one-sided Mann-Whitney test). Thus, we conclude that both tactile and auditory stimuli can evoke climbing fiber-mediated responses in Purkinje cells of crus 1 and that the impact of the sound of the stimulator on the tactile stimuli has been small.

### *Multiple cutaneous receptive fields*

Subsequently, we addressed the question whether Purkinje cells could respond to tactile stimulation at more than one location. In total, we were able to record 189 Purkinje cells in combination with stimulations at all four facial locations. Of these, 60 Purkinje cells (34.7%) responded to a single stimulus only, 38 (20.1%) to two stimuli, 27 (14.3%) to three stimuli and 6 (3.2%) to all four stimuli. The other 58 Purkinje cells (30.7%) did not respond to any of the tactile stimuli (Fig. 3).

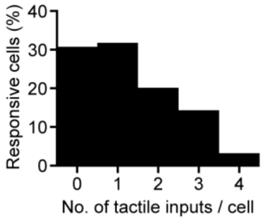

***Figure 3 – Single Purkinje cells can have complex receptive fields***
*Around 70% of the Purkinje cells from which we recorded responded to tactile stimulation at at least one location. A substantial amount of Purkinje cells responded to stimulation at more than one area.*

To find out whether some combinations of receptive fields were more favorable than others, we examined the occurrence of double responses (Fig. 4A). For all possible sets of two stimulus locations we found Purkinje cells responding to both. We wondered whether Purkinje cells tended to combine or segregate receptive fields. To test this we designed a simple model consisting out of 174 Purkinje cells in which each cell had the same chance of being responsive to a certain stimulus as we observed in our data. We then counted the number of cells being responsive to both stimuli. This procedure was repeated 10,000 times and we took the mean ± 2 sd as thresholds for significance. A $z$ transform was performed to calculate the $p$ value. Using this procedure, we found that none of the combinations occurred either more or less often than expected. Only the combination of cheek and lower lip had a (non-significant) tendency to occur more often than expected (measured: 14.9% overlap; expected: 10.6 ± 4.7% overlap; $p$ = 0.063).

We repeated this procedure for the combinations of three regions. The combinations whisker pad, cheek and upper lip and whisker pad, cheek and lower lip did not occur more or less often than expected by change ($p$ = 0.721 and 0.209, respectively), but the combination cheek, upper lip and lower lip was prevalent than expected (measured: 5.17 %; expected: 2.40 ± 1.16%; $p$ = 0.039). The combination of all four locations occurred in only 1 Purkinje cell, which is in line with the expected value (also 1 Purkinje cell). Overall, we conclude Purkinje cells neither respond to more or less tactile regions than could be expected by chance. Thus, climbing fiber-mediated input from different facial regions is not segregated at the level of Purkinje cells, neither are there many Purkinje cells that integrate all facial inputs.

*Purkinje cell responses to visual stimulation*

In a subset of experiments, we also included a session with only visual input (from a blue LED). This stimulus evoked Purkinje cell responses in 33 out of 97 cells (34.0%). The stimulus strength was not significantly different from those of tactile responses ($p = 0.135$; Mann-Withney test), but the response latency to visual stimulation was longer (tactile: 127.1 ±2.5 ms; visual: 154 ±3.9 ms; $p < 0.001$; Mann-Whitney test; Fig. 2C-F).

*Combinations of different sensory modalities*

We could not find convincing evidence for the overlap of receptive fields for cutaneous stimulation. But what about vision? In 97 Purkinje cells, we tested whether there was a response to tactile and to visual stimulation. For all four stimulation spots, we found that the number of Purkinje cells that responded to both the tactile and the visual stimulus was above the expected value (whisker pad: $p = 0.009$; cheek: $p = 0.006$; upper lip: $p = 0.042$; lower lip: $p < 0.001$; Fig. 4C). Thus, the somatosensory input from the face and visual input tended to converge on Purkinje cells.

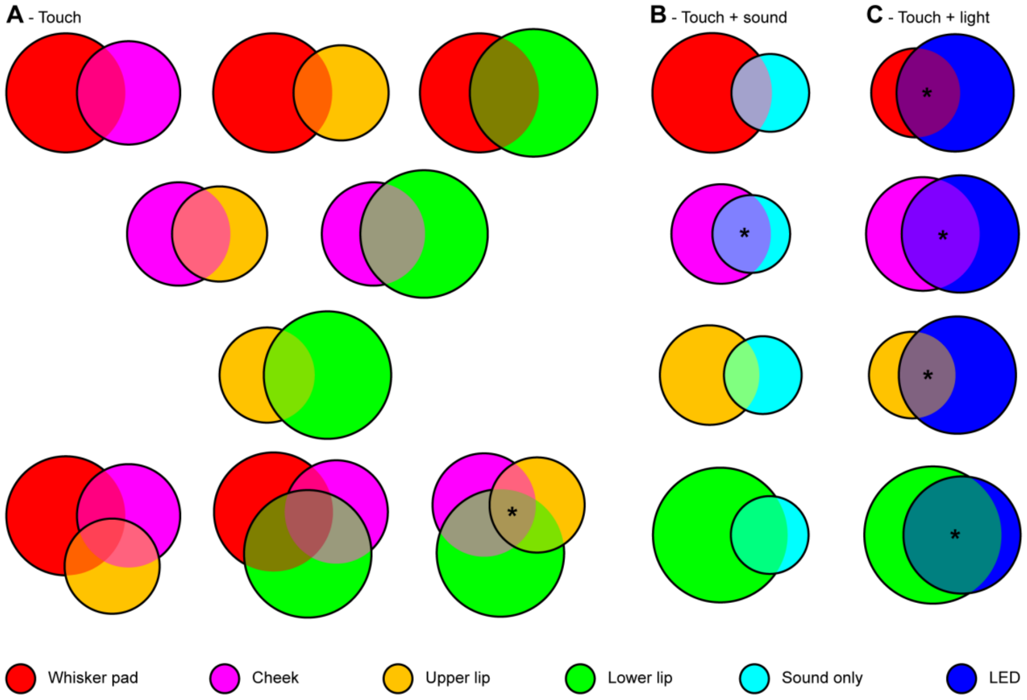

***Figure 4 – Tactile receptive fields are independent from each other, but overlap with that of visual input***
***A*** *– Venn diagrams representing the (overlap in) responsiveness to tactile stimulation of four different areas of the face. The area of each circle corresponds to the fraction of responsive Purkinje cells and the area of the overlap is proportional to the fraction of Purkinje cells responsive to both stimuli. In none of the combinations of two stimulus locations we could find a significantly smaller or larger fraction of overlap than could be predicted by chance. Only the combination of cheek, upper lip and lower lip occurred remarkably often.* ***B*** *– Purkinje cells responsive to cheek and to lower lip stimulation had an unexpectedely large chance of also responding to sound only. However, due to the low sound intensity of the stimulus, the responses to sound only are relatively unreliable.* ***C*** *– Remarkably, there was a very large overlap between responsiveness to tactile stimulation of all four facial areas tested and visual stimulation.* * $p < 0.05$.

*Grouping of Purkinje cells with the same receptive field*

There is a strong convergence of adjacent Purkinje cells to the cerebellar nuclei. Indeed, nearby Purkinje cells tend to have a high degree of complex spike synchrony (Sugihara et al., 2007; Hoogland et al., 2015). From this perspective it is highly interesting to know whether adjacent Purkinje cells indeed process the same information. To this end we calculated the distances between Purkinje cell pairs of which both cells responded to a particular stimulus with those between heterogeneous pairs of which one cell did and the other did not respond to that particular stimulus. We found that responsive Purkinje cell pairs indeed tend to be closer to each other than heterogenous pairs (*p* = 0.037; Kolmogorov-Smirnov test; Fig. 5). We found that this ordening is, however, not strict, in the sense that stimuli are encoded by continuous block of neighboring Purkinje cells.

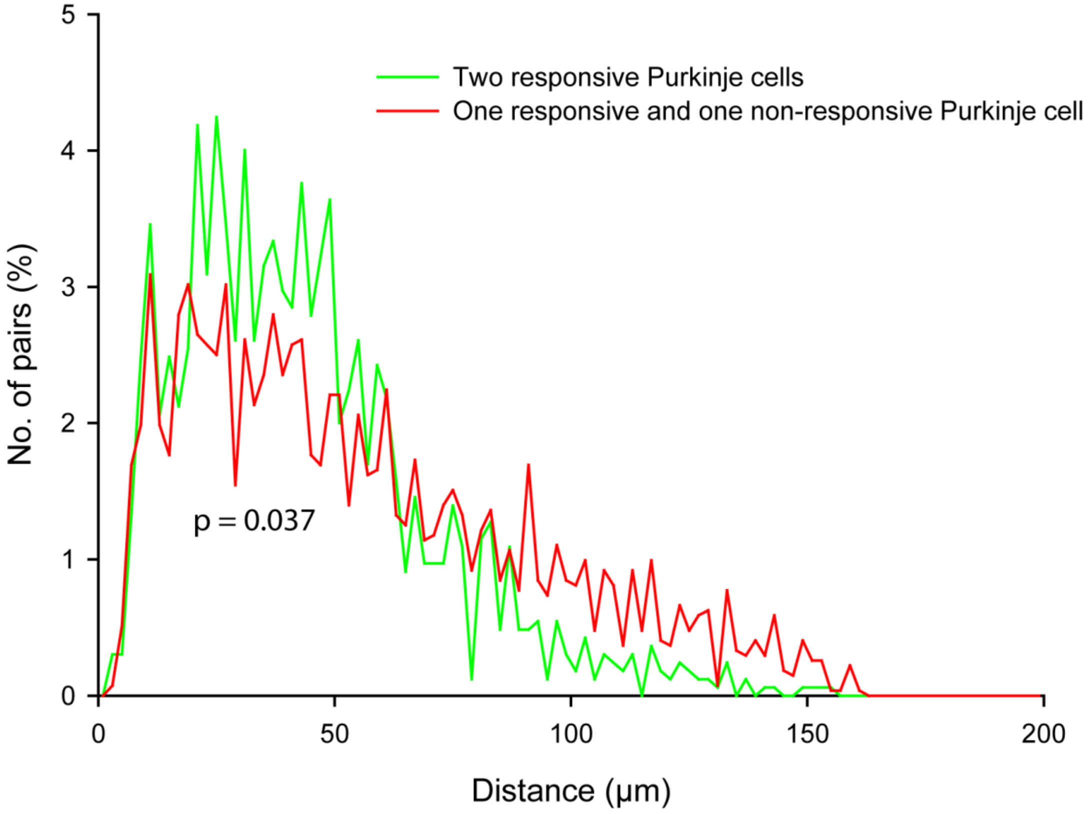

***Figure 5 – Alike Purkinje cells tend to be nearby***

*Histogram showing the distributions of distances between homogenous Purkinje cell pairs responding to the same stimulus (red) and heterogenous Purkinje cell pairs (green). The heterogenous pairs consist of one responsive and one non-responsive Purkinje cell. Homogenous cell pairs were – on average – closer together than heterogenous pairs (p = 0.037; Kolmogorov-Smirnov test), indicating that Purkinje cells with the same functional indentity were located more often in each other vicinity than Purkinje cells with different functional identities.*

## Discussion

Groups of nearby Purkinje cells collectively project to a single neuron in the cerebellar nuclei. In this chapter, we addressed the spatial aspects of climbing fiber-mediated sensory input in crus 1 of awake mice. We used *in vivo* two-photon $Ca^{2+}$ imaging to study sensory-induced responses in groups of adjacent Purkinje cells. First, we compared tactile input from four different facial areas. We found that the number of Purkinje cells recruited by each type of stimulus varied, but that the response properties of individual Purkinje cells were comparable. Thus we conclude that the sensitivity to facial areas depend on the number of Purkinje cells involved rather than on modulation of the response strength at the level of individual neurons. Although Purkinje cells encoding the same stimulus tended to be closer to each other than to other Purkinje cells, we were not able to find clear clusters of Purkinje cells responding to a specific stimulus. This could indicate that Purkinje cells are more involved in the integration of sensory input than on the segregation of different inputs. In line with this, we found that a substantial portion of Purkinje cells responded to touch of more than one area. And even more, Purkinje cells responsive to tactile input were often also responsive to visual input, and vice versa. However, while the combination of responsiveness to touch and vision was encountered more than expected, there was no systematic clustering of tactile input from different areas. This implies that there are many types of Purkinje cells, with varying responsiveness. Taken together, crus 1 is composed of a myriad of Purkinje cells, with many different sensory profiles. During normal behavior, many different combinations of sensory input occur in specific sequences and this could be reflected in the organizaition of Purkinje cell receptive fields.

### *Anatomical organization of climbing fiber projections*

In the adult brain, Purkinje cells are usually innervated by a single climbing fiber only, with a minority receiving input from two climbing fibers (Nishiyama and Linden, 2004; Bosman and Konnerth, 2009). The climbing fiber-to-Purkinje cell synapse is remarkably strong and climbing fiber activity leads invariably to a postsynaptic complex spike (Simpson et al., 1996). A complex spike involves, apart from the typical $Na^+$ and $K^+$ currents also a strong influx of $Ca^{2+}$ so that it can be monitored reliably using two-photon $Ca^{2+}$ imaging (De Zeeuw et al., 2011). The climbing fibers originate exclusively from the contralateral inferior olive and each climbing fiber innervates approximately five to ten Purkinje cells located within a parasagittal plane (Sugihara et al., 1999; De Gruijl et al., 2013). Climbing fibers from adjacent neurons in the inferior olive project to nearby Purkinje cells, again organized in the parasagittal plane (Groenewegen, Voogd, and Freedman 1979). As the inferior olivary neurons are tightly coupled, this creates microzones of Purkinje cells with increased complex spike synchrony(Zeeuw et al. 2003; Leznik and Llinás 2005; Marshall et al. 2007; De Gruijl, Hoogland, and De Zeeuw 2014).

At a larger scale, each subnucleus of the inferior olive projects to a specific parasagittal zone in the cerebellar cortex and the Purkinje cells of each of these zones all project to specific cerebellar nuclei (Ruigrok, 2011). A nucleo-olivary connection closes the olivo-cerebellar loop, thus creating parasagittal modules including the inferior olive, the cerebellar cortex and the cerebellar nuclei (Dietrichs and Walberg 1981; Bazzigaluppi et al. 2012). Some of these modules can be largely identified by their expression pattern of zebrin II (Voogd and Ruigrok 2004; Apps and Hawkes 2009; Sugihara 2011). As shown in chapter 2, zebrin-positive and zebrin-negative bands differ in their Purkinje cell activity patterns at rest. This study created, for the first time, a link between anatomical and physiological heterogeneity in the cerebellar cortex. In the current chapter, we zoomed in on a zebrin-positive region and studied functional heterogeneity, in terms of receptive fields, within this region.

### *Spatial organization of "sensory climbing fibers"*

Quite some attention has been devoted to the spatial organization of mossy fiber-mediated somatosensory input to the cerebellar hemispheres. This organization has been described as a "fractured somatotopy": all body parts have multiple representations that are not organized in the same way as on the body surface (Shambes et al., 1978; Kassel et al., 1984). For the limbs it has been shown that the climbing fibers are organized in a similar way as the mossy fibers (Ekerot and Jörntell, 2001). And also for the whole body, the existence of a fractured somatotopical organization has also been described for the climbing fibers (Rushmer et al., 1980; Castelfranco et al., 1994). The existence of such a mosaic projection pattern already indicates that parasagittal stripes should not be considered as monolithical objects but have differentiated functions.

To study this in more detail, we applied gentle cutaneous stimulation during Purkinje cell recordings with single cell resolution. This resolution is required to observe whether adjacent Purkinje cells, that tend to project to the same or neighboring cells in the cerebellar nuclei, encode the same sensory stimulus. Using a broad, unspecific facial stimulus, cooperative activity of Purkinje cells indicated that neighboring Purkinje cells can act as functional ensembles, together reliably coding sensory input (Ozden et al., 2009; Schultz et al., 2009). In this study we investigated whether this hypothesis holds true for specific, localized tactile inputs.

We found a heterogeneous answer. Purkinje cells encoding the same input tend to be closer together than other Purkinje cell pairs, supporting the idea that functionally similar Purkinje cells group together. Yet, this grouping together is far from perfect. Purkinje cells combine different cutaneous receptive fields in an apparently random manner and Purkinje cells with identical receptive fields are seperated by other Purkinje cells. While the proximity of Purkinje cells with the same receptive field supports the notion of functional ensembles of Purkinje cells with the same function (Ozden et al., 2009; Schultz et al., 2009), the many combinations of receptive fields and the intermingled locations of the Purkinje cells involved point towards a role for Purkinje cells in sensory integration.

Our experiments with visual stimuli confirm the latter: Purkinje cells responsive to visual input are very often also responsive to tactile input. The observation that visual and tactile input converge on Purkinje cells strengthens the hypothesis that the cerebellum gathers all information required for fine adjustments of movements.

### *The inferior olive as sensory area?*

The inferior olive and its efferent climbing fibers are generally considered to be part of the motor system. In the “error theory”, however, climbing fiber activity is hypothesized to convey “errors” or mismatches between expected and actual input (Ito 1982; Marr 1969; Albus 1971). The problem for regarding climbing fiber responses as reporters of sensory input is that they are unreliable. Studies using whisker stimulations have shown that the climbing fiber responses have low response rate, large jitter and long latency (Thomson et al. 1989; Bosman et al. 2010). Also in our hands, we found that subtle stimulation in general did not induce complex spikes in much more than 10% of the trials – although there were some outliers. This is in line with previous studies using electrophysiology in the same area using whisker stimulation (Bosman et al., 2010). It implies that only a relatively small fraction of the complex spikes are actually related to the sensory input under study.

We also found long latency times. Again, this has been shown before and the more subtle the stimulus, the longer the latency to response (Bosman et al., 2010). Nevertheless, the latency following a visual stimulus was almost 150 ms which was longer than observed before using tactile input.

It should be noticed, however, that strong and preferably unexpected stimuli are able to trigger complex spikes in a more reliable manner (Bosman et al. 2010; Najafi et al. 2014). But what could be the physiological relevance of climbing fiber-responses to weak stimuli? A possible explanation comes from previous two-photon imaging experiments were it has been shown that groups of adjacent Purkinje cells are reliable reporters of sensory events (Ozden et al., 2009; Schultz et al., 2009). We show here that clusters of adjacent Purkinje cells with the exact same receptive field do probably not exist in crus 1. Instead, adjacent Purkinje cells seem to integrate various receptive fields. This could be in line with providing the sensory feedback for different types of facial behavior – often involving different regions (e.g. during grooming).

## *References*

*Bosman LWJ, Konnerth A (2009) Activity-dependent plasticity of developing climbing fiber-Purkinje cell synapses. Neuroscience 162:612-623.*

*Bosman LWJ, Koekkoek SKE, Shapiro J, Rijken BFM, Zandstra F, van der Ende B, Owens CB, Potters JW, de Gruijl JR, Ruigrok TJH, De Zeeuw CI (2010) Encoding of whisker input by cerebellar Purkinje cells. The Journal of physiology 588:3757-3783.*

*Castelfranco AM, Robertson LT, McCollum G (1994) Detail, proportion, and foci among face receptive fields of climbing fiber responses in the cat cerebellum. Somatosensory & motor research 11:27-46.*

*Chaplan SR, Bach FW, Pogrel JW, Chung JM, Yaksh TL (1994) Quantitative assessment of tactile allodynia in the rat paw. J Neurosci Methods 53:55-63.*

*De Gruijl JR, Hoogland TM, De Zeeuw CI (2014) Behavioral correlates of complex spike synchrony in cerebellar microzones. J Neurosci 34:8937-8944.*

*De Gruijl JR, Bosman LWJ, De Zeeuw CI, De Jeu MTG (2013) Inferior olive: All ins and outs. In: Handbook of the Cerebellum and Cerebellar Disorders (Manto M, Schmahmann JD, Rossi F, Gruol DL, Koibuchi N, eds), pp 1013-1058. Dordrecht: Springer Netherlands.*

*De Zeeuw CI, Hoebeek FE, Bosman LWJ, Schonewille M, Witter L, Koekkoek SK (2011) Spatiotemporal firing patterns in the cerebellum. Nature reviews Neuroscience 12:327-344.*

*Eccles JC, Provini L, Strata P, Táboříková H (1968) Analysis of electrical potentials evoked in the cerebellar anterior lobe by stimulation of hindlimb and forelimb nerves. Experimental brain research 6:171-194.*

*Ekerot CF, Jörntell H (2001) Parallel fibre receptive fields of Purkinje cells and interneurons are climbing fibre-specific. The European journal of neuroscience 13:1303-1310.*

*Ekerot CF, Garwicz M, Schouenborg J (1991) Topography and nociceptive receptive fields of climbing fibres projecting to the cerebellar anterior lobe in the cat. The Journal of physiology 441:257-274.*

*Groenewegen HJ, Voogd J, Freedman SL (1979) The parasagittal zonation within the olivocerebellar projection. II. Climbing fiber distribution in the intermediate and hemispheric parts of cat cerebellum. The Journal of comparative neurology 183:551-601.*

*Hoogland TM, De Gruijl JR, Witter L, Canto CB, De Zeeuw CI (2015) Role of synchronous activation of cerebellar Purkinje cell ensembles in multi-joint movement control. Current biology : CB 25:1157-1165.*

*Joseph JW, Shambes GM, Gibson JM, Welker W (1978) Tactile projections to granule cells in caudal vermis of the rat's cerebellum. Brain, behavior and evolution 15:141-149.*

*Kassel J, Shambes GM, Welker W (1984) Fractured cutaneous projections to the granule cell layer of the posterior cerebellar hemisphere of the domestic cat. The Journal of comparative neurology 225:458-468.*

*Miles TS, Wiesendanger M (1975) Organization of climbing fibre projections to the cerebellar cortex from trigeminal cutaneous afferents and from the SI face area of the cerebral cortex in the cat. The Journal of physiology 245:409-424.*

*Nishiyama H, Linden DJ (2004) Differential maturation of climbing fiber innervation in cerebellar vermis. J Neurosci 24:3926-3932.*

*Oscarsson O (1969) Termination and functional organization of the dorsal spino-olivocerebellar path. The Journal of physiology 200:129-149.*

*Ozden I, Sullivan MR, Lee HM, Wang SSH (2009) Reliable coding emerges from coactivation of climbing fibers in microbands of cerebellar Purkinje neurons. J Neurosci 29:10463-10473.*

*Ozden I, Dombeck DA, Hoogland TM, Tank DW, Wang SS (2012) Widespread state-dependent shifts in cerebellar activity in locomoting mice. PloS one 7:e42650.*

*Ruigrok TJH (2011) Ins and outs of cerebellar modules. Cerebellum 10:464-474.*

*Rushmer DS, Woollacott MH, Robertson LT, Laxer KD (1980) Somatotopic organization of climbing fiber projections from low threshold cutaneous afferents to pars intermedia of cerebellar cortex in the cat. Brain Res 181:17-30.*

*Schultz SR, Kitamura K, Post-Uiterweer A, Krupic J, Häusser M (2009) Spatial pattern coding of sensory information by climbing fiber-evoked calcium signals in networks of neighboring cerebellar Purkinje cells. J Neurosci 29:8005-8015.*

*Shambes GM, Gibson JM, Welker W (1978) Fractured somatotopy in granule cell tactile areas of rat cerebellar hemispheres revealed by micromapping. Brain, behavior and evolution 15:94-140.*

*Simpson JI, Wylie DR, De Zeeuw CI (1996) On climbing fiber signals and their consequence(s). Behav Brain Sci 19:384-398.*

*Sugihara I, Wu H, Shinoda Y (1999) Morphology of single olivocerebellar axons labeled with biotinylated dextran amine in the rat. The Journal of comparative neurology 414:131-148.*

*Sugihara I, Marshall SP, Lang EJ (2007) Relationship of complex spike synchrony bands and climbing fiber projection determined by reference to aldolase C compartments in crus IIa of the rat cerebellar cortex. The Journal of comparative neurology 501:13-29.*

# Chapter 5

# Cellular resolution imaging of climbing fibers responding to single whisker stimulation

Chiheng Ju[1,2], Laurens W.J. Bosman[1,2,3], Tycho M. Hoogland[4], Mario Negrello[1] and Chris I. De Zeeuw[1, 4]

[1]Department of Neuroscience, Erasmus MC, 3000 CA Rotterdam, The Netherlands
[4]Netherlands Institute for Neuroscience, Royal Netherlands Academy of Arts and Sciences, 1105 BA Amsterdam, The Netherlands

**in preparation**

## Abstract

Facial whiskers are typically arranged in grid-like patterns on the snout. In several sensory brain regions, whisker input is organized in a similar arrangement as the whiskers on the snout. The best-known example of this strict somatotopy is found in the barrel cortex. During exploration mice use their whiskers extensively and many brain regions concertedly ensure integration of sensory input and motor output. In recent studies we highlighted the role of the cerebellum in perception and decision-making based on whisker input in mice. Despite our understanding at physiological and behavioral levels, the anatomy of whisker input to the cerebellar cortex is still largely unknown. In particular, the organization of climbing fiber inputs carrying whisker-related input has not been studied at a cellular level. Here, we used two-photon $Ca^{2+}$ imaging in anesthetized mice in conjunction with single-whisker stimulation to map the climbing fiber projections to cerebellar lobules crus 1 and crus 2. We found that in these lobules climbing fibers carry mainly input from single whiskers. We describe that, although whisker-responsive Purkinje cells are interspersed between other Purkinje cells, the input pattern of whisker-responsive Purkinje cells is organized based on whisker identity: Purkinje cells processing input from the same whisker were often found to be in each other’s neighborhood. Thus, although crus 1 and crus 2 lack clear “barrels” and have an anatomy that seems to favor data integration rather than segregation, we for the first time show a structure in the sensory input channels to the cerebellar cortex at a cellular resolution.

## Introduction

The cerebellum integrates sensorimotor pathways in order to precisely control the coordination, timing and adjustment of movements (De Zeeuw et al., 2011) including locomotion and whisking (Proville et al., 2014; Vinueza Veloz et al., 2014). When exploring their environment, mice rhythmically protract and retract their mystacial whiskers at frequencies between 5 and 30 Hz (Rahmati et al., 2014; Sofroniew et al., 2014). Such rhythmic pacing of active touch requires fast integration of sensory and motor pathways (Hartmann, 2009; O'Connor et al., 2013). The cerebellum could therefore be of great importance in sustaining such rhythmicity for the mouse whisker system. Whisker sensory input reaches the cerebellar cortex via the two main afferent pathways: the mossy fibers and the climbing fibers (Axelrad and Crepel, 1977; Bosman et al., 2010; Bosman et al., 2011; Chu et al., 2011) with the strongest receptive fields localized in lobules crus 1 and crus 2 (Shambes et al., 1978; Sharp and Gonzalez, 1985) (Fig. 1A).

Most likely, the cerebellum contributes to sensorimotor integration via reciprocal signaling with the somatosensory and motor cortices. It is important, therefore, to understand how the cerebellar receptive fields relate to those in the cortex. The somatosensory cortex has a continuous somatotopy of the body surface with an extensive representation of the whiskers (Welker, 1971; Woolsey et al., 1975; Brecht, 2007). In contrast, the mossy fiber input to the cerebellar cortex follows a patchy and discontinuous body map (Shambes et al., 1978; Apps and Hawkes, 2009). The somatotopy of the other main input pathway to the cerebellar cortex, the climbing fibers, has not been described in any detail for the whisker system. We recently showed that climbing fiber input can pattern mossy fiber input (Badura et al., 2013), underscoring the importance of understanding the spatial arrangement of climbing fiber input in relation to whisking behavior.

The climbing fibers exclusively originate from the contralateral inferior olive. In turn, the inferior olive receives sensory input from the whiskers both directly from the trigeminal nuclei as well as indirectly via many other brain regions (De Gruijl et al., 2013; Voogd et al., 2013). The primary sensory neurons convey information from the whisker mechanoreceptors to all parts of the sensory trigeminal nuclei (Hayashi, 1980). The inferior olive receives trigeminal input only from the spinal nucleus (SpV) and not from the principal nucleus (PrV). The densest projections are to the rostral parts of the dorsal accessory olive (DAO) and of the principal olive (PO). In the PO, the innervation is largely confined to the dorsal leaf and to the dorsomedial cell group of the ventral leaf. The medial accessory olive (MAO) is only sparsely innervated from the SpV (Huerta et al., 1983; Swenson and Castro, 1983; Molinari et al., 1996; Yatim et al., 1996) (Fig. 1B). Each of these olivary regions projects contralaterally to specific rostro-caudal zones in the cerebellar cortex (Voogd and Glickstein, 1998; Apps and Hawkes, 2009).

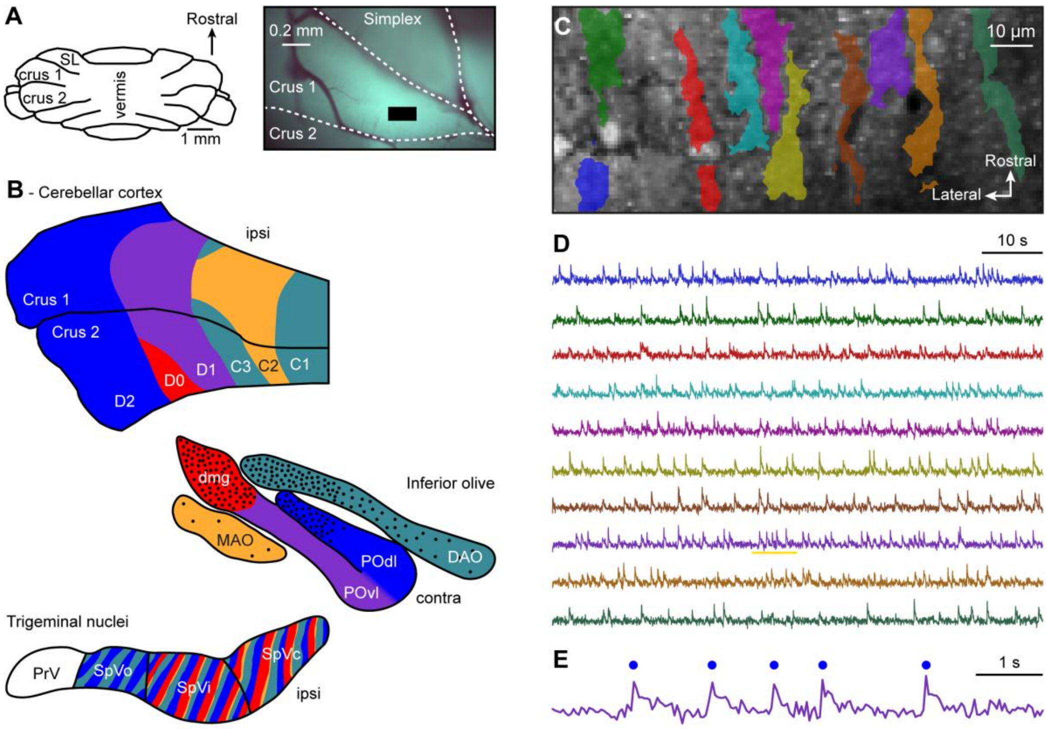

***Figure 1 – In vivo two-photon imaging of Ca2+ transients in Purkinje cell dendrites.***
***A** - Schematic diagram of the lobules of the cerebellar cortex (left) and epifluorescent image of the left crus 1 following dye injection. The black rectangle indicates the location of the recording shown in panels C-E. **B** – Schematic representation of the information flow from the trigeminal nuclei via the inferior olive to the cerebellar cortex. The principal trigeminal nucleus (PrV) does not project directly to the inferior olive, but in contrast to the three parts of the spinal trigeminal nucleus (SpV). The oral (SpVo), interpolar (SpVi) and caudal (SpVc) parts of the SpV all project to the dorsal accessory olive (DAO) and the dorsal leaf of the principal olive (POdl). The SpVi and SpVc in addition project to the dorsomedial cell group (dmg) of the ventral leaf of the principal olive (POvl) and sparsely to the medial accessory olive (MAO). The density of the black dots in the inferior olive symbolizes the density of the projections. The inferior olive, in turn, projects via climbing fibers to the cerebellar cortex. Corresponding colours indicate the interconnected regions. For references: see main text. **C** – Recording location in the molecular layer of crus 1 (see panel A) showing 13 Purkinje cell dendrites identified following independent component analysis of the fluorescent signal. This recording was made using OGB and at a recording depth of approximately 50 µm. **D** – Fluorescent traces of the 13 Purkinje cell dendrites shown in panel C. The colors of the traces correspond to those of the Purkinje cells. A part (indicated by yellow line) of these recordings is enlarged (**E**) showing identified Ca2+ transients (indicated with blue symbols).*

In order to obtain a cellular resolution map of climbing fiber projections that encode sensorimotor information of single whiskers, we applied *in vivo* two-photon Ca$^{2+}$ imaging in lobules crus 1 and 2 of the cerebellum during mechanical stimulation of single whiskers. We found that these climbing fiber projections are mostly related to single rather than multiple whiskers and that climbing fibers with input from the same whisker tended to group together: not in a barrel-like fashion, but intermingled with other climbing fibers in a pattern facilitating integration rather than segregation of sensory input.

## Materials and Methods

### *Animals*

We used male C57Bl/6 mice of 4-12 weeks of age (Charles Rivers, Leiden, the Netherlands). All experimental procedures involving animals were in agreement with Dutch and European legislation and guidelines and approved in advance by the institutional animal welfare board (Erasmus MC, Rotterdam, the Netherlands). A 2 mm craniotomy was made above the medial part of crus 1 ipsilateral to the side of whisker stimulation (Fig. 1A). The dura mater was left intact and the brain surface was covered with 2% agarose dissolved in saline (0.9% NaCl) in order to reduce motion artifacts. A metal head plate was attached to the skull using dental cement (Simplex Rapid, Kemdent, Swinden, UK) to allow the animals to be head-fixed in the recording setup. During the surgical procedure and the subsequent recordings the mice were under anesthesia (intraperitoneal injection of ketamine (initial dosis of 100 mg/kg and maintenance of approximately 60 mg/kg/h; Alfasan, Woerden, the Netherlands) and xylazine (10 mg/kg and maintenance of approximately 3 mg/kg/h; AST Farma, Oudewater, the Netherlands)). To prevent dehydration, the mice receive 1 ml of saline subcutaneously before the start of the surgery and the eyes were protected using eye ointment (Duratears, Alcon, Fort Worth, TX). Body temperature was continuously measured and kept constant at 37 ℃ with a heating pad.

### *Dye injection and* in vivo *two-photon $Ca^{2+}$ imaging*

Multi-cell bolus-loading of the $Ca^{2+}$ indicator dyes Oregon Green BAPTA-1 AM (OGB, Invitrogen, Grand Island, NY) or Cal-520 (0.2 mM; AAT Bioquest, Sunneyvale, CA) was performed according to the method described by Stosiek et al. (2003). Briefly, the dye was dissolved with 10% w/v Pluronic F-127 in DMSO (Invitrogen) and diluted 20x with extracellular solution composed of (in mM) 150 NaCl, 2.5 KCl, 2 $CaCl_2$, 1 $MgCl_2$ and 10 HEPES (pH 7.4, adjusted with NaOH). In a subset of experiments, we also added Alexa 594 dye (20 µM; Invitrogen) to monitor the staining procedure. The dye solution was pressure injected into the molecular layer (50–80 µm below the surface) at 0.35 bar for 5 min. Starting at least 30 min after dye injection, *in vivo* two-photon $Ca^{2+}$ imaging was performed of the molecular layer using a setup consisting of a TriM Scope II system (LaVision BioTec, Bielefeld, Germany) with a Chameleon Ultra Ti:Sapphire laser (Coherent, Santa Clara, CA), a 20x 1.0 NA water immersion objective (Olympus, Tokyo, Japan) and GaAsP photomultiplier detectors (Hamamatsu, Iwata City, Japan). Frames (40 x 200 µm) were acquired at a rate of 24 Hz.

### *Whisker stimulation*

Multiple whisker stimulation was achieved by applying brief air puffs (0.3 bar and 0.1 s) to the mystacial macro-vibrissae. The air flow was directed away from the skin to avoid stimulation of skin or eyes. Single whiskers were stimulated using a piezo linear drive (M-663, Physik Instrumente, Karlsruhe, Germany). The maximal deflection was 4°-6°. It took the stimulator 30 ms to reach this position. At the extreme position, the stimulator was paused for 150 ms before returning to the neutral position. The stimulator was designed to minimize contact with other whiskers. Each stimulation experiment consisted of five sessions in random order. During each block one of the ipsilateral whiskers B2, C1, C2, C3 and D2 was stimulated. In a subset of experiments, we separately tested air puff stimulation to multiple whiskers. Each session consisted of 150 stimuli at 2 Hz.

*Data analysis*

Image analysis was performed offline using algorithms described and validated before (Ozden et al., 2012; De Gruijl et al., 2014) and involved segmentation of responding Purkinje cell dendrites using spatial independent component analysis (ICA) (Fig. 1C). The fluorescent intensities for each Purkinje cell dendrite were averaged per frame and a point-wise high-pass filter was applied that involved dividing each averaged intensity by a baseline that was set to the minimum 8% percentile value within a time window of 500 ms (Ozden et al., 2012). $Ca^{2+}$ transient event times were detected using an approach described earlier (Ozden et al. 2012) (Fig. 1D-E).

Using the obtained event times, we constructed peri-stimulus time histograms (PSTHs) using the inter-frame time (approx. 42 ms) as bin size. Significance of responses was tested using a bootstrap method: we replaced for each cell the list with measured complex spike times with that of a list of fake spike times created by randomly shuffling the measured inter-spike intervals. This procedure was repeated 1000x and the resultant bootstrap-PSTHs were averaged (Fig. 2C). As threshold we used the average + 2 sd. Bootstrap methods were also employed to estimate the expected variation in the fraction of Purkinje cells or cell pairs that exhibit responses with a specific stimulation. Unless specified otherwise, data are represented as mean ± sd.

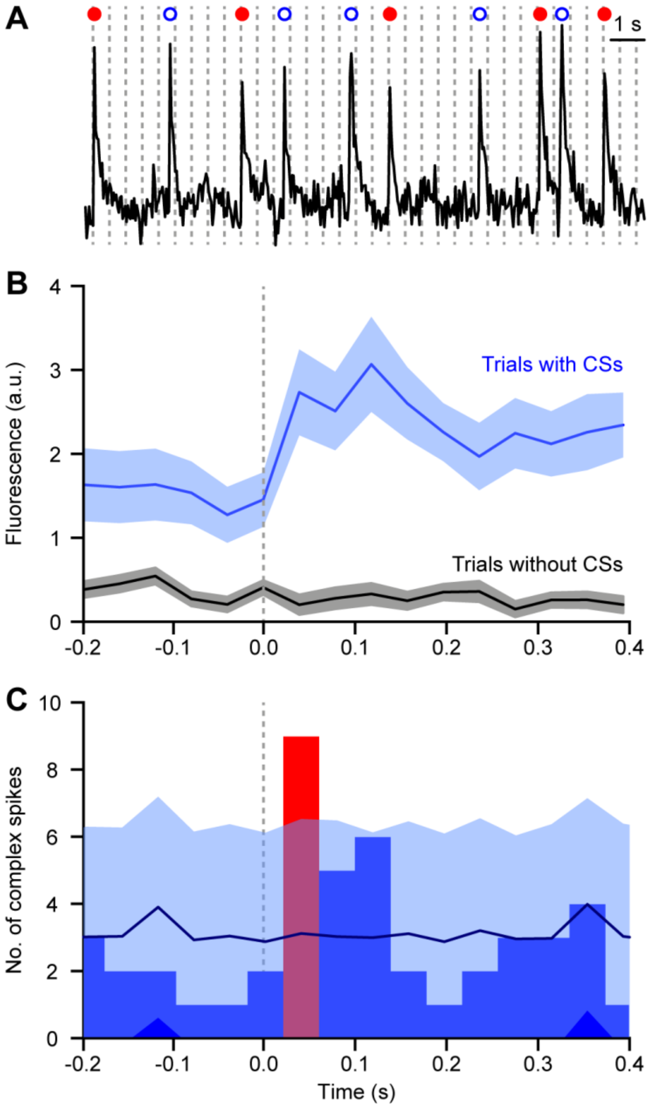

***Figure 2 – Purkinje cells react to single whisker deflection.***
***A** – A representative recording from a Purkinje cell dendrite during 2 Hz stimulation of the ipsilateral C1 whisker. The moments of stimulation are indicated with vertical dashed lines. Ca$^{2+}$ transients following a stimulus are indicated with (red) filled symbols (see also panel C). Spontaneous Ca$^{2+}$ transients are indicated with (blue) open symbols. **B** – Averaged fluorescent traces of all trials (of the same recording as shown in A) with (blue) and without (grey) identified complex spikes showing that increase in fluorescence occurred predominantly after the stimulus. In the trials that did not show a complex spike, no correlation between the stimulus and the fluorescence was observed, indicating that the changes in fluorescence were due to complex spikes rather than to other mechanisms increasing the intracellular Ca$^{2+}$ concentration. Shaded areas indicate SEM. **C** – Peri-stimulus histogram of Ca$^{2+}$ transients of the same Purkinje cell dendrite as shown in A and B. The dark blue line indicates the average of 1000 bootstraps (see Methods) and the shaded area indicates the average ±2 s.d.. A response was considered significant if it exceeded the average + 2 s.d. of the bootstrapped trace (as illustrated with the red bar).*

The distance between two Purkinje cells was defined as the Euclidean distance between the two centers of gravity. To calculate the center of gravity we evaluated the region of interest of each Purkinje cell (as defined using independent component analysis (see above)) and identified the pixel that had the smallest sum of (Euclidean) distances with all pixels of that region of interest.

## Results

### *Cellular resolution imaging of whisker evoked complex spikes*

Facial whisker sensory input reaches the cerebellar cortex both via the climbing fibers and the mossy fibers (Bosman et al., 2011). Here, we investigated the climbing fiber projection areas of individual whiskers in lobules crus 1 and crus 2 of the cerebellar cortex. Climbing fibers evoke complex spikes in Purkinje cells that can be recorded using *in vivo* two-photon $Ca^{2+}$ imaging during single-whisker stimulation in anaesthetized mice. Previous studies have demonstrated that the observed $Ca^{2+}$ transients represent complex spike activity (Ozden et al., 2008; Schultz et al., 2009; Tada et al., 2014).

Following bolus injection of OGB we could record spontaneous complex spike activity with a frequency of 0.47 ± 0.16 Hz (average ± s.d.; $n = 172$). This was lower than previously reported using electrophysiology in the same area with the same type of anesthesia (Bosman et al., 2010), implying an underestimation of the true number of complex spikes. To improve the signal to noise of our recordings we used a novel $Ca^{2+}$ indicator: Cal-520 (Tada et al., 2014), which resulted in data with superior signal-to-noise and consequently a higher spontaneous firing rate (0.70 ± 0.24 Hz; average ± s.d.; $n = 43$; $p < 0.001$ compared to OGB; data not shown), similar to the frequency found previously with electrophysiology (0.6 ± 0.1 Hz; Bosman et al. (2010)).

### *Receptive fields of Purkinje cells*

First, we verified whether we could image Purkinje cell complex spike responses to air puff stimulation of multiple whiskers. In four mice, we trimmed all but five whiskers (B2, C1, C2, C3 and D2) and applied 150 air puffs at a frequency of 2 Hz. In all four experiments we could identify responses in some, but not in all Purkinje cells. In total, we found responses in 14 out of 62 cells measured (23%). Strikingly, responsive and non-responsive Purkinje cells were intermingled (Fig. 3). Thus, whisker-responsive Purkinje cells were not clustered together but dispersed between other Purkinje cells.

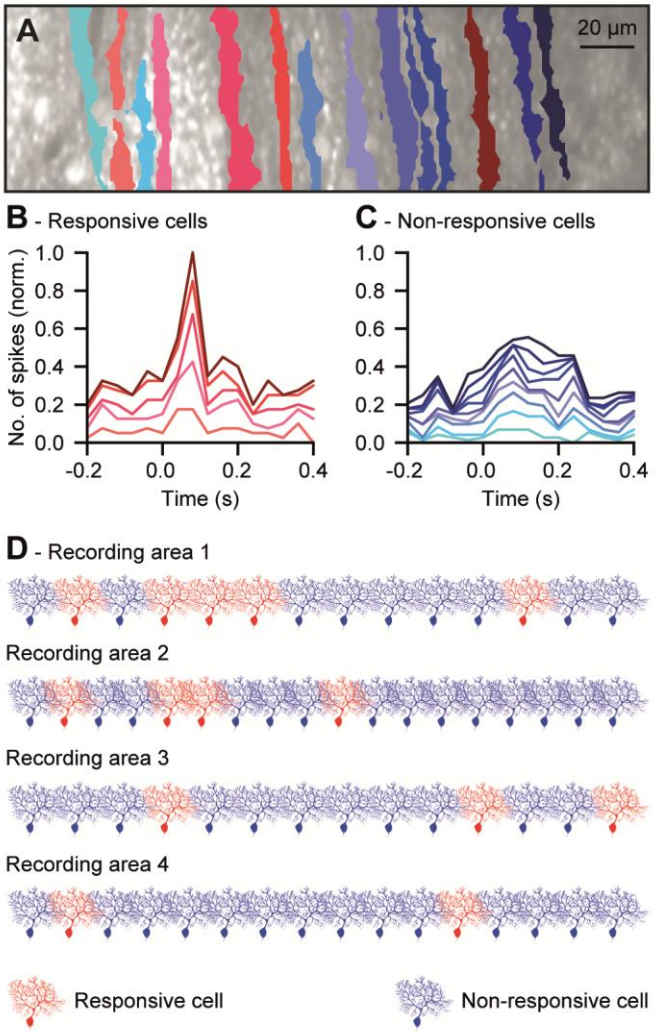

***Figure 3 – Purkinje cell responses to multi-whisker stimulation***
***A** – Field of view of a representative recording showing the masks of identified Purkinje cells. The masks shown in shades of red correspond to Purkinje cells that responded to repeated air puff stimulation of the ipsilateral whiskers. The masks shown in shades of blue are of non-responsive Purkinje cells. Summed line plots of the PSTHs of all responsive (**B**) and non-responsive (**C**) Purkinje cells of the recording shown in panel A. These plots were normalized for the number of Purkinje cells in each category. Identical colors in panels A, B and C refer to the same cell. **D** – Schematic representation of the four experiments involving multiple whisker air puff stimulation showing that responisve (red) and non-responsive (blue) Purkinje cells were largely interspersed.*

Subsequently, we investigated whether whisker-responsive Purkinje cells received input from a single or from multiple whiskers. To this end, we stimulated – in a random order – five anatomically identified whiskers (B2, C1, C2, C3 and D2) using a piezo linear drive (Fig. 4A). Out of 530 Purkinje cells (*n* = 17 mice) 124 responded to at least one of the whiskers (23%). Note that the fraction of responsive cells was identical for air puff stimulation of the five whiskers simultaneously and for piezo-stimulation of the five whiskers consecutively, indicating that our two methods of stimulation yielded comparable results. Of the Purkinje cells that responded to piezo-stimulation, the large majority (110 Purkinje cells (89%)) only showed single whisker responses. The rest responded to two (13 Purkinje cells (10%)) or three whiskers (1 Purkinje cell (1%); Fig. 4B). As a rule, if a Purkinje cell received input from two whiskers these were adjacent whiskers (12 out of 13 Purkinje cells (92%)). In most pairs (*n* = 9 out of 12 (75%)) the whiskers were oriented diagonally (Fig. 4C).

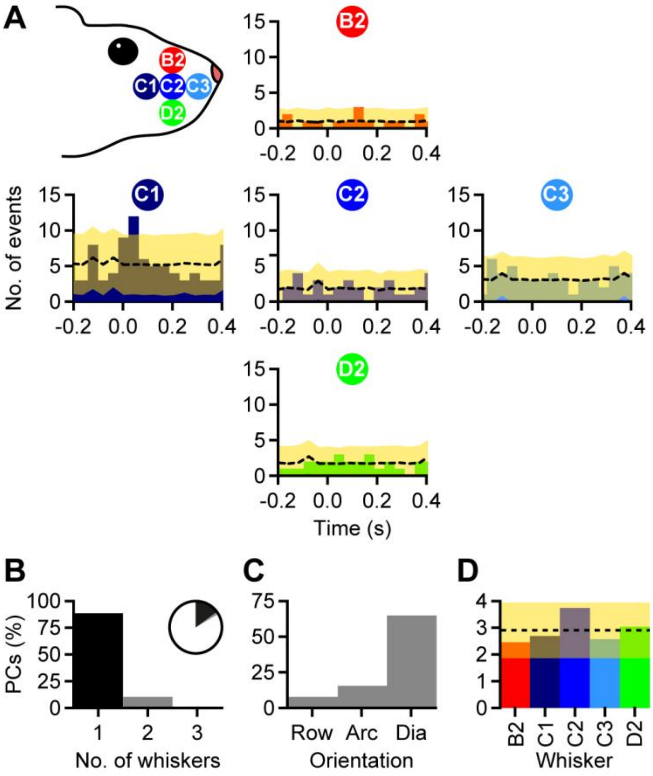

***Figure 4 – Most Purkinje cells respond to a single whisker only***
***A*** *– Representative example showing a Purkinje cell that responded to stimulation of whisker C1 but not to any of the other whiskers tested. The black dashed line indicates the average of the bootstrapped PSTH (see methods). The yellow area depicts the bootstrap average ± 2 sd.* ***B*** *– We could identify responses to single whisker stimulation in 124 out of 831 Purkinje cells (inset). The large majority responded to a single whisker only, but a few Purkinje cells responded also to a second or even a third whisker.* ***C*** *– In case a Purkinje cell responded to two whiskers, these whiskers were usually oriented diagonally on the whisker pad.* ***D*** *– None of the whiskers tested evoked responses in significantly more or less Purkinje cells than the other whiskers. Thus we conclude that all whiskers are represented approximately equally in crus 1 and crus 2.*

Finally, we tested whether all whiskers were represented by equal numbers of Purkinje cells. On average, each individual whisker triggered responses in 2.09 ± 0.52% of all cells recorded. Although whisker C2 activated more Purkinje cells than the other whiskers, this was not significant (*z* = 1.6222; *p* = 0.4474; Fig. 4D). Thus, most Purkinje cells received climbing fiber input from a single whisker only. In the exceptional case that a Purkinje cell received input from multiple whiskers this usually involved adjacent whiskers. All whiskers were represented in roughly equal numbers of Purkinje cells.

The above dataset comprised both recordings with OGB and with Cal-520. Since we established that we could measure more events with Cal-520 than with OGB, we wondered whether the use of two different dyes could have biased our results. Therefore we evaluated whether it was easier to find whisker responsive cells using Cal-520 than OGB. This proved not to be the case: using OGB we found whisker responses in 89 out of 373 Purkinje cells (24%) compared to 35 out of 152 Purkinje cells (23%) with Cal-520 ($p = 0.910$; Fisher's exact test). Since the the use of two indicators with different signal-to-noise ratios led to near identical responsiveness to single whisker stimulation we combined the two datasets.

### *Contribution of non-complex spike responses*

The largest observed $Ca^{2+}$ elevations in the molecular layer are generated by Purkinje cell complex spikes. Nonetheless, other sources can contribute to the measured $Ca^{2+}$ signal. For example changes in $Ca^{2+}$ concentration unassociated with complex spikes have been described in response to corneal air puffs in awake mice (Najafi et al., 2014). In the large majority of the Purkinje cells (506 out of 530 cells; 95.5%) recorded for this study, we did not observe changes in fluorescence to stimulation of single whiskers (Fig. 2B). Small responses were observed in 24 out of 530 Purkinje cells (4.5%). We conclude that in our hands and under ketamine/xylazine anesthesia the contribution of non-complex spike mediated changes in fluorescence following whisker stimulation was neglibile.

### *Spatial arrangement of Purkinje cells responding to single whisker stimulation*

We first mapped whisker receptive fields of Purkinje cells and determined that on average individual Purkinje cells are responsive to only a single whisker. We then wanted to examine the anatomical location of Purkinje cells that encode deflection of the same whiskers. In particular, we wanted to know whether we could identify a "barrel-like pattern" in lobules crus 1 and crus 2 as in many other brain regions. For such a barrel-like pattern, we reasoned, Purkinje cells encoding the same whisker should be closer to each other than to Purkinje cells not encoding that whisker. However, we found that - similar as for the multi-whisker stimulation experiments (Fig. 3) – Purkinje cells responsive to single-whisker stimulation were spatially segregated (Fig. 5A-C). To quantify this observation, we calculated the distance between pairs of Purkinje cells responsive to the same whisker ("homogenous pairs") and between heterogenous pairs of one responsive and one non-responsive Purkinje cell (see Methods). From this analysis we conclude that the distances homogenous and heterogenous cell pairs were indiscernable ($p = 0.955$ unpaired t test; Fig. 5D). Thus we conclude that there are no spatial clusters of Purkinje cells responsive to a single whisker.

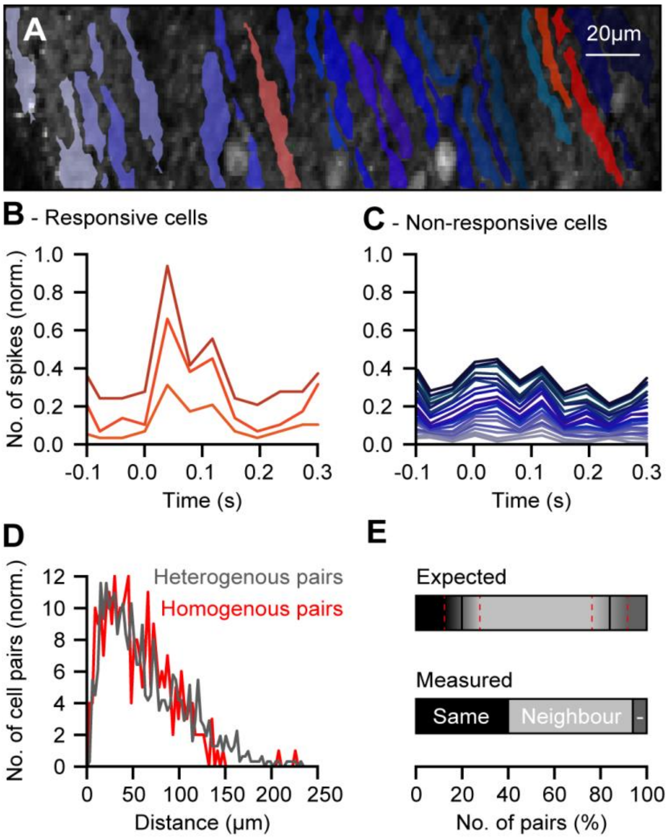

***Figure 5 – Grouping of Purkinje cells***

***responsive to the same whisker***
***A** – Field of view of a representative recording showing the masks of identified Purkinje cells. The masks shown in red colours corresponded to Purkinje cells that responded to repeated piezo stimulation of a single whisker (C1). The masks shown in blue are of non-responsive Purkinje cells. Summed line plots of the PSTHs of all responsive (**B**) and non-responsive (**C**) Purkinje cells of the recording shown in panel A. These plots were normalized for the number of Purkinje cells in each category. **D** – Histograms of the distance between the centers of gravity of pairs of two responsive Purkinje cells ("homogenous pairs", red) and of pairs consisting of one responsive and one non-responsive Purkinje cell ("heterogenous pairs", dark gray). Responsive cells were not clustered together. **E** – When taking only the responsive Purkinje cells into account, it turned out that adjacent Purkinje cells encoded more often than expected for the same whisker or for two neighbouring whiskers. Only a small fraction of neighbouring Purkinje cells encoded non-neighbouring whiskers ("-").*

The absence of a barrel-like somatotopy in crus 1 and crus 2, however, does not necessarily implicate the absence of any ordering principle. To further investigate this issue we now examined only the responsive Purkinje cells. Since we tested in total five different whiskers for each Purkinje cell, the chance that a neighboring, responsive Purkinje cell responds to the same whisker is 20%. This is true under the assumptions that each Purkinje cell responds to a single whisker only (cf. Fig. 4B) and that all Purkinje cells are distributed randomly. However, we found that 40.0% of pairs of adjacent responsive Purkinje cells shared the same whisker identity. This is more than expected ($n$ = 105 pairs; $z$ = 5.224; $p < 0.0001$). As a control, since some Purkinje cells responded to more than one whisker, we repeated this calculation excluding multi-whisker Purkinje cells and found that 41.1% of the pairs to respond to the same whisker ($n$ = 56 pairs; $z$ = 4.030; $p$ = 0.0001). In addition we identified those pairs of neighboring cells in which each cell responded to a different whisker how these whiskers were located on the snout. We found that 92 pairs (87%) responded to adjacent whiskers (taking also diagonal neigbors (e.g. B2 and C1) into account) and only 14 pairs (13%) responded to non-neighboring whiskers. Based on the geometry of the tested whiskers, we would have expected 80% of the pairs to respond to neighboring whiskers. Although we observed more pairs of Purkinje cells to respond to adjacent whiskers than expected, this was not quite significant ($n$ = 106 pairs; $z$ = 1.724; $p$ = 0.085). Thus, although Purkinje cells do not cluster anatomically based on their sensory input, we observed that – within the group of whisker-responsive Purkinje cells – adjacent cells have an increased chance of sharing the input from the same whisker or from neighboring whiskers.

### *Whisker responses and Purkinje cell synchrony*

Complex spike activity of adjacent Purkinje cells can be synchronized. Previous studies showed that such synchrony is mainly organized in parasagitally organized microzones (Lang, 2001; Sugihara et al., 2007). Sensory stimulation had only a minor impact on spatial extent of the synchronicity of Purkinje cells (Mukamel et al., 2009; Ozden et al., 2009). Microzones with increased within-band synchrony have been proposed to act as functional ensembles (Ozden et al., 2009; Schultz et al., 2009; Ozden et al., 2012). In order to determine if the Purkinje cells that respond to a single whisker could be identified as a functional ensemble based on their co-activation. To this end, we recorded from many Purkinje cells simultaneously and cross-correlated their complex spike event patterns (Fig. 6A). We found that Purkinje cell co-activation was enhanced during whisker stimulation (Fig. 6B-E). However, when responsive and non-responsive Purkinje cells were compared we could not find a difference in the degree of co-activation between these groups ($n$ = 34; $p$= 0.313; paired t test). We therefore conclude that Purkinje cells responsive to a single whisker do not assemble into microbands but instead form looser larger scale functional ensembles.

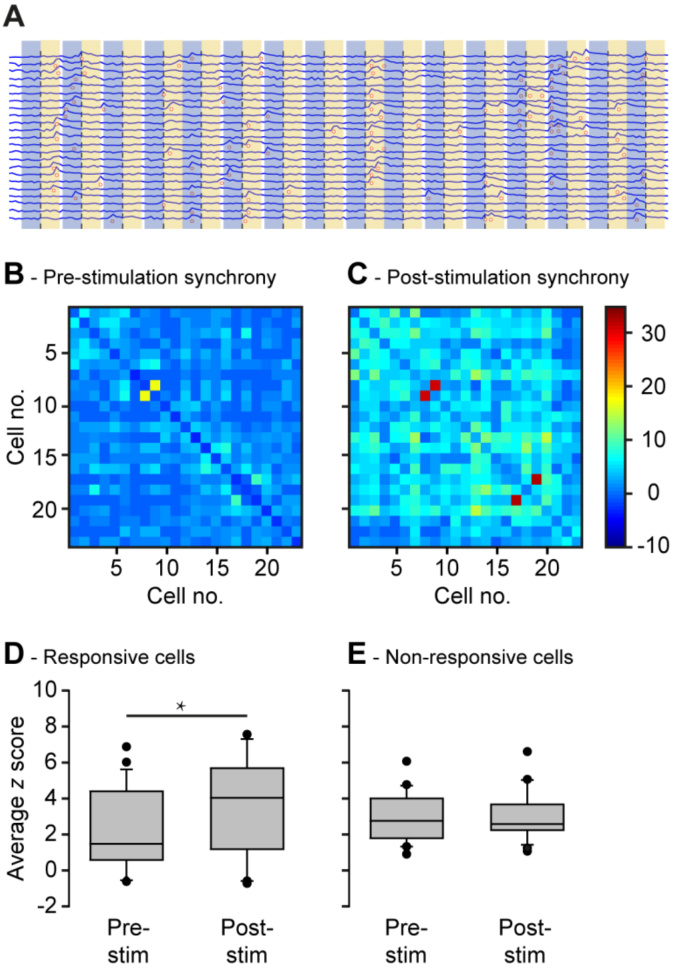

***Figure 6 – Synchrony is not linked to groups of Purkinje cells encoding the same whisker***
***A** – Fluorescent traces of simultaneously recorded Purkinje cells. Dashed vertical lines indicate the onsets of (D2) whisker stimulation. The yellow and blue areas indicate the response and the pre-response windows, respectively. Heat plots depicting the z-score of synchronous complex spikes between cell pairs during the pre stimulation intervals ("blue areas" in A; **B**) and during the post-stimulation intervals ("yellow areas" in A; **C**). The diference between average z scores of pre and post-stimulation intervals among Purkinje cell pairs of responsive Purkinje cells ("homogenous pairs") was statistically significant (**D**), but not for heterogeneous pairs consisting of one responsive and one non-responsive Purkinje cell (**E**) .*

## *Discussion*

### *Organization of the cerebellar cortex*

The two main afferent pathways of Purkinje cells in the cerebellar cortex have a strikingly different anatomy. Climbing fiber terminals in the cerebellar cortex are organized in parasagittally oriented modules. Each of these modules is innervated by climbing fibers originating from a specific part of the inferior olive and the Purkinje cells in each modules, in turn, project to a well-defined part of the cerebellar nuclei (Groenewegen et al., 1979; Glickstein et al., 2011). The parallel fibers are oriented perpendicular to theses parasagittal modules. Functionally, the Purkinje cells seem to adhere predominantly to the parasagittal, rather than the transversal, orientation of the cerebellar modules (Zhou et al., 2014; Tsutsumi et al., 2015).

*Receptive fields of Purkinje cells*

Despite the existence of both parasagittal and transversal zones, somatosensory input to the cerebellum occurs in a patch-like fashion. This has been demonstrated extensively for the granular layer (Shambes et al., 1978; Kassel et al., 1984; Apps and Hawkes, 2009) but also for the Purkinje cells (Bower and Woolston, 1983). In the latter study, the focus was on the simple spike responses and thus more on the mossy fiber/parallel fiber pathway than on the climbing fiber pathway.

Climbing fibers are also organized topographically. This has been studied most extensively for the cutaneous projections from the cat forelimb. Around 30 receptive fields could be identified on the forelimb, typically bordered by joints, each of which had a small, microzonal sagittal projection area in zone C3 of the cerebellar cortex (Ekerot et al., 1991). Although the mossy fiber projections generally adhered to the microzones defined by the climbing fiber projections (Garwicz et al., 1998), the receptive fields of individual Purkinje cells differed for the complex spike and the simple spike responses (Ekerot and Jörntell, 2001). The preponderance of the climbing fiber projection in patterning the mossy fiber projection is in line with a developmental study in which the climbing fibers were rerouted and the mossy fiber activity followed the new wiring scheme (Badura et al., 2013).

However, the inferior olive is not exclusively a receiver of low level sensory input. Rather, input is multimodal, from broad innervations of Purkinje cells and diencephalic sources. Moreover, input to the olive is combined with ongoing network oscillations. We have solely mapped responses to sensory inputs, and find considerable variability in cellular responses. The variability (both in latency and probability of responses) indicates that the olivary nucleus is not primarily concerned with the reliable transmission of low level sensory stimulus, but rather, that it contextualizes incoming information, spike emmission being a function of its state (possibly oscilatory). In this sense, though we find that there are receptive fields for single whiskers, it is crucial to discover what are the other streams that converge onto the inferior olive nuclei, to know what is the integration performed in the inferior olive, and how that signal relates to the output of the cerebellum.

*Somatotopy of the whiskers*

In our study we examined the climbing fiber projections of individual whiskers – and thus of very small, but highly reproducible receptive fields. In combining single whisker-stimulation with *in vivo* two-photon $Ca^{2+}$ imaging we could obtain a very high spatial resolution, both on the level of the periphery and of the Purkinje cells. The topography of whisker input has been extensively studied in many brain pathways and regions. The best known example is the lemniscal pathway connecting single-whisker responsive areas in the principal sensory trigeminal nuclues, the ventroposterior medial nucleus of the thalamus and the input layer of the primary somatosensory cortex (Woolsey et al., 1975; Yu et al., 2006; Bosman et al., 2011; Feldmeyer, 2012). Many other pathways in the whisker system, however, are aimed at integrating rather than seperating data streams (Bosman et al., 2011). The latter has been elegantly shown using optical imaging of neuronal activity in the cerebral cortex: stimulation of an individual whisker initially leads to activity of a small region in the somatosensory cortex, but the activity spreads rapidly over a much larger area, seemingly undiscernible from the response area evoked by stimulating a different whisker (Ferezou et al., 2007).

In a previous study, we examined the receptive fields of Purkinje cells using *in vivo* electrophysiology (Bosman et al., 2010). We found that the receptive fields of complex spikes were generally composed of a single whisker while those of simple spikes were usually multi-whisker. Here we confirm that the complex spike reponse to whisker stimulation is indeed most often evoked by one whisker only.

In previous studies, no evidence for a clear somatotopy in crus 1 and crus 2 could be found (Axelrad and Crepel, 1977; Bosman et al., 2010). This could, however, also be attributed to the sparse sampling of Purkinje cells using electrophysiology. With a much improved spatial resolution we could – again – not find a somatotopy like in the primary somatosensory cortex. However, we did find a certain patterning in the organization of whisker projections to Purkinje cells. Interestingly, we found that whisker-responsive Purkinje cells were often interspersed with other Purkinje cells. Taking only the whisker-responsive Purkinje cells into account, there was a clear tendency of neighbouring Purkinje cells to respond either to the same whisker or to two adjacent whiskers. In conclusion, whisker-responsive Purkinje cells were located based on their connectivity to individual whiskers – grouping functionally similar cells together – but the overall organization of the Purkinje cells did resemble a fractured somatotopy rather than an organized somatotopy.

### *Functional implications*

Observations on the implication of the cerebellum in sensory and cognitive task challenge the classical view of the cerebellum as a dedicated motor region. Sensory input from the whiskers reaches the cerebellar cortex both via the mossy fibers and via the climbing fibers (Loewenstein et al., 2005; Bosman et al., 2010; Chu et al., 2011; Popa et al., 2013; Proville et al., 2014). Our current data confirm earlier reports that the projection areas for individual whiskers are irregular and seem to be tailored for data integration (Axelrad and Crepel, 1977; Bosman et al., 2010). As the same part of the cerebellar cortex is involved in the control of whisker movement (Esakov and Pronichev, 2001; Lang et al., 2006; Proville et al., 2014), a role for of the cerebellum in sensorimotor integration within the whisker system is likely. Recently, we showed that impaired cerebellar potentiation comprimised learning a whisker-based discrimination task (Rahmati et al., 2014). Taken together, our data support the notion of the cerebellum being involved both in primary sensory and motor function as well as in integrative and even cognitive functions, especially in complex and time-critical situations.

## Acknowledgements

We thank the Dutch Organisation for Medical Sciences (ZonMw), NWO (ALW and MaGW), Neuro-Basic (FES) and ERC-Advanced and ERC-POC for their financial support to C.I.D.Z. In addition, we wish to thank Olesya Shevchouk and Wouter Teunissen for help with setting up the two-photon microscope, Jochen Spanke and Pascal Warnaar for help with programming and Dr. Tom Ruigrok for valuable discussions.

## *References*

*Apps R, Hawkes R (2009) Cerebellar cortical organization: a one-map hypothesis. Nature reviews Neuroscience 10:670-681.*

*Axelrad H, Crepel F (1977) Représentation sélective des vibrisses mystaciales au niveau des cellules de Purkinje du cervelet par la voie des fibres grimpantes chez le rat. C R Acad Sci Hebd Seances Acad Sci D 284:1321-1324.*

*Badura A, Schonewille M, Voges K, Galliano E, Renier N, Gao Z, Witter L, Hoebeek FE, Chedotal A, De Zeeuw CI (2013) Climbing fiber input shapes reciprocity of Purkinje cell firing. Neuron 78:700-713.*

*Bosman LWJ, Koekkoek SKE, Shapiro J, Rijken BFM, Zandstra F, van der Ende B, Owens CB, Potters JW, de Gruijl JR, Ruigrok TJH, De Zeeuw CI (2010) Encoding of whisker input by cerebellar Purkinje cells. The Journal of physiology 588:3757-3783.*

*Bosman LWJ, Houweling AR, Owens CB, Tanke N, Shevchouk OT, Rahmati N, Teunissen WHT, Ju C, Gong W, Koekkoek SKE, De Zeeuw CI (2011) Anatomical pathways involved in generating and sensing rhythmic whisker movements. Front Integr Neurosci 5:53.*

*Bower JM, Woolston DC (1983) Congruence of spatial organization of tactile projections to granule cell and Purkinje cell layers of cerebellar hemispheres of the albino rat: vertical organization of cerebellar cortex. J Neurophysiol 49:745-766.*

*Brecht M (2007) Barrel cortex and whisker-mediated behaviors. Curr Opin Neurobiol 17:408-416.*

*Chu CP, Bing YH, Liu QR, Qiu DL (2011) Synaptic responses evoked by tactile stimuli in Purkinje cells in mouse cerebellar cortex crus II in vivo. PloS one 6:e22752.*

*De Gruijl JR, Hoogland TM, De Zeeuw CI (2014) Behavioral correlates of complex spike synchrony in cerebellar microzones. J Neurosci 34:8937-8944.*

*De Gruijl JR, Bosman LWJ, De Zeeuw CI, De Jeu MTG (2013) Inferior olive: All ins and outs. In: Handbook of the Cerebellum and Cerebellar Disorders (Manto M, Schmahmann JD, Rossi F, Gruol DL, Koibuchi N, eds), pp 1013-1058. Dordrecht: Springer Netherlands.*

*De Zeeuw CI, Hoebeek FE, Bosman LWJ, Schonewille M, Witter L, Koekkoek SK (2011) Spatiotemporal firing patterns in the cerebellum. Nature reviews Neuroscience 12:327-344.*

*Ekerot CF, Jörntell H (2001) Parallel fibre receptive fields of Purkinje cells and interneurons are climbing fibre-specific. The European journal of neuroscience 13:1303-1310.*

*Ekerot CF, Garwicz M, Schouenborg J (1991) Topography and nociceptive receptive fields of climbing fibres projecting to the cerebellar anterior lobe in the cat. The Journal of physiology 441:257-274.*

*Esakov SA, Pronichev IV (2001) Motor representations of facial muscles and vibrissae in cerebellar cortex of the white mouse Mus musculus. J Evol Biochem Physiol 37:642-647.*

*Feldmeyer D (2012) Excitatory neuronal connectivity in the barrel cortex. Frontiers in neuroanatomy 6:24.*

*Ferezou I, Haiss F, Gentet LJ, Aronoff R, Weber B, Petersen CCH (2007) Spatiotemporal dynamics of cortical sensorimotor integration in behaving mice. Neuron 56:907-923.*

*Garwicz M, Jörntell H, Ekerot CF (1998) Cutaneous receptive fields and topography of mossy fibres and climbing fibres projecting to cat cerebellar C3 zone. The Journal of physiology 512:277-293.*

*Glickstein M, Sultan F, Voogd J (2011) Functional localization in the cerebellum. Cortex 47:59-80.*

*Groenewegen HJ, Voogd J, Freedman SL (1979) The parasagittal zonation within the olivocerebellar projection. II. Climbing fiber distribution in the intermediate and hemispheric parts of cat cerebellum. The Journal of comparative neurology 183:551-601.*

*Hartmann MJZ (2009) Active touch, exploratory movements, and sensory prediction. Integr*

*Comp Biol 49:681-690.*

*Hayashi H (1980) Distributions of vibrissae afferent fiber collaterals in the trigeminal nuclei as revealed by intra-axonal injection of horseradish peroxidase. Brain Res 183:442-446.*

*Huerta MF, Frankfurter A, Harting JK (1983) Studies of the principal sensory and spinal trigeminal nuclei of the rat: projections to the superior colliculus, inferior olive, and cerebellum. The Journal of comparative neurology 220:147-167.*

*Kassel J, Shambes GM, Welker W (1984) Fractured cutaneous projections to the granule cell layer of the posterior cerebellar hemisphere of the domestic cat. The Journal of comparative neurology 225:458-468.*

*Lang EJ (2001) Organization of olivocerebellar activity in the absence of excitatory glutamatergic input. J Neurosci 21:1663-1675.*

*Lang EJ, Sugihara I, Llinás R (2006) Olivocerebellar modulation of motor cortex ability to generate vibrissal movements in rat. The Journal of physiology 571:101-120.*

*Loewenstein Y, Mahon S, Chadderton P, Kitamura K, Sompolinsky H, Yarom Y, Häusser M (2005) Bistability of cerebellar Purkinje cells modulated by sensory stimulation. Nature neuroscience 8:202-211.*

*Molinari HH, Schultze KE, Strominger NL (1996) Gracile, cuneate, and spinal trigeminal projections to inferior olive in rat and monkey. The Journal of comparative neurology 375:467-480.*

*Mukamel EA, Nimmerjahn A, Schnitzer MJ (2009) Automated analysis of cellular signals from large-scale calcium imaging data. Neuron 63:747-760.*

*Najafi F, Giovannucci A, Wang SSH, Medina JF (2014) Coding of stimulus strength via analog calcium signals in Purkinje cell dendrites of awake mice. eLife 3:e03663.*

*O'Connor DH, Hires SH, Guo ZV, Li N, Yu J, Sun QQ, Huber D, Svoboda K (2013) Neural coding during active somatosensation revealed using illusory touch. Nature neuroscience 16:958-965.*

*Ozden I, Lee HM, Sullivan MR, Wang SSH (2008) Identification and clustering of event patterns from in vivo multiphoton optical recordings of neuronal ensembles. J Neurophysiol 100:495-503.*

*Ozden I, Sullivan MR, Lee HM, Wang SSH (2009) Reliable coding emerges from coactivation of climbing fibers in microbands of cerebellar Purkinje neurons. J Neurosci 29:10463-10473.*

*Ozden I, Dombeck DA, Hoogland TM, Tank DW, Wang SS (2012) Widespread state-dependent shifts in cerebellar activity in locomoting mice. PloS one 7:e42650.*

*Popa D, Spolidoro M, Proville RD, Guyon N, Belliveau L, Léna C (2013) Functional role of the cerebellum in gamma-band synchronization of the sensory and motor cortices. J Neurosci 33:6552-6556.*

*Proville RD, Spolidoro M, Guyon N, Dugué GP, Selimi F, Isope P, Popa D, Léna C (2014) Cerebellum involvement in cortical sensorimotor circuits for the control of voluntary movements. Nature neuroscience.*

*Rahmati N, Owens CB, Bosman LWJ, Spanke JK, Lindeman S, Gong W, Potters JW, Romano V, Voges K, Moscato L, Koekkoek SKE, Negrello M, De Zeeuw CI (2014) Cerebellar potentiation and learning a whisker-based object localization task with a time response window. J Neurosci 34:1949-1962.*

*Schultz SR, Kitamura K, Post-Uiterweer A, Krupic J, Häusser M (2009) Spatial pattern coding of sensory information by climbing fiber-evoked calcium signals in networks of neighboring cerebellar Purkinje cells. J Neurosci 29:8005-8015.*

*Shambes GM, Gibson JM, Welker W (1978) Fractured somatotopy in granule cell tactile areas of rat cerebellar hemispheres revealed by micromapping. Brain, behavior and evolution 15:94-140.*

*Sharp FR, Gonzalez MF (1985) Multiple vibrissae sensory regions in rat cerebellum: a ($^{14}C$)*

*2-deoxyglucose study. The Journal of comparative neurology 234:489-500.*

*Sofroniew NJ, Cohen JD, Lee AK, Svoboda K (2014) Natural whisker-guided behavior by head-fixed mice in tactile virtual reality. J Neurosci 34:9537-9550.*

*Stosiek C, Garaschuk O, Holthoff K, Konnerth A (2003) In vivo two-photon calcium imaging of neuronal networks. Proceedings of the National Academy of Sciences of the United States of America 100:7319-7324.*

*Sugihara I, Marshall SP, Lang EJ (2007) Relationship of complex spike synchrony bands and climbing fiber projection determined by reference to aldolase C compartments in crus IIa of the rat cerebellar cortex. The Journal of comparative neurology 501:13-29.*

*Swenson RS, Castro AJ (1983) The afferent connections of the inferior olivary complex in rats. An anterograde study using autoradiographic and axonal degeneration techniques. Neuroscience 8:259-275.*

*Tada M, Takeuchi A, Hashizume M, Kitamura K, Kano M (2014) A highly sensitive fluorescent indicator dye for calcium imaging of neural activity in vitro and in vivo. The European journal of neuroscience 39:1720-1728.*

*Tsutsumi S, Yamazaki M, Miyazaki T, Watanabe M, Sakimura K, Kano M, Kitamura K (2015) Structure-Function Relationships between Aldolase C/Zebrin II Expression and Complex Spike Synchrony in the Cerebellum. J Neurosci 35:843-852.*

*Vinueza Veloz MF, Zhou K, Bosman LWJ, Potters JW, Negrello M, Seepers RM, Strydis C, Koekkoek SKE, De Zeeuw CI (2014) Cerebellar control of gait and interlimb coordination. Brain structure & function:612-623.*

*Voogd J, Glickstein M (1998) The anatomy of the cerebellum. Trends Neurosci 21:370-375.*

*Voogd J, Shinoda Y, Ruigrok TJH, Sugihara I (2013) Cerebellar nuclei and the inferior olivary nuclei: Organization and connections. In: Handbook of the Cerebellum and Cerebellar Disorders (Manto M, Schmahmann JD, Rossi F, Gruol DL, Koibuchi N, eds), pp 377-436. Dordrecht: Springer Netherlands.*

*Welker C (1971) Microelectrode delineation of fine grain somatotopic organization of (SmI) cerebral neocortex in albino rat. Brain Res 26:259-275.*

*Woolsey TA, Welker C, Schwartz RH (1975) Comparative anatomical studies of the SmI face cortex with special reference to the occurrence of "barrels" in layer IV. The Journal of comparative neurology 164:79-94.*

*Yatim N, Billig I, Compoint C, Buisseret P, Buisseret-Delmas C (1996) Trigeminocerebellar and trigemino-olivary projections in rats. Neuroscience research 25:267-283.*

*Yu C, Derdikman D, Haidarliu S, Ahissar E (2006) Parallel thalamic pathways for whisking and touch signals in the rat. PLoS Biol 4:e124.*

*Zhou H, Lin Z, Voges K, Ju C, Gao Z, Bosman LWJ, Ruigrok TJH, Hoebeek FE, De Zeeuw CI, Schonewille M (2014) Cerebellar modules operate at different frequencies. eLife 3:e02536.*

# Chapter 6

# General discussion

## 6.1

In this thesis, we investigated spatial heterogeneities in Purkinje cell functioning. We found that, contrary to earlier believe, the activity patterns of Purkinje cells are not the same throughout the cerebellar cortex. In contrast, Purkinje cells operate at different frequencies, depending on the expression pattern of zebrin. We also found heterogeneity in the firing pattern of individual Purkinje cells in the form of the occurrence of long pauses interrupting the sustained high firing rate of simple spikes. These pauses are potentially important instrumental properties of Purkinje cells, but we show that they could also be a sign of unphysiological perturbation. Then we zoomed in on the largely zebrin-positive area, crus 1, to study how individual Purkinje cells respond to multimodal peripheral stimulation. We applied gentle tactile input to various facial regions as well as auditory and visual stimuli. We found that climbing fiber-mediated responses in Purkinje cells were only weakly grouped based on the nature of the stimulus. Such a weak grouping of Purkinje cells according to their receptive field was also present when we used single whisker displacement as a stimulus. Whereas we found a considerable amount of overlap between receptive fields for larger stimulation areas, most Purkinje cells did not respond to more than one whisker. Taken together, in this thesis we challenge the notion of the cerebellum as a spatially homogeneous structure. Instead, we describe functional domains at different levels, some of these having clear borders while others are more dispersed. There seems to be a balance between spatial ordering, promoting efficient processing of separate data streams, and spatial mixture, promoting the integration of data streams.

## 6.2 *Homogeneity and heterogeneity in the cerebellum.*

A striking feature of the cerebellum is the beautifully regular and simple cellular organization, which is repeated across its cortex (Ito 1984; Ramnani 2006). The repeated regularity has long been considered as a sign that the cerebellar cortex is a homogenous structure that performs a particular type of information processing on different types of data streams. But within this homogeneous structure a number of longitudinally organized modules can be recognized based on the cortico-nuclear and olivo-cerebellar connections (De Zeeuw and Ten Brinke 2015). These modules could potentially act as different functional entities. The progress in mapping the functional connectivity of the cerebellum has provided evidence that the cerebellum is functionally heterogeneous as each cerebellar module has distinct sources (Witter and De Zeeuw 2015; De Zeeuw and Ten Brinke, 2015).

Zebrin bands form large modules according to which we can divide Purkinje cells into two categories: zebrin-positive and zebrin-negative cells. In chapter 2 we show that functional heterogeneity in Purkinje cell activity is not exclusively based on different input sources. Instead, the Purkinje cells with different zebrin-identities have intrinsically different firing properties. This finding splits the “homogeneous cerebellum” into two distinct cerebellar compartments. But why do we need two cerebellar compartments with different firing rates? While the ultimate answer to this question is not known, a possible explanation could lie in the observation that Purkinje cells in different zebrin-bands could favor the opposite form of synaptic plasticity (De Zeeuw and Ten Brinke, 2015). Zebrin-positive cells may be more prone to express long-term depression and zebrin-negative cells may be more prone to express long term potentiation (Wadiche and Jahr 2005; Wang et al. 2011). This would imply that the zebrin-identity of a specific module has significant implications for motor behavior and learning.

The functional heterogeneity of the cerebellar cortex is in line with its afferent connections, both in terms of ponto-cerebellar mossy fibers and olivo-cerebellar climbing fibers (Witter and De Zeeuw 2015). There are strong projections from various parts of the cerebral cortex to the pontine nuclei. In human, the cortico-pontine connections are 20 times stronger than the cortico–spinal projections (Tomasch 1969). Both cortico–spinal and cortico–bulbar fibers give off collaterals to pontine cells (Ugolini and Kuypers 1986). The inputs to the inferior olive come from various nuclei in the mesodiencephalic junction and the spinal cord (Gruijl 2013). Mossy fibers as well as climbing fibers convey somatosensory input that is projected to the cerebellar cortex in the form of a fractured somatotopy (Robertson 1984; Bosman et al. 2010; Witter and De Zeeuw 2015). For the climbing fiber-mediated inputs recent studies have shown that a band of adjacent cells, which could be called a microband, could act as a functional unit that responds to a coarse of sensory stimulations (Ozden et al. 2009). We describe in chapters 4 and 5 interspersed maps of Purkinje cells that respond to specific types of subtle stimulation. Clear microbands, in terms of synchronously activated neighboring Purkinje cells, were not observed, however. This suggests that cerebellar heterogeneity can even be found within regions as small as microbands.

### 6.3 *Reliability of activity at surface of cerebellar cortex*

Purkinje cells show a sustained, high firing rate of simple spikes, but pauses in their firing pattern have been noticed for decades with electrophysiological recordings in vitro (Llinás and Sugimori 1980) as demonstrated by in vivo studies showing that the regular simple spike activity was separated by intermittent periods of quiescence (Loewenstein et al. 2005; Yartsev et al. 2009). Indeed, the parallel fibers, climbing fibers, molecular layer interneurons and Bergman glia cells were all reported to modulate the two states of purkinje cell membrane potential: upstates with high firing rate and downstates with pauses that can last for seconds (De Schutter and Steuber 2009; Shin et al. 2007; Steuber et al. 2007; F. Wang et al. 2012). There is also evidence that whisker stimulation induced complex spikes can mediate a switch between these two states in vivo (Loewenstein et al. 2005). The functional relevance of the downstates in the awake brain has been questioned, however, since the downstate with long pauses, was subsequently reported to be promoted by the use of anesthetics (Schonewille et al. 2006). In chapter 3 we describe that particularly long pauses are typically found close to the brain surface near the craniotomy. The surgical damage and the low local temperature are contributors to this phenomenon. In this respect, it is of interest that in zebrafish, which live at relatively low temperatures, bistability occurs more frequently (Sengupta and Thirumalai 2015). Thus, we provide evidence that unfavorable experimental conditions in mammals can promote the occurrence of exceptionally long pauses in simple spike firing. These long pauses were, at rest, almost never found in the deeper, seemingly healthy tissue.

In vivo $Ca^{2+}$ imaging has a penetration depth that is limited to the upper cell layers of the cerebellar cortex. A following question from this result could be: what kind of influence the craniotomy and temperature could have on in vivo two-photon experiments? Are the data we record from the surface layer cells still reliable? Several aspects should be considered in this respect: First, during our two-photon experiments the brain surface was protected better than during electrophysiological experiments in that the dura mater was preserved both during surgery and imaging, limiting surgically inflicted brain damage. Second, the craniotomy during our two-photon experiments entailed agar coverage and a glass slide, which not only provided protection but also prevented evaporation and thereby a decrease of local brain temperature. Third, the infrared laser pumps energy into the tissue and could thus prevent excessive cooling. This implies that the major risk factors for generating pathological Purkinje cell activity in superficial layers during the electrophysiological recordings were largely absent during the imaging experiment. Furthermore, with two-photon $Ca^{2+}$ imaging we focused on the climbing fiber-responses that are dictated by activity of the inferior olive that is located on the ventral side of the brainstem, thus far away from the craniotomy at the dorsal surface. Thus, although we cannot exclude that our experimental conditions affected normal brain function, we eliminated the most important risk factors.

### 6.4 *What is the size of sensory maps in the cerebellum?*

Sensory maps can be made at different levels of detail. The climbing fiber-mediated responses depend on the size of the stimulated area, as single whiskers evoked responses in less Purkinje cells (Chapter 5) than whisker pad stimulation (Chapter 4). In addition, climbing fiber-mediated responses depend on stimulus strength (Bosman et al., 2010). Thus, to avoid indirect stimulation of surrounding tissue, we choose to use precise and gentle stimuli of the whisker system, which allows very precise and reproducible types of stimulation.

We coupled these precise stimulations with recordings at the single cell level. Since adult Purkinje cells are normally innervated by a single climbing fiber, the single cell level is the lowest level, at which one can study the extent of climbing fiber-mediated sensory maps. We show here that our stimuli induced responses in nearby, but dispersed Purkinje cells. Thus, somatotopic representation in crus 1 is not according to a somatotopic arrangement nor does it strictly adhere to microbands, defined as groups of synchronized Purkinje cells, as has been suggested before (Ozden et al. 2009). Instead, we show that the input organization of Purkinje cells is aimed at the convergence of different input streams. This was particularly striking when comparing the Purkinje cells responding to tactile and to visual stimulation: they practically coincide.

But why do we need a finely grained map? More and more evidence shows that the cerebellum conveys and processes information not only by rate coding but also by spatio-temporal coding (De Zeeuw et al. 2011). In other words, we are dealing with a vast neuronal network that acts as a whole to perform its function. A detailed sensory map, as provoked by subtle stimulation, could involve relatively many small-sized networks, together allowing the creation of an internal world permitting predictions and state estimates (Wolpert, Miall, and Kawato 1998). Hence, taking advantage of two-photon imaging, the current work empowered us to cover a relatively large portion of this network and thereby to understand better how the network may operate as a whole.

### 6.5 *Sensorimotor integration at lower and higher levels*

Most of the functional knowledge we know about the brain originally derived from clinical observations and lesion studies of animals. According to these studies, the cerebellum can considered as the region that controls motor movement coordination, balance, equilibrium and muscle tone (Sherrington, 1916; Ito, 1984). Cerebellar focal damage commonly results in motor symptoms: muscle weakness (hypotonia), ataxia and tremor (Thach and Bastian 2004). Other studies, particularly propelled by Bower and colleagues claim that the cerebellum is mostly involved in sensory integration (Bower 1997). Finally, there is also evidence that the cerebellum is involved in control of cognition and emotion (Strick, Dum, and Fiez 2009; de

Zeeuw et al. 2012; Schraa-Tam et al. 2012). Indeed, patients with cerebellar lesions have been diagnosed with the so-called cerebellar cognitive affective syndrome, a condition that can be described by deficits in language, executive function and impaired emotions (Schmahmann 2010). However, the distinction between sensorimotor functions and cognitive functions may not be as clear as the words themselves suggest. After all, in the end most, if not all, cognitive activity ultimately serves to prepare for movements, whether in the near or far future. Moreover, this preparation always requires processing of sensory information. Thus, when merging these ideas together, this makes the cerebellum an ideal candidate for sensorimotor integration at both lower and higher levels.

### 6.6 *Future directions*

This dissertation provides several new insights in the physiology of cerebellar Purkinje cells and the spatial organization of sensory input to the cerebellar cortex. The sensory information input is, however, only part of the whole story of cerebellar function. The long-term goal of our study is to know how sensory information can modulate cerebellar output and hence coordinate the motor behavior of the animal. Though quite some models have been proposed to explain the mechanisms behind cerebellar function, it is still difficult to validate those models without solid answers to some basic questions. For instance, more detailed knowledge of the cerebellar connectome is still required. Our findings presented here indicate that a high-resolution map of cerebellar function should be met with high-resolution tracing studies of its afferents. We should find out to what extent the precise convergence of sensory relays is mediated by specific afferents at the anatomical level and/or whether it is embedded in the physiological strength of specific synaptic connections. Along the same line, we should complement the sensory recording maps following natural stimulation as provided in the current thesis with behavioral motor mappings following optogenetic stimulation of the smallest possible unit in the cerebellar cortex, i.e. at the single cell level. Thus, before we can fully grasp the essentials of the cerebellar connectome, we have to also investigate the pure motor side of the cerebellum. As such, optogenetic stimulation of crus 1 Purkinje cells together with registration of animal behavior could be a powerful tool to explore the correlation between the local activities within the cerebellum and the resultant behavioral output. Alternatively, one might train the animals for repetitive stereotyped movements, like licking or jumping. Using stereotyped movements as a behavioral read out, we might also be better able to observe putative correlations of neuronal activity and manipulations with optogenetics. Finally, non-invasive techniques like fMRI are also very powerful tools to map the functional connections within the network of the whole cerebellum or even brain. Though it is an indirect way to image brain activity and it has relatively poor resolution, still the power of monitoring the whole brain at the same time makes it a valuable method to explore the main functional connections (eg Timmann study during eyeblink conditioning). Hence, it could provide us with the big picture of how the cerebellum interacts with other regions. This also pertains to the questions as to whether the cerebellum is more sensory than motor, and/or whether the cerebellum is just as cognitive as sensorimotor. Thus, functional mapping at both the micro and macro level is required to help us understand how the brain works. The current thesis does not provide a full picture of all the mapping studies required to unravel cerebellar function, but certainly it provides a myriad of principles that have to be taken into account to reach that goal in the future.

## References

*Bosman, Laurens W. J, Sebastiaan K. E Koekkoek, Joël Shapiro, Bianca F. M Rijken, Froukje Zandstra, Barry Van Der Ende, Cullen B Owens, et al. 2010. "Encoding of Whisker Input by Cerebellar Purkinje Cells." The Journal of Physiology 588 (19): 3757–83. doi:10.1113/jphysiol.2010.195180.*

*Bower, J. M. 1997. "Is the Cerebellum Sensory for Motor's Sake, or Motor for Sensory's Sake: The View from the Whiskers of a Rat?" Progress in Brain Research 114: 463–96.*

*De Schutter, E., and V. Steuber. 2009. "Patterns and Pauses in Purkinje Cell Simple Spike Trains: Experiments, Modeling and Theory." Neuroscience 162 (3): 816–26. doi:10.1016/j.neuroscience.2009.02.040.*

*De Zeeuw, Chris I., Freek E. Hoebeek, Laurens W. J. Bosman, Martijn Schonewille, Laurens Witter, and Sebastiaan K. Koekkoek. 2011. "Spatiotemporal Firing Patterns in the Cerebellum." Nature Reviews. Neuroscience 12 (6): 327–44. doi:10.1038/nrn3011.*

*De Zeeuw, Chris I., and Michiel M. Ten Brinke. 2015. "Motor Learning and the Cerebellum." Cold Spring Harbor Perspectives in Biology 7 (9). doi:10.1101/cshperspect.a021683.*

*de Zeeuw, Patrick, Juliette Weusten, Sarai van Dijk, Janna van Belle, and Sarah Durston. 2012. "Deficits in Cognitive Control, Timing and Reward Sensitivity Appear to Be Dissociable in ADHD." PloS One 7 (12): e51416. doi:10.1371/journal.pone.0051416.*

*Gruijl, Jornt de. 2013. "Timing and Graded Signals in the Inferior Olive," January. http://repub.eur.nl/pub/38598/.*

*Ito, M. 1984. "The Modifiable Neuronal Network of the Cerebellum." The Japanese Journal of Physiology 34 (5): 781–92.*

*Itō, Masao. 1984. The Cerebellum and Neural Control. Raven Press.*

*Llinás, R, and M Sugimori. 1980. "Electrophysiological Properties of in Vitro Purkinje Cell Dendrites in Mammalian Cerebellar Slices." The Journal of Physiology 305 (August): 197–213.*

*Loewenstein, Yonatan, Séverine Mahon, Paul Chadderton, Kazuo Kitamura, Haim Sompolinsky, Yosef Yarom, and Michael Häusser. 2005. "Bistability of Cerebellar Purkinje Cells Modulated by Sensory Stimulation." Nature Neuroscience 8 (2): 202–11. doi:10.1038/nn1393.*

*Ozden, Ilker, Megan R. Sullivan, H. Megan Lee, and Samuel S.-H. Wang. 2009. "Reliable Coding Emerges from Coactivation of Climbing Fibers in Microbands of Cerebellar Purkinje Neurons." The Journal of Neuroscience 29 (34): 10463–73. doi:10.1523/JNEUROSCI.0967-09.2009.*

*Ramnani, Narender. 2006. "The Primate Cortico-Cerebellar System: Anatomy and Function." Nat Rev Neurosci 7 (7): 511–22. doi:10.1038/nrn1953.*

*Robertson, L. T. 1984. "Topographic Features of Climbing Fiber Input in the Rostral Vermal Cortex of the Cat Cerebellum." Experimental Brain Research 55 (3): 445–54.*

*Schmahmann, Jeremy D. 2010. "The Role of the Cerebellum in Cognition and Emotion: Personal Reflections since 1982 on the Dysmetria of Thought Hypothesis, and Its Historical Evolution from Theory to Therapy." Neuropsychology Review 20 (3): 236–60. doi:10.1007/s11065-010-9142-x.*

*Schonewille, Martijn, Sara Khosrovani, Beerend H. J. Winkelman, Freek E. Hoebeek, Marcel T. G. De Jeu, Inger M. Larsen, J. Van der Burg, Matthew T. Schmolesky, Maarten A. Frens, and Chris I. De Zeeuw. 2006. "Purkinje Cells in Awake Behaving Animals Operate at the Upstate Membrane Potential." Nature Neuroscience 9 (4): 459–61; author reply 461. doi:10.1038/nn0406-459.*

*Schraa-Tam, Caroline K. L., Willem J. R. Rietdijk, Willem J. M. I. Verbeke, Roeland C. Dietvorst, Wouter E. van den Berg, Richard P. Bagozzi, and Chris I. De Zeeuw. 2012. "fMRI Activities in the Emotional Cerebellum: A Preference for Negative Stimuli and Goal-Directed Behavior." Cerebellum (London, England) 11 (1): 233–45. doi:10.1007/s12311-011-0301-2.*

*Sengupta, Mohini, and Vatsala Thirumalai. 2015. "AMPA Receptor Mediated Synaptic Excitation Drives State-Dependent Bursting in Purkinje Neurons of Zebrafish Larvae." eLife 4. doi:10.7554/eLife.09158.*

*Sherrington, Charles Scott. 1916. The Integrative Action of the Nervous System. CUP Archive.*

*Shin, Soon-Lim, Freek E. Hoebeek, Martijn Schonewille, Chris I. De Zeeuw, Ad Aertsen, and Erik De Schutter. 2007. "Regular Patterns in Cerebellar Purkinje Cell Simple Spike Trains." PloS One 2 (5): e485. doi:10.1371/journal.pone.0000485.*

*Steuber, Volker, Wolfgang Mittmann, Freek E. Hoebeek, R. Angus Silver, Chris I. De Zeeuw, Michael Häusser, and Erik De Schutter. 2007. "Cerebellar LTD and Pattern Recognition by Purkinje Cells." Neuron 54 (1): 121–36. doi:10.1016/j.neuron.2007.03.015.*

*Strick, Peter L., Richard P. Dum, and Julie A. Fiez. 2009. "Cerebellum and Nonmotor Function." Annual Review of Neuroscience 32: 413–34. doi:10.1146/annurev.neuro.31.060407.125606.*

*Thach, W. Thomas, and Amy J. Bastian. 2004. "Role of the Cerebellum in the Control and Adaptation of Gait in Health and Disease." Progress in Brain Research 143: 353–66.*

*Tomasch, Joseph. 1969. "The Numerical Capacity of the Human Cortico-Pontocerebellar System." Brain Research 13 (3): 476–84. doi:10.1016/0006-8993(69)90261-3.*

*Ugolini, G., and H. G. J. M. Kuypers. 1986. "Collaterals of Corticospinal and Pyramidal Fibres to the Pontine Grey Demonstrated by a New Application of the Fluorescent Fibre Labelling Technique." Brain Research 365 (2): 211–27. doi:10.1016/0006-8993(86)91632-X.*

*Wadiche, Jacques I., and Craig E. Jahr. 2005. "Patterned Expression of Purkinje Cell Glutamate Transporters Controls Synaptic Plasticity." Nature Neuroscience 8 (10): 1329–34. doi:10.1038/nn1539.*

*Wang, Fushun, Qiwu Xu, Weishan Wang, Takahiro Takano, and Maiken Nedergaard. 2012. "Bergmann Glia Modulate Cerebellar Purkinje Cell Bistability via Ca2+-Dependent K+ Uptake." Proceedings of the National Academy of Sciences of the United States of America 109 (20): 7911–16. doi:10.1073/pnas.1120380109.*

*Wang, Xinming, Gang Chen, Wangcai Gao, and Timothy J. Ebner. 2011. "Parasagittally Aligned, mGluR1-Dependent Patches Are Evoked at Long Latencies by Parallel Fiber Stimulation in the Mouse Cerebellar Cortex in Vivo." Journal of Neurophysiology 105 (4): 1732–46. doi:10.1152/jn.00717.2010.*

*Witter, Laurens, and Chris I. De Zeeuw. 2015. "Regional Functionality of the Cerebellum." Current Opinion in Neurobiology 33 (August): 150–55. doi:10.1016/j.conb.2015.03.017.*

*Wolpert, Daniel M, R.Chris Miall, and Mitsuo Kawato. 1998. "Internal Models in the Cerebellum." Trends in Cognitive Sciences 2 (9): 338–47. doi:10.1016/S1364-6613(98)01221-2.*

*Yartsev, Michael M., Ronit Givon-Mayo, Michael Maller, and Opher Donchin. 2009. "Pausing Purkinje Cells in the Cerebellum of the Awake Cat." Frontiers in Systems Neuroscience 3: 2. doi:10.3389/neuro.06.002.2009.*

# Summary

The regularity of the cellular organization of the cerebellar cortex has long been considered as a sign of structural homogeneity, where all parts perform a similar type of information processing on different types of data streams. In contrast to the structural homogeneity of the neuronal network, the inputs to the cerebellar cortex are not homogeneously distributed. Instead, they project to distinct parasagittal zones based on their origin. The zones can be observed in the patterning of the climbing fiber projections from the inferior olive to the cerebellar cortex and in that of the projections from the cerebellar cortex to the nuclei. The parasagittal zones can be recognized, apart from by its connections, by their alternating expression patterns of the protein “zebrin II”. The parasagittal zones can be subdivided into smaller “microbands” that could function as synchronized ensembles. For this thesis, we first investigated the basic electrophysiological properties of Purkinje cells in parasagittal zones with different zebrin-identities. Then we zoomed in to single cell resolution to observe the responses of Purkinje cells to different sensory inputs via climbing fiber projections.

In chapter 2 we compared, using single unit recordings across the whole cerebellar cortex, the spontaneous firing rates of Purkinje cells in zebrin-positive and -negative bands. Between these, we found clear differences between Purkinje cells in terms of their simple spike and complex spike firing frequencies. Simple spike and complex spike frequencies are significantly higher in Purkinje cells located in zebrin-negative than zebrin-positive modules. We speculate that this finding could indicate that Purkinje cells in different zebrin-bands could favor the opposite form of synaptic plasticity. Zebrin-positive cells may be more prone to express long-term depression and zebrin-negative cells may be more prone to express long term potentiation.

In chapter 3 we studied the phenomenon of pauses in Purkinje cell simple spike firing. We found the occurrence of long pauses (>500 ms) correlated with tissue damage and lower temperature. The short pauses (<500 ms) distributions differ between purkinje cells of different lobule or cerebellar modules. The simple spike pauses are potentially important instrumental properties of Purkinje cells, but we showed that long pauses could also be a sign of unphysiological perturbations.

In chapter 4, using the two photon $Ca^{2+}$ imaging technique, we mapped tactile, auditory and visual responses of lobule crus 1 Purkinje cells. We found interspersed projections from different sensory sources, and overlapping projections of sensory modalities. We have shown that clusters of adjacent Purkinje cells with the exact same receptive field do probably not exist in crus 1. Instead, adjacent Purkinje cells seem to integrate various receptive fields. This could be in line with providing the sensory feedback for different types of facial behavior – often involving different regions (e.g. during grooming).

In chapter 5, we mapped, using the whisker system as a reliable and precise source of tactile inputs, the single whisker sensory projections to lobule crus 1. We found that whisker-responsive Purkinje cells were located based on their connectivity to individual whiskers – grouping functionally similar cells together – but the overall organization of the Purkinje cells did resemble a fractured somatotopy rather than an organized somatotopy.

In conclusion, our findings expand our view of the heterogeneity in cerebellar cortex on two

different levels. On macro level, zebrin identity separates cerebellar cortex into two heterogeneous groups. On micro level, in the range of microbands, there is also heterogeneity of sensory inputs. All these results provide us a fascinating complicated multilayer organization of cerebellum which could underline the functional diversity of cerebellum.

# Samenvatting

De regelmaat in de neuronale opbouw van de cerebellaire cortex doet structurele uniformiteit veronderstellen welke de verwerking van verschillende soorten input op één gelijke wijze faciliteert. De input naar de cerebellaire cortex is daarentegen niet homogeen verdeeld en projecteert naar afzonderlijke parasagitale zones op basis van hun oorsprong. Deze zones worden gekenmerkt door de banen van klimvezelprojecties vanuit de olijfkernen naar de cerebellaire cortex en connecties van de cerebellaire cortex naar de cerebellaire kernen. De parasagitale zones kunnen, naast hun netwerkverbindingen, ook herkend worden aan de hand van alternerende expressiebanden van het ‘zebrin II’ eiwit. De parasagitale zones kunnen verder verdeeld worden in zogenoemde microbanden welke als gesynchroniseerde ensembles kunnen functioneren. In deze dissertatie is allereerst ingegaan op de algemene electrophysiologische karakteristieken van Purkinje neuronen naar gelang van zijn zebrin indentiteit. Vervolgens is ingezoomd op individuele Purkinje neuronen om de responsiviteit voor verschillende sensorische stimuli via klimvezelprojecties te onderzoeken.

In hoofdstuk twee vergeleken we de spontane vuurfrequenties tussen Purkinje neuronen die in zebrin-positieve en -negatieve banden gelokaliseerd zijn over de gehele cerebellaire cortex. Tussen deze twee groepen werden duidelijke verschillen gevonden in de simpele en complexe actiepotentiaalfrequenties. De frequenties voor de twee types actiepotentialen zijn significant hoger in Purkinje neuronen die zich in zebrin-negatieve banden bevinden. Deze resultaten suggereren dat Purkinje neuronen in de verschillende zebrin banden een diametrale vorm van plasticiteit kennen. Zebrin-positieve neuronen zouden meer geneigd zijn tot de expressie van lange termijn depressie, terwijl zebrin-negatieve neuronen eerder lange termijn potentiatie laten zien.

In hoofdstuk drie bestudeerden we de karakteristieke lange pauzes waargenomen in de vuurpatronen van simpele actiepotentialen in de Purkinje neuronen. Het voorkomen van lange pauzes (>500 ms) werd gevonden te correleren met weefselschade en lagere temperaturen. De verdeling van korte pauzes (<500 ms) verschilt tussen Purkinje neuronen in verschillende lobben en/of cerebellaire modules. Ondanks dat de pauzes tussen simpele actiepotentiaal treinen mogelijk een belangrijk instrumentele eigenschap van het Purkinje neuron zijn, hebben we hier laten zien dat lange pauzes ook een indicatie kunnen zijn van een niet-physiologische verstoring van het neuron.

In hoofdstuk vier is de responsiviteit van Purkinje neuronen in de Crus I lobule in kaart gebracht voor tactiele, auditieve en visuele input met behulp van twee-photon $Ca^{2+}$ visualisatie. We vonden zowel gemengde als overlappende projecties voor de verschillende sensorische input. We laten zien dat de clusters van aangrenzende Purkinje neuronen met gelijke receptieve velden waarschijnlijk niet in Crus I zijn te vinden. Aangrenzende Purkinje neuronen laten daarentegen juist een integratie van verschillende receptieve velden zien. Dit ligt in lijn met een terugkoppelmechanisme dat reageert op verschillende types van gezichtsgedrag, hetgeen vaak betrokken is met verschillende gebieden (bijvoorbeeld tijdens verzorging).

In hoofdstuk vijf is het snorhaar-systeem gebruikt als een betrouwbare en nauwkeurige bron van tactiele stimulatie om sensorische projecties van individuele snorharen naar de Crus I lobule in kaart te brengen. Ons onderzoek wijst uit dat snorhaar-responsieve Purkinje neuronen gelocaliseerd zijn op basis van hun connectiviteit naar individuele snorharen, waardoor functioneel gelijke neuronen gegroepeerd zijn. De algehele organisatie van Purkinje neuronen liet echter een gefractureerde dan georganiseerde somatotopy zien.

Ter conclusie, onze bevindingen verbreden ons inzicht in de heterogeniteit van de cerebellaire cortex op twee niveaus. Op macroscopisch niveau wordt de cerebellaire cortex onderscheiden in twee heterogene groepen door de zebrin identiteit. Op microscopisch level zien we heterogeniteit van sensorische input in het gebied van microbanden. Deze resultaten verschaffen ons een fascinerende inkijk in de gecompliceerde multi-laag organisatie van het cerebellum welk zijn functionele diversiteit onderstreept.

# Curriculum vitae

## PERSONAL DATA

| | |
|---|---|
| Family Name: | Ju |
| First Name: | Chiheng |
| Birth date: | 1975.12.03 |
| Gender: | Male |

## EDUCATION

| | |
|---|---|
| April .2007 | *-Present*<br>**ERASMUS NIVERSITY, MEDICAL CENTER**<br>Rotterdam, NETHERLAND<br>*PhD student in neuroscience* |
| July .2007 | *-January 2011*<br>**SHANGHAI JIAO TONG UNIVERSITY, MEDICAL SCHOOL** Shanghai, CHINA<br>*Master/PhD student in neurology (not finished)* |
| Sept.1994 | -July.1999<br>**LIAONING COLLEGE OF TRADITIONAL CHINESE MEDICINE**<br>Shenyang, CHINA<br>*Bachelor in clinical medicine* |

# PhD Portfolio

| | |
|---|---|
| *Student's name* | Chiheng Ju |
| *University* | Erasmus University Rotterdam |
| *Department* | Neuroscience |
| *Research school* | ONWAR |
| *PhD duration* | April 2011- January 2016 |
| *Supervisor* | Prof.Dr. Chris I. De Zeeuw |
| *Co-supervisor* | Dr. L. W. J. Bosman |

## General Courses

| | |
|---|---|
| 2012 | Laboratory animal science |
| 2012 | Imaging Life at the Molecular Level |
| 2012 | Academic English Writing |

## Teaching

| | |
|---|---|
| 2012-2014 | Neuroscience Summer school: two photon imaging demonstration |
| 2012-2015 | Master of Neuroscience: two photon imaging demonstration |

# Acknowledgments

When looking back at my five years journey as a PhD student in Rotterdam, I would like to thank all those people who made it possible.

First I would like to thank my supervisor Chris. Not only because everything started from where you kindly give me the PhD position offer but also because of your continueously guidance and support along the way. You always warmly response to my questions and always encourage me to try exciting new experiments. Your enthusiasm for science & research has been infectious to me and will continuously fuel my motivation as a researcher in future career!

I am very grateful to my co-supervisor Laurens for all the helps along the journey. Whenever I got a problem in work you were always there to help. Whenever I feel depressed and down in experiments you were always there offering me 'Chicken Soup for the Soul'. Whenever I made a progress you were always the one who gave me first congratulations. Outside the lab, You also kindly invited my wife and I to have dinner in your house after we arrived and when my son was born you and your lovely family visited us to share the happy moments. You also dedicated a lot of time helping me prepare this book. Thank you for being such a great mentor and a great friend!

Without the help and support from all our department members I could also not be here. First thanks to Prof.Dr. Hans van de steen for the interview you gave me in Shanghai 5 years ago, which was the crucial step that literally helped me got here. And also thank you very much for the invitation to your great birthday party!

As soon as my wife and I arrived in Rotterdam we were invited by Dr. Zhenyu Gao couple to visit 'great wall' (a restaurant) and had a great chinese dinner there. You made us instantly felt the warmth as at home. Thank you very much Gao for your advises and support from the very beginning to the end!

After been introduced to the whisker lab, I met two former Master students in our group Olesya and Wouter, I would like to say thanks to you for trained me to use our two photon setup. And great big thanks to Tycho and Rudiger for your very kind support to make it works! Tycho, thank you so much for all your instrutions and valuable suggestions! I really enjoy working with you in the lab. Rudiger, you are the coolest and most warm hearted scientist I have ever met!

Thanks to our group mates Wei, Sanders(Senior and Junior), Vincenzo, Lorenzo, Marizio, Cullen, Negah Rahmati Andami, Pavithra, Arthiha, Siyang for all the valuable discussions about my projects and thesis! After acquired data I am blessed to have my 'Matlab genies' Johan, Mario and Pascal. Thanks for helping me to automize the analysis with matlab scripts. You guys are literately life saving by saving so much of my time from bushcrafting with excel! Thanks Mario for your valuable inputs to my projects. Whenever I asked questions you were always ready to provide inspiring answers and constructive arguments. Thanks to Pascal for all the efforts you made to the analysis and I always enjoy our discussion about culture and science! Dear Sander Senior, thank you for always willing to listen to my problems and kindly offered great suggestions! Dear Sander Junior, thanks for always supported me and taught me Dutch!

In the middle of my PhD study, I got a great opportunity to cooperate with Schonewille group. Big thanks to Martijn, Haibo and Kai for their help during the experiments. It was a great joy to work with such an experienced and effective team!

Other members in out department also offered great help when I need it. Thanks to Prof.Dr.Bas Koekkoek , Dr.Freek. E. Hoebeek ,Prof.Dr. Gerard Borst, Dr. Tom Ruigrok, Dr.Dick Jaarsma and .Dr. Joan Holstege for their valuable suggestions and help. Thanks to Prof.Dr.John Simpson for your great advises about my future career. Thanks to our Coordinator Loes and Elise for always being there to give me effective support. Thanks to Kees, Elize, Laura and Annette for the technical support. Thanks to Job Lassche who helped me got all the bureaucracy paper works done. Thanks to Jackie Zhou, Bin Wu, Rui Cai, Tianshi wang, Andrius Plauska, Suman Das, Mafer Vinueza Veloz, Martijn Sierksma, Zhanmin Lin, Malik Bechakra, Christos Strydis, Grazia Iaffaldano, Robert Seepers, Tiantian Wang, Zhouqiao Wu, Aaron Wong. I am lucky to have you guys as colleagues and friends! Thank you all for your help and support along the way! I'd like to give special thanks to my Paranimfen Jackie and Pascal for taking care of the defense preparation.

Last but not least, I want to thank my family members. Thanks to my wife Viviane for taking good care of our son Vincent at home. Thanks for all the great Chinese dishes you cooked. Thanks for all you have done for the family. Thanks to my son Vincent to be such a great little guy, you could always cheer me up no matter how tired I feel after work. To my parents and my sister, 亲爱的爸爸妈妈，谢谢你们一直支持我追逐梦想，谢谢你们永远无条件的站在我的背后，你们的爱是我前进的最大动力，希望我的梦想也是你们的梦想，我会继续为之努力。亲爱的妹妹蕾俐，感谢你在我远在海外的时候照顾妈妈，感谢你与我同悲同喜，不论顺境逆境你都是我最值得信赖的亲人和朋友。我爱你们。

This work is supported in part by a scholarship from China Scholarship Council (CSC) No.2010623033 to C.J